Water Erosion Modelling using Fractal Rainfall Disaggregation, a Study in Semiarid Tunisia

Jebari, Sihem

2009

DEPARTMENT OF WATER RESOURCES ENGINEERING
Lund Institute of Technology, Lund University, Sweden

Water erosion modeling using fractal rainfall disaggregation - A study in semi-arid Tunisia

Sihem Jebari

Report No 1047
Lund, Sweden, 2009

Organization: LUND UNIVERSITY Water Resources Engineering Box 118, S-221 00 Lund, Sweden	**Document name:** DOCTORAL DISSERTATION
	Date of issue June 2009
	Coden: LUTVDG/(TVRL-1047) (2009)

Author:
Sihem Jebari

Title and subtitle

Water erosion modelling using fractal rainfall disaggregation – A study in semiarid Tunisia

Abstract

In the Tunisian semiarid area, water erosion processes have led to negative economic and environmental consequences in a context of limited water resources. To characterize and predict these degradation phenomena, a comprehensive high-resolution data base on erosive rainfall, together with siltation records for 28 small reservoirs were analyzed. The studied small reservoir network displays a general life-span of about 14 years. The average soil loss is 14.5 tonnes/ha/year. The complex relationship between the erosive rainfall events and the annual soil loss rates can be explained by two important factors. The first factor is related to the soil "degradation cycle". It determines the soil particle delivery potential of the catchment. The second factor corresponds to the "degradation front". The latter presents a north-western/south-eastern direction.

To investigate rainfall disaggregation possibilities, a regionalization of fine time-scale and daily rainfall was undertaken. The results showed that the spatial properties are typically non-isotropic. Clustering showed that two different homogeneous rainfall subgroups are closely related to the predominant convective and frontal rainfall types. The comparison illustrated important similarities between the maximum 15-min and the daily rainfall data.

The above findings were an incentive to explore the multiplicative properties of a 4-year rainfall time series. The time series showed scaling behavior for time scales up to 100 min that coincides with the most active erosion process time scale. Moreover, the temporal structure of rainfall was reproduced using a disaggregation model (Olsson, 1998). The observed and generated rainfall time series displayed several similar characteristics. This allowed the reproduction of erosivity for erosive rainfall events longer than 45 minutes. The erosion modeling was performed using the USLE/GIS approach. Maps of observed and generated spatial erosion distribution were combined with the Masson's and Wischmeier-Smith's erosion limit intervals. According to the above, the potential of rainfall scaling-based approaches to predict water erosion levels in semiarid areas seems promising. Using this approach may help soil and water authorities in semiarid areas to better manage soil erosion problems.

Key words: Atlasic mountain range, erosive events, fractal analysis, regionalization, reservoir siltation, semiarid area, soil loss, Tunisia.

Classification system and/or index terms (if any)

Supplementary bibliographical information		Language English
ISSN and key title: ISSN: 1101 – 9824		ISBN:
Recipient´s notes	Number of pages	Price
	Security classification	

Distribution by Division of Water Resources Engineering, Faculty of Engineering, Lund University, Box 118, S-221 00 Lund, Sweden

Signature_____ Date_____

DEPARTMENT OF WATER RESOURCES ENGINEERING
LUND INSTITUTE OF TECHNOLOGY, LUND UNIVERSITY
CODEN: LUTVDG/TVVR-1047 (2009)

Doctoral Thesis

Water erosion modeling using fractal rainfall disaggregation - A study in semiarid Tunisia

By

Sihem Jebari

June 2009

Water erosion modeling using fractal rainfall disaggregation-
A study in semiarid Tunisia

Doktorsavhandling
Institutionen för Teknisk vattenresurslära
Lunds Tekniska Högskola, Lunds Universitet

Doctoral Thesis
Water Resources Engineering
Lund Institute of Technology, Lund University
Box 118
SE-221 00 Lund
Sweden

http://aqua.tvrl.lth

Cover:
The Tunisian semiarid areas, photos taken by Sihem Jebari.

CODEN: LUTVDG/(TVRL-1047) (2009)
ISBN:
ISSN: 1101 – 9824

Printed by Media-Tryck, Lund, Sweden, 2009

To the memory of my father Abdelkader, to my mother Habiba
who taught me the perseverance that made my dream come true
&
To my sweet hearts Omar and Walid for making my life so joyful

Acknowledgments

First and foremost I would like to thank my supervisor Prof. Ronny Berndtsson for all the efforts, the patience and the time he devoted to communicate the scientific reasoning to a young researcher. He has been a great source of inspiration to me. Indeed, his support, guidance and constructive criticism were crucial for the completion of this thesis. My gratitude goes also to my co-supervisor Dr. Akissa Bahri, who provided help, continued interest in my progress, and an exceptional contact network.

It has been a real privilege to work with Prof. Cintia B. Uvo, Dr. Jonas Olsson, and Prof. Fethi Lebdi "as paper co-authors". They have provided invaluable advice and tools for data analysis. Their involvement is gratefully acknowledged. Many thanks also go to Mrs. Mary Fraser Berndtsson who not only checked the language of the summary but also is a good friend to me.

I would like to express my gratitude to Prof. Abdelaziz Mougou President of IRESA (Tunisian Agricultural Institute for Research and Higher Education) and Dr. Nejib Rejeb head of INRGREF (Tunisian National Research Institute for Rural Engineering, Water and Forestry) for facilitating the cooperation with Lund University and for providing all facilities for this research work.

We are especially thankful to Mr. Habib Farhat, head of the Farmland Conservation and Management Department (DG/ACTA) at the Ministry of Agriculture and Water Resources in Tunisia as well as his staff for enabling us to access databases. I would also like to thank Mr. Moncef Rajhi head of the Tunisian National Meteorological Institute (INM). His team of dynamic engineers introduced me to the interpretation of the meteorological maps.

The financial support provided by the Swedish Agency for International Development Cooperation (SIDA), the Swedish Institute (SI) and the Tunisian National Research Institute for Rural Engineering, Water and Forestry (INRGREF) is gratefully acknowledged.

I very much enjoyed working with all my colleagues at INRGREF, Tunisia. I am grateful to Dr. Raoudha Mougou for sharing her climatological knowledge, Dr. Hedia Chakroun for helping with GIS tool, and Dr. Thameur Chaibi for his advice and encouragement. It was also a real pleasure to share experiences and discuss with all my colleagues at the Department of Water Resources Engineering, Sweden. Special thanks to my good friends Dr. Justyna Czemiel, Ms. Lijun Liao, Dr. Dinis Juizo, and Mr. Osama Ali Maher.

I am also obliged to my teachers at INAT. I am especially thankful to Prof. Ennebli Noureddine for encouraging me to do further research. I am also grateful to Prof. Mohamed S. Slimani who revealed statistical hydrology to me and passed me his passion to this research field. Great thanks go to Mr. Moustpha Saadaoui from the Tunisian Department of Water Resources, Mr. Louati Ben Younes and Aymen Lassoued for sharing their professional experiences.

My deepest appreciation goes to my sister Dalila and her husband Khaled Abassi, they have been invaluable supporters, patient listeners and devoted advisers. With their daughter Asma they

have given me a helping hand whenever needed. They have always been a source of comfort for my kids during my stays at Lund.

Finally, I dedicate my work to all my family: my brothers, sisters, brothers in law, sisters in law, nieces and nephews. Without forgetting the precious help of Ms. Wassila, I want you all to know that this is a product of your contribution. I love you all.

Abstract

In the Tunisian semiarid area, water erosion processes have led to negative economic and environmental consequences in a context of limited water resources. To characterize and predict these degradation phenomena, a comprehensive high-resolution data base on erosive rainfall, together with siltation records for 28 small reservoirs were analyzed. The studied small reservoir network displays a general life-span of about 14 years. The average soil loss is 14.5 tonnes/ha/year. The complex relationship between the erosive rainfall events and the annual soil loss rates can be explained by two important factors. The first factor is related to the soil "degradation cycle". It determines the soil particle delivery potential of the catchment. The second factor corresponds to the "degradation front". The latter presents a north-western/south-eastern direction.

To investigate rainfall disaggregation possibilities, a regionalization of fine time-scale and daily rainfall was undertaken. The results showed that the spatial properties are typically non-isotropic. Clustering showed that two different homogeneous rainfall subgroups are closely related to the predominant convective and frontal rainfall types. The comparison illustrated important similarities between the maximum 15-min and the daily rainfall data.

The above findings were an incentive to explore the multiplicative properties of a 4-year rainfall time series. The time series showed scaling behavior for time scales up to 100 min that coincides with the most active erosion process time scale. Moreover, the temporal structure of rainfall was reproduced using a disaggregation model (Olsson, 1998). The observed and generated rainfall time series displayed several similar characteristics. This allowed the reproduction of erosivity for erosive rainfall events longer than 45 minutes. The erosion modeling was performed using the USLE/GIS approach. Maps of observed and generated spatial erosion distribution were combined with the Masson's and Wischmeier-Smith's erosion limit intervals. According to the above, the potential of rainfall scaling-based approaches to predict water erosion levels in semiarid areas seems promising. Using this approach may help soil and water authorities in semiarid areas to better manage soil erosion problems.

Contents

Appended papers

The present thesis is based on the following papers:

I. Jebari, S. (2009) Temporal aspects of soil erosion in Tunisia. *Hydrological Sciences Journal* (Submitted).

II. Jebari, S., Berndtsson, R., Lebdi, F. & Bahri, A. (2008) Sediment, discharge and precipitation variation in the wadi Mellegue catchment during the last 50 years. *Annales de l'INRGREF* **11**, 116-122.

III. Jebari, S., Berndtsson, R., Bahri, A. & Boufaroua, M. (2008) Exceptional rainfall characteristics related to erosion risk in semiarid Tunisia. *The Open Hydrology Journal*, **2** (9), 25-33.

IV. Jebari, S., Berndtsson, R., Bahri, A. & Boufaroua, M. (2009) Spatial soil loss risk and reservoir siltation in semiarid Tunisian. Accepted for publication in *Hydrological Sciences Journal.*

V. Jebari, S., Berndtsson, R., Uvo, C. & Bahri, A. (2007) Regionalizing fine time-scale rainfall affected by topography in semi-arid Tunisia. *Hydrological Sciences Journal*, **52** (6), 1199-1215.

VI. Jebari, S., Berndtsson, R. & Olsson, J. (2008) A scaling approach to enhance rainfall data for erosion estimation in semiarid Tunisia. *Hydrology and Earth System Sciences* (Submitted).

VII. Jebari, S. & Olsson, J. (2009) Soil erosion estimation based on rainfall disaggregation. *Hydrology and Earth System Sciences* (Submitted).

1. Introduction

1.1 Background

Water erosion problems are often related to important issues like food security, water storage capacity and environmental management and sustainability (Pimentel *et al*., 1995; Lal, 1998; WCD, 2000; Eswaran *et al*., 2001; Lomborg, 2001; ILEC, 2003). Thus, water erosion has direct negative economic and environmental consequences. Water erosion processes are sensitive on the one hand to anthropogenic effects and on the other hand to global warming (Yang *et al.*, 2003; Nearing *et al*., 2004; Cudennec *et al*., 2007). Recent research indicates that intensive rainfall is the main contributor to sediment transport (Dhakal & Sidle, 2004; Jen *et al*., 2006; Boix-Fayos *et al*., 2007). However, the prediction of soil loss distribution still remains a difficult research challenge (Herath, 1999; Price *et al.*, 2000; Coppus *et al.*, 2002; De Vente, 2005; Goel *et al.*, 2005). In fact, the non-availability of recorded short-term rainfall data appears to be a major limitation for statistical modeling of soil erosion risk (White *et al*., 1997; De Vente, 2005; Haregeweyn *et al*., 2006). This fact is especially disadvantageous for areas in the semiarid Mediterranean and the Middle East, since the soil erosion is especially severe in these locations (Sivapalan *et al*., 2003).

Soil erosion is likely to worsen in the future. This is especially true in the northern Mediterranean basin where studies have emphasized the importance of soil erosion (Poesen & Hooke, 1997; EEA, 1999; Boix-Fayos, 2007). However, the situation can be even more serious in the southern parts of the basin, more specifically in the North African countries where water and soil resources are expected to continue to deteriorate (Gobin *et al*., 2004; GOPA & GTZ, 2005; Ennabli, 1998; 2007). The obvious consequence of water erosion is the increasing area of a barren arid belt, as can be observed in countries in the south of the Maghreb. An example of this is Tunisia. In this country, water erosion seems to be a persistent phenomenon, affecting 20% of the total area. Annually, 15000 hectares of arable farming land and 500 million m^3 of runoff water are lost (DG/ACTA, 1993). Presumably from now until 2030 the Tunisian reservoir capacity will gradually decrease by 40 million m^3 per year due to siltation (GOPA & GTZ, 2005). Tunisia is one of the countries in the Mediterranean basin that is likely to suffer from water scarcity and loss of storage capacity for water in reservoirs (FAO, 1994). At the same time, the maximum capacity of rainwater harvesting will reach 95% in 2010.

In this context, the strong variability of rainfall influences rural development progress in terms of water and soil resource availability and use (Cudennec *et al*., 2005). Water storage systems, flood protection, water harvesting structures, and silting trap design, are common tasks for rural engineers. Consequently, there is a great need to establish links between exceptional rainfall event characteristics and the erosion process. In this study, the utilized data were taken from a unique high-resolution rainfall data base together with siltation data from 28 reservoirs originally collected in an EU-funded project (SERST-IRD, 2000). By combining the two sources of data the aim was to improve the understanding of the erosion process and to delineate important links between field rainfall characteristics and deposited sediments in small reservoirs. Moreover, the comparison between short time scale and daily rainfall in view of disaggregation possibilities was conducted through the Olsson cascade disaggregation model (1998; 2008). Scaling and disaggregation approaches for rainfall especially have been an intense research area

in recent years (e.g., Ormsbee, 1989; Olsson, 1998; Olsson & Berndtsson, 1998; Guntner *et al*., 2001; Lovejoy & Schertzer, 2005; Molnar & Burlando, 2005; Veneziona *et al*., 2006; Elshamy, 2007; Kantelhardt, 2008). The research challenge in this thesis was consequently to investigate if daily rainfall time series could be disaggregated to 15-min rainfall data that can be used to estimate rainfall erosivity. If this is possible it would also be possible to predict rainfall erosion and the siltation of reservoirs. Development of such a methodology would aid in the management of soil and water conservation projects and eventually better the handling of water shortage in a context of an increasing need for water.

1.2 Objectives

The main objective of this study was to develop a methodology that can be used to predict siltation in reservoirs and thus loss of reservoir capacity in view of large spatial and temporal rainfall variability and lack of short-term rainfall data. For this purpose several partial objectives had to be fulfilled. The first partial objective was to establish links between short-term rainfall variability and water erosion in the studied area. The second partial objective was to develop a technique to generate short-term rainfall input which is crucial for water erosion modeling. The third partial objective was to use the generated short-term rainfall data to simulate water erosion. For this purpose the following work schedule was applied in the study:

- Analysis of temporal and spatial water erosion patterns using observed siltation in reservoirs.

- Definition of the most important erosive rainfall characteristics.

- Exploration of disaggregation possibilities through a comparison between short-term and daily rainfall time scales.

- Evaluation of the performance of a rainfall cascade disaggregation model to generate erosive rainfall intensities for short time steps.

- Performance of soil loss modeling based on the fractal rainfall model in order to estimate and to spatially distribute the erosion risk.

2. Literature review

2.1 Rainfall characteristics and soil erosion processes

Raindrop impact initiates detachment of soil particles and causes the formation of a crust (Ellison, 1947; Greene *et al*., 1994; EEA, 2002) which seals the surface and limits the infiltration. Once the rainfall intensity exceeds the infiltration rate of the soil, overland flow of water occurs across the land surface, generating hydraulic forces that erode and transport sediments in a down-slope direction (Weggel & Rustom, 1992). In the Mediterranean areas, very low values of saturated hydraulic conductivities are often found after 10 min of simulated rain (Ramos & Nacci, 1997). As a consequence of weak aggregate stability of the soil surface, rainfall is often laterally distributed by Hortonian overland flow even for low intensity rainfall (Cerdan *et al*., 2004). Runoff is the most important direct driver of severe soil erosion (EEA, 2002). It often occurs at catchment scale, when rainfall intensities reach a minimum threshold of about 25 mm/h in 10 min (e.g., Cammeraat, 2002). For other semiarid areas, observations have shown that about a 15-mm rain may be needed to produce 1 to 2 mm of runoff (Coppus & Imeson, 2002). High-intensity rainfall events affect runoff generation and erosion processes which are known to be highly non-linear (Kandel *et al*., 2004). This is also considered the major contributor to long-term soil loss (Gilley *et al*., 2000; Martinez-Mena *et al*., 2002; Spaan *et al.*, 2005). The lowest rainfall intensities leading to runoff on humid soil range from about 2 to 23 mm/h in Tunisian semiarid areas (Collinet & Jebari, 2000). Rainfall characteristics determine the erosive action of raindrops and overland flow. They also define the most common water erosion processes namely, interrill, rill, and gully erosion.

Interrill erosion concerns the uniform removal of soil and is assumed to be the first phase of the erosion process. Its rate is assumed to be low (Toy *et al*., 2002), but it affects the largest areas and plays an essential role in the erosion system (EEA, 2002; Malam Issa *et al.*, 2006). Rill erosion presumably begins when interrill erosion reaches about 15 tonnes/ha/year (Toy *et al.*, 2002). Interrill and rill erosions affect about 40% of the sediment moving into the reservoirs (Plata Bedmar *et al.*, 1997). However, gully erosion which is a localized process supplies about 60% of the total sediment yield to reservoir siltation (Plata Bedmar *et al.*, 1997; Martínez-Casasnovas, 2003; Lesschen *et al.*, 2007).

Return period intervals that characterize the rainfall events are crucial in describing the erosion impacts on the landscape. Bull *et al.* (1999) and Hooke *et al.* (2000) showed that important events transporting sediments have a return period of more than 1 to 7 years. Coppus *et al.* (2002) and Garcia-Ruiz *et al.* (2003) described 1-year return period events as mobilizing bed load and 5-year return period events as mobilizing small rock avalanches and channelizing debris flows. According to Maas *et al.* (2000) events with an occurrence of 5 to 15 years change the valley floor considerably. Harvey (1984) showed that 25-year event rainfall can modify the channel morphology. Finally, the 100-year return period rainfall shows a reactivation of large, deep mass movements and exceptional events with a return period that exceeds 100 years and are considered to be a catastrophic geomorphic process (Coppus *et al*., 2002; Garcia-Ruiz *et al*., 2003).

2.2 Soil erosion modeling and rainfall erosivity factor

The erosion modeling approach can evaluate soil erosion and sediment yield related to many conditions. Physically-based models require large data bases and still have limitations in predicting basin sediment yields (Renschler & Harbor, 2002). However, empirical models such as the Universal Soil Loss Equation (USLE) (Wischmeier & Smith, 1965) present a simple structure, an easy application, and require relatively small data sets (Bartsch *et al*., 2002). It reasonably estimates soil erosion and sediment yield worldwide caused by interrill and rill erosion. The latter erosion processes affect the largest areas and play major role in the erosion systems (EEA, 2002; Malam Issa *et al*., 2006).

According to previous research, the rainfall erosivity used in the USLE model is considered being the most important factor in estimating erosion response as compared to other environmental variables (e.g., Nearing *et al*., 1990). It is based on short term rainfall intensity (Wischmeier & Smith, 1958; Lal, 1976). Areas with a high potential rainfall erosivity factor present high risk of severe soil erosion; thus soil conservation structures become necessary. Finally, if it is possible to generate short time scale rainfall, the erosivity factor could be calculated. The R values would be used as input to erosion modeling in order to estimate erosion rates and to better manage erosion risks in catchments with serious degradation.

2.3 Rainfall disaggregation models

The non-availability of recorded short-term rainfall data is considered the principal limitation to water erosion modeling. In fact, to describe the ability of the rainfall to erode soil through the erosivity factor is rarely undertaken, worldwide. However, a possible way to resolve this problem would be to use a fractal approach recently developed as an effective method in disaggregation rainfall modeling which can preserve the fine time scale rainfall properties (e.g., Olsson and Berndtsson, 1998; Gunter *et al.*, 2001; Molnar and Burlando, 2005; Lovejoy and Schertzer, 2005; Veneziona *et al*., 2006; Kantelhardt, 2008). The temporal rainfall disaggregation is performed by means of the invariant scaling theory (Schertzer and Lovejoy, 1987; Over and Gupta, 1996; Olsson, 1998; Menabde and Sivapalan, 2000; Sivakumar *et al*., 2001; Schertzer *et al*., 2002, Gaume 2007). The above mentioned scaling behavior is modeled by a cascade process, an approach discussed by Schertzer and Lovejoy (1987), Lovejoy and Shertzer (1990), and Gupta and Waymire (1990; 1993), and originally used in statistical turbulence (e.g., Yaglom, 1966; Mandelbrot, 1974). Cascade models distribute rainfall mass on successive regular subdivisions of an interval in a multiplicative manner. Their performance is usually assessed in terms of reproducing some statistical characteristics of the observed time series, such as variance, wet/dry properties, rainfall amount quantiles, autocorrelation, etc. (e.g., Marsan *et al*., 1996; Svensson *et al*., 1996; Harris *et al*., 1998; Menabde *et al*., 1999; Deidda, 2000; Gunter *et al*., 2001; Olsson & Burlando, 2002; Veneziano & Furcolo, 2002; 2003; Hingray *et al*., 2005; Molnar & Burlando, 2005; Olsson, 2008). However, applications still remain rare and restricted to characterize the complex systems (e.g., Thauvin *et al*., 1998; Venezianoa *et al*., 2006). Moreover, the physical reasons behind the rainfall scale invariance remain a widely debated topic. Consequently, specialist researchers call for increasing the confidence in scaling assumptions, refining analysis techniques, and improving the modeling ability. Thus, scaling

behavior has to be established for rainfall data over different climates and geographical regions (Olsson, 1996; Olsson & Berndtsson, 1998; Kantelhardt, 2008).

3. Description of studied area and data used

3.1 Tunisian semiarid rainfall characteristics

Rainfall in semiarid Tunisia is characterized by strong irregularities. In winter, the rain originates on the Mediterranean and is usually of a frontal type. Conversely, summer and fall rain, is generally of a convective type and bursts in storms on the heights. It is often sudden and strong with more frequent occurrences (e.g., Dhonneur, 1985). This can cause a great raindrop impact triggering detachment of soil particles especially in the beginning of the rainy period. The semiarid climate covers the Dorsal area, which is defined as an important orographic region that influences the water resources and natural environment in an important way (Gammar, 1999). The mountain crest line is often described as the southern boundary of northern Tunisia and corresponds approximately to the 400 mm/year rainfall isohyet (Fig. 1). The latter is of a great importance since it is the limit for growing dry cereals (Houérou, 1969). A maximum of 110 rainfall days yearly has been observed in the extreme east of the studied area and a minimum of 58 rainfall days yearly in the centre.

3.2 Physical features and water erosion context of the Dorsal area

The Dorsal Mountains represent the last part of the Atlas chain towards the east (Fig. 1). They stretch through Tunisia from the southwest to the northeast and end at the Cap Bon Peninsula. Their width in the west is about 40 km, and falls to less than 10 km in the northeast. Altitudes continue to decrease in the same direction. They include a chain of high mountain peaks, the highest of which is Chaambi (1544 m). The Tunisian Dorsal region covers a total area of 12 490 km^2 and plays an important role in the hydrology of the country. In fact, its mountain chain links the main wadis, e.g., Mejerda, Meliane, Nebhana, Merguellil, and Zeroud (Fig. 1). The hydrological regime of this region means a hot dry summer of 4 to 5 months during which the high potential evaporation causes the formation of calcareous crusts at about 50 cm depth. The latter prevents water from seeping downwards and obstructs efficient drainage. Water resources are based on surface water use, while agriculture is based on cereal crops and cattle rising.

Due to the specific bioclimatic conditions of the Mediterranean area, the soils are better characterized by the degradation of rock material rather than their organic matter content. Consequently, they are not well developed and often shallow. The young geological relief and the rate of erosion prevent them from reaching maturity. Consequently, soil degradation characterizes the Dorsal areas, where it leads to serious water erosion problems. In fact, a thin and uneven soil cover often exposes the underlying bare bedrock. The erosion mechanisms and sediment deposits are spectacular for exceptional floods. During one of these catastrophic events, the solid transport concentration and the soil loss rate reached respectively 400 g/l and 4250 tonnes/km^2 (Claude *et al*., 1977; Bouzaine & Lafforgue, 1986; Ben Mammou, 1998). It has been estimated that 7% of the Dorsal area are badly damaged by erosion and 70% are moderately

damaged. During the national decadal plans, the Dorsal area management was based on water and soil conservation practices that covered about 20% of the total area.

3.3 The hydrological monitoring network

The present hydrological network includes 28 experimental catchments at representative sites along the Tunisian Dorsal range (Fig. 1). Each catchment discharges into a small dam, called a hill reservoir, usually built in an agricultural area. An automatic rain gage is located at each site (D/CES & ORSTOM, 1998). The rain gage network was set up by the EU-funded Program HYDROMED (Research program on hill reservoirs in the semiarid Mediterranean periphery, 1992–2002; IRD, 2000). At present the observation network is managed by the Tunisian Farmland Conservation and Management Department (DG/ACTA). The rainfall measurements were made by tipping bucket rain gages (type Oedipe V.4, pluvio 91 and pluvio-limni 92; designed and provided by the French Elsyde and SERPE-IESM, respectively). The rain gages are fully automatic and data are downloaded once a month through data loggers. The collection area of each gage is 400 cm^2. The capacity of the tipping bucket is 0.5 mm of rainwater and the adding tip diameter of the bucket is 3.5 mm. The rain gages were calibrated for average precipitation intensity. According to SERPE-IESM (1993), the measurement accuracy is ±4% up to 250 mm/h intensity (for 5-min time scale). The rainfall observation system was designed to give reliable rainfall estimates down to at least 1-min values (Colombani, 1988). Time is recorded every second. Therefore, rainfall amounts and intensities can be computed with great accuracy for the range of durations used in the current study. The gage density corresponds to approximately one gage per 500 km^2. The descriptive statistics for recorded rainfall event during the analyzed periods display missing data less than 1% of the total time. A rainfall event is defined as separate from another event if a rain gage shows less than one tip per hour.

3.4 Catchment characteristics and siltation measurements

The observed small catchments over the Dorsal area have an average area of about 4 km^2. Their drainage density is 5.1 km/km^2; their mean height difference is about 245 m, and their mean slope is 11.2%. Estimates of concentration time were made using the Kirpich (1940) formula useful for small agricultural catchments, which gave values of about 11 min. The average runoff coefficient is about 10%, but values up to about 80% have been recorded for some intense rainstorms. Bathymetric measurements were undertaken for all reservoirs. These measurements were made by echo-sounding the water depths along pre-defined transects (Camus *et al*., 1995). At least 400 measuring points defined by three Cartesian coordinates (x, y, and z) were used. The change in reservoir volume was calculated as the difference from one observation time to another. Siltation data for the reservoirs are available from annually published hydrological reports (DCES/IRD, 1994-2002). These are used to estimate average and maximum siltation rates delivered at the outlet of a catchment usually needed to design reservoirs and to preserve the storage water capacity.

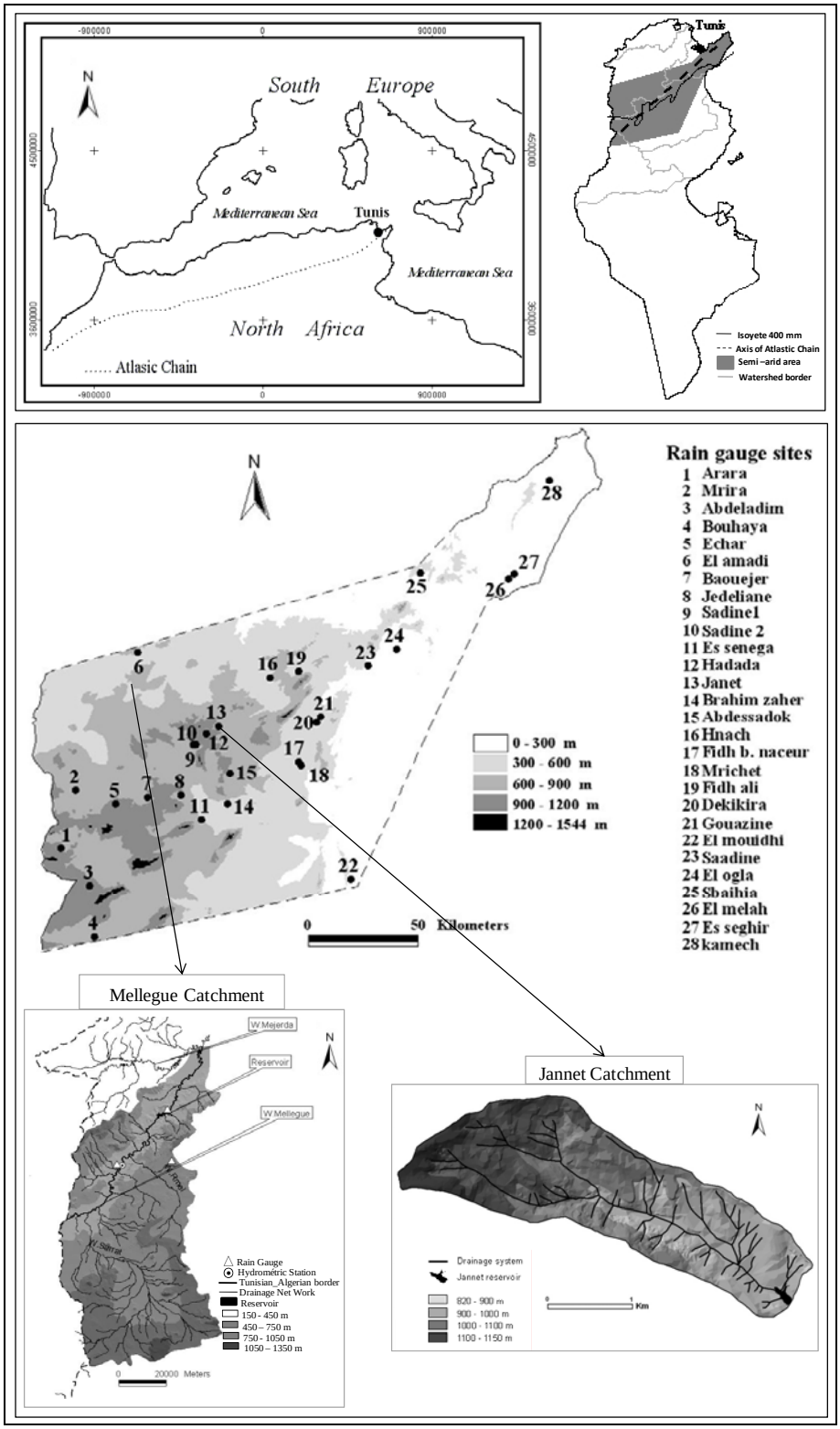

Figure 1. Study area and observation network.

3.5 Specifically studied sites

From the above described hydrological and sedimentological network, the Jannet catchment was chosen for the erosion modeling based on the fractal rainfall model. This catchment is located at the heart of the Dorsal area and appears representative of the semiarid area in terms of rainfall properties and soil loss rate. Similarly for the whole network, the Jannet rain gage is located on the dike of the reservoir itself. The 10-year old reservoir represented an average annual soil loss of 32.5 tonnes/ha/year since it was completely silted up by the end of the hydrological year 2002-2003.

From the extreme north-western Dorsal area, daily precipitation and yearly sediment load time series covering about 50 years were used to perform a trend analysis that is crucial for the prediction of soil loss. The two stations used were Mellegue (1947-2006) and K13 (1955 to 2005). The K13 station is situated a 25 km distance upstream from the Mellegue reservoir. The reliability of the data has previously been investigated by the DG/RE (Department of water resources) and DG/EGTH (Department of study and construction of big hydraulic infrastructure). Missing data correspond to about 3%.

4. Methodology

4.1 Progress of farming landscape degradation

Agriculture has always been important in semiarid Tunisia. Its rich grazing and fertile lands have been continuously exploited over time. However, farming on sloping lands and deforestation led, to serious water erosion. To analyze the degradation phenomena, historical records of erosion were investigated. Through this analysis the shaping of the Tunisian landscape through different agricultural systems could be determined (e.g., Kassab, 1979; Decret & Fantar, 1981; Ennabli, 1993). The historical analysis was compared to a macro-scale analysis of the present-day soil degradation over the Dorsal area. This analysis was performed through field visits and the recording of soil depth and properties, bed rock visibility, and general soil particle availability to erosion processes. These soil morphological changes were analyzed spatially using arc-view mapping tools. The latter made it possible to interpret the erosion potential in terms of the soil degradation cycle over the Dorsal area.

4.2 Precipitation and sedimentation trend analysis

The analyses of trend in precipitation, and sedimentation time series may explain natural and anthropogenic effects in prevailing climatic conditions. The current research used simple linear regression to detect the trend, followed by a Mann-Kendall test to determine the trend and its statistical significance at the 95% level (e.g., Salas, 1993). The Mann-Kendall test is a non-parametric test commonly used to assess the trend in the hydro-meteorological time series (Zhang & Zwier, 2004). The two methods are complementary. Accordingly, the linear regression fits a linear equation to data. However, the Mann-Kendall method does not assume a distribution of the data but requires non-seasonality and no autocorrelation for the data and the residual

series. The above procedure was used to analyze Mellegue time series data for the last 50 years (Fig.1). The latter data are, yearly sediment load, daily precipitation, and number of rainy days according to two thresholds related to erosion processes (3 & 12 mm) given by Kowal et al., (1976) and Wischmeier & Smith (1978).

4.3 Rainfall and erosion process assumptions

Recorded rainfall events for the analyzed 10-year period (1993-2003) were statistically described. A specific analysis was done regarding exceptional rainfall with an approximate return period of equal to or superior to 1 year. The focus of the analysis was on rainfall with maximum intensities for rainfall event duration of 1-60-min. For these durations, several thousands of rainfall events from the 28 experimental catchments were identified for erosion process analyses. Each exceptional rainfall event was characterized by its depth, duration, average, and maximum intensity. The investigated period was shown to be representative of longer periods in terms of maximum intensities corresponding sometimes to more than 100-year return period.

In order to compare siltation rates for the different reservoirs, the deposited sediment volume on the bottom of the reservoirs was converted into transported mass of soil using an average of 1.5 tonnes/m^3 as an apparent density (Ben Mammou, 1998). The amount of sediment is an observation used to estimate the average water erosion for the catchment since it is produced by all erosive sources (e.g., Toy *et al.*, 2002). The representativity of the studied period versus long-term siltation conditions was verified.

Exceptional rainfall events are responsible for most of the soil erosion taking place in the Mediterranean areas (e.g., Boix-Fayos *et al.*, 2007). They are characterized by short event durations (Ramos *et al.*, 1997; Cammeraat, 2002; EEA, 2002;) and specific return period intervals (Bull *et al.*, 1999; Hooke *et al.*, 2000; Coppus *et al.*, 2002; Garcia-Ruiz *et al.*, 2003). The following relationships are an attempt to summarize important soil erosion research concerning return period and soil erosion type for semiarid areas in general as well as semiarid Mediterranean regions in particular:

1) Interrill erosion: $1 \leq T < 5$
2) Rill erosion: $5 \leq T < 10$
3) Gully erosion: $10 \leq T$

where T is rainfall return period in years and the duration of rainfall is 1 to 60 min.

The maximum rainfall intensities were analyzed in order to determine the resulting deposited sediment amount during specific periods. They were also used to determine the erosion process's contribution to the soil loss rate for all catchments. The spatial distributions of erosive rainfall together with erosion processes were analyzed.

4.4 Regionalization of the rainfall data

4.4.1 Data treatment

The regionalization work was performed on normalized and standardized rainfall time series (1995-1998), (e.g., Uvo, 2003; Livezey, 2005). They concern 1-, 30-min, and 1 day rainfall scales. All numerical computations were made using standard routines of the Matlab software. In order to evaluate the representativity of the rather short observation period as compared to long-term rainfall conditions, a number of comparisons were made. It was revealed that the studied period does not display any tendencies of being unusual in terms of either short-term or long-term spatial rainfall distribution.
Multivariate techniques were used on the bases of covariance or correlation between stations to study rainfall on a regional basis (e.g., Van Regenmortel, 1995; Uvo & Berndtsson, 1996; Lana *et al*., 2004; Livezey, 2005). Spatial correlation functions were used to investigate the spatial dependence of fine time scale rainfall. The empirical orthogonal function (EOF) was used to delineate spatial and dynamic properties of rainfall as used by, e.g., Svensson, (1999), Andres *et al*. (2000), Todd *et al*. (2003), and Tosic (2004). After this, hierarchical clustering was performed for regionalization purposes.

4.4.2 Spatial correlation

The spatial correlation gives a general quantitative measure of the rainfall variability within an investigated area. It can be expressed in a general way as a function of distance (h) and direction (φ). The lag k (k = time lag) correlation rh,φ,k may be plotted with respect to either distance only, or both distance and direction. If the spatial correlation function is isotropic, the correlation–distance diagram contains all the necessary information. Otherwise, the correlation function is non-isotropic and the directional information needs to be included (Berndtsson, 1988; Uvo & Berndtsson, 1996). Rainfall gradients in mountainous areas as observed by Gilles *et al*. (2006) result in large anisotropy in spatial rainfall distribution. Similar properties may be expected for the Dorsal Mountain rainfall.

4.4.3 Empirical orthogonal function (EOF)

The EOF technique is similar to the principal component analysis (PCA; Hotelling, 1933; Preisendorfer, 1988). The EOF patterns are the eigenvectors (e), of a covariance matrix and, as such, they contain important information about the probability distribution of the variables themselves. These eigenmodes are characterized by several useful properties such as mutual orthogonality and efficient representation of the initial field. The eigenvalues (λ) are defined as the variance of the amplitude, and the rank of each eigenvector is ordered by the magnitude of their eigenvalues, so that the first mode represents the largest part of the total variance, the second mode is the second largest part of the total variance, and so on. The initial data set can be efficiently represented by the first k dominant modes of the analysis. The amplitude of the modes particularly characterizes the time evolution. The space vectors were found using the covariance matrix of the rainfall time series. In general, all modes that were statistically significant or

physically justifiable were retained (e.g., Andres *et al*., 2000; Gurgel & Ferreira, 2003; Singh, 2004; Tosic, 2004). To obtain physically meaningful and statistically stable EOF patterns, careful consideration of several factors is needed. These factors include the choice of dispersion matrices, sampling errors (e.g., North *et al*., 1982), and rotation of the EOF axes (Richman, 1986). Most commonly, the rotated EOFs are used in the regionalization procedure to resolve the domain dependence problem that is associated with non-rotated EOFs (e.g., Busuioc *et al*., 2001; Livezey, 2005). In this study, results of the EOF analysis were rotated through use of the varimax (orthogonal rotation) procedure (Richman, 1986).

4.4.4 Cluster analysis

The clustering was achieved by means of routines included in the Matlab software. This analysis was performed with two kinds of input, namely the retained EOF modes on the one hand and the correlation matrix on the other hand. The EOF and correlation data between all rain gages stations were compared with the specific similarity/dissimilarity, using selected linkage methods grouped into clusters. All analysed time scales were included in this comparison. A classification scheme using Euclidean distance for similarity measurement, together with several linkage techniques, was tested (Kalkstein *et al*., 1987). However, Ward's method (Ward, 1963) appeared to be the most appropriate linkage technique, which gave the most stable and consistent results. This method often produces the most consistent groups in climatic research (e.g., Unal *et al*., 2003). The number of groups was assessed graphically through a dendrogram and then interpreted on a map together with topography and atmospheric circulation.

4.5 Soil loss prediction using USLE model

The USLE model has been developed by Wischmeier & Smith (1960-1978) after 20 years of erosion analysis and of more than 10000 of yearly measurements of soil loss. Actually, for several decades, USLE has been the most frequently applied model in the assessment of the annual soil loss. Moreover, it has been widely applied at the watershed scale (Williams & Berndt, 1972; Griffin *et al*., 1988; Dickinson & Collins, 1998; Jain *et al*., 2001; Lee, 2004), the country scale (Gay *et al*., 2002), and at the continent scale (Van der Knijff *et al*., 2000). For the current research work, the USLE model is used for the Jannet catchment (Fig. 1) in order to determine its mean annual soil loss A (tonnes/ha/year). The latter value is calculated as a function of six erosion factors:

$$A = R * K * L * S * C * P \qquad (1)$$

where R is a rainfall erosivity factor (m.tonnes/ha.h), K (tonnes.ha/m.t) is a soil erodibility factor, L is a length factor (m), S is a slope factor (%), C is a crop management factor (unit-less), and P is a conservation practice factor (unit-less).

4.5.1 Rainfall erosivity factor (R)

The rainfall erosivity factor is based on the kinetic energy (KE) and the maximum intensity (I) in a 30-min period (Wischmeier & Smith, 1958; Lal, 1976). The kinetic energy of rainfall is the potential ability of rain to detach soil and to splash (Mihara, 1951; Free, 1960). It can be evaluated above 3 mm (Kowal *et al*., 1976) and remains constant for rainfall intensities exceeding 76 mm/h (Hudson, 1965). The erosivity factor is calculated for precipitation exceeding 12.7 mm, a rate proposed by Wischmeier & Smith (1978) as erosive rainfall. The rainfall erosivity factor of Jannet station was computed by analyzing observed and simulated rainfall for 15-min periods. This time period was found representative regarding the occurrence of erosion processes in the Tunisian semiarid Dorsal catchments (Jebari *et al.*, 2008). Each erosive event in the Jannet area was characterized by its depth, duration, average, and maximum intensity. Moreover, the observed and the generated erosivity factor (R) were calculated from the different erosive rainfall events. The erosivities were assumed constant and used as input to the USLE model for the entire Jannet catchment.

4.5.2 Soil erodibility factor (K)

The soil erodibility factor (K), represents the susceptibility of soil to erosion under standard plot conditions. Their values can be locally measured since they depend on soil properties. In fact, soils differ in their resistance to erosion, according to the texture, structure, soil moisture, roughness, and organic matter content. The Jannet K factors were defined by using the Tunisian soil map (DRES 1979, scale: 1/200000), Tunisian experiments conducted in semiarid areas, and tables given in literature (Wishmeier & Smith, 1978; Dangler *et al*., 1976; Cormary, 1963)

4.5.3 Topographic factor (LS)

The percent slope layer was determined from digital elevation model (DEM) developed for the Jannet area using the topographical map with a vertical resolution of 10 m (Tunisian National Topographical Service, Makthar map 1922, sheet 53, 1:50000). The contour lines were digitized, rastered and linearly interpolated. The slope length was assumed to be fixed as 15 m according to Ogawa *et al.* (1997). The topographical factor LS was determined by using the equation recommended by Morgan & Davidson (1991).

4.5.4 Crop management (C) and conservation practice (P) factors

The crop management factor C, is defined as the ratio of soil loss from land cropped under specified conditions to the corresponding clean-tilled continuous fallow on identical soil and slope under the same rainfall conditions (Wischmeier & Smith, 1978). Their values account for different types of cover in a catchment and lower value was given to the forest cover which indicates a better cover as compared to the other land cover types. The conservation practice factor (P) is the ratio of soil loss with a specific support practice to the corresponding loss with up and down slope cultivation. These factors depend on land/cover information of the catchment

area. For Jannet catchment, they were derived from the aerial photo interpretation (Agricultural and Water Resources Ministry, mission 1998; scale: 1/20000; photo: TU_17_28/ TU_18_28 TU_18_29/). The digitalization of these photos was used as a tool to guide the allocation of C and P factors for different land use classes. Their corresponding values are defined as recommended by the literature (Wischmeier, 1975; Hudson, 1985; Masson, 1971; Heusch, 1970, CTFT, 1979). The values and the spatial distribution of both factors were determined for the entire Jannet catchment.

4.6 Generation of the erosivity factor based on fractal rainfall model

The generation of rainfall erosivity factors concerns exclusively the Jannet catchment (Fig.1). This catchment is especially characterized by serious water erosion problems. The period corresponding to the disaggregation analysis involved two bathymetric measurements (12/10/1994-12/5/1998) and showed a soil loss rate of 27 tonnes/ha/yr. The used rainfall time series present data at 15 min resolution (1995-1998).

4.6.1 Scaling and multifractal analysis

The scale invariant behavior characterizes the temporal rainfall process (e.g., Hubert *et al*., 1993; Olsson *et al*., 1993; Menabde *et al*., 1997; Gunter *et al*., 2001). It implies that statistical properties of the process observed at different scales resolutions are governed by the same relationship. Literature offers power spectrum and probability distribution function as two ways to show the existence of scaling behavior. The spectral analysis (Fourier transform) is considered a powerful tool to assess the scaling invariance in rainfall time series (Malamud & Turcotte, 1999). It requires stationarity of the data and calculates the power spectrum E(f) as a function of the frequency to determine self affine scaling behavior (Hunt, 1951). If the time series spectrum fits a power law form according to (2), thus, the scaling regime characterizes the range of the defined power law. Spectral analysis is applied to a double logarithmic plot of E(f). Within the above mentioned range, fluctuations at all scales are related to each other by the same scale independent relationship. This indicates that multifractal behavior of the data may be assumed.

$$E(f) \ \alpha \ f^{-\beta} \qquad (2)$$

where, f is the frequency and β the spectral exponent deduced from the slope of a linear regression.

To investigate the multifractal temporal structure of the rainfall process is to study scaling of the probability distribution function (pdf) of the data (Schertzer & Lovejoy, 1987). If the tail of the probability distribution of the rainfall intensity obeys a power law form, then a hyperbolic intermittency characterizes the series (Fraedrich & Larnder, 1993). Moreover, to study the scaling properties of the data series, the scaling of the statistical moments of the rainfall intensity is examined (Over & Gupta, 1994). The scaling of the moments is described by the exponent function K(q).

4.6.2 Random cascade model

For rainfall, cascade models have been used to explore the temporal structure (e.g., Hubert *et al*., 1993; Olsson, 1995; Menabde *et al*., 1997). In this study, the model type was tested to investigate disaggregation possibilities that can capture properties of the high resolution rainfall data base (e.g., Olsson, 1998; Olsson & Berndtsson, 1998; Gunter *et al*., 2001; Molnar & Burlando, 2005). In a multiplicative cascade process the flux of water is transferred into successively smaller scales by means of multiplicative weights, and the generator specifies the statistical distribution of these weights (Davis *et al*., 1994). In a random cascade, the ensemble moments are shown to be a log-log linear function of the scale of resolution λ_n. The slope of this scaling relationship is a function (Mandelbrot, 1974; Kahane & Peyriere, 1976). The latter function contains important information about the distribution of the cascade generator w, and thus determines the scaling properties of rainfall.

4.6.3 Rainfall disaggregation procedure and erosivity factors computation

The current study focuses on the performance of the modified cascade disaggregation model developed by Olsson (1998). The model was modified in order to be applied on semiarid rainfall data (Olsson, 2008). For this, a Matlab code for disaggregation, parameters, and settings defined to fit the observed data was developed using the scale invariant properties of observed rainfall time series. The probability values P(0/1), P(1/0), and P(x/x) were estimated and the weights extracted (Fig.2). For this, the observed 15-min time series values were sequentially aggregated

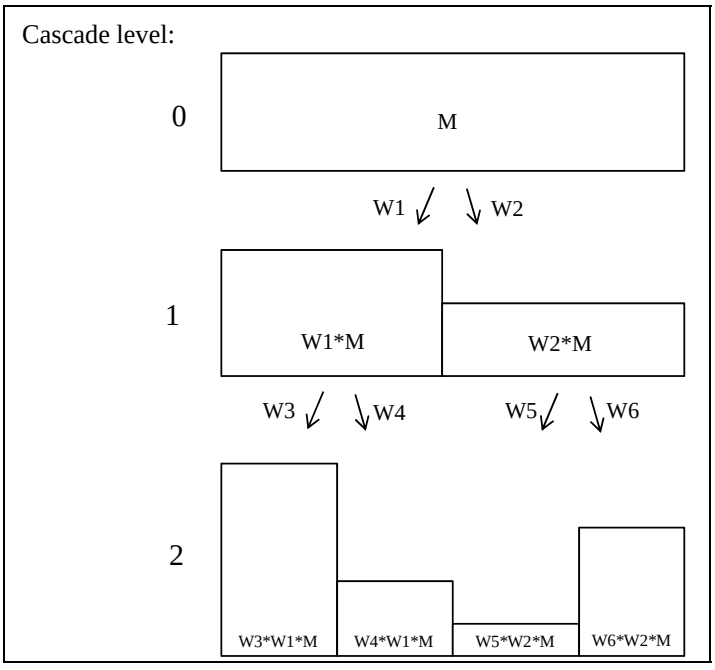

Figure 2. Cascade process principle in one dimension. Between two cascade levels, each interval is divided into two halves. The mass in each half is obtained by multiplying the total interval mass by a weight W_i. (After Olsson, 1998).

into daily values (96 by 96). The daily values were then disaggregated back to 15-min values using the cascade model (8 cascade steps) calibrated for the same series. The mean of the empirical probabilities in the range 15 min to 1 day was used as probability values. The disaggregation from 1 day resolution was reproduced 10 times. Consequently, ten 15-min time series were generated. The latter series were averaged and compared to the observed time series.

The generated rainfall erosivity factors for the Jannet catchment were then determined on the bases of the above approach that provided the simulated fine time scale rainfall data. The erosivity factors were defined by means of five specific rainfall intensities. In fact, the generated erosive events were defined according to durations equal to 30, 45, 60, 75, and 90 min. This procedure allowed a comparison of short erosive event characteristics and the most suitable duration limit for erosion in the Jannet catchment. Finally, a comparison was made between observed erosivity and results from the calculated erosivity values.

4.7 Generation of the thematic layers and estimation of soil loss rate

4.7.1 Mapping eroded areas according to the USLE/GIS approach

The GIS and aerial photo interpretation provided spatial input data for the Universal soil loss equation (USLE) model (literature review). Together, they allowed an analysis of soil erosion in a much more detailed way and offered an accurate, quick, and inexpensive tool for estimating erosion within a watershed (Millward & Mersey, 1999; Wang *et al*., 2003; Onyando *et al*., 2005; Panday *et al*., 2007). The GIS technique discretizes the studied area into small regular grid cells which are considered a basic operational unit for erosion analysis and assumed a closed plot (Renschler *et al*., 1997; Kinnell, 2001; Fistikoglu & Harmancioglu, 2002). Subsequently, annual average soil loss for the catchment is computed from the sum of the grid cells. For Jannet catchment, the preparation of various thematic maps as a spatial data base was performed to run the USLE model. In fact, the watershed boundary, land cover aerial photos, and soil map were digitized and/or transferred as GIS layers in ARC View 3.3. The 10 m resolution DEM (digital elevation model) of the watershed is performed by interpolating the digitized contour intervals. All data were spatially organized in the GIS with the same resolution and co-ordinate system. The Jannet watershed was subdivided into cells of a regular grid of 25*25 m and the erosivity factor was used as a uniform layer presenting a constant value. Finally, these steps were followed by an overlay procedure for five parameter layers (R, K, LS, C, and P). The USLE/GIS approach was calibrated for the Jannet catchment where the soil loss rate was validated by the sediment amount deposited downstream in the reservoir.

4.7.2 Spatial presentation of soil loss rates

The spatial distribution of the soil loss values were elaborated for the observed and the generated rainfall erosivity factors. The comparison between these different cases was undertaken over the entire Jannet catchment on the basis of three erosion cluster references. The first reference is related to Masson’s erosion classes. The latter classes were defined throughout experiments all over the Tunisian semiarid area. They have determined the average tolerable soil loss to be about

2.5, 5, and 10 tonnes/ha/year for thin, average, and thicker soils (Masson, 1972). The second cluster referred to Wischmeier & Smith (1978) work. The authors determined the soil loss tolerance to 12 tonnes/ha/year as "the maximum level of soil erosion that will permit a level of crop productivity to be sustained economically and indefinitely". The third cluster reference was inspired from the recent published research works which present different soil loss intervals (Toy *et al*., 2002; Irvem *et al*., 2007; Onyando *et al*., 2005; Pandey *et al*., 2007). These intervals reflect the impact of the main erosion processes in the Mediterranean semiarid areas. This allows us to summarize the soil loss classes into five intervals namely, 0-15, 15-30, 30-60, 60-100, and >100 tonnes/ha/year.

The rainfall erosivity factors, together with the three erosion clusters were used to present the spatial distribution of soil loss over the Jannet catchment. The comparison between observed and generated maps was made in terms of eroded area. This focused on the difference in erosivity and corresponding soil loss interval. The approach allowed displaying the most suitable assumption that reproduced the extension of eroded areas according to their observed degradation.

5. Major results and discussion

5.1 Long and short term soil loss characteristics in Tunisia

5.1.1 Water erosion consequences

Water erosion implies negative consequences for rural development. It leads to several changes which affect the catchment and its river bed. For more than 3000 years, Tunisia has witnessed agricultural practices that have been based on intensive exploitation rather than sustainable management of its natural resources. This has greatly affected the soil cover, led to excessive water erosion, and reduced the farmland productivity by about 4%/century. This has also led to great morphological changes of river beds and affected downstream infrastructure. The wadi Mejerda exemplifies the above. The large sediment load carried by the water effectively prevented navigation on the river since the beginning of the Christian period and gradually silted up the famous Utique harbor from the 5th century. Moreover, it led to an increase in the hydrological network from 13 to 65 km, and moved the river mouth about 15 km further out into the sea by extending the deltaic plain. During the last three centuries, upstream and downstream areas of the wadi Mejerda have displayed a greater frequency of increasing flood plains (Kassab, 1979). Collet (1953) stated that in the beginning of the last century, Mejerda used to change parts of its river bed location every 2 or 3 years. These changes led to the development of natural dikes that are two meters higher than the surrounding areas. Over the two last decades the over-flows have become increasingly threatening. The decreasing flow and larger flood plains have changed 20 and 30% in 15 years, respectively (Zahar *et al*., 2008). Also, nowadays floods occur with gradually smaller discharge (Lebdi *et al*., 2006; Zahar *et al*., 2008). Consequently, it is obvious that the sedimentological and hydrological characteristics of the wadi Mejerda catchment, have changed continuously over time as a result of the impact of water erosion processes. These changes need to be considered in any water and soil management work or design of construction that is to be undertaken.

5.1.2 The temporal cycle of degradation

Evaluation of the long-term progress of the Mejerda deltaic plain displays an increasing trend of the solid transport from the last 2nd millennium B.C to at least the 1st millennium A.C. The average sediment transport over one century, doubled between the 2nd and the 1st millennium B.C. In fact, the Mejerda deltaic plain grew from 6.6 to 12 km^2/century during this period. The maximum value was observed between 200 B.C. and 400 A.C. with 14.5 km^2/century. Then a decreasing tendency until about 1900 A.C. was noticed (Fig. 3). The intensive exploitation during the Roman era is well illustrated by the maximum amount of solid transport during this period. However, the period of decrease in solid transport does not indicate any effort of land conservation, but simply the probably of a decrease in the sediment available to be carried downstream (Fig.3). The water erosion follows a specific temporal cycle of degradation through the watershed. Knowledge of this cycle could be a valuable tool in the design of a management plan for the watershed damaged by water erosion.

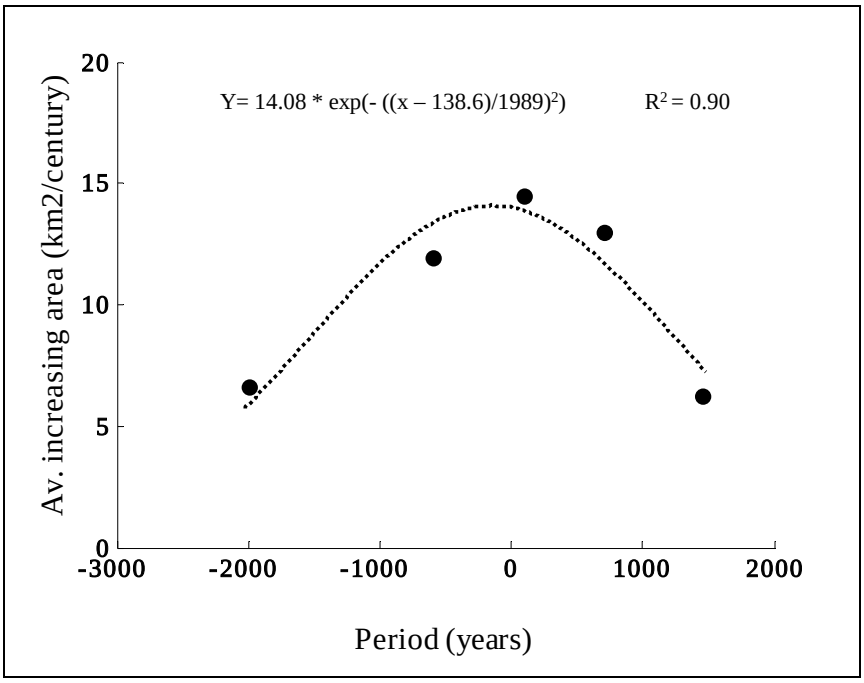

Figure 3. Trend for progress of the deltaic plain of Mejerda.

5.1.3 Erosive events and siltation trend

The trend for erosive rainfall events and sediment load were evaluated for the latest 50-year period. The number of erosive events appears in general to decrease (Fig. 4(a)). The decrease in depth concerns exclusively the rainiest months (October, November, December, January, February, and March). However, the decrease in erosive rainfall does not seem to reduce the water erosion process as seen from Fig. 4(b). Consequently, a dryer climate in semiarid Tunisia decreases the volume of water but still appears to continue to impoverish the soil cover.

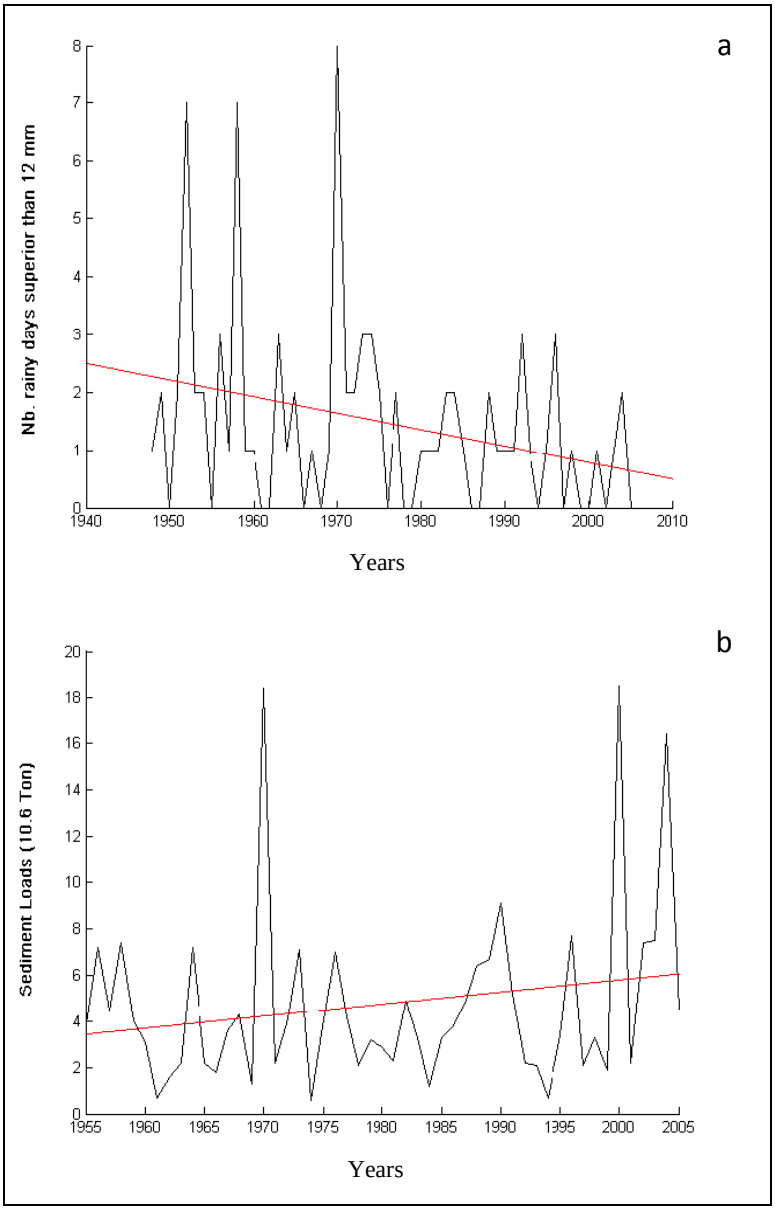

Figure 4. (a) Negative significant trend for daily rainfall larger than 12 mm at Mellegue station.
(b) Positive non-significant trend of sediment load at the K13 station.

5.2 Erosive events and water erosion risks

5.2.1 Exceptional 15-min rainfall intensities and erosion types

In semiarid Tunisia, exceptional rainfall events represent about 12% of the annual rainfall station events (about 10-20 events per year). Rainfall with less than a 10-year return period represents several hundred station events, while, rainfall with a larger than a 10-year return period corresponds to about 10-20 events. The 15-min duration exceptional rainfall intensities seem to

be more homogeneous compared to other duration rainfalls. Figure 5 shows the average temporal distribution for the 15-min duration exceptional rainfall events. The distribution appears somewhat skewed with a centre of gravity towards the first half of the events. The maximum intensity occurs after about 5-10 min. The standard deviation displays a large variation for the first minutes that then gradually decreases. This indicates that some rainfall events may have large intensities right from the start which can cause great raindrop impact initiating detachment of soil particles. The erosion types can be linked to the different return periods (cf. Methods). According to this, the risk of erosion may be related to specific exceptional 15-min intensities. This yields the following relationships:

1) Interrill erosion: $38 \leq I_{15} < 65$
2) Rill erosion: $65 \leq I_{15} < 75$
3) Gully erosion: $75 \leq I_{15}$

where I_{15} is the 15-min exceptional rainfall intensity in mm/h.
The above relationships should be regarded as a simplified way to estimate the occurrence of different erosion types depending on the maximum 15-min duration rainfall intensity. As such, the intensity boundaries should not be regarded as fixed but rather indicative. Together with additional information on a particular situation of catchments in the soil degradation cycle, the relationships can be used to estimate the risk for different types of erosion in the dorsal region. The results can be used to better manage erosion-prone catchments and also give input to erosion modeling.

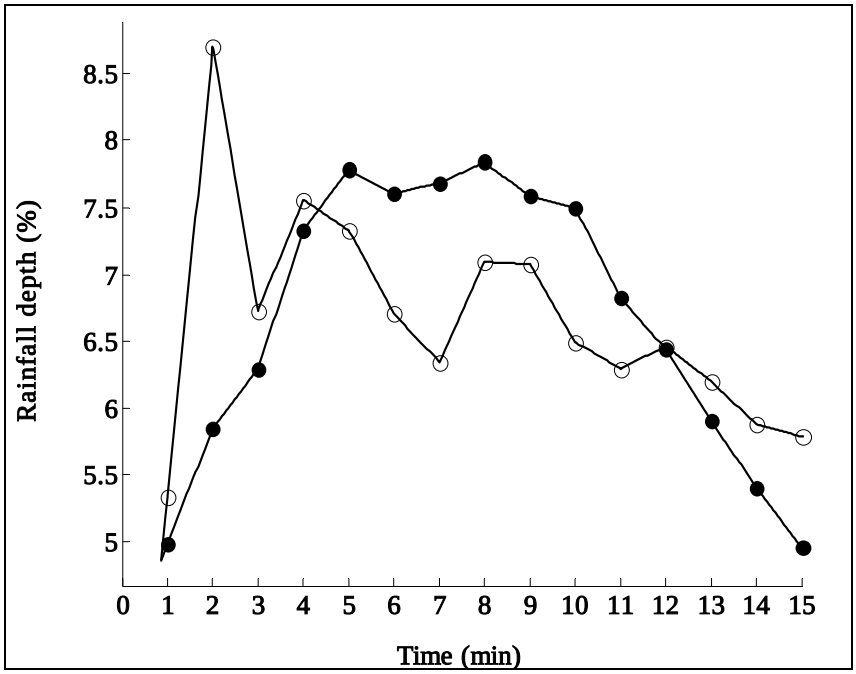

Figure 5. Temporal distribution of the identified 15-min duration exceptional rainfall events. Line connecting filled circles shows average properties and line connecting empty circles shows standard deviation (about 500 station events).

5.2.2 Exceptional rainfall characteristics and soil loss rates

According to the above erosion types, the studied area shows an average of about 60 erosive events per year. They are unevenly distributed depending on the recorded exceptional 15-min rainfall intensities. The average erosive event was 2.2 per station and year. The average erosive event duration was 105 min with a depth of 24.6 mm, a maximum intensity of 56 mm/h, and an average intensity of 23.5 mm/h. The total number of erosive events representing interrill, rill, and gully erosion was 342, 84, and 65, respectively. The number of rainfall events related to the different erosion types varied depending on the rainfall station. Interrill rainfall events, however, are present for all stations, while rill and gully rainfall events occurred occasionally depending on the year.
A large variation between the erosive rainfall events and the annual average soil loss rate was found. The total number of erosive rainfall events during the 10-year observation period varied from 8 to 29 depending on station. About 8 erosive events at Arara and Barhim Zaher corresponded to an average siltation of 14 and 25 tonnes/ha/year, while 17 erosive events at Abdeladim, Hadada, and Abdessadok gave a siltation of 3.2, 11.2, and 15.9 tonnes/ha/year, respectively. About 29 erosive events at Kamech and Ogla corresponded to 24.9 and 36.4 tonnes/ha/year, respectively. At stations like Jedeliane and Mrichet 20 erosive events gave the same siltation rate of 11.4 tonnes/ha/year. Similarly, for Dekikira and Mouidhi with 22 erosive events resulted in a soil loss equal to 21 tonnes/ha/year. Notably, Ogla displayed the maximum average soil loss rate among all the studied reservoirs. This station also had the largest number of erosive rainfall events per year (3.7).

Nine stations experienced interrill erosion only. The observed soil loss during these events was 62.8, 49.5, 30.8, and 72.1 tonnes/ha/year for Janet, Fidh Ali, Es-Senega, and Dekikira, respectively. This indicates how important the contribution of interrill erosion is for the reservoir siltation throughout the Tunisian Dorsal area in the absence of rill and gully erosion. For two occurring rill events the maximum soil loss rate reached 88.3 tonnes/ha/year at Ogla. However, a catchment that displays gully erosion is Saadine. This catchment has a maximum soil loss of 152.2 tonnes/ha/year.

Finally, a larger number of erosive events do not necessarily mean a larger soil erosion rate. We have to keep in mind that each catchment has its own specific response to the number and the type of erosive rainfall events.

5.2.3 Soil loss rates and soil degradation cycle

The mean annual soil loss for all catchments was 14.5 tonnes/ha/year, while the maximum soil loss rate was 44.2 tonnes/ha/year. Among the 28 catchments studied, about 30% display an annual soil loss of more than the permissible limits given in the literature (Wischmeier & Smith, 1978; Masson, 1972). At the end of the hydrological year 2006-2007, almost half of the reservoirs were already completely filled up with silt. This occurred for an average life span of about 14 years. Referring to the depreciation time mentioned in the literature, the Dorsal reservoir lifetime is well below average rates.

Predisposition and resistance of small catchments to soil loss depend on the ability of the catchments to deliver soil particles. This ability is conditioned by the soil degradation cycle for each specific catchment. The degradation cycle can be described by three different catchment erosion states according to Fig. 6:

- The first state (group I in Fig. 6) is related to low soil loss rate and concerns catchments that are protected against rainfall erosivity by several parameters such as erosion and soil restoration management practices.

- The second state corresponds to catchments that are more active in the degradation process since they display deeper soil layers and a soft original bed rock (group II in Fig. 6). The catchments yield soil particles in a generous way and soil loss rate is large. Actually, most of the catchments belong to this second state characterized by badlands.

- The third state of the cycle includes catchments that are in their last stage of degradation (group III in Fig. 6). The majority of available soil particles have already been lost to downstream areas. Catchments display modest soil loss rates where the original hard bedrock is uncovered. This last state is displayed by a few catchments to differing degrees.

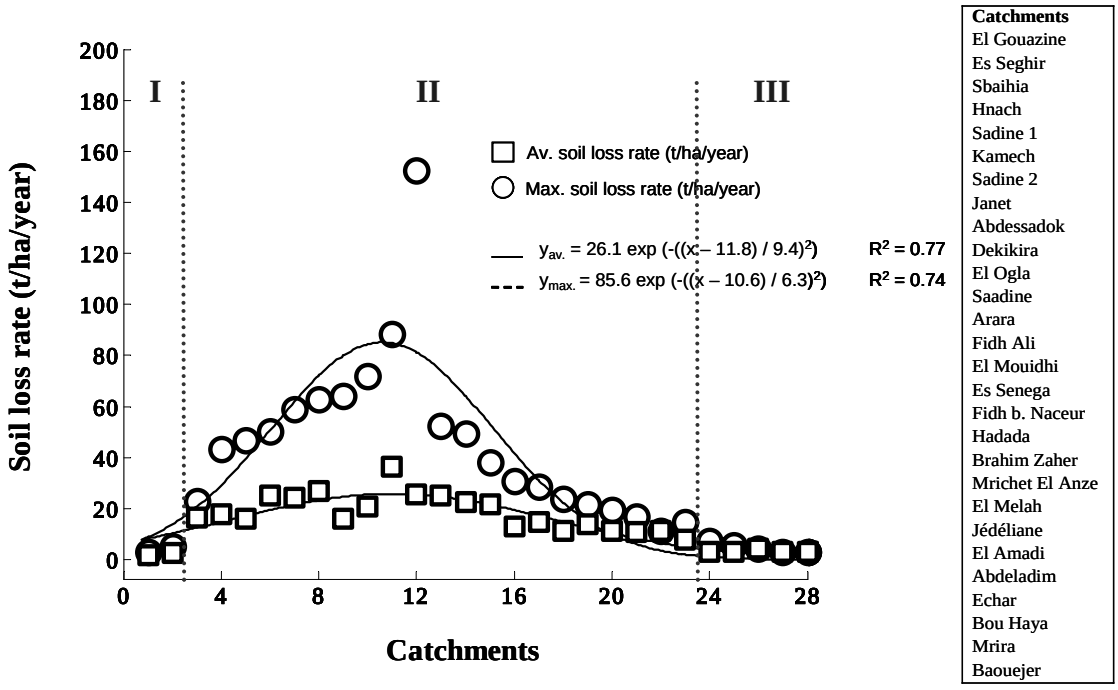

Figure 6. Soil degradation cycles (I, II, and III) depending on average and maximum soil loss rates. Stations are arranged according to their degradation levels as determined during field visits (according to list to the right).

5.2.4 Spatial erosive rainfall and soil erosion

By using the above relationship between erosive rainfall intensity and soil erosion type, it is possible to delineate spatial properties of erosive rainfall and soil erosion. Figure 7(a) shows the spatial distribution of erosive rainfall over the Dorsal area estimated from the maximum 15-min duration rainfall (1993-2003). The Dorsal area appears to be divided into an eastern and a western part according to a specific centre localized on the main Dorsal axis along the Saadine-Ogla stations (300 m altitude). A comparison between the eastern and the western parts in terms of rainfall characteristics then also translates into spatial erosion properties. For rainfall, the eastern part displays exceptional events that are 25% more recurrent, 40% more intense, 45% longer in duration, and 28% more important in amount as compared to conditions in the western part. One of the reasons for this is that the eastern part presents no continuous major physical barrier for rainfall. Catchment areas here are smaller (30%) presenting shorter concentration times (42%). For erosion, 30% and 40% greater average and maximum soil loss are found here. The eastern area also presents an advanced soil degradation level as compared to the western area.

Figure 7(b,c,d) shows the distribution of soil erosion risk expressed as the average number of erosive events per year based on the spatial pattern for maximum 15-min rainfall intensity (I_{15}; Fig. 7(a)). Figure 7(e,f) shows the spatial distribution of observed soil erosion loss in tonnes/ha/year calculated from the bathymetric data. The similarity between Fig. 7(b,c,d) and 7(a) is not perfect, at least not at the detailed level. However, the general conformity at a larger scale is quite striking. All estimated erosion types reach their maximum near the north-eastern or north-western parts of the Dorsal. This is the same general pattern as for the observed erosion. The interrill risk map displays the largest values for the north-eastern parts of the Dorsal, whereas the rill and the gully erosion risks appear to be greatest in the north-west and the central north-eastern areas.

As seen from Fig. 7(e,f), the observed spatial average and maximum erosion is similar over the Dorsal area. The western part of the Dorsal displays the lowest erosion rates while the mid-eastern parts have the highest rates. Consequently, there is a clear general trend for observed erosion along the Dorsal axis (broken line in Fig. 7). The trend is increasing towards the mid-eastern Dorsal. The maximum erosion is observed for the Ogla-Saadine stations. These stations present the most important difference in height (735 m) and the maximum observed soil loss for the whole network.

Some of the discrepancy between estimated and observed erosion rates depends on differences in the erosion cycle for the observed catchments. If all catchments had had similar soil surfaces, the observed erosion would probably have been closer to the estimated one (from extreme rainfall).

From a large-scale point of view the erosive processes and the availability of potential erosive material can be viewed as a slowly moving “soil degradation front”. This soil degradation front coincides with the 300 m altitude at the level of the Ogla-Saadine transverse. It is continuously progressing westward from lower to higher altitude following the main Dorsal axis. Consequently, the situation of the catchments in the soil degradation cycle clearly displays the soil particle delivery potential for the dorsal area. This then determines the progress of the soil degradation front as influenced by extreme rainfall.

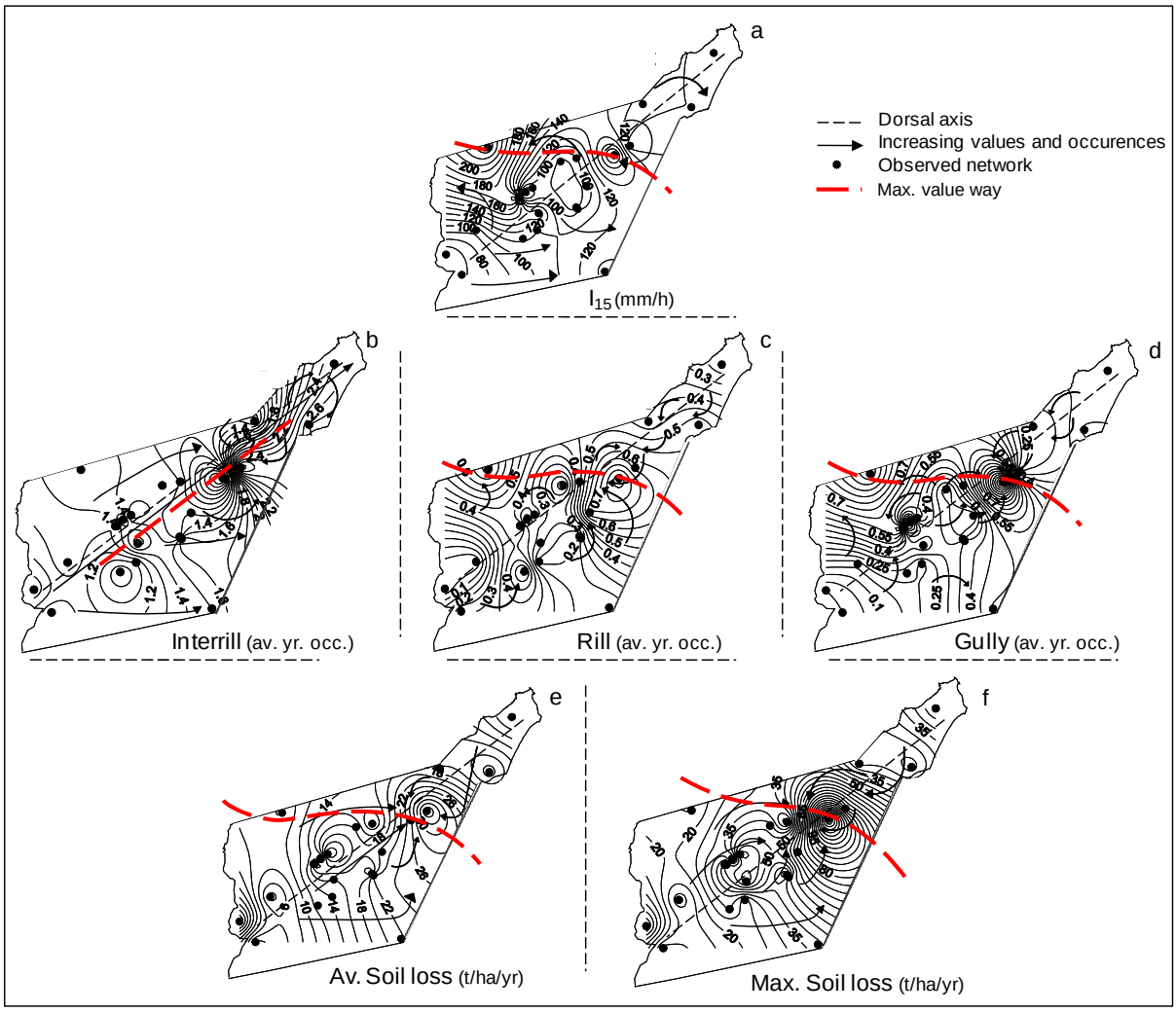

Figure 7. a) Spatial distribution of maximum 15-min duration rainfall intensity (1993-2003; Jebari *et al.*, 2008), b) c) d) estimated number of annual events for different erosion types namely interrill, rill, and gully erosion, and e) f) observed average and the maximum soil loss in tonnes/ha/year.

The above findings are crucial for determining the most urgent areas where soil erosion control needs to be developed. For this purpose, factors like the main erosion type, exposure to extreme rainfall, degradation front direction, and the most vulnerable catchments within the degradation cycle need to be taken into account. For the Dorsal area it is clear that the 300 m altitude cross-section is an erosion front that needs to be closely monitored and further investigated. Similarly, areas surrounding the Dorsal ridge and areas at mid-slope locations must also be monitored. All these areas need urgent management to halt severe erosion.

5.3 Rainfall disaggregation

5.3.1 Characteristics of the spatial correlation

The spatial correlation for 25 rainfall stations and a 4-year observation period is shown to be typical non-isotropic. It increases with time scale and varies according to topography and local meteorological settings. The decorrelation distances are between 2 and 15 km for 1- to 30-min rainfall, respectively. Meanwhile it is about 70 km for the daily time step. Shorter convective rainfall appears to be less affected by topography as compared to daily accumulation which corresponds to the frontal rainfall. These two kinds of rainfall may in general illustrate the localized rill-gully event areas and the generalized interrill event region, respectively.

5.3.2 Pattern distribution modes

In the empirical orthogonal function (EOF) analysis six modes were kept due to their statistical significance and, more importantly, their physical explanation (Yarnal, 1984; Kozuchowski et al., 1992; Chen, 2000; Busuioc et al., 2001). They display quite good interpretation in terms of the topography and atmospheric circulation patterns known in Tunisia. In general, it seems as if

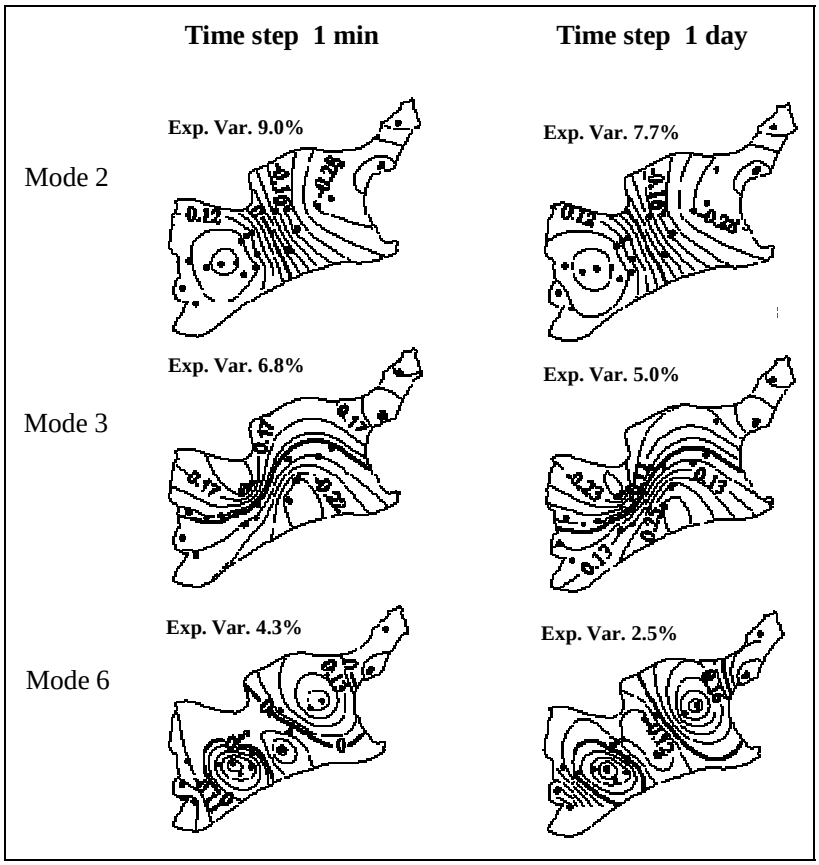

Figure 8. Comparison of three spatial modes for 1-min and daily rainfall.

the finer the time scale of the rainfall, the more noise and small-scale variation are at hand in the data. Thus, fine time-scale rainfall has a low explained variance. This may indicate the complexity of fine time-scale rainfall and that many different physical variables are responsible for its variation.

The spatial presentation of the daily and the short time step modes are quiet similar. They are closely related to the 600 m altitude, the Dorsal crest axis and the summit locations. All these display relationships according to the synoptic large scale processes and the small local scale meteorological phenomena. Thus, they display a spatial dependence regarding areas with predominant convective and frontal rainfall. Moreover, the comparison of the mode patterns and the spatial distribution of exceptional events reveals many similarities. The area for the maximum 15-min rainfall intensities can be easily recognized. Consequently, the EOF analysis defines the most important areas related to the exceptional rainfall intensities which are crucial for water erosion processes all over the Dorsal area.

5.3.3 Hierarchical cluster subgroups

The cluster analysis performed using the EOF modes shows two rather clear sub-groups (Fig. 9(a)). The general pattern related to the minute time scale, is a first subgroup covering the entire Dorsal area surrounding a second subgroup located in the central part. Similarly, the daily scale rainfall displays subgroup 2 covering the central southern slope of the Dorsal area with wider extension eastward. The clustering using the correlation matrix as input displays similar clusters as mentioned above. The subgroup 2 is delimited as seen in Fig. 9(c) and (d) according to the 600 m altitude for the 1-min time scale and extend eastward to reach the 300 m altitude for the daily time step.

The results from the EOF and correlation display similar results in terms of regionalization which indicate robust results. However, the EOF results also indicate a better relation to the maximum rainfall intensity areas (Fig. 7(a)). And the correlation results appear more related to the isolines of the most recurrent exceptional events (Fig. 7(b,c,d)) indicating erosion risks.

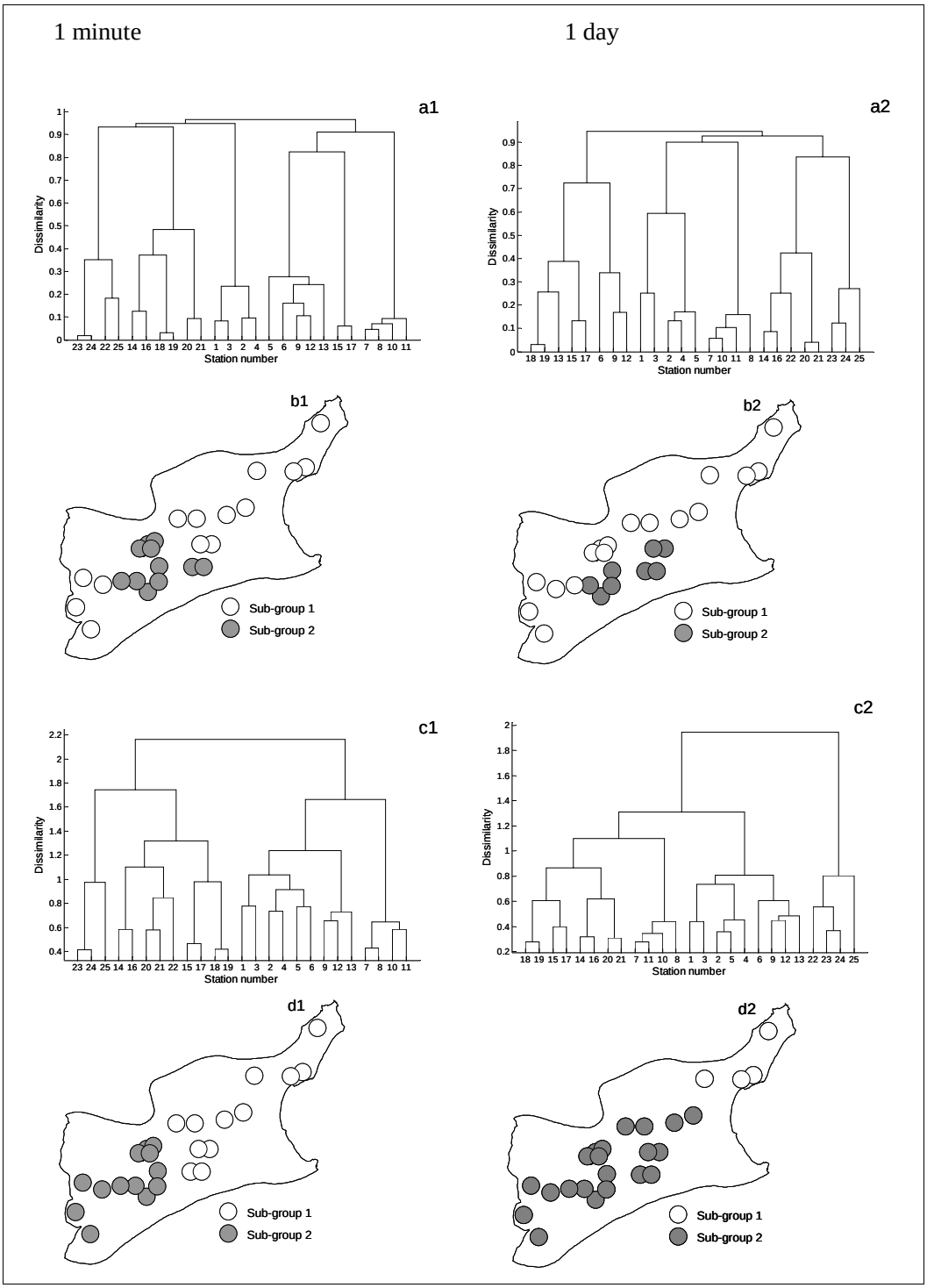

Figure 9. (a) Cluster dendrogram (6 modes); (b) regionalization (6 modes); (c) cluster dendrogram (correlation matrix); and (d) regionalization (correlation matrix): for 1-min time scales (left) and 1-day time scales (right).

5.4 Fractal rainfall characteristics and water erosion modeling

5.4.1 Fractal properties and temporal scaling behavior of erosive rainfall

A random cascade model according to the Methodology chapter was used to generate rainfall time series. The generation of 15-min rainfall time series, using the cascade model appears to reproduce the observed time series in a satisfactory way. High intensities, e.g., seem well represented. Also, the number of 3 and 12 mm rainfalls is almost the same. However, the model in general overestimated the rainfall depth event and underestimated the rainfall duration, thus inducing larger average and maximum intensities.

In order to test the applicability of the fractal disaggregation model the fractal and scaling properties of the rainfall time series were tested using different methods. The autocorrelation for the generated time series was in general larger as compared to the original series, especially for short time lags. Between 1 and 4 time lags the significant autocorrelation of the observed time series decreased strongly, while the generated one takes about 25 more time steps to reach the same level of autocorrelation. It is observed that a significant correlation exists up to about 40 min for the observed data and about 1000 min for the generated one. The autocorrelation reaches zero at 600 and 1500 min, respectively. This delay in the autocorrelation function could be due to a temporal persistence that may be related to the fractal properties of the time series (Rodriguez-Iturbe *et al*., 1989).

The power law shapes for the observed and the generated time series, respectively, were shown to exist over a range of frequencies of $f^{0.62}$ and $f^{0.91}$. The scaling regime was estimated to be from 15 min up to 375 min for the observed data and from 15 min up to 225 min for the generated time series. The power spectrum for the generated time series was in general larger than for the original one. However, looking at Fig. 10(a,b)) it is seen that differences are mainly for frequencies corresponding to longer time scales than one day. The upper limit of the scaling regime appears to be very different as compared to some previous studies where they were found to be several days (Ladoy, 1993; Olsson, 1995, 1998; Svensson *et a*l., 1996). However, these studies used rainfall data from mainly humid regions. A reason for the different upper limit of the scaling region may be due to the different climate and that individual meso-scale storms often characterize the semiarid areas.

The scaling behavior of the observed and the generated time series was confirmed by the statistical moments of various orders. Accordingly it appears that the model preserves this specific characteristic. It was shown that this behavior is respected from 260 to 360 min for the observed series and from 140 to 260 min for the generated one. The scaling regime consequently concerns a time range of about 100 min for both series. This time range seems to fit the erosive event durations very well. The latter coincides with the time structure of the most crucial erosion process that is responsible for the most important soil loss. In fact, after a few hours of rainfall, it is clear that the soil is water-soaked and all cohesion between surface soil particles has been lost. Consequently, after this time period huge soil losses are often observed. Consequently, this may show an important link between the temporal scaling structure of erosive rainfall events in semiarid areas and the soil loss process.

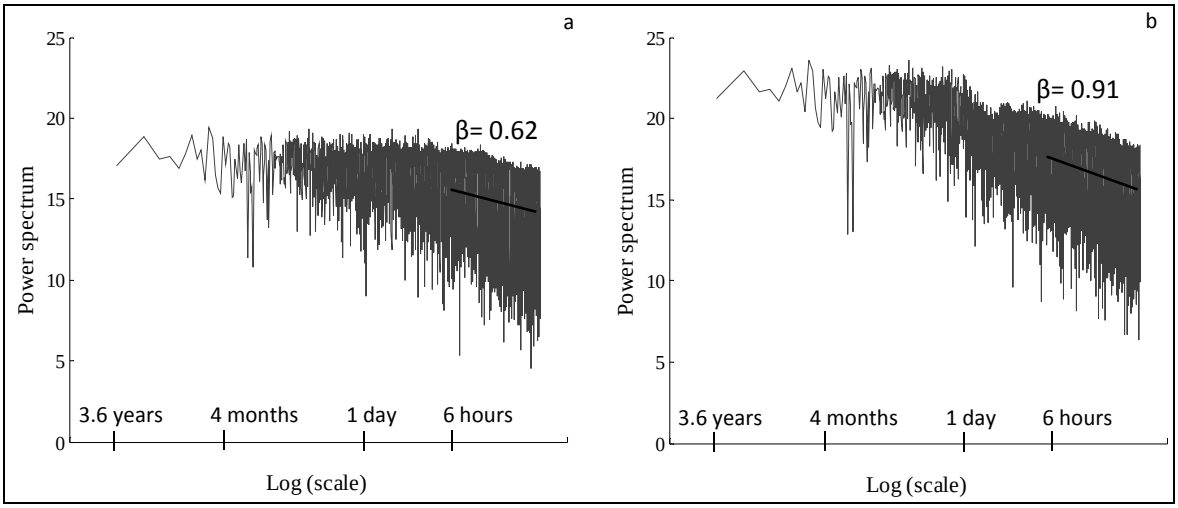

Figure 10. (a) Spectral density function for the observed time series. (b) Spectral density function for the generated time series. The straight lines have been fitted by regression respecting the significance for Fourier power spectrum.

5.4.2 Performance of Olsson's disaggregation model in predicting rainfall erosivity

Preliminary results comparing observed and generated series for the erosivity factor and spatial distribution of soil loss resulted in an overestimation of 30%. Observed and generated erosion rates from the Jannet catchment, displayed 27.0 and 37.4 tonnes/ha/year, respectively. However, the use of partially generated series based on the event duration limit concept, provided better results. The disaggregation model performance curve shows that generated erosivities are increasing when the duration limit is decreasing (Fig. 11). The cause for this is revealed when comparing observed and generated short duration erosive events. Even though this category of events is rare, it is highly over-estimated by the disaggregation model (65% over-estimation). According to this and the model performance curve, it can be seen that the best results were achieved by using a duration limit of 50 min (Fig. 11). However, available time step from the model generation limited data to the 45-min duration was the best alternative for generating erosivity factors and average soil loss rate. These were 83.5 m tonnes/ha.h and 28.5 tonnes/ha/year (Table 1). Compared to observed values, these represent a small overestimation of less than about 5%.

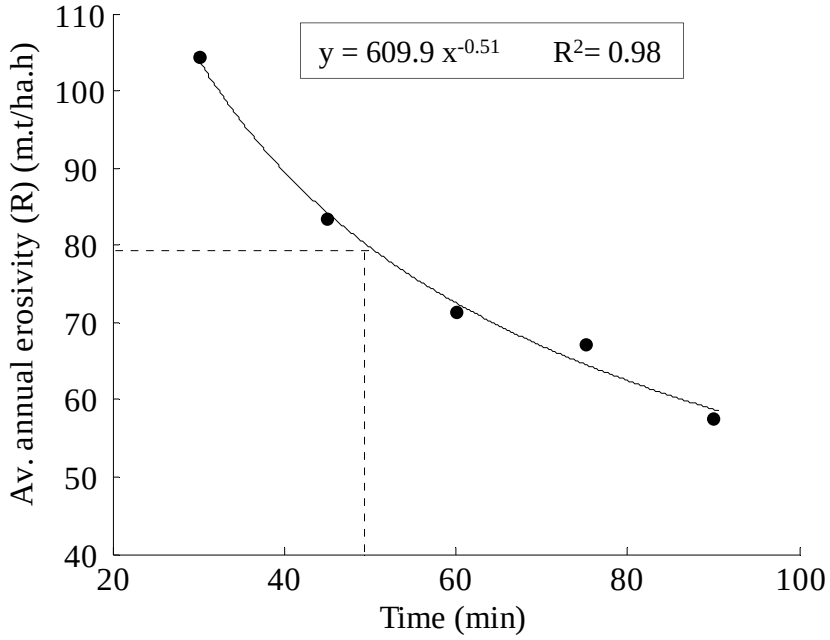

Figure 11. Generated erosivity factors for different duration limits.

Table 1. Comparison between observed and partially generated data series ($Gen._{Part}$) that take into account only events longer than 45 min.

Erosive event characteristics	Obs. data	Part. gen. data	Perfor. (%) (Obs-Part. gen.)
No. of events	23	17.5	-23.9
Tot. depth (mm)	420.1	355.2	-15.4
Av. depth /ev. (mm)	18.3±7.9	21.5±9.5	+17.4
Av. duration/ev. (min)	267±217	235±149	-12.0
Av. I_{max15} /ev. (mm/h)	18.8±14.5	22.5±16.4	+19.6
Av. Int./ev. (mm/h)	9.3±11.5	8.5±7.3	-8.6
Av. KE/ev. (MJ/ha.mm)	359±199	432±236	+16.8
Av. R/ev. (m.tonnes/ha.h)	11.4±14.4	18.0 ±24.6	+36.6
Max. I_{max15} (mm/h)	52.0	67.2	+22.6
Max. KE (MJ/ha.mm)	1198	1087	-10.2
Max. R (m.tonnes/ha.h)	66.4	96.0	+30.8
Annual KE (MJ/ha.mm)	2361	2012	-17.3
Annual R (m.tonnes/ha.h)	79.9	83.5	+4.3

5.4.3 Comparison between observed and simulated spatial soil loss distribution

Three different methods were used to calculate annual soil loss distributions from the simulated data, namely; Masson´s erosion classes, Wischmeier-Smith's erosion classes, and the most used recent erosion classes. The results from these three methods were compared to the observed erosion. The results appear promising. For the erosion class less than 30 tonnes/ha/year, the results display a total overlay map (Fig.12). However, for the erosion intervals ranging from 30-60, 60-100, and above 100 tonnes/ha/year, the recent erosion classes display 71.0 and 41.7 ha which are under-estimated and 119.6 ha which are over-estimated.

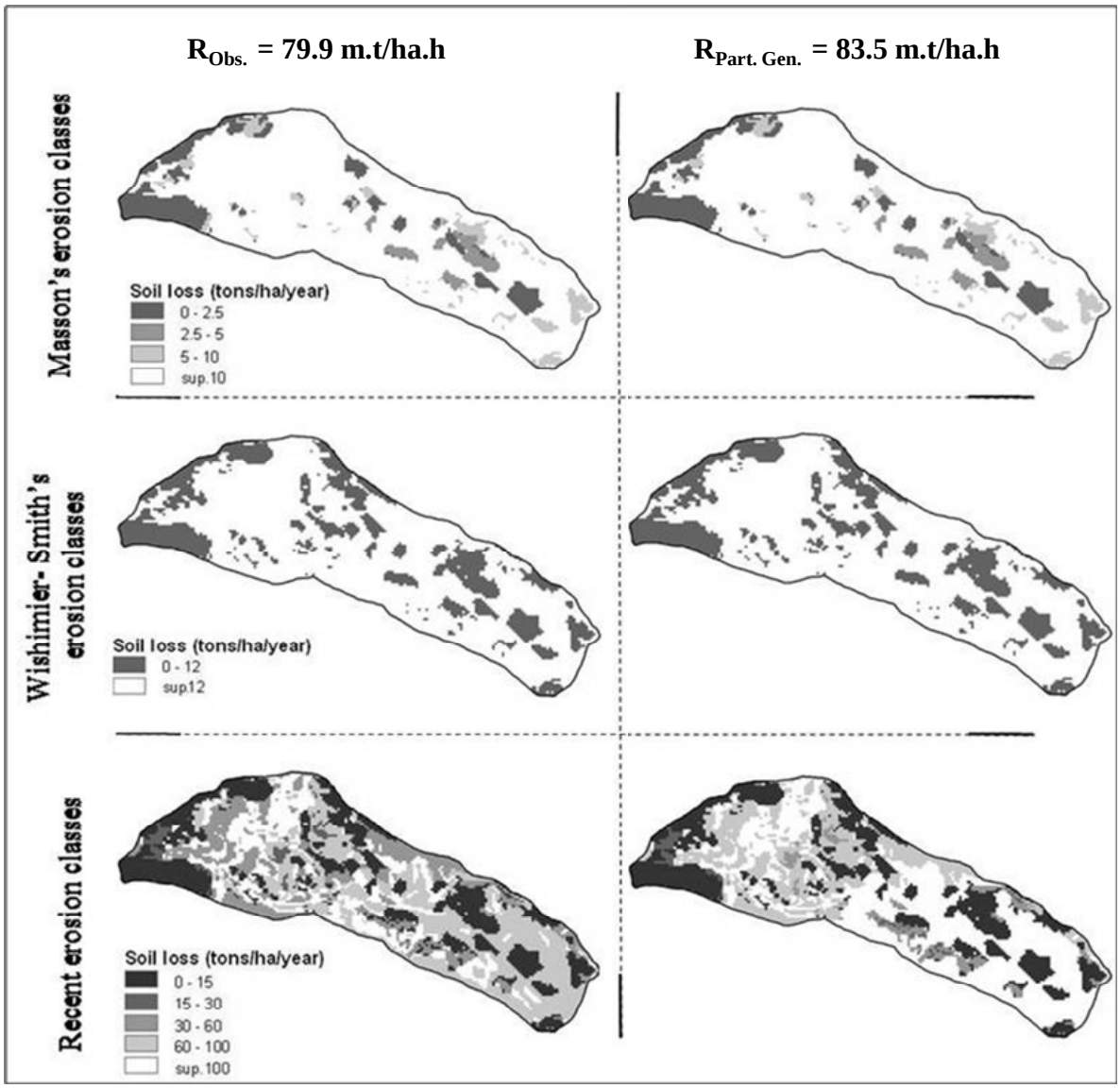

Figure 12. Comparison between spatial distribution of erosion using observed and generated soil loss in the Jannet watershed. This was performed by means of three erosion calculation methods, namely: a) Masson's erosion classes, b) Wischmeier-Smith's erosion classes, and c) recent erosion classes.

Usually, over-estimated or under-estimated areas are compensated for, through the different soil loss intervals. However, over-estimated areas characterize the highest soil loss level (>100 tonnes/ha/year) but under-estimated areas involve low soil loss intervals. The spatial distribution of the extreme soil loss values were exactly the same for the two used erosivity factors.

While comparing observations with simulations from the recent erosion classes, we noticed that observation results for 60-100 tonnes/ha/year are uniformly distributed over the entire catchment. On the other hand, for the same category of soil loss rate, the generated maps show mainly upstream areas involved in this soil loss. Also, the map for the observed soil loss rate that was superior to 100 tonnes/ha/year displays active areas situated rather evenly over the catchment while the map for generated soil loss displays active areas mainly downstream in the catchment.

6. Conclusions and further studies

The active water erosion process observed all over the Tunisian semiarid areas is a serious problem that causes degradation of fertile catchments. The latter are badly affected by erosive events, which lead to sedimentological and hydrological changes. This process worsens the situation of the catchments and makes water and soil conservation projects relatively inefficient. Consequently, more efficient methods to predict soil loss rates are urgently needed especially for ungaged catchments. In line with this, this thesis aims at developing improved techniques for rainfall erosivity prediction using rainfall data that are normally too coarse in time to use for this purpose.

Soil loss rate based on siltation measurements in reservoirs in the Dorsal area showed that the average soil loss is about 14.5 tonnes/ha/year. This soil loss results from about 12% of the rainfall events which display exceptional 15-min duration intensities. The latter define the different erosion types and generate meaningful maps of erosion risks at large scales. The results show that soil particles are provided from two main areas. The first area corresponds to the vulnerable catchments, located all over the soil “degradation cycle”. The second area corresponds to the “degradation front” currently located at about 300 m altitude.

A random cascade rainfall model was applied to disaggregate daily rainfall time series into 15-min time steps. The model was shown to reproduce the scaling region of observed data. It also displayed a multifractal behavior for the duration of 100 min. The generated series were used as input into a soil loss model. The estimation of siltation at the downstream reservoir at Jannet catchment provided reliable results. Only when erosive events beyond 45 min were considered, did the overestimation of the erosivity factor and the soil loss rate become 5% higher than observations. The corresponding spatial soil loss distribution performed in Masson’s and Wischmeier-Smith’s erosion classes was shown to mimic observations. For the recent erosion classes there were slight differences between observations and simulations. Finally, for the Jannet catchment, the use of the Olsson model and partially-generated series provided a good estimation of most important spatial soil loss areas.

The above results seem to be very promising. Results indicate that a scaling-based approach for rainfall can be used in soil loss applications. In order to better calibrate the Olsson model, several other analyses for larger databases relative to the semiarid areas need to be performed in the future. Moreover, the presented methodology for soil loss estimation should be applied to other small experimental catchments in order to strengthen the results and allow tests in other areas where erosion is a serious problem. The above results can be helpful for planning and management to develop mitigation strategies for soil erosion at large scale.

References

Andrés, M., Tomás, C., & De Pablo, F. (2000). Spatial patterns of the daily non-convective rainfall in Castilla y León (Spain). *Int. J. Climatol.* **20**, 1207–1224.

Bartsch, K.P., Mietgroet, H.V., Boettinger, J., & Dobrowolski, J.P. (2002). Using empirical erosion models and GIS to determine erosion at Camp William, Utah. *J. Soil Water Cons.* **57**(1), 29–37

Ben Mammou, A. (1998). Barrages Nebeur, Sidi Salem, Sidi Saad et Sidi Bou Baker. Quantification, étude sédimentologique et géotechnique des sédiments piégés. Apport des images satellitaires. Thèse de Doctorats Es-Sciences géologiques, présentée à l'Université de Tunis II, Faculté des Sciences de Tunis.

Berndtsson, R. (1988). Spatial hydrological processes in a water resources planning perspective. An investigation of rainfall and infiltration in Tunisia. PhD Thesis, Rep. 1009, Dept of Water Resour. Engng, Lund Univ, 1–315.

Boix-Fayos, C., Martinez-Mena, M., Calvo-Cases, A., Arnau-Rosalén, E., Albaladejo, J., & Castillo, V. (2007). Causes and underlying processes of measurement variability in field erosion plots in Mediterranean conditions. *Earth Surf. Process. Landforms* **32**, 85–101.

Bouzaiane, S., & Lafforgue, A. (1986). Monographie hydrologique des oueds Zeroud et Merguellil. Publication commune de la Direction Générale des Ressources en Eau et de l'Institut Français de Recherche Scientifique pour le développement en Coopération. République Tunisienne, Ministère de l'Agriculture.

Bull, L.J., Kirkby, M.J., Shannon, J., & Hooke, J.M. (1999). The impact of rainstorms on floods in ephemeral channels in southeast Spain. *Catena* **38**, 191–209.

Busuioc, A., Chen, D., & Hellström, C. (2001). Temporal and spatial variability of precipitation in Sweden and its link with the large-scale atmospheric circulation. *Tellus* **53**A, 348–367.

Cammeraat, L.H. (2002). A review of two strongly contrasting geomorphological systems within the context of scale. *Earth Surf. Process. Landforms* **27**, 1201–1222.

Camus, H., Guiguen, N., & Ben Younes, M. (1995). Note sur l'envasement des lacs collinaires en zone semi-aride Tunisienne. Rapport publié par la Direction de la Conservation des Eaux et du Sol (D/CES) & l'Institut de Recherche pour le Développement en Coopération (ORSTOM).

Cerdan, O., Le Bissonnais, Y., Govers G., Lecomte, V., Van Oost, K, Couturier, A., King, C., & Dubreuil, N. (2004). Scale effect on runoff from experimental plots to catchments in agricultural areas in Normandy. *J. Hydrol.* **299**, 4–14.

Chen, D. (2000). A synoptic climatology based on the Lamb classification for Sweden and its application to winter temperature study. *Int. J. Climatol*. **20**, 1067–1076.

Claude, J., Francillon, G., & Loyer, J.Y. (1977). Les alluvions déposées par l'oued Medjerda lors de la crue exceptionnelle de mars 1973. *Cahier ORSTOM, Sér. Hydrol*. **14**, 37–109.

Collet, C. (1953). Les moyens mis en œuvres en Tunisie pour l'étude des crues de la Medjerda. *La Houille blanche*, 395–408.

Collinet , J., & Jebari S. (2000). Étude expérimentale du ruissellement et de l'érosion sur les terres agricoles de Siliana. Rapport publié par l'INRGREF & l'IRD.

Colombani, J. (1988). Autopsie d'un hyétogramme. In: Troisièmes journées hydrologiques de l'ORSTOM (Montpellier, 23–24), 28–37. Publication du laboratoire d'hydrologie de Montpellier, France.

Coppus, R., & Imeson, AC. (2002). Extreme events controlling erosion and sediment transport in a semi-arid sub-andean valley. *Earth Surf. Process. Landforms* **27**, 1365–1375.

Cudennec, C., Leduc, C., & Koutsoyiannis, D. (2007). Dry-land hydrology in Mediterranean regions : A review. *Hydrol. Sci. J.* **52**, 1077- 1087.

Cudennec, C., Slimani, M. & Le Goulven, P. (2005). Accounting for sparsely observed rainfall space–time variability in a rainfall–runoff model of a semiarid Tunisian basin. *Hydrol. Sci. J.* **50**, 617–630.

Davids, A., Marshak, A., Wiscombe, W., & Cahalan, R. (1994). Multifractal characterizations of non-stationarity and intermittency in geophysical fields: Observed, retrieved or simulated. J.Geophys. Rs, 99, 8055–8072.

DCES/IRD. (1994-2002). Annuaires hydrologiques des lacs collinaires. Rapports publiés par la Direction Générale de l'Aménagement et de la Conservation des Terres Agricoles & l'Institut de Recherche pour le Développement. République Tunisienne.

D/CES et ORSTOM. (1998). L'acquisition numérique et autonome de données hydro-pluviométriques. L'expérience d'un réseau pilote Tunisien. Rapport édité par la Direction de Conservation des Eaux et du Sol ainsi que l'Institut Français de Recherche Scientifique pour le développement en Coopération, 01–33.

Deidda, R. (2000). Rainfall downscaling in a space time multifractal framework. *Wat. Resou. Res.* **36**, 1779–1794.

Decret, F., & Fantar, M. (1981). L'Afrique du nord dans l'antiquité. Histoire et civilisation des origines au V^{e} siècle. Edition Payot, Paris.

De Vente, J., Poesen, J., & Verstraeten, G. (2005). The application of semi-quantitative methods and reservoir sedimentation rates for the prediction of basin sediment yield in Spain. *J. Hydrol.* **305**, 63–86.

Dhakal, AS., & Sidle RC. (2004). Distributed simulations of landslides for different rainfall conditions. *Hydrol. Process.* **18**, 757–776.

Dhonneur, G. (1985). Traité de Météorologie Tropicale, 1–151. Publication de la Direction de la Météorologie, France.

Dickinson, A., & Collins, R., (1998) Predicting erosion and sediment yield at the catchment scale. Soil erosion at multiple scales. CAB Int 317–342;

DG/ACTA. (1993). Stratégie nationale pour la conservation des eaux et des sols. Publication de la Direction de la Conservation des Eaux et des Sols. Ministère de l'Agriculture et des Ressources Hydrauliques. République Tunisienne.

EEA. (2002). Assessment and reporting on soil erosion. Background and workshop report. European Environmental Agency, Copenhaguen.

EEA. (1999). Environment in the European Union at the Turn of the Century. European Environmental Agency.

Ellison, WD. (1947). Soil erosion studies - part I. *Agric. Eng.* **28**,145-146.

Ennabli, M., Margat, M., & Vallee, D. (1998). Pour prévenir les crises de l'eau en Méditerranée, priorité à une meilleure maîtrise des demandes. Conférence internationale « Eau et Développement durable », Paris, 19-21 Mars.

Ennabli, M. (2007). La gestion durable des ressources en eau. Communication présentée lors des journées scientifiques de l'INRGREF à Hammamet.

Ennabli, N. (1993). Les aménagements hydrauliques et hydro-agricoles en Tunisie. Institut National Agronomique de Tunis. Ministère de l'Agriculture et des ressources hydrauliques.

Eswaran, H., Lal, R.& Reich, P.F.(2001). Land degradation: an overview. In: Bridges, E.M., Hannam, I.D., Oldeman, L.R., Penning de Vries, F.W.T., Scherr, S.J., Sombatpanit, S.

(Eds.), Response to Land Degradation. Science Publishers Inc, Enfield, NH, USA, pp. 20–35.
Fistikoglu, O., & Harmancioglu, N.B. (2002). Integration of GIS with USLE in assessment of soil erosion. *Water Resour. Manag.* **16**, 447–467.
FAO. (1994). Situation mondiale de l'alimentation et de l'agriculture 1993. *FAO Agriculture* **26**, 326 p.
Fraedrich, K., & Larnder, C. (1993). Scaling regimes of composite rainfall time series. *Tellus* **45**, 289–298.
Gammar, A. M. (1999). La dorsale Tunisienne, entre la représentation linéaire et réalité régionale, 39–52. Publication de la faculté des lettres de Manouba, Tunisie.
García-Ruiz, J.M., Martí-Bono, C., Lorente, A., & Begería, S. (2003). Geomorphological consequences of frequent and infrequent rainfall and hydrological events in Pyrenees Mountains of Spain. *Mitig. Adapt. Strat. Global Change* **7**, 303–320.
Gaume, E., Mouhous, N., & Andrieu, H. (2007). Rainfall stochastic disaggregation models: Calibration and validation of a multiplicative cascade model. *Adv. Water Ress.* **30**, 1301–1319.
Gay, M., Cheret, V. & Denux, J.P. (2002). Apport de la télédétection dans l'identification du risque d'érosion. *La Houille Blanche* **1**, 81– 86.
Gilles, D., Christian, W., Nicole, M., Lucien, H. & Laurent, P. (2006). Topography and recent winter rainfall regime change in temperate western European areas: A case study in the Rhine–Meuse basin. *Int. J. Climatol*. **26**, 785–796.
Gilley, JE., Eghball, B., Kramer, LA., & Moorman, TB. (2000). Narrow grass hedge effects on runoff and soil loss, *J. Soil Water Cons*. **55**, 190–196.
Gobin, A., Jones, R., Kirkby, M., Campling, P., Govers, G., Kosmas, C. & Gentile, A.R. (2004). Indicators for pan-European assessment and monitoring of soil erosion by water. *Environ. Sci. Policy* **7**, 25–38.
Goel, A.K., & Kumar, R. (2005). Economic analysis of water harvesting in a mountainous watershed in India**.** *Agricultural Water Management* **71**, 257–266.
GOPA & GTZ. (2005). *Elaboration d'une stratégie nationale d'adaptation de l'agriculture Tunisienne et des écosystèmes aux changements climatiques*. Pré-rapport 1ère phase.
Greene , RSB., & Ringrose-Voase, AJ. (1994). Micromorphological and hydraulic properties of surface crusts formed on a red earth soil in the semi-arid rangelands of eastern Australia, Conference Proceedings, Townsville, Queensland, Elsevier.
Griffin, M.L., Beasley, D.B., Fletcher, J.J. & Foster, G.R. (1988). Estimating soil loss on topographically non-uniform field and farm units. *J. Soil Water Cons.* **43**, 326–331
Güntner, A., Olsson, J., Calver, A., & Gannon, B. (2001). Cascade-based disaggregation of continuous rainfall time series: the influence of climate. *Hydrol. Earth Syst. Sci.* **5**, 145–164.
Gupta, V.K., & Waymire, E. (1990). Multiscaling properties of spatial rainfall and river flow distributions. *J. Geophy. Res.* **95**, 1999–2009.
Gupta,V. K., & Waymire, E.C. (1993). A statistical analysis of mesoscale rainfall as a random cascade. *J. Appl. Meteo*. **32**, 251–267.
Gurgel, H., C. & Ferreira N. J. (2003). Annual and interannual variability of NDVI in Brazil and its connections with climate. *Int. J. Remote Sensing* **24**, 3595–3609.
Haregeweyn, N., Poesen, J., Nyssen, J., & al. .(2006). Reservoirs in Tigray (Northern Ethiopia): characteristics and sediment de position problems. *Land. Degr. Dev.* **17**, 211–230.

Harris, D., Menabde, M., Seed, A., & Austin, G. (1998). Breakdown Coefficients and scaling properties of rain fields. *Nonlinear Proces. Geophy.* **5**, 93–104.

Harvey, AM. (1984). Geomorphological response to an extreme flood: a case from southeast Spain. *Earth Surf. Process. Landf.* **9**, 267– 279.

Herath, M.G., & Gopalakrishnan, C. (1999). The Economics of Reservoir Sedimentation: A Case Study of Mahaweli Reservoirs in Sri Lanka. *Int. J. Wat. Ress. Develop*. **15**, 511–526.

Hingray, B., Ben Haha, M. (2005). Statistical performances of deterministic and models for rainfall series disaggregation. *Atmospheric Research* **77**, 152–175.

Hooke, J.M., & Mant, J.M. (2000). Geomorphological impacts of a flood event on ephemeral channels in SE Spain. *Geomorph*, **34**, 163–180.

Hubert, P., Tessier, Y., Lovejoy, S., Schertzer, D., Schmitt, F., Ladoy, P., Carbonnel, J. P., Violette, S. & Desurosne, I. (1993). Multifractals and extreme rainfall events. *Geophys. Res. Lett.* **20**, 931–941.

Hudson, N.W. (1965). The Influence of Rainfall on the Mechanics of Soil Erosion with particular reference to Northern Rhodesia. MSc. Thesis, Univ. of Cape Rown.

Hunt, G.A. (1951). Random Fourier transforms. *Trans. Amer. Math. Soc*. **71**, 1–38.

ILEC & UNEP. (2003). World lake vision- A call to action. International Lake Environment Committee Foundation, and United Nations Environment Programme, Nairobi.

Irvem, A., Topaloglu, F. & Uygur, V. (2007). Estimating spatial distribution of soil loss over seyhan river Bassin in Turkey. *J. Hydrol*. **336**, 30-37.

Jain, SK., Kumar, S., & Varghese, J. (2001). Estimation of soil erosion for a Himalayan watershed using a GIS technique. *Water Resour Manag*. **15**, 41–54

Jen, CH., Lin, JC., Hsu, ML., & Petley, DN. (2006). Fluvial transportation and sedimentation of the Fu-shan small experimental catchments. *Quarter. Int*. **147**, 34–53.

Kahane, J.P., & Peyriere, J. (1976). Sur certaines martingales de Benoit Mandelbort. *Adv. Math*. **22**, 131–145.

Kalkstein, L. S., Tan, G. & Skindlov, J. A. (1987). An evaluation of three clustering procedures for use in synoptic climatological classification. *J. Climat. Appl. Met*. **26**, 717–730.

Kandel, DD., Western, AW., Grayson, RB., & Turral, HN. (2004). Process parameterization and temporal scaling in surface runoff and erosion modelling. *Hydrol. Process.* **18**, 1423–1446

Kantelhardt, J.W. (2008). Fractal and Multifractal Time Series. arXiv:0804.0747v1 [physics.data-an: date of access, 4 Apr. 2008].

Kassab, A. (1979). L'évolution de la vie rurale dans les régions de la moyenne Medjerda et de Bèja Mateur. Thèse de Doctorat Es-Lettres, Géographie. Faculté des Lettres et Science Humaines de Tunis.

Kinnell, P. I. A. (2001). Slope length factor for applying the USLE-M to erosion in grid cells. *Soil & Tillage Research* **58**, 11–17.

Kirpich, Z.P. (1940). Time of concentration of small agricultural watersheds. *Civil Engineering* **10**, 1– 362.

Kowal, J.M., & Kassam, A.H. (1976). Energy load and instantaneous intensity of rainstorms at Samaru Nigeria. *Tropical Agric*. **53**, 185-197.

Kozuchowski, K. M., Wibig, J. & Maheras, P. (1992). Connections between air temperature and precipitation and the geopotential height of the 500 hPa level in a meridional cross-section in Europe. *Int. J. Climatol.* **12**, 343–352.

Ladoy, P., Schmitt, F., Schertzer, D., & Lovejoy, S. (1993). Variabilité temporelle multifractale des observations pluviométriques a Nîmes. *C. R. Acad. Sci*. **317**, 775–782.

Lal, R. (1976). Soil Erosion problems on Alfisols in Western Nigeria and Their Control. IITA Monograph 1, IITA, Ibadan, Nigeria pp 208.

Lana, X., Martínez, M. D., Serra, C. & Burgueno, A. (2004). Spatial and temporal variability of the daily rainfall regime in Catalonia (northeastern Spain), 1950–2000. *Int. J. Climatol.* **24**, 613–641.

Lebdi, F., Fdhila, M.K. & Hzami, A. (2006). Modélisation de la dynamique fluviale de la Medjerda : Impact de l'évolution morphologique du lit sur l'écoulement. Conférence scientifique internationale " L'avenir des terres sèches : Cas des bassins Méditerranées ". Tunis, 19-21 Juin.

Lee, S. (2004). Soil erosion assessment and its verification using the universal soil loss equation and geographic information system: A case study at Boun, Korea. *Environmental Geology*. **45**, 457–465.

Lesschen, J.P., Kok, K., Verburg, P.H,. & Cammeraat, L.H. (2007). Identification of vulnerable areas for gully erosion under different scenarios of land abandonment in Southeast Spain. *Catena* **71**, 11–0121.

Livezey, B. (2005). Best practices vs. misuse of PCA in the analysis of climate variability. The 30th Annual Climate Diagnostics and Prediction Workshop (24–28 October, The Pennsylvania State University) [proceedings/cdw30_proceedings/Livezey_PCA_PSU. ppt; date of access 2006].

Lomborg, B. (2001). The Skeptical Environmentalist: Measuring the Real State of the World. Cambridge University Press, Cambridge, UK.

Lovejoy, S. & Schertzer, D. (1990). Multifractals, universality classes and satellite and radar measurements of cloud and rain fields. *J. Geophy. Res.* **95**, 2021–2034.

Lovejoy, S., & Schertzer, D. (2005). Multifractals, cloud radiances and rain. *J. Hydrol*. **322**, 59–88.

Maas, GS., Macklin, GE., Warburton, J,. & Woodward, JC., Meldrum, E. (2000). A 300-year history of flooding in an Andean mountain river system: The Rio Alizos, southern Bolivia. Technical Report, Balkema, Rotterdam.

Malam, Issa, O., Le Bissonnais, Y., Planchon, O., Favis-Mortlock, D., Silvera, N., & Wainwright J. (2006). Soil detachment and transport on field- and laboratory-scale interrill areas: Erosion processes and the size-selectivity of eroded sediment. *Earth Surf Proc Landf*. **31**, 929–939.

Malamud, B., & Turcotte, D. (1999). Self affine time series: Measure of weak and strong persistence. *J. Stat. Plan. Inference* **80**,173–196.

Mandelbrot, B. (1974). Intermittent turbulence in self similar cascades: divergence of high moments and dimension of the carrier. *J. Fluid Mech*. **62**, 331–350.

Marsan, D., Schertzer, D., & Lovejoy, S. (1996). Causal space time multifractal processes: Predictability and forecasting of rain fields. *J. Geophy. Research* **101**, 26333–26346.

Martínez-Casasnovas, J.A. (2003). A spatial information technology approach for the mapping and quantification of gully erosion. *Catena* **50**, 293– 308.

Martinez-Mena, M., Castillo, V., Albaladejo, J. (2002). Relations between interrill erosion processes and sediment particle size distribution in a semiarid Mediterranean area of Spain. *Geomorph*. **45**, 261- 275.

Masson, J.M. (1972). L'érosion des sols par l'eau en climat Méditerranéen. Méthodes expérimentales pour l'étude des quantités érodées a l'échelle du champ. *La Houille Blanche* **8**, 673–679.

Menabde, M., Harris, D., Seed, A., Austin, G., & Stow, D. (1997). Multiscaling properties of rainfall and bounded random cascades. *Water Resour. Res*. **33**, 2823–2830.

Menabde, M., Seed, A., & Pegram, G. (1999). A simple scaling model for extreme rainfall. *Water Resour. Res.* **35**, 335– 339.

Menabde, M., & Sivapalan, M. (2000). Modeling of rainfall time series and extremes using the bounded random cascades and Levy-stable distributions. *Water Resour. Res*. **36**, 3293–3300.

Millward, A. A., & Mersey, J. E. (1999). Adapting the RUSLE to model soil erosion potential in a mountainous tropical watershed. *Catena*, **38**, 109–129.

Molnar, P., Burlando, P. (2005). Preservation of rainfall properties in stochastic disaggregation by a simple random cascade model. *Atmos. Res*.**77**, 137–151.

Nearing, M.A., Ascough, L.D. & Laften, J.M. (1990). Sensitivity analysis of the WEPP hilloslope pofile erosion model. *Trans. ASAE*. **33**, 839-849.

Nearing, M.A., Pruski, F.F. & O'Neal, M.R. (2004). Expected climate change impacts on soil erosion rates: A review. *J. Soil and Water Cons.* **59**, 43– 50.

North, G .R., Bell, T. L., Cahalan, R. F. & Moeng, F. J. (1982). Sampling errors in the estimation of empirical orthogonal functions. *Mon. Weather Rev*. **110**, 699–706.

Olsson, J., & Berndtsson , R. (1998). Temporal rainfall disaggregation based on scaling properties. *Water Sci. Technol*. **37**, 73–79.

Olsson, J., & Burlando, P. (2002). Reproduction of temporal scaling by a rectangular pulse rainfall model. *Hydrol. Process.* **16**, 611–630.

Olsson, J., Niemczynowicz, J., & Berndtsson, R. (1993). Fractal analysis of high resolution rainfall time series. *J. Geophys. Res.* **98**, 65–74.

Olsson, J. (1995). Limits and characteristics of the multifractal behavior of a high-resolution rainfall time series. *Nonlinear Proces. Geophy*. **2**, 23–29.

Olsson, J. (1996). Scaling and fractal properties of rainfall. Analysis and modeling of rain gauge data. PhD Thesis, Rep. 1014, Dept of Water Resourc. Engng, Lund Univ.

Olsson, J. (1998). Evaluation of a cascade model for temporal rainfall disaggregation. *Hydrol. Earth Syst. Sci.* **2**, 19–30.

Olsson, J. (2008). Development and Matlab implementation of the cascade-based disaggregation model. Report.

Onyando, J.O., Kisoyan, P. & Chemelil M.C. (2005). Estimation of potential soil erosion for River Perkerra catchment in Kenya. *Water Resour Manag*. **19**, 133–143.

Ormsbee, L.E. (1989). Rainfall disaggregation model for continuous hydrologic modeling. *J. Hydraul. Eng.* **115**, 507–525.

Over, T. M., & Gupta,V. K. (1994). Statistical analysis of mesoscale rainfall: dependence of a random cascade generator on large-scale forcing. *J. Appl. Meteorology* **33**, 1526–1542.

Over, T. M., & Gupta, V. K. (1996). A space–time theory of mesoscale rainfall using random cascades. *J. Geophys. Res.* **101**, 26319– 26331.

Panday, A., Chowdary, V.M. & Mal, B.C., (2007). Identification of critical erosion prone areas in the small agricultural watershed using USLE, GIS and remote sensing. *Water Resour Manag.* **21**,729-746.

Pimentel, D., Harvey, C., Resosudarmo, P., Sinclair, K., Kurz, D., McNair, M., Crist, S., Shpritz, L., Fitton, L., Saffouri, R. & Blair, R. (1995). Environmental and Economic Costs of Soil Erosion and Conservation Benefits. *Science* **267**, 1117– 1123.

Plata Bedmar, A., Cobo Rayan, R., Sanz Montero, E., Go´mez Montan˜a, J.L., Avendan˜o & Salas, C. (1997). Influence of the Puentes reservoir operation procedure on the sediment accumulation rate between 1954–1994. Commission Internationale des Grands Barrages, Proc. 19th Congress Grands Barrages, Florence, Italy, 1997,Q.74, R.52, 835– 847.

Poesen, J.W.A., & Hooke, J.M. (1997). Erosion, flooding and channel management in the Mediterranean environments of southern Europe. *Prog. Phys. Geogr.* **21**, 157–199.

Price, L.E., Fawcett, C.P., & Young, P.C. (2000). Modeling reservoir sedimentation and estimating historical deposition rates using a data-based mechanistic (DBM) approach. *Hydrol. Sci. J.* **45**, 237–248.

Ramos, M.C., & Nacci, S. (1997). Estabilidad de agregados superficales en suelos del Anoia-penedès (Barcelona) frente al humedecimiento y al impacto de las gotas de lluvia. *Edafologia* **3**, 3–12.

Renschler, C., Diekkruger, B. & Mannaerts, C. (1997). Regionalization in surface runoff and soil erosion risk evaluation, in Regionalization of Hydrology. *IAHS Publishers*, UK. **254**, 233–241

Richman, M. B. (1986). Rotation of principal components. *J. Climatol*. **6**, 293–335.

Renschler, C.S. & Harbor, J. (2002). Soil erosion assessment tools from point to regional scales-the role of geomorphologists in land management research and implementation. *Geomorph*. **47**, 189–209.

Rodriguez-Iturbe, I., DePower, F., Sharifi, M., & Georgakakos, K. (1989). Chaos in rainfall. *Water Resour. Res.* **25**, 67–75.

Salas, J.D. (1993). Analysis and modeling of Hydrologic time series. In D.R. Maidment (Ed), Handbook of Hydrology, Mc. Graw-Hill, New York, chapter 19.

Schertzer, D., & Lovejoy, S. (1987). Physical modeling and analysis of rain and clouds by anisotropic scaling of multiplicative processes. *J. Geophys. Res.* **92**, 9693–9714.

Schertzer, D., Tchiguirinskaia, I., Lovejoy, S., Hubert, P., & Bendjo-udi, H. (2002). Which chaos in the rainfall-runoff process? A discussion on ‘‘evidence of chaos in the rainfall-runoff process’’l. *Hydrol. Sci. J.* **47**, 139–147.

SERPE-IESM. (1993). Pluviomètre transducteur à impulsions R01-3032. Notice d'utilisation, France.

SERST-IRD. (2000). Evaluation du programme lacs et barrages collinaires en Tunisie "Hydromed". Rapport édité par l'Institut de Recherche Développement.

Singh, C. V. (2004). Empirical Orthogonal Function (EOF) analysis of monsoon rainfall and satellite-observed outgoing long-wave radiation for Indian monsoon: A comparative study. *Meteorol. Atmos. Phys*. **85**, 227–234.

Sivakumar, B., Sorooshian, S., Gupta, H. V., & Gao, X. (2001). A chaotic approach to rainfall disaggregation. *Water Resour. Res*. **37**, 61–72.

Spaan, WP., Sikking AFS., & Hoogmoed, WB. (2005). Vegetation barrier and tillage effects on runoff and sediment in an alley crop system on a Luvisol in Burkina Faso. *Soil Till Res.* **83**, 194–203.

Svensson, C., Olsson, J., & Berndtsson, R. (1996). Multifractal properties of daily rainfall in two different climates. *Water Resour. Res*. **32**, 2463–2472.

Svensson, C. (1999). Empirical orthogonal function analysis of daily rainfall in the upper reaches of the Huai River Basin, China. *Theoret. Appl. Climatol.* **62**, 147–161.

Thauvin, V., Gaume, E., & Roux, C. (1998). A short time-step point rainfall stoshastic model. *Water Sci. Technol*. **11**, 37–45.

Todd, M. C., Washington, R., & James, T. (2003). Characteristics of summer time daily rainfall variability over South. Atlantic Convergence Zone. *Meteorol. Atmos. Phys.* **83**, 89–108.
Tosic, I. (2004). Spatial and temporal variability of winter and summer precipitation over Serbia and Montenegro. *Theoret. Appl. Climatol*. **77**, 47–56.
Toy, J.T., Foster, G.R., & Renard, K.G. (2002). Soil erosion: Processes, prediction, measurement and control. Library of congress cataloging-in-publication data. Edited by Jhon Wiley et & Sons, Inc., NewYork. 338 pp.
Unal, Y., Kindap, T., & Karaca, M. (2003). Redefining the climate zones of Turkey using cluster analysis. *Int. J. Climatol.* **23**, 1045–1055.
Uvo, B. C. (2003). Analysis and regionalization of northern European winter precipitation based on its relationship with the North Atlantic Oscillation. *Int. J. Climatol*. **23**, 1185–1194.
Uvo, C., & Berndtsson, R. (1996). Regionalization and spatial properties of Ceara State rainfall in Northeast Brazil. *J. Geophys. Res. Atmos*. **101**, 4221–4233.
Van der Knijff, J.M., Jones, R.J.A., & Montanarella, L. (2000). Soil erosion risk assessment in Europe. EUR 19044 EN, European Soil Bureau, Space Application Institute, JRC, Ispra, Italy, p. 34.
Van Regenmortel, G. (1995). Regionalization of Botswana rainfall during the 1980s using Principal Component Analysis. *Int. J. Meteorol*. **15**, 313–323.
Veneziano, D., & Furcolo, P. (2002). Multifractality of rainfall and scaling of the IDF curves. *Water Res. Research* **38**, 12–42.
Veneziano, D., & Furcolo, P. (2003). Marginal distribution of stationary multifractal measures and their haar wavelet coefficients. *Fractals* **11**, 253–270.
Veneziano, D., Furcolo, P., & Iacobellis, V. (2006). Imperfect scaling of time and space –time rainfall. *J. Hydrol.* **322**, 105–109.
Wang, G., Gertner, G., Fang, S., & Anderson, A. B. (2003). Mapping multiple variables for predicting soil loss by geostatistical methods with TM images and a slope map. *Photog. Eng. Remote Sensing* **69**, 889–898.
Ward, J. H. (1963). Hierachical grouping to optimize an objective function. *J. Am. Statist. Assoc*. **58**, 236–244.
WCD. (2000). Dams and development. A new framework for Decision-Making. Earth-scan Publications Ltd, London , 356 pp.
White, S., García-Ruiz, JM., Martí, C., Valero, B., Errea, MP., & Gómez- Villar, A. (1997). The 1996 Biescas campsite disaster in the Central Spanish Pyrenees, and its temporal and spatial context. *Hydrol. Process*. **11**, 1797-1812.
Weggel, JR., & Rustom, R. (1992). Soil erosion by rainfall and runoff - State of the art. *Geotext. Geomembr*. **11**, 551-572.
Williams, R. & Berndt, H.D. (1972). Sediment yield computed with universal equation. *J. Hydrau. Div, ASCE* **98**, 2087–2098.
Wischmeier, W.H., & Smith, D.D. (1958). Rainfall energy and its relationship to soil loss. *Trans. Am. Geophys. Union* **39**, 285–291.
Wischmeier, W.H., & Smith, D.D. (1965). Predicting rainfall-erosion losses from cropland east of Rocky Mountains: Guide for selection of practices for soil and water conservation. US Department of Agriculture, Agricultural handbook 282.
Wischmeier, W.H., & Smith, D.D. (1978). Predicting rainfall erosion losses – A guide to conservation planning. USDA Agriculture Handbook 537, Washington D.C: GPO.

Yaglom, Y. (1966). The influences of fluctuations in energy dissipation on the shape turbulence characteristics in the inertial interval. *Sow. Phys. Dek*l. **11**, 26–29.

Yang, H., Shen, J., & Hu, S. (2003). Evaluating waste treatment, recycle and reuse in industrial system, an application of the emergy approach. *Ecol. Model*. **160**, 13–21.

Yarnal, B. (1984). The effect of weather map scale on the results of a synoptic climatology. *Int. J. Climatol*. **4**, 481–493.

Zahar, Y., Ghorbel, A., & Albergel, J. (2008). Impact of large dams on downstream flow conditions of rivers: Aggradation and reduction of the Medjerda channel capacity downstream of the Sidi Salem dam (Tunisia). *J. Hydrol*. **326**, 318 330.

Zhang, X.B., & Zwiers F.W. (2004). Comment on "Applicability of prewhitening to eliminate the influence of serial correlation on the Man- Kendall test" by Sheng Yue and Chun Yuan Wang. *Wat. Res. Res*. **4**, (30), W03805.

I

Sihem Jebari, (2009). **Temporal aspects of soil erosion in Tunisia**.

Hydrological Sciences Journal (Submitted)

II

Jebari, S., Berndtsson, R., Lebdi, F. & Bahri, A. (2008). **Sediment, discharge and precipitation variation in the wadi Mellegue catchment during the last 50 years.** *Annales de l'INRGREF* 11, 116-122

III

Jebari, S., Berndtsson, R., Bahri, A. & Boufaroua, M. (2008). **Exceptional Rainfall Characteristics Related to Erosion Risk in Semiarid Tunisia**. *The Open Hydrology Journal*, 2 (9), 25-33.

IV

Jebari, S., Berndtsson, R., Bahri, A. & Boufaroua, M. (2009). **Spatial soil loss risk and reservoir siltation in semi arid Tunisian.** Accepted for publication in *Hydrological Sciences Journal*.

V

Jebari, S., Berndtsson, R., Uvo, C. & Bahri, A. (2007). **Regionalizing fine time-scale rainfall affected by topography in semi-arid Tunisia**. *Hydrological Sciences Journal*, 52 (6), 1199-1215.

VI

Jebari, S., Berndtsson, R., Olsson, J. (2008). **A scaling approach to enhance rainfall data for erosion estimation in semiarid Tunisia**. *Hydrology and Earth System Sciences (*Submitted).

VII

Jebari, S., Olsson, J. (2009). **Soil erosion estimation based on rainfall disaggregation**. *Hydrology and Earth System Sciences (*Submitted).

Temporal aspects of soil erosion in Tunisia

SIHEM JEBARI[1,2]

[1]*National Research Institute for Rural Engineering, Waters, and Forestry, Box 10, Ariana 2080, Tunis, Tunisia*
Sihem.jebari@iresa.agrinet.tn
[2]*Department of Water Resources Engineering, Lund University, Box 118, S-22100 Lund, Sweden*

Submitted for publication to Hydrology and Earth System Sciences

Abstract Water erosion implies negative consequences for rural development. It leads to significant changes in the sedimentological and hydrological characteristics of watersheds. This research work aims at studying short and long-term temporal effects of water erosion. The site of the Tunisian semi arid was chosen for this research work. We referred to historical texts and archeological excavations that go back to 1000 year B.C as well as archives of the last century. The relationship between the different types of agricultural landscape managements has been debated according to the soils potential production, to their solid transport and deposit, to the development of hydrographical network and finally to flood frequency. The results proved that water erosion is at the origin of - an important decrease in soil fertility – a development of the hydrographic network reaching 65 km and a progression of the deltaic plain that amounts to 15km^2/century. Moreover, due to a river choking, the number of overflooding occurrences has multiplied over at least one century. Finally, it was revealed that water erosion follows a specific cycle of degradation through the watershed. This cycle could be a valuable tool to design the settlements that must be undertaken in order to rehabilitate the watersheds spoilt by water erosion. This new approach will contribute to better manage soil and water in a context of a sustainable development.

Key words water erosion; semi-arid; Tunisia; temporal degradation pattern

INTRODUCTION

Since ancient times, man has adapted soil and water conservation practices to farming lands located on slopes (El Amami, 1984; Ennabli, 1993). These techniques favored protection of the soils, their fertility as well as their content in rain water (Bennet, 1950; FAO, 1996). Nowadays, the extension of the water erosion process continues to erode the farming landscape. Recent research has shown that the semiarid areas are very vulnerable to this phenomenon. In fact, they result in decrease in crops, a loss in the water potential, and source of recurrent natural catastrophes. The obvious consequence of water erosion is the increasing area of the arid belt, as we can observe in the south of the Maghreb countries. In Tunisia water erosion seems to be a chronic phenomenon. It affects 20% of the total land area. Yearly, 15000 hectares of farming arable land and 500 million m^3 of runoff water are lost (DG/ACTA, 1993). Erosion is also responsible for sediment deposit in the reservoirs that amounts to 40 million m^3/year (GOPTA & GTZ, 2005). At present, the sustainability of the farming systems in Tunisia will depend on the ability of the farming policies to deal with rural landscaping, to stop soil degradation and to rationalize water management (Jebari, 2003). Thus, we must clearly determine the degradation level of our environment as well as its temporal evolution. This research is essentially based on historical documents and

archeological excavations that go back more than 3000 years. Hydrological and sedimentological data of typical watersheds in semiarid Tunisia have also been used. The finding regarding short-term and long-term soil erosion evolution will provide a better understanding of the soil erosion process and allow decision makers in the field of land settlement as well as in the field of water and soil management, to better understand the erosive phenomena and to prevent them. As a result, we can design better sustainable development strategies.

STUDIED AREA

Tunisia represents a Northern occidental region with high and elevated plains. This area is crossed by the Atlas mountain chain which displays a South-Western/North-Eastern direction. The vast Kairouan plains cover the oriental part. As a result of these physical features, the hydrological network has developed its catchments towards the North-West and flows towards the East. When rainfall is abundant, the wadis have a regular flow towards the sea. This is the case of wadi Mejerda, the main permanent river of the country. It is 485 m long and drains a catchment of 23500 km^2, of which 7600 km^2 are located in Algeria. At present, the flow is regulated by a number of dams. When rain is scarce, climatic conditions are clearly more arid, thus the wadi waters do not reach the sea and flow towards small depressions called sebkha. This is the case of the central Tunisian wadis, of which the most important is Zeroud. The latter covers a catchment of 9000 km^2.

The average annual rainfall is about 450 mm. It is characterized by yearly and seasonal irregularity. In winter, the rain is usually of a frontal type and originates on the Mediterranean. Whereas, summer and fall rain, is generally of a convective type and bursts in to storms on the heights. During the 20th century, Tunisia suffered 10 major flooding events (1907, 1928, 1953, 1962, 1966, 1969, 1973, 1975, 1979, 1982, and 1990). The floods that occurred in the centre of the country in 1969 and the one in the Mejerda catchment in 1973 are the most devastating (Sakiss et al., 1991; 1994; Slimani, 2001). The maximum daily rainfall reached 185 and 114 mm, respectively. In the first flood, the rain lasted 2 days (max. 2 day rainfall 495 mm). The second lasted 4 days (max. 4 days rainfall 202 mm). The erosion and subsequent sediment deposits were spectacular. The solid concentration reached 374 g/l in wadi Zeroud and 170 g/l in wadi Mejerda (Ben Mammou, 1998). The water carried 6 million tonnes (700 tonnes/km^2) and 100 million tonnes (4250 tonnes/km^2) of sediments, respectively (Bouzaine and Lafforgue, 1986; Claude et al., 1977; Fig.1).

METHODOLOGY

Since independence, national water and soil conservation programs, changed very often, due a change in administration and therefore in approach. The general coherence of the programs was very often affected by the limited financial means, the lack of technical support, the absence of follow up and maintenance, and finally, by the insufficient efficiency of the available technologies (DG/ACTA, 1993). Semiarid Tunisia has always offered good farming possibilities to its population. The land has rich grazing and fertile lands crossed by the Atlas mountain chain (Knight, 1928; Ennabli, 1995). However, farming on sloping land and deforesting triggered of water erosion. This phenomenon was the origin of morphological

changes of the landscape. This is exemplified by the Mejerda, the development of its hydrographical network, the formation of its terraces as well as the deltaic plain (Fig. 2). The farming landscape degradation was conditioned by political events. In fact, all over its 3000-year history, every Tunisian era contributed in shaping the rural landscape through various land occupation ways and farming exploitation techniques (Kassab, 1979). This has included cultures such as the numid, roman, arab, turkish, colonial, and the modern times. This study intends to give an historical account for how the land management has changed catchment physiography and erosional pattern. For this purpose morphological changes of solid transport will be discussed, interpreted, and quantified by means of arc-view mapping tools. For the Mejerda watershed analysis of the hydrologic network evolution as well as progress of the deltaic plain are performed. The ancient hydrographic network suggested by Lancel (1999) for the Punic era is used for and compared to the present state by DGRE (1983). For the deltaic plain, graphs of Jauzein (1971) and Oueslati *et al*. (2006) have been used. Also, historical texts, accounts of archeological excavations, and data from catastrophic floods have been used. Data from floods were used to quantify the soil loss, define the watershed behavior, determine the human impact, and finally to suggest a temporal cycle of watershed degradation.

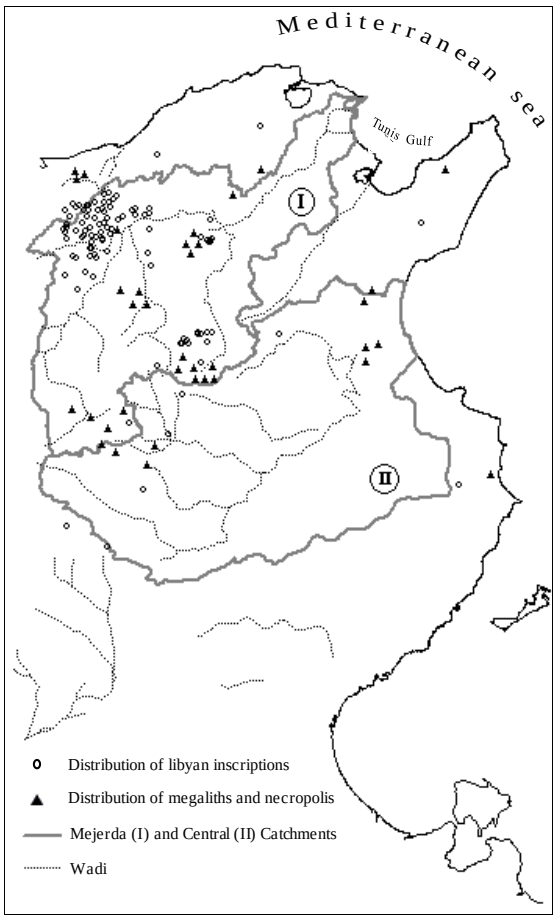

Fig. 1 Distribution of the archeological investigations in analyzed catchments.

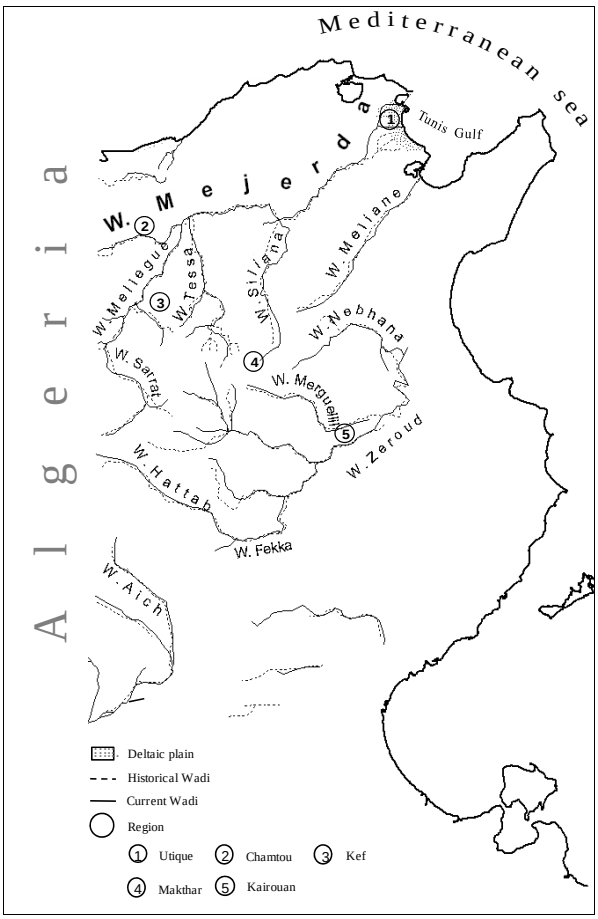

Fig. 2 Comparison between ancient and present hydrographical network.

HISTORICAL BACKGROUND OF THE NATURAL RESOURCES MANAGEMENT

North African agriculture goes back to the end of prehistoric times. The native numid farmers grew cereals using farming tools of the Bronze Age (Decret and Fantar, 1981). These tools had the great advantage of ploughing only the arable shallow layer of the land and thus allowing sustainable soil exploitation. The Numids, also called Libyans, make up a fraction of the North African population, the territory of which was located in the western part of Carthage (according to Polybe). They farmed the fertile plains of the Dorsal up to the Algerian Eastern border. Archeological investigations show that numidic habitats covered a large portion of the Dorsal area and the Mejerda catchment (Fig.1). The border of this land went from the plateaus of the Constantine province and ending in the Mejerda valley. Their capital was located at the present town of Makthar at center of the Tunisian Dorsal (Lepelly and Dupuis, 1999). The Numidian civilization was well organized with economical and cultural contacts over the Mediterranean as well as with the Egyptian civilization. As a matter of fact, when the Phoenicians came into contact with this native population, they found them well established with their own political, religious, and administrative organization (Decret and Fantar, 1981; Peyras, 1991).

In 1101 B.C, the Phoenician came and settled downstream the agricultural numidic habitats. They built a trading post at Utica, located at the wadi Mejerda discharge point. The choice of this site, accessible by sea, seems to be wisely thought as it was a rich agricultural and commercial region. The economic wealth of the maritime power of the Phoenicians increased during several centuries and Utica became a large settlement. The historical texts indicate a political coexistence between the Phoenicians and Numids. For example, a special tax had to be paid to the landlords (Camps, 1979). The Phoenicians that came from Tyr had lost their farming lands which had been totally devastated by water erosion as a result of deforestation and intense exploitation of downstream lands (Lowdermilk, 1953). The farming culture appears to have been converted into commerce in order to survive. However, they have been thrown out by the Greek from the oriental Mediterranean Sea and were forced to develop maritime trade in the occidental Mediterranean Sea. Many historical texts mention the mixed Punic civilization during which Numids and Phoenicians succeeded in connecting the orient to the occident (Lancel, 1999). This new civilization was embodied by the creation of Carthage (814 B.C.). It later became well-known for its economic wealth and military power. In fact, the original sustainable agriculture as well as the old Phoenician “know how” were put in to practice through the alluvial Mesopotamia and Nile plains during several centuries. This became the fabulous cereal, olive, and many fruit crops that are mentioned in historical texts. Besides, Greek texts recognize that Numidia has an abundant and over production of cereals. This food excess that was mainly exported (Jaidi, 1990; CNRS, 1994). In the 4th century B.C. the Carthagians invented mechanical agricultural devices that thresh wheat in order to achieve a better profitability. In the 3rd century B.C. Magon wrote an agronomy book in 28 volumes that both Greek and Romans translated. Under the reign of Massinissa, Strabon spoke about “double-crop lands, the wheat yield was 240 grains for one …” (Decret and Fantar, 1981; Lancel, 1999). Carthage was then responsible of a vast empire made up of rich colonies scattered and settled on both banks of the occidental Mediterranean Sea. However, it was on Tunisian lands that Carthage had its own territories. Thus, it became the first agricultural power of the west of the Mediterranean (Fig. 3). It exploited the most fertile and richest areas of 300 towns where sedentary life reigned (Lepelly and Dupuis, 1999). On the eve of the destruction of Carthage by the roman in 146 B.C., and after six centuries of reign, the Numidic lands were over-full of wheat and fruit of all sorts (Decret and Fantar, 1981).

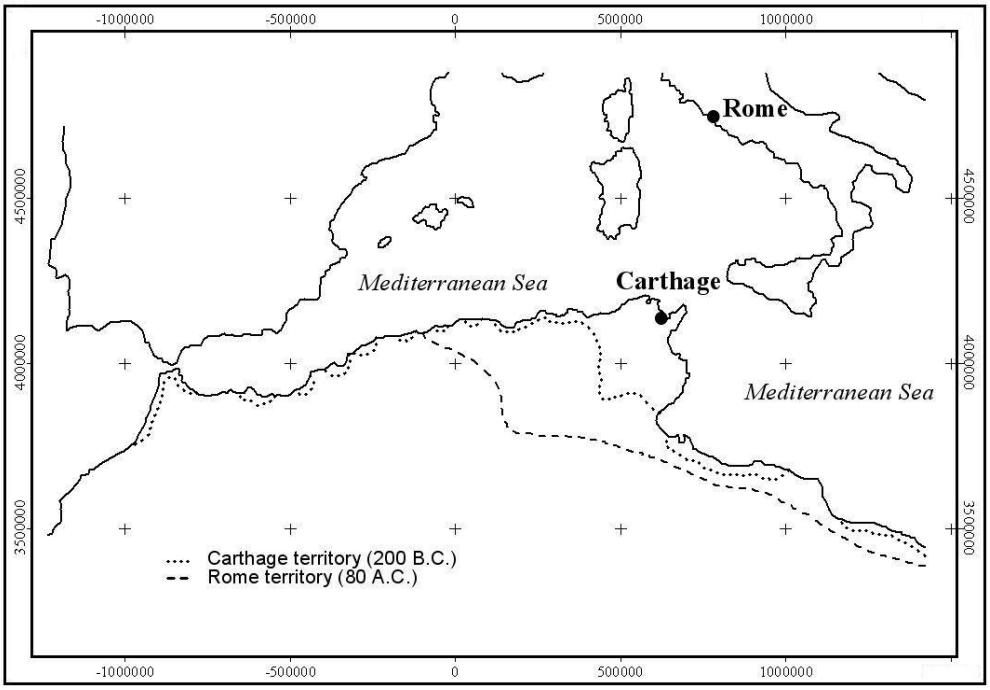

Fig. 3 The Carthagian and Roman boundaries in Tunisia

In the beginning of the Christian era, Pline l'Ancien described the province of Africa (now Tunisia) as a fertile land where cereals are lovely and crops are huge reaching 150 grains for one. The Roman consumption of wheat necessitated a total production of almost 10 million quintals in order to feed 3 to 4 million inhabitants (Decret and Fantar, 1981, Jaidi, 1990). The Romans considered Carthage as an agricultural colony. In fact, the whole territory became public property of the state and the native inhabitants had to pay a tax. Cereal farming covered Tunisia and the present Algerian lands of Constantine until the borders of the desert (Fig.3). All types of fields were needed for farming and even wetlands were drained and cultivated (Peyras, 1991). Towards 380 A.D. Rome suffered from a general agricultural crisis as well as a depopulation (Decret and Fantar, 1981). In fact, the lands of wheat, worn out, due to an intensive production, had to be replaced by other cultures. And thus, interest for tree planting was born (grape and olive trees). This new farming trend, focused on exploiting the soil wealth in depth, after the surface layer of the soil was impoverished. They also resorted to irrigation in order to improve the yield. Thus, the spring-water development, rain water harvesting, and numerous well digging were undertaken. The hill slopes destroyed by erosion necessitated a new kind of management. Consequently, terraces, water collection areas, and rain water collection were developed. A quotation by Coripe in the 6th century confirms the state of soil degradation and the persistence of the farmers to continue a non-sustainable exploitation of an over-exploited land: "The farmers of the altered land of Libya used to watch the clouds and when they see the first flashes of lightening, the strokes of thunder, the gusts of wind they rushed to the dried fields and expected rain. They cleaned up, made the fields even to receive rain water in suitable paths to prepare for a greening fields they build sand obstacles on the slopes of the soil" (Decret and Fantar, 1981). After nearly 8 centuries of reign, repeated Arab incursions occurred.

The Arab era (734 A.C.) is characterized by the construction of huge hydraulic structures. These structures collected and stored surface water in order to provide support for an increasing cattle raising industry. In fact, instead of resorting to extending farming lands and

irrigation an intensive cattle raising seemed to be more suitable and beneficial for soil conditions of that time. In fact El Bekri (1000) mentions in his road notes that the cereal crops of the center reached 100 grains for one at the best (Sakiss et al., 1994; Ennabli, 1993; 1995). In the 11th century (1050), conflicts led converted some of the Tunisian population in to a nomadic lifestyle and cities and town life started disappearing from the Dorsal area (Mahjoubi, 1992). This Arabic period seems to have introduced a farming system that combined cereal farming and cattle breading in agricultural areas. Moreover, pressure on the upper soil cover was continued. Unfortunately, in no way was the inherited historical sustainable management knowledge taken into account in the context of land exploitation. Thus the area sank into a more severe degradation.

At the time when Tunisia became part of the Ottoman Empire (1534), the central administration made most of the farming lands its own property. The new owners were city dwellers living in luxury in the capital Tunis. They hired people who collected taxes from the tribes on their behalf. The amount of taxation imposed on the land was higher than that imposed on cattle. Therefore, cattle rising became more popular with the rural communities. The latter was indeed poor and frequently decimated by epidemics and starvation. Their state clearly reflects that of their environment which was eroded and poorly drained. Their cereal crops didn't exceed 30 grains for one (Kassab, 1979). Eventually, this farming technique was unsuccessful and the policy of increasing taxation was a failure as they led to severe financial problems. And this induced France to benefit from the disastrous situation to colonize Tunisia which seemed a strategic stake owing to its geographical location and its potential farming advantages mentioned in Roman texts.

The French protectorate seized the Tunisian territory without any difficulty (Niox, 1890) due to the degraded agricultural landscape and low rural density. Moreover, Tunis the cosmopolitan capital drew all sorts of population from everywhere thanks to its active trade. The new invader quickly started to develop agriculture on vast lands and designed a plan to build big dams (Coignet, 1917). Faced with the pressing needs of an increasing European population, France hoped to greatly increase its production through an intensive agriculture. However, at its great surprise the crop yield was only 15 grains for one (Gsell, 1921). The cattle were hard to keep alive due to a high mortality during dry periods. Once again, the perseverance and determination of the colonial power didn't restrain from impoverishing the land even more. It also prevented the rural communities from development by depriving them from their water resources and pushing them out of their own lands. This population was pushed towards the mountains and the marginal lands. Thus, degradation of the land worsened and all means to safeguard or re-establish natural resources were simply ignored.

When independence came (1956), soil exploitation continued and the French hydraulic policy was wholly adopted by the new government (Coignet, 1917). The main streams that fed from the Dorsal area were chosen as privileged sites for water resources development. Nevertheless, setting up reservoirs was undertaken without paying attention to the upstream management of the watershed involved. Therefore water erosion and early sedimentation of dams were soon noticed. Despite the efforts to avoid soil loss and to use new technology in agriculture, cereal crops remained 15 grains for one (DG/PA, 2008). In spite of the adoption of a national policy for the protection of farming lands and for soil and water conservation, the erosion pressure was severe. In fact, the lack of important environmental protection made the semiarid area hardly developed (Gammar 1995).

CONSEQUENCES OF AN UNSUSTAINABLE MANAGEMENT FOR THE AGRICULTURAL ENVIRONMENT

During 3000 years Tunisia has witnessed successive agricultural systems which have practiced an intensive exploitation rather than a sustainable management of its natural resources. This has seriously affected the soil cover, the fertility level of the soils, the water erosion area, the hydrological and sedimentological regime of the wadis, the morphological changes of river beds, and finally the damage to the downstream infrastructure. For example, wadi Mejerda has been well described since the beginning of written history. The importance of its water and solid transport are mentioned by the poet Silius Italicus during the Punic war (2^{nd} century B.C.); "a river with muddy troubled waters, and a slow flow that digs the dry sand, the Bagrada, and no other river, on Libyan land extends its muddy waters and no longer the beds of its sleeping water sheets" (Chelbi et al., 1995).

Most historical texts show that wadi Mejerda allowed navigation during the Numid and Punic times. The Phoenicians used to practice their sea trade along this river. Thus, they came into contact with the Numid habitats and reached its population in the most remote areas located on the plateau of Constantine. They sold colorful material, glassware pearls, metal, and pottery to the native people and received local products and cattle (cereals, wood, animal skins, elephant tusks, raw metals; Rougé, 1975; Decret and Fantar, 1981; AIECM, 1976; Lepelley and Dupuis, 1999). During the Punic civilization this river used to supply the city of Utica then Carthage and their respective harbors with metals from the Kef, with marble from Chemtou and with wood from the Dorsal (Barkaoui, 2003; Fig.2). In addition to that, the river allowed the setting up of a permanent military camp in Kef at a distance of 170 km from Carthage, where many thousands of mercenaries used to gather, once back from wars against Rome (Lancel, 1999; Fig. 2). Two rock drawings illustrating warships from the archaic times (620 B.C.) in the northwest of Tunisia in the continental part of Numidia were found indicating navigation. Navigation on wadi Mejerda appears very likely, owing to its morphology and especially its width. In fact, it has a width that varies from 35 to 170 m (Niox, 1890; Zahar et al., 2008; Abidi, 2007). This indicates that navigation occurred by Carthagian trade ships (max. width 5 m) as well as war ships (max. width 7.4 m; Barkaoui, 2003; Lancel, 1999). Finally, wadi Mejerda has always represented a vital artery for the Punic maritime empire. In fact, the decline of Carthage was only possible by barring the river and thus isolating the city from its supporting land areas (Meyran, 2008).

The high solid load in Mejerda continued during the entire Roman period. Probably it even worsened. It seems that navigation was prevented since the beginning of the Christian period. In fact, the Romans who came and settled on the Punic lands started the building of a large road network (Decret and Fantar, 1981; Niox, 1890). This probably replaced the navigation needs in order to ensure communication, commercial trade, and military operations. The massive sedimentation affected the Utica harbor too. Historical texts show that it started to silt up in the beginning of the 5^{th} century while the town itself was deserted in the 7th century. On the eve of the destruction of Carthage it was described as a very important military and commercial harbor. However, recent archeological excavation rather depicts it as a river harbor (Reyniers, 1952). The Romans had to continuously dredge the harbor from silt. Thus, the importance of this harbor decreased because of the sedimentation pressure from the wadi Mejerda. During the Roman Empire, water erosion seemed to have been spectacular. This could be shown by the reluctance of farmers to fertilize their agricultural lands (Decret and Fantar, 1981). The agricultural lands either received new sediment deposits or were eroded due to the scouring of their upper layers. Finally, if we compare the Roman period with the

Punic one, it is obvious that the land fertility deteriorated and cereal yields decreased by 40% (Fig. 4).

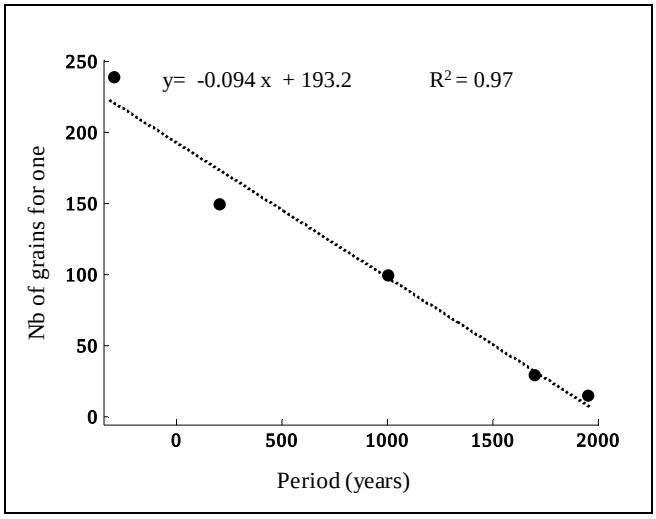

Fig. 4 Cereal yield from a single sowed grain.

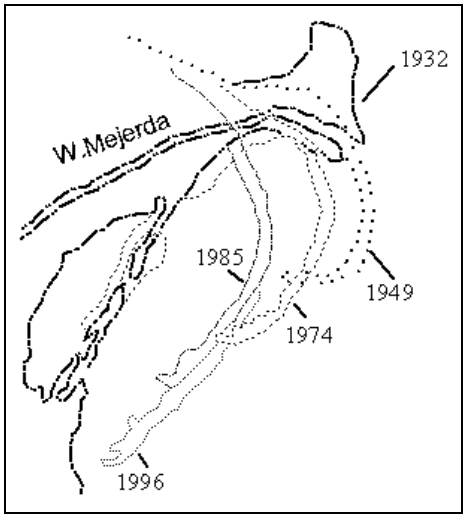

Fig. 5 The progress of the Mejerda delta. The figure was modified from Oueslati et al. (2006).

The water erosion process was generated on a large scale. Arabic settling basins in central Tunisia had to be included in hydraulic networks every time water came from wadis (Ennabli, 2001). These basins were essential in order to separate water from its solid content. However, the Mejerda basin remains the most obvious evidence of the importance in soil loss (Paskoff and Trousset, 1992). It created a deltaic downstream plain that gained more than 450 km^2 from the sea. At present, it is intensively exploited by farmers. The chronology of its formation as well as the importance of the climatic, hydrologic, and human factors in its evolution have been well documented (Tissot, 1884; Bernard, 1911; Reyniers, 1952; Jauzein, 1971; Barjot, 1952; Chelbi et al., 1995; Oueslati et al., 2006). Its extension is due to the existence of a sheltered coastal shallow environment to a river characterized by an abundant solid load. The delta is made up of old off-shore bars which delimited the lagoons that have been slowly covered by silt (Paskoff and Trousset, 1985). The best image that illustrates this phenomenon is the present sandy arrow of Kalaat Landalous which originates at the river delta (Fig. 5). The latter, is morphologically active, it is progressing with an average speed of 100 m/year and stretches from the north towards the south by nearly 4.5 km (ScetTunisie-Apal, 2005; Studi-Apal, 2001). This continuous nowadays observed silting process coincides with the historical description of Polybe. The latter, described the mercenary war in the middle of the 3rd century B.C. He wrote that Amilcar the leader of the Carthagian army: "… as he couldn't drive out the enemy of ambush … he knew that when the wind blew during some days, the river bed became sand-blocked, so that he could wade through it. He used to wait patiently for the sand to gather and crossed to the other river bank with his troops and elephants …" (Chelbi et al., 1995; Paskoff and Trousset, 1993).

Evaluating the long-term progress of the delta plain was possible by referring to Jauzein's mapping (1971) which were later modified by Oueslati (2006). An increasing trend of solid transport during 3 millennia is clearly noticeable (Fig. 6). The average progress of the delta per century doubled between the 2nd and the 1st millennium B.C. (Table 1). The advance grew

from 6.6 km^2/century to 12 km^2/century. The maximum value was observed between 200 B.C. and 400 A.C. with 14.5 km^2/century. Then, a tendency to decrease is noticed and it continued until the 1900s (Fig. 6). The time of increasing rates perfectly coincides with the farming of the lands and their extension through North Africa, as quoted by Jauzein (1971).

Table 1 Development of the delta according to Oueslati et al. (2006).

Period	Surface area of delta (km^2)
3000 BC – 1000 BC	132.7
1000 BC – 200 BC	228.6
200 BC – 400 AD	315.6
400 AD – 1000 AD	39.3

The intensive exploitation during the Roman period is well illustrated by the maximum amount of solid transport during the studied period. However, the decreasing tendency in solid transport during the last millennium may not be a result of land conservation. Rather this is probably a decrease in sediment available to be carried downstream. Consequently, the graph coincides rather well with the degradation cycle suggested by Jebari et al. (2009). Consequently, the progress of the Mejerda delta plain illustrates the temporal sedimentary dynamics for the semiarid catchments (Fig. 6).

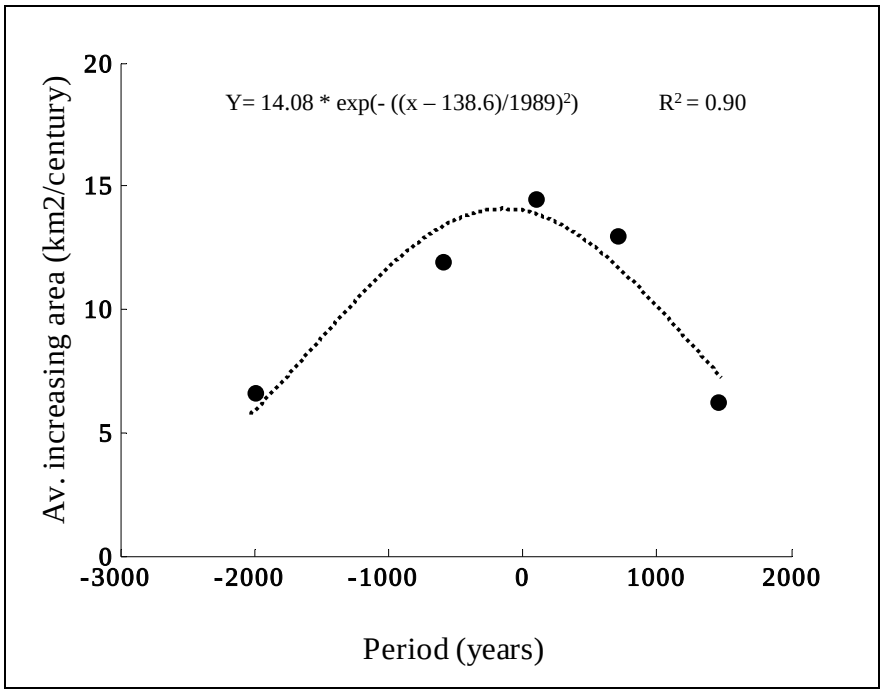

Fig. 6 The average progress trend of the deltaic plain of Mejerda

A comparison between the ancient and the current hydrographical network displays in general a rather permanent situation (Fig. 2). However, an increase in the river length from 13 to 65 km characterized the Mellegue and Siliana wadis, respectively. A probable first cause may be the population pressure that always has been strong in both watersheds (Fig. 1). A second explanation for the increasing degradation may be due to the wood exploitation. Indeed wood was among the most valuable goods in the Mediterranean Sea trade circle. Among the 14 recorded species from historical wrecks, the Atlas wood amounted to about half (Barkaoui, 2003). The Siliana and Mellegue woods were rich in pines (Gammar, 1979). This species was highly appreciated for boat building since it creates light ships. This type of wood was transported to Carthage where round-shaped ships for trade and long-shaped ones for war were continuously built. The carpenters assembled and put afloat boats on an average of one vessel each 2 days. This was done, in order to cover the needs of the maritime empire (Barkaoui, 2003). The nearest pine-forest to Carthage via Mejerda was that of Siliana, which underwent an even stronger pressure than the farther located Mellegue forest (Fig. 1).

During the last three centuries, a more and more frequent overflowing of the wadi Mejerda has been noticed. Consequently, water swamps areas have been created both up and downstream in the wadi. These areas are malaria sources and this was probably a cause of the decrease in rural population density that characterized that time (Kassab, 1979). In 1898 exceptional floods downstream led to the silting of 3000 hectares which varies from 50 cm to 1 m deposits. From 1931 to 1973 on the occasion of other floods, wadi Mejerda swells again and overflows to its nearby river arms located in the surrounding of its mouth (Jauzein, 1971). In fact, geomophologists have discovered six arms like this (Oueslati, 2006). The latter may have been developed during periods of even more frequent floods. Indeed, Collet (1953) quoted that in the beginning of the last century, Mejerda used to flow over from its bed every 2 or 3 years. These swellings developed in to two meter high natural dikes on its banks. Thus, it has been necessary to design hydraulic structures along its downstream 80 km drain in order to allow for evacuation of about 1200 m^3/s and avoid overflow. During exceptional events, the amount of solid transport is excessive and can result in morphological changes of the wadi's river beds. In fact the Mejerda mouth used to be located at 15 km from the present one. It carries an average amount of 25 g/l of solid matter. Before the building of the dams in 1953, its annual solid transport at Tunis gulf amounted to 22 million m^3 (Pimienta, 1959). This yields an average erosion of the whole watershed of 0.41 m/1000 years. At present, the yearly solid transport of Mejerda to the Tunis gulf amounts to 5 million tons (LCHF, 1978; SOGREAH, 1983; Studi-Scet, 1989 d).

Also, the increasing population pressure of the farming environment, during the last 50 years, is partly responsible for some over-flowing. The building of hydraulic infrastructure as well as road building triggers recurring floods downstream of Mejerda. These floods have become more and more threatening with the urbanization of the area. In fact, studies of the impact of the morphological changes of Mejerda have recently been undertaken. They showed that the fattening of the Mejerda river bed increased by 20% in 15 years and decreased in flow by 30% (Zahar et al., 2008). The choking of the river bed is mainly due to releasing too small amounts of water from upstream reservoirs. The current water management includes irrigation water supply to the downstream and desilting of reservoirs (Lebdi et al., 2006). Vegetation also worsens the effects of solid deposit (DGRE, 2006). In fact, the decrease in the water speed through the river bed does no longer allow for a natural desilting. All these factors have led to a reduced water flow by 75% at downstream parts of Mejerda. In fact, at Sloughuia station, the recorded discharge were 762, 371, 274, and 183 m^3/s for 1989, 1997, 2003, and

2006, respectively (Lebdi, 2006; GOPA-GTZ, 2005). Also, floods occur with gradually lessening discharge (Zahar et al., 2008; Lebdi et al., 2006).

CONCLUSION AND DISCUSSION

The farming environment in the Tunisian watersheds has undergone hydrological and sedimentological changes due to the different management strategies during the last 3 millennia. Severe floods have been mentioned in central Tunisia since 861 A.D. (MARH, 2000; El Louati et al., 1998; Floury, 2003). However, in Mejerda they have only been mentioned in historical texts since the 18th century. This relatively late triggering of overflows shows a better resistance against the human influence as compared to, e.g., the wadi Zeroud in central Tunisia. Probably, this ability is closely linked to the potential capacity of the watershed to preserve its soil and water. In fact, infiltration through the surficial substratum of soil and draining water all over the hydrographic network are crucial for a stable catchment.

The watershed behavior during natural catastrophes depends on its degree of degradation (Fig. 6; Jebari et al., 2009). If we compare the floods of 1969 and 1973, we can deduce an average rainfall 2.5 times larger for wadi Zeroud. However, sedimentation was 6 times larger in Mejerda. If the first catchment is illustrating that the soils have already lost most of its soil particles, the Mejerda catchment gives us an idea about the long and short term human impacts. In fact, it allows us to assume a soil degradation cycle over the last 3000 years. Moreover, it reveals why floods became more frequent and how important sediment deposits were during a century. During the period 1900-1960, 1960-2000, and 2000-2007 the number of floods were 12, 7, and 3, respectively. The first period illustrates a watershed that has been used in a non-sustainable manner regarding its resources. The second period, displays great changes to the land by introducing big hydraulic structures that lead to noticeable decrease in overflows. The third period illustrates consequences of imbalanced population pressure over the rural landscape. We record frequent severe floods, excessive loss in the storage water capacity of reservoirs, poor water quality, deterioration and choking of the hydraulic structures. During millennia when water erosion became severs farmers utilized different small-scale hydro-agricultural techniques to uphold their farming activities. They were needed to store and to spread water for irrigation. Besides, they created new soil substratum downstream when upstream soils were eroded. Nowadays, these traditional techniques are more or less forgotten. In fact, the centralized water and soil management turned the rural community into a passive actor (Ennabli, 1993).

We cannot give up a watershed because it is eroded. The loss in the potential production of its arable lands must be regained. As well as its ability to store water. For this purpose, we must first define its degradation level which shows us its general behavior during exceptional events. History shows that it is important to promote balanced land settlements over the catchments. Small and big hydraulic structures have to complement each other and be constructed in order to control soil loss efficiently. Scientists and rural engineers have to jointly set up different scenarios due to catchment settlement. They need to take into consideration where the position of the hydrological unit is on the soil degradation cycle. When the sedimentological and hydrological characteristics continuously change due to the water erosion process, hydrological calculations and resulting parameters should be revised. This would necessitate a better participation by hydrological researchers in the technological development of agricultural management. Eventually, this approach would strengthen the

national policy for the water erosion control. Indeed it would better emphasize the plans of action and efficiency of the development of projects in soil and water conservation aimed at preserving the farming areas.

Acknowledgments Sihem Jebari thanks Prof. Fethi Lebdi head of the Tunisian National Institute of Agronomy (INAT), Dr. Taoufik Redissi from the National Institute of Patrimony (INP), Ms. Rabaa Ben Salah from the Department of Agricultural Production (DG/PA) and Mr. Mehdi Ben Haj from the Coastal Protection and Planning Agency (APAL), for the generous literature material, the interesting discussions and the valuable advice they provided.

REFERENCES

Abidi, M. (2007) Etude et modélisation de la dynamique fluviale de l'oued Mellegue en période de crue. M.Sc. Institut National Agronomique de Tunisie.

AIECM (1976) Actes du 2e Congrès International d'Etude des Cultures de la Méditerranée Occidentale. La société nationale d'édition et de diffusion, Alger.

Barjot, P. (1952) Le Golf d'Utique dans l'antiquité. Le dessin d'Utique, de Carthage et de Bizerte. Rev.gén. de l'hydraulique, **68**, 59-68.

Barkaoui, A. (2003) *La marine carthaginoise. Approche des activités militaires des carthaginois sur mer depuis les origines jusqu'en en 146 av. J.-C.* Publication de la Faculté des Lettres et des Sciences Humaines de Sfax. Ouvrage édité par l'Or du Temps.

Ben Mammou, A. (1998) Barrages Nebeur, Sidi Salem, Sidi Saad et Sidi Boubaker. Quantification, étude sédimentologique et géotechnique des sédiments piégés. Apport des images satellitaires. Thèse de Doctorat Es-sciences Géologiques. Université de Tunis II Faculté des Sciences de Tunis.

Bennet, H.H. (1950) *Manuel de conservation du sol N°53*. Publication du Département de l'Agriculture des Etats Unis.

DG/PA. (2008) Les terres céréalières en Tunisie : leurs distributions, leurs productions et leurs principales problématiques. *Atelier organisé par l'association des sols à l'UTAP en Juin.*

Bernard, C. (1911) Le golfe d'Utique et les bouches de la Medjerda. Extrait du bulletin de géographie historique et descriptive. Imprimerie Nationale de Paris.

Bouzaiane, S., Lafforgue, A. (1986) *Monographie hydrologique des oueds Zeroud et Merguellil.* Publication commune de la Direction Générale des Ressources en Eau et de Institut Français de Recherche Scientifique pour le développement en Coopération. Ministère de l'Agriculture.

Camps, G. (1979) Les numides et la civilisation punique. Dans Antiquités africaines, pp. 43-53.

Chelbi, F ., Paskoff, R., Trousset, P. (1995) La baie d'Utique et son évolution depuis l'Antiquité : une réévaluation géoarchéologique. Antiquités Africaines tome (31), 7-51.

Claude, J., Francillon, G Loyer, J.Y. (1977) Les alluvions déposées par l'oued Medjerda lors de la crue exceptionnelle de mars 1973. Cahier ORSTOM, *Sér. Hydrol.* **14,** 37–109.

CNRS (1994) Le ravitaillement en blé de Rome et des centres urbains des débuts de la république jusqu'au haut empire. *Actes du colloque international organisé par le Centre Jean Bérard et l'URA 994*. Naples, 14-16 Février.

Coignet, J. (1917). La Medjerda : Hydraulique en Tunisie et les grands barrages réservoirs. Bureau d'inenieurs conseils Coyne & Bellier, Paris.

Collet, C. (1953) Les moyens mis en œuvres en Tunisie pour l'étude des crues de la Medjerda. La *Houille blanche*, p. 395-408.

Coripe, Inscriptionum Simiticarum (C.I.S), I, Pars prima (Paris, à partir de 1881).

Decret, F., Fantar, M. (1981) *L'Afrique du nord dans l'antiquité. Histoire et civilisation des origines au Ve siècle*. Edition Payot, Paris.

DG/ACTA (1993) *Stratégie nationale pour la conservation des eaux et des sols*. Publication de la Direction de la Conservation des Eaux et des Sols. Ministère de l'Agriculture et des Ressources Hydrauliques.

DGRE (1983) Carte du réseau hydrographique Tunisien ; Echelle 1/1000000. Reproduction de l'Office de la Topographie et de la Cartographie.

DGRE (2006) Actualisation de la courbe de tarage de la station de Jedeida au pont route n°7. Note interne de la Direction Générale des Ressources en Eau.

El Amami, S. (1984) *Les aménagements hydrauliques traditionnels de Tunisie*. Centre de Recherche du Génie Rural. Ministère de l'Agriculture.

El Bekri, « Description de l'Afrique septentrionale ». Textes traduits de l'arabe par De Slane (1913).

Ennabli, N. (1993) *Les aménagements hydrauliques et Hydro-Agricoles en Tunisie*. Institut Nationl Agronomique de Tunis. Ministère de l'Agriculture et des Ressources Hydrauliques.

Ennabli, N. (Tunis 1995) *L'irrigation en Tunisie*. Institut National Agronomique de Tunis. Ministère de l'Agriculture et des Ressources Hydrauliques.

Ennabli, N. (2001) Les circuits hydrauliques. Institut National Agronomique de Tunis.

FAO (1996) *Introduction à la gestion conservatoire de l'eau de la biomasse et de la fertilité des sols (GCES).* Bulletin pedologique (70).

Floury, C. (2003) Modélisation de la dynamique fluviale de l'oued Mejerda pendant les inondations de Janvier-Février 2003 en Tunisie. Projet de fin d'études de l'école Nationale Superieure d'Agronomie de Rennes.

Gammar, A.M. (1979) Etude et carte écologique de la région de Kessra (Dorsale Tunisienne). Thèse de Doctorat de 3eme cycle. Université Scientifique et Médicale de Grenoble.

Gammar, A.M. (1995) La dorsale Tunisienne, entre représentation linéaire et réalité régionale. *Actes du 2eme colloque du département de géographie du 14-16 Décembre*. Publication de l'Université de Tunis I, Faculté des lettres Manouba.

GOPA & GTZ (2005) *Elaboration d'une stratégie nationale d'adaptation de l'agriculture tunisienne et des écosystèmes aux changements climatiques*. Pré-rapport 1ère phase.

Gsell, S. (1921) Histoire ancienne de l'Afrique du Nord. Ed. Hachette, 1992, t. I, 544 pp. (1).Paris.

Jaidi, H. (1990) L'Afrique et le blé de Rome au IVeme et Veme siècle. Serie histoire, volume XXXIV. Publications de la Faculté des Sciences Humaines et Sociales de Tunis.

Jausein, A. (1971) *Les agents de la morphogenèse. Evolution récente du delta de la Medjerda*. Cours et documents du Laboratoire de Géologie. Ecole Normale Supérieure, Université de Paris VI.

Jebari, S. (2003) Les methodes traditionnelles de CES et l'initiative Wocat. Rapport interne de l'Institut National de Génie Rural, Eaux et Forets. Ministère de l'Agriculture et des Ressources Hydrauliques.

Jebari, S., Berndsson, R., Bahri, A. & Boufaroua, M. (2009) Spatial soil loss risk and reservoir siltation in semiarid Tunisia. Accepted for publication in Hydrogical Sciences Journal.

Kassab, A. (1979) L'évolution de la vie rurale dans les régions de la moyenne Medjerda et de Bèja-Mateur. Thèse de Doctorat Es-Lettres, Géographie. Faculté des Lettres et Science Humaines de Tunis.

Knight M.M. (1928) Water and the course of empire in north Africa. [http://www.jstor.org. date of access 2007].

Lancel, S. (1999) *Carthage*. Cérès édition. Librairie Arthème Fayard.

LCHF , (1978). Etudes des problèmes sédimentologiques du port de Gar El Melh. Rapport général n° R79017 établi pour le compte du Ministère de l'Equipement.

Lebdi, F., Fdhila, M.K. & Hzami, A. (2006) Modélisation de la dynamique fluviale de la Medjerda : impact de l'évolution morphologique du lit sur l'écoulement. Conférence scientifique internationale " L'avenir des terres sèches : cas du bassin Méditerranées ". Tunis, 19-21 Juin.

Lepelly, C., Dupuis, X. (1999) Frontières et limites géographiques de l'Afrique du nord antique. *Actes de la table ronde réunie à Paris les 2-3 Mai*. Publication de la Sorbonne.

Louati M.H. et al (1998) Eau 21. Strategie du secteur de l'eau en Tunisie à long terme 2030. Ministère de l'Agriculture et des Ressources Hydrauliques.

Lowdermilk, W.C. (1953) Conquest of the land-Through seven thousand years. [http://www.amazon.fr/Conquest-land-through-years-Lowdermilk/dp/B0017XT474 date of access 2007].

MARH (2000) Eau 2000. Ministère de l'Agriculture et des Ressources Hydrauliques.

Mahjoubi, A. (1992) La province romaine d'Afrique à la fin de l'époque sévérienne (235 ap. J.C.) – in « Atlas National de Tunisie », Centre d'études et de recherches Economiques et Sociales, Tunis.

Meyran, R. (2008) Les derniers jours de Carthage. Dans « Les cahiers de science et vie », 104.

Niox, C. (1890) Géographie militaire (VI) – Algérie et Tunisie. Destiné par [http://aj.garcia.free.fr. date of access 2005].

Oueslati, A . , Charfi, F. , Baccar, F. (2006). La basse vallée de oued Mejerda et la lagune de Ghar El Melh. *Wadi Project fifth international meetin*g. Tunis 6-9 December.

Paskoff, R . , Trousset P. (1993) L'ancienne baie d'Utique : du témoignage des textes à celui des images satellitaires. Mappemonde.

Paskoff, R., (1985) Les plages de la Tunisie. Editec, Caen, 198 p.

Peyras, J. (1991) *Etude d'antiquités africaines. Le tell Nord-Est tunisien dans l'antiquité. Essai de monographie régionale*. Editions du Centre National de la recherche scientifique, France.

Pimenta, J. (1959) Le cycle Pliocène actuel dans les bassins paraliques de Tunis, 171 p. Mém. Soc. Géol. De France, n° 85.

Pline l'Ancien, Naturalis Historia, éd. C. Mayoff, coll. Teubner (5 vol.), 1892-1909 (reprod. 1967).

Polybe, éd. Th. Büttner-Wobst, coll. Teubner, 1882-1904 (rééd. 1962-1963); trad. Française de D. Roussel, coll. « La Pléiade », 1970.

Reyniers, F. (1952) *Port à Utique*. Correspondance de la société des antiquaires de France.

Rougé, J. (1975) La marine dans l'Antiquité. Presses Universitaires de France.

Sakiss, N., Ennabli, N., Slimani, M.S., Baccour, H. (1994) *La pluviométrie en Tunisie a-t-elle changé depuis 2000 ans ?* Production commune de l'Institut National de la Météorologie, Institut National Agronomique de Tunisie et l'Agence Nationale de Protection de l'Environnement. République Tunisienne.

Sakiss, N., Ennabli, N., Slimani, M.S. (1991) *La pluviométrie en Tunisie.* Ouvrage édité par l'Institut National Agronomique de Tunis et l'Institut National de la Météorologie. République Tunisienne.

Slimani, M.S. (2001) *Les inondations en Tunisie.* Rapport interne de l'Institut National Agronomique de Tunis.

Silius Italicus, la guerre punique, VI, trad. Miniconi, P., et Devallet, G., Paris, 1981, p .38.

Studi-Apal (2001) Etude de protection du site abri de pêche côtière de Kalaat Landlous. Rapport phase II. Etude faite pour le compte des Ministères de l'Agriculture et des Ressources Hydraulique et de l'équipement et de l'habitat.

Sect-Tunisie-Apal (2005) Campagne de reconnaissance de gites de sable en mer pour le rechargement de plages sous lot nord. Etude réalisé pour le compte du Ministère de l'Environnement et du Développement Durable.

SOGREAH, (1992) Cité touristique de Gar El Melh. Etude préliminaire des problèmes d'hydraulique et connexes. Rapport n°351486 établi pour le compte de KAL Tunisie.

Tissot, C. (1884) Géographie comparée de la province romaine d'Afrique. Imprimerie nationale,Paris.

Zahar, Y., Ghorbel, A., Albergel, J. (2008) Impact of large dams on downstream flow conditions of rivers: Aggradation and reduction of the Medjerda channel capacity downstream of the Sidi Salem dam Tunisia). *J. Hydrol*. **326**, 318 330.

Sediment, discharge and precipitation variation in the wadi Mellegue catchment during the 50 past years

Sihem Jebari[(1)], R. Berndtsson[(2)], Fathi Lebdi[(3)], & Akissa Bahri[(4)]

[1]*Institut National de Recherches en Génie Rural, Eaux et Forêts, B.P.N°. 10, Ariana 2080, Tunisie. Tel : 216-230039, Fax : 216-717951, E-mail: Sihem.jebari@iresa.agrinet.tn*
[2]*Department of Water Resources Engineering, Lund University.*
[3]*Institut National Agronomique de Tunisie.*
[4] *International Water Management Institute, PMB,CT 112, Cantonments Accra, Ghana.*

ملخص - تغيرات الرواسب، التدفق و الأمطار في حوض وادي ملاق طيلة الخمسون سنة الماضية. يعتبر انجراف التربة مؤشرا للتغيرات الهيدرولوجية و المناخية، وهو يؤدي في المنطقة الشبه الجافة التونسية إلى تراكم الترسبات وسط السدود مما يقلل من قدرتهم على الخزن بصفة سريعة. كما يؤثر بصفة سلبية على النتائج الاقتصادية والبيئية بصفة عامة و ذلك نظرا لما ينجر عنه من نقصان في حجم المياه المخزنة و الصالحة للري و الشراب كما أن له عواقب متعلقة بالوقاية ضد الفيضانات. وفي هذا الإطار وقع اختيار حوض ملاق للقيام بالدراسة الحالية مساهمة منا في رصد ظاهرة الانجراف المائي، معتمدين في ذلك على أهم النشريات العلمية و بعض تقنيات التحليل الإحصائي، نذكر من أهمها: الارتداد الخطي وتحليل الاتجاه حسب "مان كندال". و قد وقع تطبيقهما على مستوى المعطيات الخاصة بالترسبات و التدفق و الأمطار بالنسبة للمدة الزمنية التي تغطي الخمسين سنة الأخيرة.كما تقترح هذه الدراسة مناقشة جميع أنماط التغيرات التي وقع رسمها بالنسبة لهذه البارامترات. و من المتوقع أن النتائج المتحصل عليها من خلال هذا البحث ستكون جد مفيدة على مستوى المشاريع التنموية المبرمجة خلال السنوات المقبلة، و نذكر منها خاصة تحديد مدة استغلال وصلوحية السدود، تخفيف وطأة الفيضانات و أخيرا إحكام وترشيد التصرف في الأودية.
الترسبات/ التدفق/ الأمطار/ تحليل الاتجاه/ وادي ملاق /المناخ الشبه الجاف التونسي.

Summary - Sediment, discharge, and precipitation variation in the "wadi Mellegue" catchment during the 50 past years. Soil erosion is an indicator of hydrological and climatic change. It leads to siltation which has direct, negative, economic and environmental consequences on society. In fact, less siltation means more water for irrigation, water supply, and better flood control. This is especially important in the Tunisian semiarid regions where water needs are close to potential water resources and siltation is reducing the reservoir capacity rapidly. "Wadi Mellegue" in (semi-arid) central Tunisia was chosen in order to study possibilities for water erosion prediction. Trend and variational analyses were performed to study sediment, discharge, and precipitation patterns in the area during the latest 50 years. The results may be used to predict erosion and reservoir capacity decrease as well as flood mitigation and the fluvial management for the next decades.
Discharge / precipitation / semi-arid / siltation / time series / trend / Tunisia

Résumé - Variabilité de la sédimentation, du débit et des précipitations au bassin versant"Oued Mellegue" à travers les cinquante dernières

années. L'érosion des sols est un indicateur hydrologique pour l'étude du changement climatique. Elle entraîne aussi l'envasement de l'infrastructure hydraulique qui, à son tour présente des conséquences négatives d'ordre économique et environnemental pour la société en général. En effet, moins d'envasement signifie une meilleure disponibilité de la ressource pour l'irrigation, pour l'eau potable et pour une meilleure protection contre les inondations etc. Ceci est d'autant plus important dans la région semi-aride Tunisienne où les besoins en eau sont proches du volume de la ressource en eau mobilisable et où l'envasement ne cesse de réduire rapidement la capacité de stockage des réservoirs d'eau. "Oued Mellegue", au semi aride tunisien, a été choisi pour caractériser la variabilité et définir la tendance de la sédimentation, du débit et de la pluie. La présente analyse concernera les cinquante dernières années d'observation. Les résultats recueillis peuvent être utiles pour prévoir le phénomène d'érosion hydrique, pour estimer la durée de vie des ouvrages de stockage d'eau et pour permettre une meilleure gestion des cours d'eau pour les prochaines décennies.
Débit / pluie / semi-aride / sédimentation / tendance / Tunisie

1. INTRODUCTION

Water erosion processes are sensitive to climatic change and anthropogenic effects. These conditions have tremendous consequences on reservoir siltation which are of great international concern (Coppus et al., 2002; Goel, 2005). Trend analysis is often carried out to assess the human impact on the environment under the influence of natural fluctuations. Detection of temporal trends is one of the most important objectives for climatic, hydrological, and siltation monitoring (Jonsdottir et al., 2006; Zhang et al., 2006). Therefore, a variety of statistical procedures have been developed to distinguish between random fluctuations and more persistent temporal changes in general that are also useful in the water and soil field in particular.

Tunisia is one of the countries where are storage of water resources in reservoirs is important. It is expected that from now on until 2030 the Tunisian reservoir capacity will gradually decrease with 40 million m^3 per year due to siltation (GOPA & GTZ, 2005). In order to balance this lost capacity, maximum dam heights are increased and construction of new reservoirs are planned.

Recent research indicates that the prediction of sediment yield is one of the main challenges in soil erosion studies. The objective of this paper is hence to analyse the sedimentation trend which is highly correlated with rainfall conditions in Tunisia. The utilized data are from the Mellegue catchment which discharges into one of the oldest reservoirs in Tunisia. For this reason the catchment conditions are also closely monitored. Precipitation, discharge, and sediment load observations were analyzed in this paper to better understand the causes of siltation and its temporal pattern for the

Mellegue reservoir. Results of these analyses would enable decision makers and engineers to improve the management of water and soil resources throughout the Tunisian semiarid area.

2. DATA

In this study we used daily precipitation at Kef (1915-2005), Mellegue (1947-2006), and K13 (1959-2006). The time series used thus had a duration of 90, 59, and 47 observation years. The K13 station is situated 25 km upstream of the Mellegue reservoir and monitors maximum discharge and suspended sediment load. Sediment concentrations were collected daily, but during floods they were collected hourly. The K13 is a hydrometric station operating since 1923. However, in this study 50 years of data only were used, namely, from 1955 to 2005.

The general situation, the drainage area, and monitoring stations are presented in Fig. 1. The reliability of the data has previously been controlled by the DG/RE (Department of Water Resources) and DG/EGTH (Department of study and construction of big hydraulic infrastructure). Missing data correspond to about 3%. Both serial and residual correlation analysis was performed. The seasonality was also checked before proceeding with significance of trend by Mann-Kendall test.

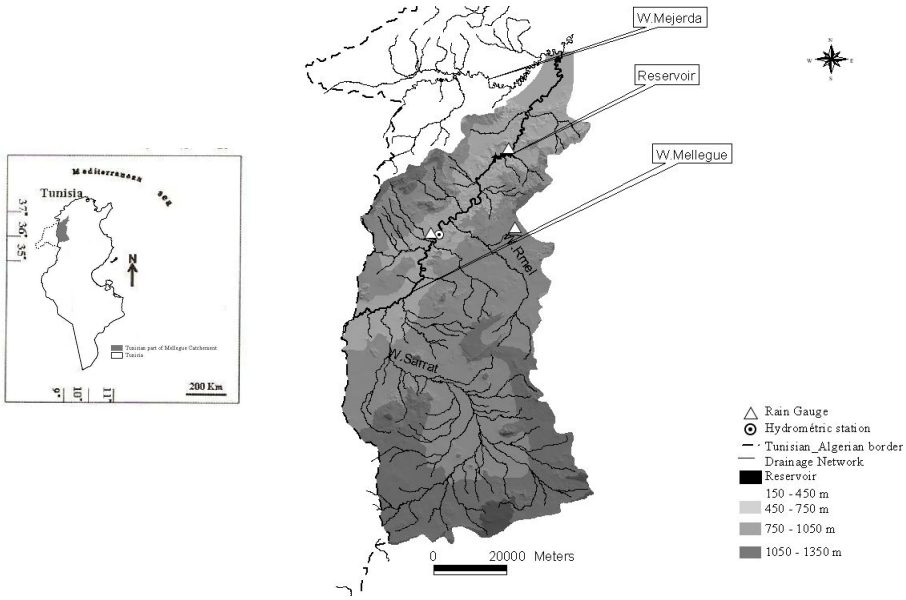

Figure 1: Drainage area and monitoring stations for the data analysed in the current study

3. METHODOLOGY

Analyses of trend in precipitation, discharge, and sedimentation time series may explain natural and anthropogenic effects in prevailing climatic conditions. The current research used simple linear regression to detect the trend followed by a Mann-Kendall test (e.g., Salas, 1993) to determine the trend and its statistical significance at 95% level. The Mann-Kendall test is a non-parametric test commonly used to assess the trend in the hydrometeorological time series (Zhang and Zwier, 2004). The two methods are complementary. Accordingly, the linear regression fits a linear equation to data. However, the Mann-Kendall method does not assume a distribution of the data but requires non-seasonality and no autocorrelation for the data and the residual series. The above procedure was used to analyse all data used in the current work, namely: daily, monthly, and annual precipitation time series. Moreover, the number of rainy days according to two thresholds and maximum discharge, and sediment load were also used in the analyses. The two thresholds mentioned above are 3 and 12 mm per day. They are related to the water erosion process and used to be considered per event (Kowal et al 1976; Wischmeier and Smith 1998). The first value corresponds to the triggering of the erosion process and the second concerns all erosion processes. The time series of number of days described as being superior or inferior to the two thresholds were also analysed.

4. RESULTS

The results of the trend analysis related to annual precipitation display a significant negative trend for the Kef station. For monthly data, the same station displays a significant negative trend for November, December, January, February, and March (Fig. 2). It displays a significant positive trend for August. The Mellegue station displays a significant negative trend for October and K13 a positive significant trend for September.

The number of rainy days during a year shows a significant positive trend at Kef. However, according to the different months they are mainly significant in September, April, May, June, and August.

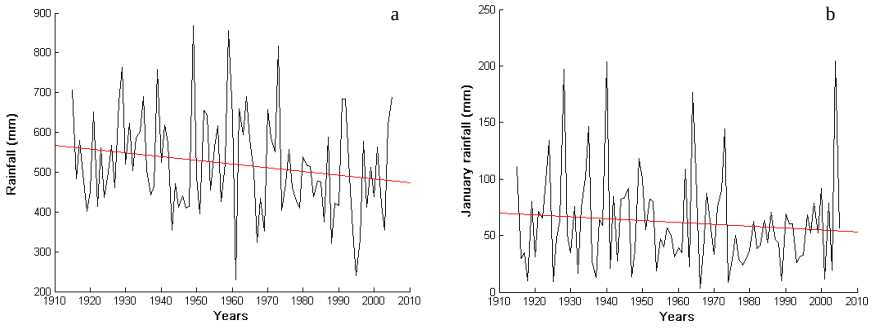

Figure 2: (a) Negative significant trend of the annual rainfall at the Kef station. (b) Negative significant trend of the January rainfall at the Kef station.

The yearly and the monthly precipitation time series for data inferior to 3 mm present a positive significant trend almost for every month. Yet, the number of days that have more than 3 mm displays a significant negative trend. This is also the case for October, November, December, January, February, and March. The significant positive trend characterizes September and August. Daily rainfall that is superior to 12 mm for annual and monthly values show a significant negative trend (Fig. 3).
Concerning the maximum discharge and sedimentation load, these display a positive but non-significant trend. This is also the case for the sediment load at the K13 station (Fig. 4).

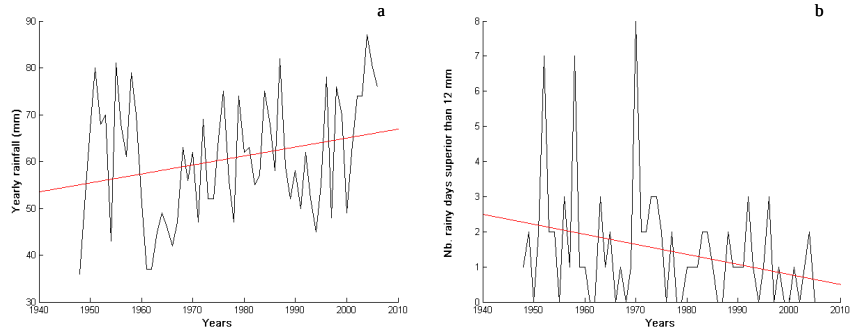

Figure 3 : (a) Positive significant trend related to the number of annual rainy days. (b) Negative significant trend for daily rainfall that are superior to 12 mm at Mellegue station.

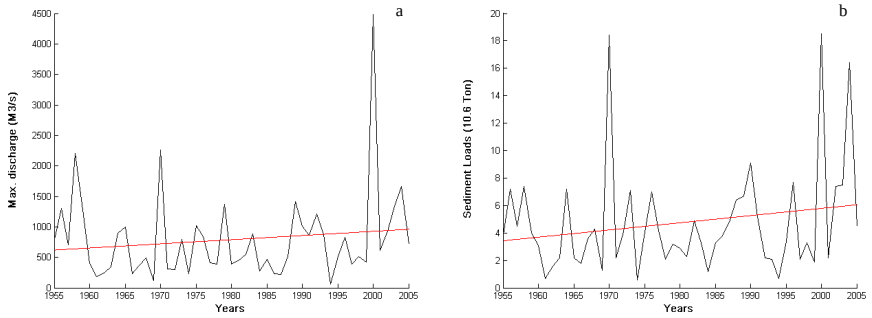

Figure 4: (a) Positive but non-significant trend for the maximum discharge at K13 station. (b)Positive non significant trend of the sediment load at the K13 station.

5. CONCLUSION

Time series for annual and monthly rainfall depth as well as the number of rainy days per year show significant trends. Moreover, we notice that the 3 mm rainfall depth is prevailing over the 12 mm daily rainfall depth. These facts are mainly controlled by climate variability. The decreasing daily rainfall depth concerns mainly and exclusively the rainiest months. This will probably mean less stored water in the soil and also in the reservoirs. Less erosive rainfall does not seem to reduce the water erosion process since the sediment load shows a positive (however non-significant) trend. The same tendency is also displayed by the maximum discharge which probably means that bare soil is becoming more common over the catchment. Finally, the dryer climate in semiarid Tunisia decreases the volume of water and impoverishes the soil cover. This would make the soil surface an easier and easier prey for the erosion phenomenon.

ACKNOWLEDGEMENTS

The authors thank Mr. M.Saadaoui from the DG/RE (Department of water resources) and K. Jammali from DG/EGTH ((Department of study and construction of big hydraulic infrastructure) for the help and for valuable time and discussions allocated to this work.

REFERENCES BIBLIOGRAPHIQUES

Coppus R., Imeson A.C., 2002 - Extreme events controlling erosion and sediment transport in a semi-arid sub-andean valley. Earth Surface Processes and Landforms 27: 1365-1375.

EGTH., 2005 - L'envasement de Mellegue après ½ siècle d'existence. Ministère de l'Agriculture et des Ressources Hydrauliques. Direction Générale des Barrages et des Travaux Hydrauliques.

Goel AK, Kumar R., 2005 - Economic analysis of water harvesting in a mountainous watershed in India. Agricultural Water Management 71: 257-266.

GOPA-ExaConsult., 2006- Stratégie nationale d'adaptation de l'agriculture tunisienne et des écosystèmes aux changements climatiques. République tunisienne, Ministère de l'Agriculture et des Ressources Hydrauliques & Coopération Technique Allemande.

GOPA&GTZ., 2005- Elaboration d'une stratégie nationale d'adaptation de l'agriculture tunisienne et des écosystèmes aux changements climatiques. Pré rapport 1ere phase.

Jonsdottir J.F., Jonsson P., Uvo B.C., 2006 - Trend analysis of Icelandic discharge, precipitation and temperature series. Nord. Hydrol. 37: 365-376

Kowal J.M., Kassam A.H., 1976- Energy load and instantaneous intensity of rainstorms at Samaru Nigeria. Tropical Agric. 53: 185-197.

Salas, J.D., 1993- analysis and modeling of Hydrologic time series. In D.R. Maidment (Ed), Handbook of Hydrology, McGraw-Hill, New York, chapter 19.

Wishmeier W.H., Smith D.D., 1978- Predicting rainfall erosion losses- a guide to conservation planning. USDA Agriculture Handbook 537, Washington D.C: GPO.

Zhang, X.B. and Zwiers F.W., 2004- Comment on "Applicability of prewhitening to eliminate the influence of serial correlation on the Man-Kendall test" by Sheng Yue and Chun Yuan Wang. Wat.Res.Res., 4, (30), W03805.

Zhang Q., Xu C., Becker S., Jiang T., 2006- Sediment and runoff changes in the Yangtze River basin during past 50 years. Jour. Hydrol., 331, 511-523.

Exceptional Rainfall Characteristics Related to Erosion Risk in Semiarid Tunisia

S. Jebari[1*], R. Berndtsson[2], A. Bahri[3], and M. Boufaroua[4]

[1]*National Research Institute for Rural Engineering, Waters, and Forestry, Box 10, Ariana 2080, Tunis, Tunisia;* [2]*Department of Water Resources Engineering, Lund University, Box 118, S-22100 Lund, Sweden;* [3]*International Water Management Institute, PMB, CT 112, Cantonments Accra, Ghana;* [4]*Farmland Conservation and Management Department, 30, Alain Savary Street, 1002 Tunis, Tunisia.*

Abstract: The Tunisian Dorsal area is representative of the semiarid Mediterranean region in terms of water resources availability as well as exceptional rainfall characteristics, runoff generation, and soil loss risk. In this context, soil properties, surface management practices together with highly intensive rainfall make the soils vulnerable to erosion. If the exceptional rainfall characteristics are linked to different erosion types, the erosion risk could be evaluated in a simple and straightforward way. In this regard, a short time-scale rainfall data base from the Dorsal area was analysed in the paper. The procedure used involves finding a representative duration between 1-60 min for the exceptional rainfall characteristics. Rainfall intensities of different return periods are then related to the different erosion types. The identified exceptional rainfall durations between 1-60 min were analyzed in terms of number of events, depth, average intensity and maximum intensity. Results show that the 15-min duration maximum intensity can be used to evaluate erosion risk based on soil erosion type. The developed methodology can be used to evaluate erosion risk in semiarid regions based on exceptional rainfall characteristics. In practical terms the results can be used to better manage catchments that are vulnerable to soil erosion.

1. INTRODUCTION

High-intensive rainfall contributes to water erosion and sediment transport (e.g., [1-5]). Consequently, strong links exist between storm rainfall characteristics on the one hand and eroded soil amount on the other hand (e.g., [6-10]). During the last decades much experimental and laboratory research work dealing with the relationship between rainfall characteristics and sediment concentration has been performed (e.g., [11-15]). Non-availability of recorded short-term rainfall data appears to be a major limitation for statistical modeling of soil erosion risk [16]. Observation of hydrological variables in small watersheds at sufficient detail is often lacking [17-19]. This is especially a drawback for areas in the semiarid Mediterranean and the Middle East, since the soil erosion is severe there [20]. These areas often display hydrological changes. The latter, are a combination of climate-induced and anthropogenic effects related to land and water management [21].

Exceptional rainfall events are responsible for most soil erosion occurring under semiarid Mediterranean conditions [5]. According to the above, the objective of this paper is to determine the erosion risk by analyzing intensive rainstorms in semiarid Tunisia. And this, considering the maximum intensity characteristics and the links to soil erosion type. The utilized data are part of a unique high-resolution rainfall data base from 28 catchments collected during an EU-funded project [22]. The paper firstly describes the data base and collection methods. After this, maximum intensities for 1-60 min durations within rainfall events are analyzed. Selected durations of these exceptional intensities are related to the risk for different soil erosion types. Finally, practical applications of the results are discussed.

*Address correspondence to this author at the National Research Institute for Rural Engineering, Waters, and Forestry, Box 10, Ariana 2080, Tunis, Tunisia; Tel: + 216 71 230 039 ; Fax: + 216 71 717 951;
E-mail: sihem.jebari@iresa.agrinet.tn

2. MATERIAL AND METHODS

2.1. Study Area and Observed Network

The Dorsal Mountains represent the last part of the Atlasic Mountain range toward the east (Fig. **1**). The major peaks correspond roughly to 1000 m a.m.s.l. The mountains are often described as the southern boundary of northern Tunisia. The Dorsal corresponds approximately to the 400 mm/year rainfall isohyet (Fig. **1**). Although the annual amount is small, rainfall is often characterized by intense storms during some periods of the year. Annual variation ranges from 250 to 550 mm. Both annual and monthly rainfalls are characterized by a large irregularity. The spatial characteristics of fine time-scale rainfall through the Dorsal were analyzed in a previous study [23]. This paper deals with the statistical time patterns of rainfall and links to soil erosion risk.

Due to specific bioclimatic conditions of the Mediterranean climate, the soils are better characterized by the degradation of rock material rather than their organic matter content. Consequently, they are not well developed and often quite shallow. Moreover, soil erosion is a serious problem throughout the Dorsal area. The soil degradation that characterizes the Dorsal has led to serious soil erosion causing a thinner and uneven soil cover, that display the underlying bare bedrock. It has been estimated that 7% of the area are badly damaged by erosion and 70% are moderately damaged. During the decadal strategies, the Dorsal area management was based on water and soil conservation practices that covered about 20% of the total area.

1874-3781/08

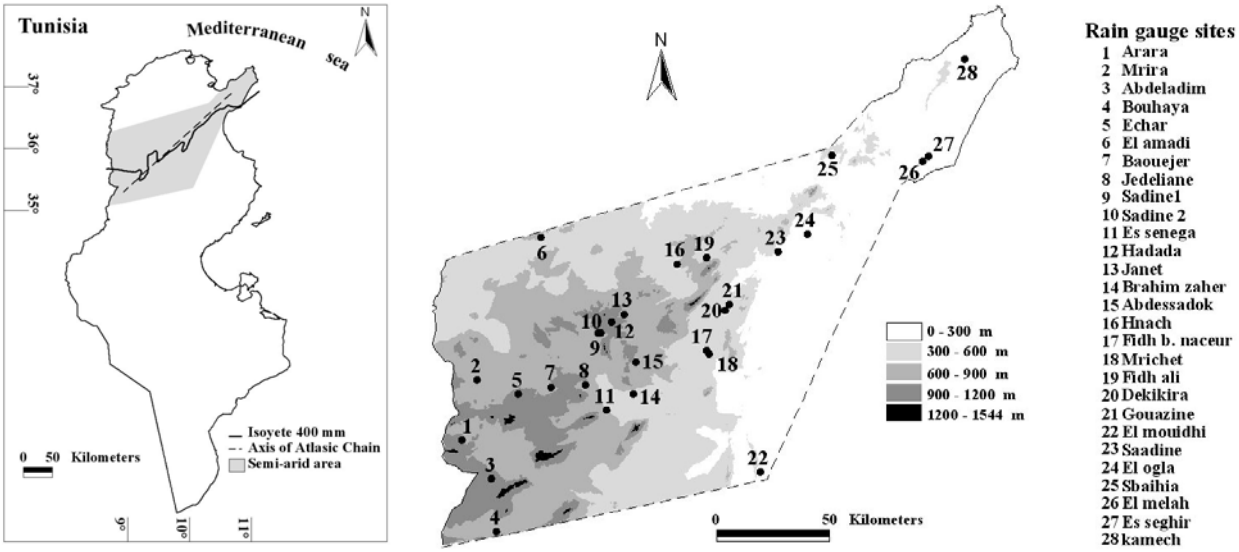

Fig. (1). Study area and observation network.

In general, the mean annual soil loss in semiarid Tunisia is about 11.5 metric tons/ha/year. This figure was determined according to the deposited sediment volume in the bottom of reservoirs. Wischmeier and Smith [24], amounted soil loss tolerance to 12 tons/ha/year. This value is defined as "the maximum level of soil erosion that will permit a level of crop productivity to be sustained economically and indefinitely". Experiments throughout the Tunisian semiarid area have determined the average tolerable soil loss [25]. This is estimated to be respectively about 2.5, 5, and 10 tons/ha/year for thin, average and thicker soil. With a very slow rate of soil formation in some parts of the Mediterranean region, any soil loss more than 1 ton/ha/year can be considered as irreversible within a time span of 50-100 years [26].

The rainfall gauge monitoring network covers 28 experimental catchments (Table **1**). The observation network was set up through the EU-funded Programme HYDROMED (Research program on hill reservoirs in the semiarid Mediterranean periphery, 1992-2002; [27] [22]. At present it is managed by the Tunisian Farmland Conservation and Management Department (DG/ACTA). Each catchment discharges into a small reservoir. An automatic rain gauge is located at each site on the dike itself, as well as an automatic water level recording.

2.2. Rainfall Characteristics and Soil Erosion Processes

Raindrop impact initiates detachment of soil particles (rain splash) and causes crust formation [28-30] which seals the surface and limits the infiltration. Once the rainfall intensity exceeds the infiltration rate of the soil, overland flow of water occurs across the land surface, generating hydraulic forces that erode and transport sediments in a down-slope direction [31]. In the Mediterranean areas, very low values of saturated hydraulic conductivities are often found after 10 min of simulated rain [32]. As a consequence of weak aggregate stability of the soil surface, rainfall is often laterally distributed by Hortonian overland flow even for low intensity rainfall [33]. Runoff is the most important direct driver of severe soil erosion [28]. It often occurs at catchment scale, when rainfall intensities reach a minimum threshold of about 25 mm/h in 10 min [e.g., 34]. For other semiarid areas, observations have shown that about 15 mm rain may be needed to produce 1 to 2 mm of runoff [2]. High-intensity rainfall events affect runoff generation and erosion processes which are known to be highly non-linear [35]. This is also considered as the major contributor to long-term soil loss [36-38]. The lowest rainfall intensities leading to runoff on humid soil range from about 2 to 23 mm/h in Tunisian semiarid areas [39].

Rainfall characteristics determine the erosive action of raindrops and overland flow. They also define the most common water erosion processes namely, interrill, rill, and gully erosion. Interrill erosion concerns uniform removal of soil and is assumed to be the first phase of the erosion process. It affects the largest areas and is of main importance in the erosion process [15] [28]. When overland flow is concentrated in well defined incisions in the soil surface, turbulent flow occurs and small rivulets are formed. This is known as rill erosion. The rill erosion amount increases with growing water inflow rate and slope [40]. Under extreme storms, rill erosion progresses to gully erosion. the latter, results in large incisions which cause severe damage to the landscape [41] [42] [31]. Gullies increase the connectivity of the drainage system, and seem to be a main component in sediment delivery [43].

Return period intervals that characterize the rainfall events are crucial in describing the erosion impacts on the landscape. Bull [44] and Hooke [1], showed that important events transporting sediments have a return period of more than 1 to 7 years. Garcia-Ruiz et *al*. [45] and Coppus et *al*. [2] described 1-year return period events as mobilizing bed load and 5-year return period events as mobilizing small rock avalanches and channelizing debris flows. According to [46], events with an occurrence of 5 to 15 years considerably change the valley floor. Harvey [47] showed that 25-year event rainfall can modify the channel morphology. Finally, the 100-year return period rainfall shows reactivation of large, deep mass movements and exceptional events with a return period that exceeds 100 years are considered to be a catastrophic geomorphic process [45] [2].

Table 1. Description of Observed Rainfall Events for the Dorsal Experimental Rainfall Network (1993 to 2003).

Rainfall Gauge	Events/Year	Mean Event Depth (mm)	Mean Event Duration (min)	Mean Event Int. (mm/h)	Max. Event Depth (mm)
1. Arara	100.7	2.1	77	4.0	40.0
2. Mrira	126.1	2.4	77	7.3	84.5
3. Abdeladim	116.6	2.4	74	3.8	52.0
4. Bou Haya	76.8	2.7	72	5.6	38.0
5. Echar	133.8	2.4	76	4.3	53.5
6. El Amadi	180.7	3.6	94	3.8	113.0
7. Baouejer	155.2	2.1	75	6.4	31.0
8. Jédéliane	100.0	2.9	80	4.1	79.0
9. Sadine1	165.9	2.7	86	4.8	107.5
10. Sadine 2	150.6	2.6	91	3.4	64.5
11. Es Senega	88.8	3.0	76	4.3	58.0
12. Hadada	170.5	2.2	84	3.5	33.5
13. Janet	144.2	2.7	84	3.8	65.5
14. Brahim Zaher	77.7	2.6	73	4.5	36.0
15. Abdessadok	106.5	3.0	82	4.2	78.0
16. Hnach	120.1	2.6	84	3.5	59.5
17. Fidh b. naceur	83.2	2.9	78	5.9	42.0
18. Mrichet El Anze	136.3	2.9	89	3.5	73.0
19. Fidh Ali	84.7	3.1	77	7.7	55.0
20. Dekikira	96.3	3.0	84	6.7	72.5
21. El Gouazine	103.1	3.0	83	4.8	84.5
22. El Mouidhi	68.7	3.5	81	5.3	53.5
23. Saadine	103.8	3.3	81	4.6	74.5
24. El Ogla	107.9	3.2	84	3.5	84.5
25. Sbaihia	135.6	2.9	85	3.5	78.0
26. El Melah	132.3	3.4	88	3.7	56.0
27. Es Seghir	135.3	3.1	85	2.9	91.0
28. Kamech	174.4	3.1	78	5.2	125.5

2.3. Rainfall Data and Treatment

Twenty eight rainfall gauges from the hydrological network were used in this study (Fig. **1**). Missing data were less than 1% and the gauging density corresponds to approximately 1 gauge per 24 km^2 catchment area. Table **1** gives descriptive statistics for recorded rainfall events during the analyzed 10-year period (1993-2003). The rain gauges are fully automatic and provide an accuracy of ±4% up to 250 mm/h intensity for a 5-min time step. However, observed rainfall intensity is available down 1-min values [48]. Rainfall intensities could be computed with great accuracy for the range of durations used in the current study. Rain gauges are of tipping bucket type connected to a logger recording data every minute. A total of about 27000 station rainfall events were included in the present analysis. A rainfall event was defined as separated from another event if a rain gauge showed less than one tip per hour. For each rainfall event, duration, accumulated depth, average, and maximum intensity for 1, 2, 5, 10, 15, 20, 25, 30, 45, and 60-min durations were determined. Corresponding maximum intensities are hereafter named I_1-I_{60}. The events with maximum intensities corresponding to a return period superior to one year were kept for further analyses. These events are called exceptional rainfall events. It should be noted that exceptional events of

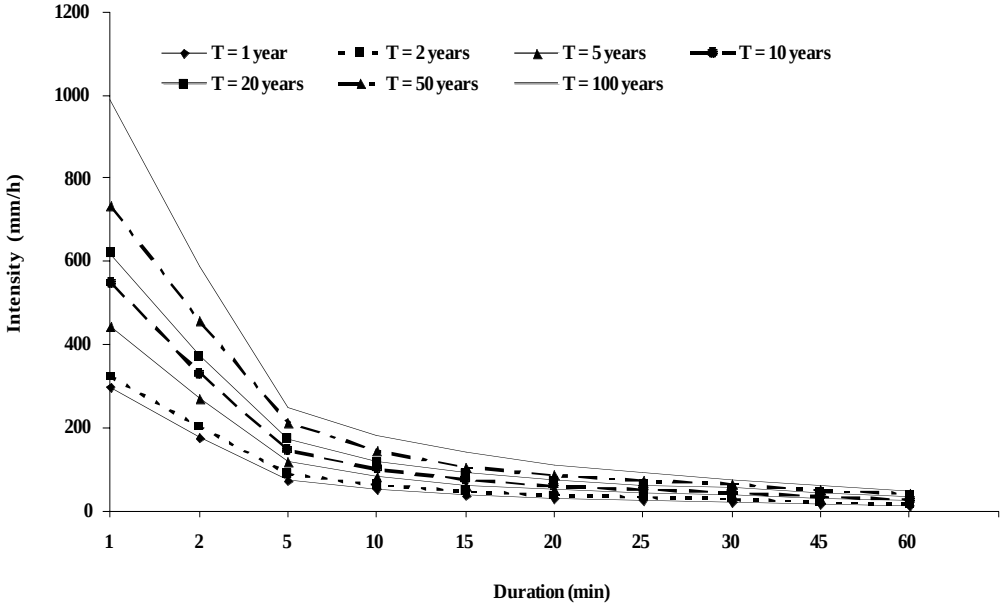

Fig. (2). Intensity-duration-frequency (IDF) curves for short-term rainfall in the Tunisian semiarid region (1964 – 2003).

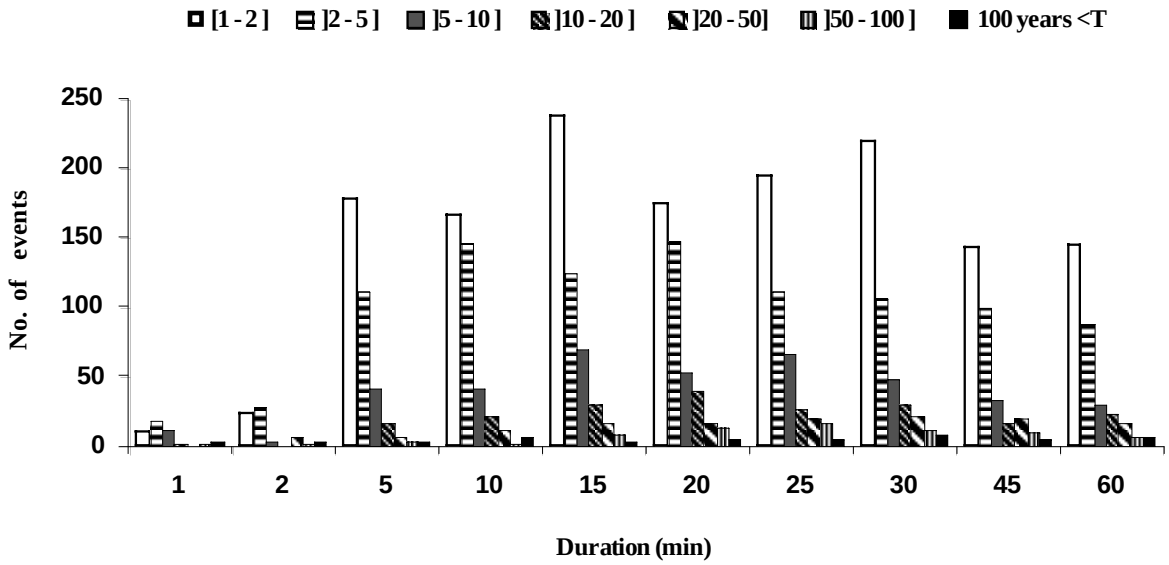

Fig. (3). Identified exceptional rainfall events depending on duration and return period (in total 3350 station events).

certain duration often contain exceptional events with shorter duration.

In order to evaluate the representativity of the observation period as compared to long-term rainfall conditions a number of comparisons were made, particularly in terms of mean rainfall depth and maximum intensities. The longest and most reliable long-term records are from 10 nearby stations in the Dorsal Mountains. The mean annual rainfall for the longer period (1969–2003) was about 406 mm (standard deviation was 124 mm). The same value for the period 1993-2003 was 365 mm (standard deviation was 102 mm). Maximum rainfall intensity for the investigated period was compared to long-term values for different time steps and return periods [49]. Fig. (**2**) shows intensity-duration-frequency (IDF) curves for the period 1964-2003. As seen in Fig. (**3**), even if the investigated period was short (1993-2003), it is still representative of longer periods in terms of maximum intensities corresponding sometimes to more than a 100-year return period.

2.4. Methods

The erosive characteristics of rainstorms and the resulting soil erosion process for the Tunisian semiarid area bring up many questions. For example, what is the importance of exceptional rainfall (rainfall intensities corresponding to a return period superior to 1 year) for the erosion risk? What time step is the most important when estimating the erosive potential of rainfall events? Which lower or upper limits of rainfall intensity characteristics could trigger erosion events? What is the most active erosion process in small catchments? Several aspects of the rainfall may be important to define events that lead to soil erosion. Different rainstorm charac-

teristics, such as return period, duration, maximum short-term intensity, and rainfall depth may be significant for the soil erosion risk. Many studies during recent years have shown that rainfall return period is one of the most important characteristic indicating soil erosion amount and type. The following relationships are an attempt to summarize important soil erosion research concerning return period and soil erosion type for semiarid areas in general as well as semiarid Mediterranean regions in particular (using the following references in alphabetical order; [50,44,34,2,51,3,45,1,47,52-54,46,37,55-56,38,57-58,7,59,14].

1) Interrill erosion: $1 \leq T < 5$

2) Rill erosion: $5 \leq T < 10$

3) Gully erosion: $10 \leq T$

where T is rainfall return period in years and the duration of rainfall is 1 to 60 min.

The above relationships can be used in a simplified way, to estimate erosion risk based on short-term rainfall characteristics. It has to be remembered that the relationships are in general only valid for semiarid areas similar to the Atlasic catchments. The return period intervals should also be seen as an approximation for a large number of samples.

3. RESULTS

3.1. General Rainfall Characteristics

Table **1** shows a summary of nearly 27000 identified station rainfall events during the observation period. The number of more or less independent rainfall events per year corresponds to between 70 and 180. The average number of rainy days is about 22% (80 days/year) for the entire rain gauge network with a maximum of 30% at Kamech and a minimum of 13% at Mouidhi. More than 80% of the events appear as afternoon rains. This is consistent with the convective storm system. The rainfall event duration does not exceed 1 hour in 70% of the cases. Rainfall events with duration of less than 6 hours represent about 28% and events superior to 6 hours only 2%. Because of this, the majority of events can be categorized as small meso-scale rainfall according to House [60]. Only 25% of the events exceed 3 mm in depth. This value is the threshold to evaluate the kinetic energy of rainfall [61]. They hold about 70% of the total rainfall depth and represent 90% of the rainfall erosivity potential.

3.2. Exceptional Rainfall Event Characteristics

The observed rainfall data during the studied period displayed a maximum rainfall event of 125.5 mm that lasted about 12 hours (Table **1**). This corresponds to a daily return period of about 50 years and the highest return period of 20 years for I_{45} and I_{60}. Among notable events the maximum values during 10, 15, and 20 min duration were respectively 24, 60, and 74 mm. For 30 and 60 min duration, 82 and 98 mm, were recorded. These values correspond to about 25% of the highest recorded rainfall intensity in the world for a duration of 15, 20, 30, and 60 min [62].

The exceptional events represent about 12% of the annual rainfall station events in semiarid Tunisia (about 10-20 events per year). Exceptional events less than a 10-year return period, represent several hundred station events, while, larger than a 10-year return period corresponds to about 10-20 events. According to Fig. (**3**), the number of exceptional events is unevenly distributed over the 1-60 min durations. One and 2-min duration exceptional events are rare. The 15-min duration displays a peak representing about 15% of all exceptional events. For instance, it displays 130, 45 and 171 more exceptional events than what is noted for the 5, 30 and 60 min durations, respectively. In general, the events occurring throughout the different durations seem to be nearly identical. If we have to choose representative durations for exceptional rainfall events, the 15-min duration, presents some advantages. When using, e.g., the universal soil loss equation (USLE; [24]). The rainfall and runoff erosivity is expressed by the so-called R factor. The R factor is calculated as a product of the total energy of rainfall, E and its maximum 30-min intensity, I_{30}. Consequently, the identified I_{30} exceptional intensities could be used to calculate the R factor. However, the I_{15} also displays possibilities to further elaborate on intensity variations within the 30-min duration. Compared to other durations it also displays the lowest stan-

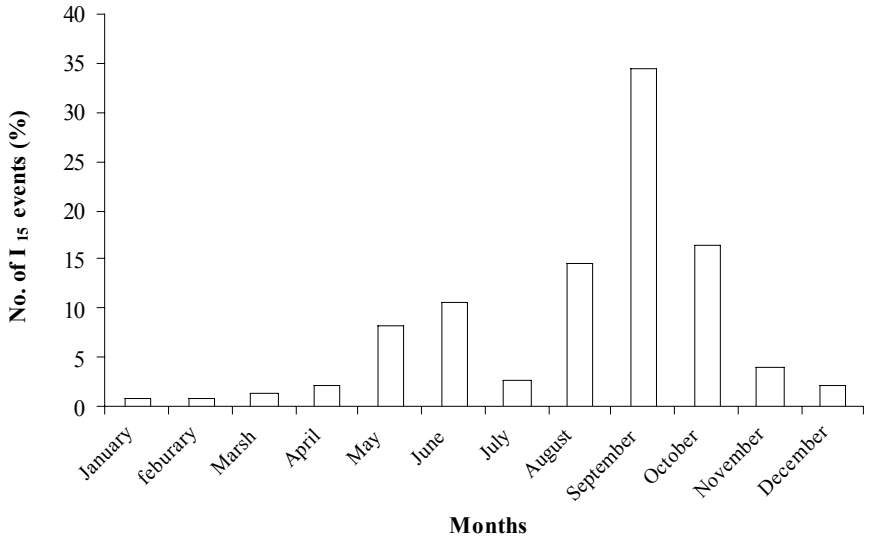

Fig. (4). Seasonality of the identified exceptional rainfall events with 15-min duration (average of about 500 station events).

Table 2. Description of Identified 15-min Duration Exceptional Rainfall Events. Depth, Intensity, and Return Period Refer to the Maximum Observed Intensity

Rainfall Gauge	Events/ Year	Mean Event Depth (mm)	Max. Int. (mm/h)	Return Period (Years)
1. Arara	1.0	28.5	60	2–5
2. Mrira	1.4	53.5	80	10–20
3. Abdeladim	1.7	44.0	68	5–10
4. Bou Haya	1.9	31.0	76	5–10
5. Echar	1.6	53.5	94	20–50
6. El Amadi	3.2	80.5	240	>100
7. Baouejer	1.4	31.0	70	5–10
8. Jédéliane	2.3	79.0	84.6	10–20
9. Sadine1	2.4	107.5	186	>100
10. Sadine 2	1.8	38.0	100	20–50
11. Es Senega	1.6	58.0	112	50–100
12. Hadada	1.9	33.5	71	5-10
13. Janet	2.1	63.0	96	20–50
14. Brahim Zaher	1.5	36.0	110	50–100
15. Abdessadok	2.4	78.0	140	>100
16. Hnach	1.7	27.0	86.6	10–20
17. Fidh b. naceur	1.6	42.0	80	10–20
18. Mrichet El Anze	2.2	73.0	98	20–50
19. Fidh Ali	2.3	50.0	100	20–50
20. Dekikira	2.2	72.5	94	20–50
21. El Gouazine	2.5	84.5	88	10–20
22. El Mouidhi	2.2	53.5	134	50–100
23. Saadine	2.5	74.5	180	>100
24. El Ogla	3.7	84.5	102	50–100
25. Sbaihia	1.9	66.5	116	50–100
26. El Melah	3.6	56.0	110	50–100
27. Es Seghir	2.5	91.0	152	>100
28. Kamech	3.5	125.5	102	50–100

dard deviation (15.8 mm) for rainfall depth and the smallest coefficient of variation (37.8%) linked to the maximum intensity values. In short, the 15-min duration, seems to be the most homogeneous sub-sample of exceptional rainfall intensities and also the most representative duration for erosive rainfall in the Dorsal area.

3.3. I_{15} Characteristics and Erosion

Fig. (**4**) shows inter-annual variation of I_{15} events. As shown in the figure, the majority of exceptional events occur with a major peak during the start of the rainy period in Tunisia between August September and October. During this specific period, the soils are the most vulnerable for rainfall erosion since they usually lie bare after the long dry period.

The average depth and duration for all identified 15-min exceptional events are respectively 25 mm and 105 min,. Corresponding average and maximum intensity are 23 and 56 mm/h. Table **2** shows a summary of the I_{15} maximum event characteristics depending on station. As seen in the table the return period for these events are often much larger than the 10-year recording period and in several cases larger than 100 years. Consequently, the observation period may well represent a much longer period in statistical terms. The

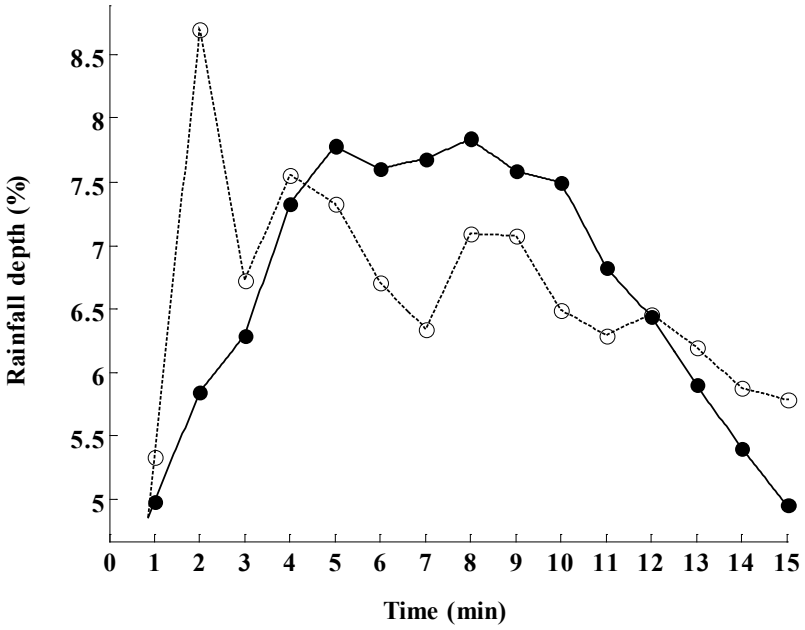

Fig. (5). Temporal distribution of the identified 15-min duration exceptional rainfall events. Line connecting filled circles shows average properties and line connecting empty circles shows standard deviation (about 500 station events).

28 different rainfall stations display varied number of exceptional 15-min duration events. Ogla, Amadi, and Kamech show more than 3 exceptional events per year while Arara only has one single exceptional event per year. The largest observed I_{15} was recorded at Amadi and Sadine 1 with a return period larger than 100 years. The corresponding intensities were 240 and 186 mm/h that correspond to respectively 450 and 200 year return period. Largest maximum intensities occur most often east of Mouidhi to Kamech. The western parts usually have the lowest maximum intensities.

Fig. (**5**) shows the average temporal distribution for the 15-min duration exceptional rainfall events. The distribution appears somewhat skew with a centre of gravity towards the first half of the events. The intensity maximum occurs after about 5-10 min. The standard deviation displays a large variation for the first minutes that then gradually decreases. This indicates that some rainfall events may have large intensities right from the start which can cause great raindrop impact initiating detachment of soil particles.

The erosion types are linked to the different return periods (cf. Methods). Consequently, the risk of erosion appears to be related to specific exceptional 15-min intensities. This yields the following relationships:

1) Interrill erosion: $38 \leq I_{15} < 65$

2) Rill erosion: $65 \leq I_{15} < 75$

3) Gully erosion: $75 \leq I_{15}$

where I_{15} is the exceptional rainfall intensity in mm/h.

The above relationships should be regarded as a simplified way to estimate the occurrence of different erosion types depending on the maximum 15-min duration rainfall intensity. As such, the intensity boundaries should not be seen as fixed but rather indicative. Together with additional information on a particular catchment´s situation in the soil degradation cycle [63], the relationships can be used to estimate the risk for different types of erosion in the Dorsal region. The results can be used to better manage erosion-prone catchments and also give input to erosion modelling.

4. CONCLUSION AND DISCUSSION

Semiarid regions are especially vulnerable to erosion due to a combination of geomorphological conditions, soil management, and the high-intensive character of rainfall. Due to this, there are needs to better develop methods and estimate the erosion risks in a simple way. The most rational means to do this is to start from the rainfall characteristics. About 12% of all rainfall events in the Tunisian semiarid region are erosive and can be categorized as being exceptional (return period equal and superior than 1 year). A literature survey of pertinent soil erosion research for semiarid regions shows that type of erosion can in a general way be related to rainfall return period. A combination of these results with the conclusions herein show that the 15-min exceptional rainfall intensity can be used to characterize erosive rainfall. And this leads forward to a simplified general relationship for the occurrence of a certain type of erosion. The relationship links erosion type with the 15-min exceptional rainfall intensity. The results can be used to estimate the risk of certain type of erosion in a simplified way based on short-term rainfall characteristics. Together with information on a certain catchment´s location in the soil degradation cycle. Results can be used as input to erosion modeling but also to better manage erosion risks in catchments with water erosion problems.

ACKNOWLEDGEMENTS

Sihem Jebari and Akissa Bahri thank Mr Habib Farhat, head of the Tunisian Farmland Conservation and Management Department (DG/ACTA) for providing data and all his staff for valuable time and discussions allocated to this work.

Ronny Berndtsson is supported by the Swedish Research Council.

REFERENCES

[1] Hooke JM, Mant JM. Geomorphological impacts of a flood event on ephemeral channels in SE Spain. Geomorph 2000; 34: 163–180.

[2] Coppus R, Imeson AC. Extreme events controlling erosion and sediment transport in a semi-arid sub-andean valley. Earth Surf Process Landforms 2002; 27: 1365-1375.

[3] Dhakal AS, Sidle RC. Distributed simulations of lanslides for different rainfall conditions. Hydrol Process 2004; 18: 757-776.

[4] Jen CH, Lin JC, Hsu ML, Petley DN. Fluvial transportation and sedimentation of the Fu-shan small experimental catchments. Quater Int 2006; 147: 34-53.

[5] Boix-Fayos C, Martinez-Mena M, Calvo-Cases A, Arnau-Rosalén E, Albaladejo J, Castillo V. Causes and underlying processes of measurement variability in field erosion plots in Mediterranean conditions. Earth Surf Process Landforms 2007; 32: 85-101.

[6] Walling DE. Measuring sediment yield from river basin, Soil Erosion Research Methods. Soil and Water Conservation Society. In: R. Lal, Editor 1994.

[7] Uson A, Ramos MC. An improved rainfall erosivity index obtained from experimental interrill soil losses in soils with a Mediterranean climate. Catena 2001; 43: 293-305.

[8] Krishnaswamy J, Richter DD, Halpin PN, Hofmockel MS. Spatial patterns of suspended sediment yields in a humid tropical watershed in Costa Rica. Hydrol Process 2001; 15: 2237-2257.

[9] Romkens MJM, Helming K, Prasad SN. Soil erosion under different rainfall intensities, surface roughness, and soil water regimes. Catena 2002; 46: 103-123.

[10] Vogel RM, Stedinger JR, Hooper RP. Discharge indices for water quality loads. Water Res Res 2003; 39: 1273-1292.

[11] Walker PH, Kinnel PIA, Green P. Transport of a non cohesive sandy mixture in rainfall and runoff experiments. Soil Sci Soc Am J 1978; 42: 793-801.

[12] Singer MJ, Walker PH, Hutka J, Green P. Soil erosion under simulated rainfall and runoff at varying cover levels. Soils Div Rep. CSIRO, Australia 1981.

[13] Kinnel PIA. The effect of flow depth on sediment transport induced by raindrops impacting shallow flows. Am Soc Agr Eng 1991; 34: 161-168.

[14] Zartl AS, Klik A, Huang C. Soil Detachment and Transport Processes from Interrill and Rill Areas. Phys Chem Earth 2001; 26: 25-26.

[15] Malam Issa O, Le Bissonnais Y, Planchon O, Favis-Mortlock D, Silvera N, and Wainwright J. Soil detachment and transport on field- and laboratory-scale interrill areas: erosion processes and the size-selectivity of eroded sediment. Earth Surf Proc Landf 2006; 31: 929-939.

[16] White S, García-Ruiz JM, Martí C, Valero B, Errea MP, Gómez-Villar A. The 1996 Biescas campsite disaster in the Central Spanish Pyrenees, and its temporal and spatial context. Hydrol Process 1997; 11: 1797-1812.

[17] Berndtsson R. Spatial hydrological processes in a water resources planning perspective. An investigation of rainfall and infiltration in Tunisia. Ph.D. diss., Dept. of Water Resources Engineering, Lund Univ, 1988.

[18] Sur HS, Bhardwaj A, Jindal PK. Some hydrological parameters for the design and operation of small earthen dams in lower Shiwaliks of northern India. Agr Water Manag 1999; 42: 111-121.

[19] Haregeweyn N, Poesen J, Nyssen J, De Wit J, Haile M, Govers G, Deckers S. Reservoirs in Tigray (Northern Ethiopia): characteristics and sediment deposition problems. Land Degr Developm 2006; 17: 211-230.

[20] Sivapalan M, Takeuchi K, Franks SW, Gupta VK, Karambiri H, Lakshim V, Liang X, McDonnel JJ, Mendiodo EM, O'Connel PE, Oki T, Pomery JW, Schertzer D, Unlenbrook S, Zehe E. IAHS Decade on prediction in ungauged basins (PUB), 2003 -2012 : Shaping an exciting future for the hydrological sciences. Hydrol Sci J 2003; 48: 857-880.

[21] Cudennec C, Leduc C, Koutsoyiannis D. Dryland hydrology in Mediterranean regions _ a review. Hydrol Sci J 2007; 52: 1077-1087.

[22] SERST-IRD. Evaluation conjointe du programme de recherché "Lacs et barrages collinaires en Tunisie », Technical Report 2000, Tunis 2000.

[23] Jebari S, Berndtsson R, Uvo C, Bahri A. Regionalizing fine time-scale rainfall affected by topography in semi-arid Tunisia. Hydrol Sci J 2007; 52:1199-1215.

[24] Wischmeier WH, Smith DD. Rainfall energy and its relationship to soil loss. Trans Am Geophys 1958; 39: 285-291.

[25] Masson JM. L'érosion des sols par l'eau en climat méditerranéen. Méthodes expérimentales pour l'étude des quantités érodées à l'échelle du champ. La Houille Blanche 1972 ; 8 : 673-679.

[26] EEA. Environment in the European Union at the turn of the century, Technical Report 1999, European Environment Agency, Brussels 1999.

[27] Albergel J, Rejeb N. Les lacs collinaires en Tunisie: enjeux, contraintes et perspectives. Comptes rendus à l'Académie d'Agriculture de France, 1997; 83: 77-104.

[28] EEA. Assessment and reporting on soil erosion. Background and workshop report, Technical Report 2002, European Environmental Agency, Copenhaguen 2003..

[29] Ellison WD. Soil erosion studies - part I. Agric Eng 1947; 28: 145-146.

[30] Greene RSB, Ringrose-Voase AJ. Micromorphological and hydraulic properties of surface crusts formed on a red earth soil in the semi-arid rangelands of eastern Australia, Conference Proceedings, Townsville, Queensland, Elsevier: 1994.

[31] Weggel JR, Rustom R. Soil erosion by rainfall and runoff - State of the art. Geotext Geomembr 1992; 11: 551-572.

[32] Ramos MC, Nacci S. Estabilidad de agregados superficales en suelos del Anoia-penedès (Barcelona) frente al humedecimiento y al impacto de las gotas de lluvia. Edafologia 1997; 3: 3-12.

[33] Cerdan O, Le Bissonnais Y, Govers G, Lecomte V, Van Oost K, Couturier A, King C, Dubreuil N. Scale effect on runoff from experimental plots to catchments in agricultural areas in Normandy. J Hydrol 2004; 299: 4-14.

[34] Cammeraat LH. A review of two strongly contrasting geomorphological systems wihin the context of scale. Earth Surf Proc Landf 2002; 27: 1201- 1222.

[35] Kandel DD, Western AW, Grayson RB, Turral HN. Process parameterization and temporal scaling in surface runoff and erosion modelling. Hydrol process 2004; 18: 1423-1446.

[36] Gilley JE, Eghball B, Kramer LA, Moorman TB. Narrow grass hedge effects on runoff and soil loss, J Soil Water Cons 2000; 55: 190-196.

[37] Martinez-Mena M, Castillo V, Albaladejo J. Relations between interrill erosion processes and sediment particle size distribution in a semiarid Mediterranean area of Spain. Geomorph 2002; 45: 261-275.

[38] Spaan WP, Sikking AFS, Hoogmoed WB. Vegetation barrier and tillage effects on runoff and sediment in an alley crop system on a Luvisol in Burkina Faso. Soil Till Res 2005; 83: 194-203.

[39] Collinet J, Jebari S. Étude expérimentale du ruissellement et de l'érosion sur les terres agricoles de Siliana, Technical Report 2000, INRGREF and IRD, Tunisia 2000.

[40] Li M, Li Z, Ding W, Liu P, Yao W. Using rare earth element tracers and neutron activation analysis to study rill erosion process. J Appl Radi Isot 2006; 64: 402-408.

[41] Bocco G. Gully erosion: processes and models. Progr Phys Geogr 1991; 15 4: 392-406.

[42] Vrieling A. Satellite remote sensing for water erosion assessment: A review. Catena 2006; 65: 2-18.

[43] Plata Bedmar A, Cobo Rayan R, Sanz Montero E, Go´mez Montan˜a JL, Avendan˜o Salas C.. Influence of the Puentes reservoir operation procedure on the sediment accumulation rate between 1954–1994, Conference Proceedings, Florence, Italy 1997.

[44] Bull LJ, Kirkby MJ, Shannon J, Hooke JM. The impact of rainstorms on floods in ephemeral channels in southeast Spain. Catena 1999; 38: 191-209.

[45] Garcia-Ruiz JM, Carlos MB, Adrián L, Santiago B. Geomorphological consequences of frequent and infrequent rainfall and hydrological events in Pyrenees Mountains of Spain. Mitig Adapt Strat Glob Change 2003; 7: 303-320.

[46] Maas GS, Macklin GE, Warburton J, Woodward JC, Meldrum E. A 300-year history of flooding in an Andean mountain river system: the Rio Alizos, southern Bolivia, Technical Report, Balkema, Rotterdam 2000.

[47] Harvey AM. Geomorphological response to an extreme flood: a case from southeast Spain. Earth Surf Process Landf 1984; 9: 267-279.

[48] Colombani J. Autopsie d'un hyétogramme, Troisièmes journées hydrologiques de l'ORSTOM , Conference Proceedings, Montpellier, France 1988.

[49] DGRE. Optimisation des réseaux de suivi des ressources en eau, étude de la pluviographie, Technical Report, Water Resources Department, Tunisia 2006.

[50] Berguaoui M, Camus H. Etude statistique des averses sur le basin versant de l'oued Ez-zioud : Djebel Semmama, Tunisie Centrale. Les Annales Maghrébines de l'Ingénieur 1994; 8 : 2-27.

[51] CGR. Les pluies en Tunisie, Technical Report, Centre de Recherches et d'Expérimentation de Génie Rural, Tunisie 1964.

[52] Hollinger E, Cornish PS, Baginska B, Mann R, Kuczera G. Farm scale storm water losses of sediment and nutrients from a market garden near Sydney, Australia. Agr Water Manag 2001; 47: 227-241.

[53] Hudson NW. The Influence of Rainfall on the Mechanics of Soil Erosion with particular reference to Northern Rhodesia. MSc. Thesis, Univ. of Cape Town 1965.

[54] Li Y, Poesen J, Yang JC, Fud B, Zhang JH. Evaluating gully erosion using ^{137}Cs and $^{210}Pb/^{137}Cs$ ratio in a reservoir catchment. Soil Till Res 2003; 69: 107-115.

[55] Sempere TD, Creutin D, Salles JD, Delrieu G. Quantification of soil detachment by raindrop impact: performances of classical formulae of kinetic energy in Mediterranean storms. Wallingford: IAHS Press 1992.

[56] Sinniger R, Martini O, De Cesare G. Apports de sédiments dans une retenue par courant de densité, Conference Proceedings, Durban 1994.

[57] Steegen A, Govers G, Nachtergaele J, Takken I, Beuselinck L, Poesen J. Sediment export by water from an agricultural catchment in the Loam Belt of Central Belgium. Geomorph 2000; 33: 25-36.

[58] Thévenin MJ. La sédimentation des barrages-réservoirs en Algérie et les moyens mis en œuvre pour préserver les capacités. Annales de l'Institut Technique du Bâtiment et des Travaux Publiques : Algérie 1960.

[59] Xie Y, Liu B, Nearing MA. Practical thresholds for separating erosive and non-erosive storms. Transactions of the ASAE 2002; 45: 1843-1847.

[60] House RA. The mesoscale and microscale structure and organization of clouds and precipitation in midlatitude cyclones, 1: A case study of a cold front. J Atmos Sci 1980; 37: 568-596.

[61] Kowal JM, Kassam AH. Energy load and instantaneous intensity of rainstorms at Samaru, Northern Nigeria. Tropical Agric 1976; 53: 185-197.

[62] Shaw EM. Hydrology in practice. London: Chapman and Hall 1994.

[63] Jebari S, Berndtsson R, Bahri A, Boufaroua M. Delineation of spatial soil loss and reservoir siltation rates in semiarid Tunisia. Forthcoming.

Received: March 11, 2008 Revised: April 01, 2008 Accepted: April 02, 2008

Spatial soil loss risk and reservoir siltation in semiarid Tunisia

SIHEM JEBARI[1], RONNY BERNDTSSON[2], AKISSA BAHRI[3], AND MOHAMED BOUFAROUA[4]

[1]*National Research Institute for Rural Engineering, Waters, and Forestry, Box 10, Ariana 2080, Tunis, Tunisia*
Sihem.jebari@iresa.agrinet.tn
[2]*Department of Water Resources Engineering, Lund University, Box 118, S-22100 Lund, Sweden*
[3]*International Water Management Institute, PMB, CT 112, Cantonments Accra, Ghana*
[4]*Farmland Conservation and Management Department, 30, Alain Savary Street, 1002 Tunis, Tunisia*

Accepted for publication in Hydrological Sciences Journal the 11 November 2008

Abstract Soil erosion vulnerability and extreme rainfall characteristics over the Mediterranean semiarid region in general and the Tunisian Dorsal in particular are crucial input for reservoir siltation rate estimation. A comprehensive high-resolution data base on erosive rainfall together with siltation records for 28 small reservoirs were analysed for this region. The general life-span of these reservoirs is only about 14 years. Depending on the soil degradation for the different catchments corresponding reservoirs display a wide variety of soil erosion rate. The average soil loss was 14.5 tons/ha/year but some catchments display values up to 36.4 tons/ha/year. The maximum 15-min duration rainfall intensity was used to display spatial distribution of rainfall erosivity. The north-western parts of the Dorsal display the most extreme rainfall erosivity. Spatial erosion patterns are to some extent similar, however, they vary greatly according to their location in the "soil degradation cycle". This cycle determines the soil particle delivery potential of the catchment. In general, the north-western parts of the Dorsal display modest soil erosion patterns due to the already severely degraded soil structure. Here, the soil surface is often the original bedrock. However the greatest soil erosion occurs in the mid-eastern parts of the Dorsal that represents the "degradation front". The latter, corresponds to the area with highest erosion, which is continuously progressing westward in the Dorsal. The large variation between the erosive rainfall events and the annual soil loss rates was explained by two important factors. The first factor is related to the soil degradation cycle. The second factor corresponds to the degradation front with the highest soil loss rates. This front is at present located at 300 m altitude and appears to be moving along an 80 km westward path starting from the east coast. A better understanding of the above can be used to better manage soils and soil covers in the Dorsal area and eventually to decrease the soil erosion and reservoir siltation risk.

Key words Atlasic mountain range; degradation cycle; erosive rainfall; gully erosion; interrill erosion; rill erosion; semiarid; siltation distribution; small reservoirs; Tunisia

INTRODUCTION

Soil erosion does not only cause serious environmental degradation but also constitutes an important indicator of hydrological and climatic change (Tafangenyasha, 1997; Sundborg, 1992). Soil erosion leads to siltation which is a major problem for lake and reservoir management all over the world (e.g., ILEC, 1993; 2003; UNEP, 1994; Keller *et al.*, 2000). Reservoir siltation has direct negative economical and environmental consequences, since less volume can be used for irrigation, water supply, and flood control. Recent research indicates that prediction of sediment yield is one of the main challenges in soil erosion research (Price *et al.*, 2000; Coppus *et al.*, 2002; De Vente, 2005; Herath, 1999; Goel *et al.*, 2005). The most

vulnerable climatic regions to soil loss are the semiarid areas (WCD, 2000; Woodward, 1995) while the geographical area with the highest rate of siltation is Africa (on average about 19% of reservoir storage volume; ILEC, 1993; 2003; UNEP, 1994). During the latest decades, research has emphasized the importance of soil erosion in the Mediterranean basin where siltation reduces the reservoir capacity rapidly (e.g., Imeson, 1990; Poesen and Hooke, 1997; EEA, 2000; Martínez-Casasnovas *et al.*, 2003). In this region, the water needs are close to the potentially available water resources (e.g., Ennabli *et al.*, 1998). Here, the water is becoming increasingly expensive and a more and more heavy burden for the economy.

Tunisia was one of the countries within the Mediterranean basin that was classified as being among the ten first that would suffer from water scarcity (FAO, 1994). In 2006, 87% of potential surface water resources were utilized through reservoirs. The maximum water harvesting will reach 95% in 2010. Presumably from now to 2030 the Tunisian reservoir capacity will gradually decrease with 40 million m^3 per year due to siltation (GOPA & GTZ, 2005). In order to balance this capacity loss, various measures are introduced. These measures include increasing dam heights and the construction of more small and average-sized reservoirs. In fact, more than 800 small reservoirs are being built in semiarid Tunisia in rough natural conditions. They constitute one of the elements of the national policy of water resources mobilization. They contribute to protect the downstream zones, to control water erosion, to refill the groundwater table and to improve the spatial distribution of the general water resources.

To mitigate siltation risks there are great needs to establish better relationships between the erosion process and exceptional rainfall event characteristics. The objective of this study is hence to examine the influence of short-term exceptional rainstorm intensity on
erosion and reservoir siltation at small and large scales. The utilized data are from a unique high-resolution rainfall data base together with siltation data from 28 reservoirs collected during an EU-funded project (IRD, 2000). By combining the two sources of data we aim at improving the understanding of the erosion process and at delineating important links between field rainfall characteristics and deposited sediments in small reservoirs. The results are based on local and spatially distributed observations. The latter, uses respectively “the soil degradation cycle” and the “degradation front” to display the soil loss dynamics and paths at the catchment and the larger Dorsal scale. These, will enable engineers to better estimate the probable life span of reservoirs, to improve measures taken against reservoir sedimentation, and finally to better face water shortage in a context of an increasing need for water.

DATA AND METHODS

Study area

The Tunisian Dorsal plays an important role in the hydrology of the country, since its mountain chain links the big wadis, e.g., Mejerda, Meliane, Nebhana, Merguellil, and Zeroud (Fig. 1). The hydrological regime of this region means a hot dry summer of 4 to 5 months during which shallow groundwater may evaporate. Water resources are based on surface water use and agriculture on cereal crops and cattle rising. The soil cover degradation that characterizes the Dorsal has led to important soil erosion meaning a thinner and more uneven soil cover often displaying the underlying bare rock surface. The soil erosion is a serious problem throughout the Dorsal area. It has been estimated that 7% of the area are badly damaged by erosion and 70% of the area are moderately damaged. At present only 28% of the

Dorsal soil cover is left. Partly, this degradation is caused by the building of large dams during the 60's and 70's which was performed without paying sufficient attention to the proper management of upper catchment areas. However, the major part of the degradation is due to the specific bioclimatic conditions of the Mediterranean climate. The soils are better characterized by the degradation of rock material rather than their organic matter content. Consequently, they are not well developed and often shallow. The young geological relief and the rate of erosion prevent them from reaching maturity. Also, the high potential evaporation causes formation of calcareous crusts at about 50 cm depth. The latter prevents water from seeping downwards and obstructs efficient drainage.

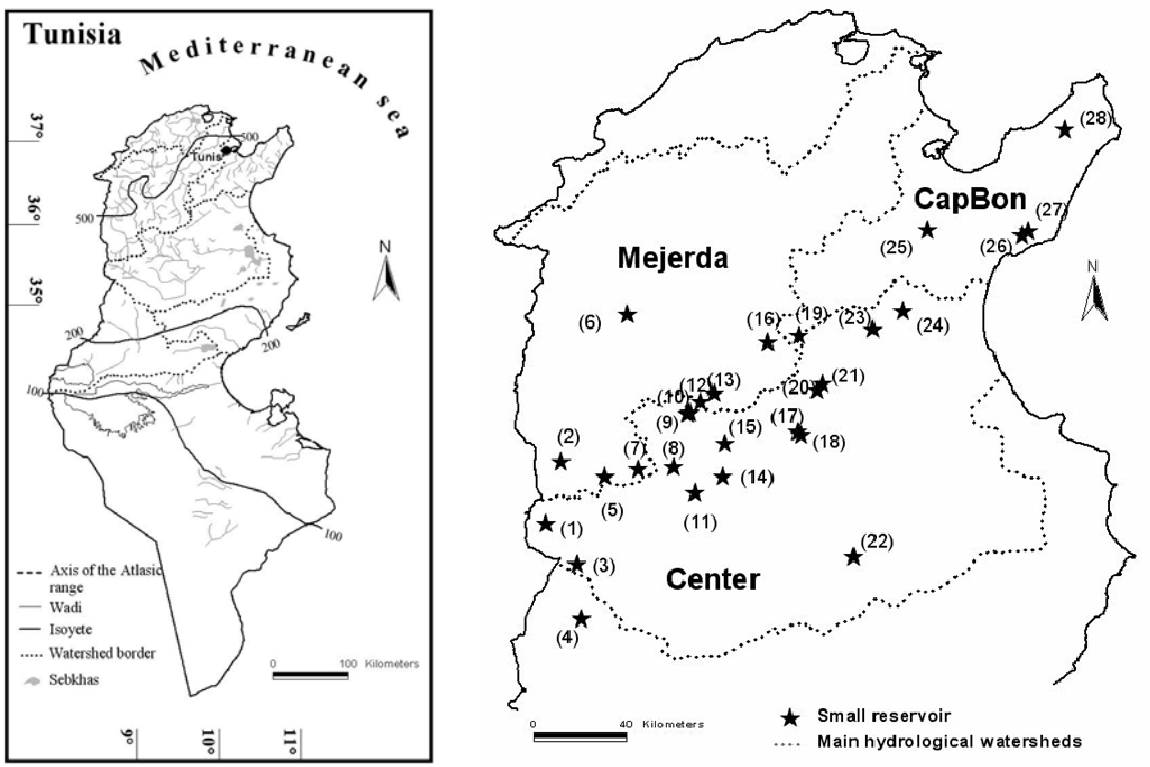

Fig. 1 Location of reservoirs in the Dorsal area.

The Dorsal area is monitored in a hydrological observation network with 28 experimental catchments (Fig. 1). Each catchment discharges into a small reservoir. An automatic rain gauge is located at each site as well as automatic water level recording. Table 1 show that the average area of 24 of these catchments is about 4 km^2. The 4 remaining catchments are fairly large with an average area of about 125 km^2. The average drainage density for these catchments is 5.1 km/km^2. The mean height difference in the catchments is about 245 m whereas the mean average slope is 11.2%. Estimates of concentration time were made using the Kirpich (1940) formula. The latter is useful for small agricultural catchments and gives values of about 11 min. The average runoff coefficient is about 10%, but values up to about 80% have been recorded for some intense rainstorms.

Rainfall data and erosivity

Totally 28 rainfall gauges from the hydrological network were used in this study (Fig. 1). Missing data are less than 1% and the gauging density corresponds approximately to 1 gauge per 24 km^2 catchment area. Table 1 gives descriptive statistics for catchment characteristics

and recorded erosive rainfall events during the analyzed 10-year period (1993-2003). The rain gauges are fully automatic and provide an accuracy of ±4% up to 250 mm/h intensity for a 5-min time step. Rain gauges are of tipping bucket type connected to a logger recording data every minute. A total of about 27000 station rainfall events were included in the present analysis. A rainfall event was defined as separated from another event if a rain gauge showed less than one tip per hour. For representativity the analyzed period was compared to long-term rainfall conditions. The mean annual rainfall for a longer period (1969–2003) was about 406 mm (standard deviation was 124 mm). The same value for the period 1993-2003 was 365 mm (standard deviation was 102 mm). The investigated period appears to be representative for longer periods. Further details are given in Jebari *et al.* (2008).

In this paper a specific analysis is made regarding exceptional rainfall with an approximate return period of equal and more than 1 year. We are focusing on rainfall with maximum intensities for a duration of 15 min. This duration was found representative regarding occurring erosion processes in the monitored catchments (Jebari *et al.*, 2008). For this duration about 500 station rainfall events were included in the analysis. Each exceptional rainfall event is characterized by its depth, duration, average and maximum intensity, and its erosivity index (R). The latter is used in the Universal Soil Loss Equation (USLE; Wischmeier and Smith, 1978) developed to predict interrill and rill erosion. The R is based on the kinetic energy (KE) and the maximum intensity (I) during a 30-min period (Wischmeier and Smith, 1958; Lal, 1976).

Siltation observations

Siltation measurements were made on the basis of bathymetric observations in the above mentioned reservoirs. Table 2 shows a summary of reservoir and siltation characteristics. Measurement campaigns started in 1993 with up to five observations for each reservoir during about 10 years (1993-2002; Table 3). The bathymetric surveys of reservoirs were made by echo-sounding the water depths along pre-defined transects (Camus *et al.*, 1995). Depending on reservoir, between 400 and 700 measuring points were obtained. The points were defined by three cartesian coordinates (x, y, and z). The change in reservoir volume was deduced from the difference from one observation time to another. Siltation data for the entire network are available from annually published hydrological reports (DCES/IRD, 1994-2002). These reports account for every reservoir and also characterize the sediments.

Catchment sediment yield is the amount of sediment delivered at the outlet of a catchment. It is used to design reservoirs and to analyse sedimentation and water quality problems. Moreover, it is an observation technique to estimate average water erosion for the catchment. Sediment yield is the sum of sediments produced by all erosive sources (e.g., Toy *et al.*, 2002). In order to compare siltation rates for the different reservoirs, the deposited sediment volume on the bottom of the reservoirs was converted into transported mass of soil using an average of 1.5 tons/m^3 as an apparent density (Ben Mamou, 1998; Tables 2 and 3).

Wischmeier and Smith (1978) give the soil loss tolerance to 12 tons/ha/year defined as “the maximum level of soil erosion that will permit a level of crop productivity to be sustained economically and indefinitely”. Experiments throughout the Tunisian semiarid area have determined the average tolerable soil loss to about 2.5, 5, and 10 tons/ha/year for a thin, average, and thicker soil, respectively (Masson, 1972). With a very slow rate of soil formation in some parts of the Mediterranean region, any soil loss of more than 1 tons/ha/year can be considered as irreversible within a time span of 50-100 years (EEA, 1999).

Table 1 Physical and hydrological characteristics of studied catchments. Rainfall events correspond to 15-min duration maximum intensity from Jebari et al., (2008).

Catchment	Area (km^2)	Drainage. density (km/km^2)	Mean slope (%)	Difference in height (m)	Mean runoff coeff. (%)	Concentr. time (min)	Mean no of excep. events /year	Mean event depth (mm)	Mean duration (min)	Mean I_{15} (mm/h)	Std. dev. I_{15} (mm/h)
1. Arara	7.08	5.5	16.6	442	14.7	7.5	1.0	18.8	55.7	49.7	6.3
2. Mrira	6.13	3.1	6.8	170	13.9	20.0	1.4	22.2	105.6	48.5	12.3
3. Abdeladim	6.42	19.2	7.6	194	3.7	7.3	1.7	19.0	89.7	49.9	9.1
4. Bou Haya	359.00	2.0	3.2	622	5.1	84.0	1.9	17.3	73.5	47.6	10.6
5. Echar	9.17	3.6	7.2	220	2.7	9.2	1.6	22.7	93.2	50.3	19.5
6. El Amadi	3.27	2.9	13.7	248	12.5	7.2	3.2	34.0	121.7	75.0	52.8
7. Baouejer	4.86	4.7	5.9	131	1.5	17.1	1.4	20.8	73.7	54.1	9.3
8. Jédéliane	47.00	3.4	6.7	466	3.2	19.2	2.3	26.4	114.4	55.1	14.2
9. Sadine 1	3.84	3.1	20.8	408	8.4	4.8	2.4	23.9	60.0	66.9	34.9
10. Sadine 2	6.53	2.7	17.0	436	21.6	8.3	1.8	20.2	47.2	56.8	18.8
11. Es Senega	3.63	4.9	13.9	265	10.0	6.1	1.6	26.4	108.8	59.4	18.2
12. Hadada	4.69	2.9	15.9	346	6.0	5.4	1.9	18.7	68.4	50.3	9.3
13. Janet	5.21	6.9	16.2	371	11.5	6.9	2.1	25.0	81.5	60.2	16.6
14. Brahim Zaher	4.64	6.0	20.6	445	10.0	5.0	1.5	18.1	75.6	53.7	24.0
15. Abdessadok	3.07	5.4	21.3	374	3.5	4.2	2.4	25.5	100.1	58.1	30.3
16. Hnach	3.95	3.5	19.4	387	8.7	4.2	1.7	17.7	68.1	50.6	15.0
17. Fidh b. Naceur	1.69	5.5	8.6	112	5.6	6.0	1.6	21.5	99.0	53.1	13.9
18. Mrichet El Anze	1.58	3.3	11.1	140	3.7	4.5	2.2	25.9	82.9	58.4	16.1
19. Fidh Ali	4.12	8.6	5.3	109	2.8	6.2	2.3	22.3	87.6	53.1	16.9
20. Dekikira	3.07	4.7	5.6	99	11.5	7.0	2.2	21.6	77.9	57.7	14.8
21. El Gouazine	18.10	4.5	4.6	199	2.4	10.0	2.5	25.1	130.5	52.1	12.7
22. El Mouidhi	2.66	8.8	7.8	128	9.9	4.5	2.2	21.5	74.3	60.5	25.6
23. Saadine	2.72	3.9	18.6	307	13.0	4.5	2.5	31.1	101.0	82.7	37.2
24. El Ogla	80.10	3.6	8.2	735	4.5	15.7	3.7	24.3	116.4	54.2	14.8
25. Sbaihia	3.24	4.5	9.6	173	5.3	5.3	1.9	31.2	169.2	56.1	19.1
26. El Melah	0.85	6.9	5.8	54	5.1	4.1	3.6	31.1	220.8	54.2	20.3
27. Es Seghir	3.09	5.9	9.1	161	4.1	5.4	2.5	36.3	242.8	56.1	24.8
28. Kamech	2.45	5.1	6.9	108	19.4	5.0	3.5	25.8	86.9	51.5	14.1

Table 2 Reservoirs and observation of siltation.

Reservoir	Height of dike (m)	Initial volume (10^3 m^3)	Year of creation/ first observation	Last bathymetric observation/ final observation	Corresponding mean soil loss (tons/ha/year)
1. Arara	10	91.1	1993	1998	25.0
2. Mrira	10.5	126.3	1991	2002	3.1
3. Abdeladim	10	164.0	1992	2002	3.2
4. Bou Haya	17.5	4420.0	1994	1999	4.2
5. Echar	11	186.8	1993	1996	2.9
6. El Amadi	9.90	200.0	1992	2002	7.8
7. Baouejer	7.40	66.0	1991	1998	2.9
8. Jédéliane	20.5	1698.9	1992	1999	11.4
9. Sadine 1	9.70	34.1	1988	1998	16.0
10. Sadine 2	10.8	82.4	1990	2000	24.5
11. Es Senega	9.85	86.4	1991	1998	12.8
12. Hadada	11	849.7	1992	1996	11.2
13. Janet	10.5	95.5	1992	1998	26.8
14. Brahim Zaher	10	86.1	1992	1999	14.0
15. Abdessadok	9.85	92.5	1990	1998	15.9
16. Hnach	10	77.4	1992	1996	17.8
17. Fidh b. Naceur	9.6	47.1	1990	1999	14.5
18. Mrichet El Anze	10	41.7	1991	1999	11.4
19. Fidh Ali	11	134.7	1991	1999	22.7
20. Dekikira	10.5	219.1	1991	1996	20.7
21. El Gouazine	10	233.3	1990	1998	1.7
22. El Mouidhi	10	142.7	1991	1998	21.7
23. Saadine	10	35.6	1992	1998	25.4
24. El Ogla	16.20	5887.0	1989	1999	36.4
25. Sbaihia	11	135.5	1993	1996	16.3
26. El Melah	10	15.3	1991	1999	10.7
27. Es Seghir	10	192.4	1992	1996	2.5
28. Kamech	10	142.5	1993	1999	24.9

The representativity of the studied period versus long-term siltation conditions was evaluated. The longest and most reliable long-term measurement has been made in 9 reservoirs belonging to the three most important catchments in semiarid middle Tunisia. Figure 2 shows the mean annual soil loss during the period 1925–2004 including also the investigated period 1993-2003. The mean annual soil loss for the longer period was about 11.5 tons/ha/year. The same value for the investigated period was 13.5 tons/ha/year. This minor difference indicates that the 1993-2003 period was not exceptional in terms of average soil loss for the area.

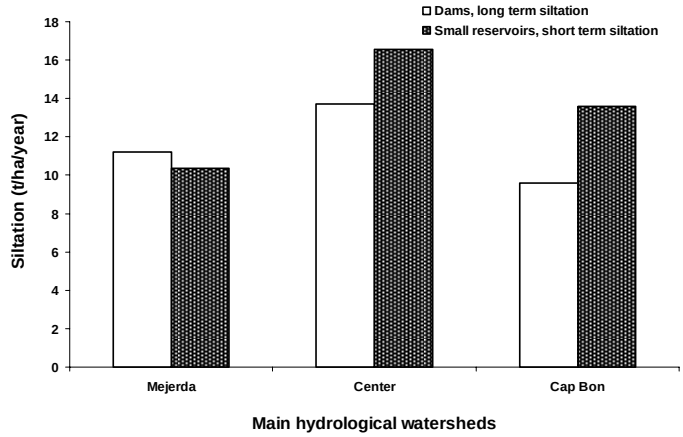

Fig. 2 Long-term (1925-2004) soil loss as compared to soil loss for the investigated period (1993-2002).

Erosion process assumptions

Erosion processes are known to be variable within and between catchments (Campbell, 1992; Li *et al.*, 2006). The three main types of water erosion are: interrill, rill, and gully erosion. Interrill erosion concerns the uniform removal of soil and is assumed to be the first phase of the erosion process. Its rate is assumed to be low (Toy *et al.*, 2002), but it affects the largest areas and has an essential role in the erosion system (Malam Issa *et al.*, 2006; EEA, 2002). Rill erosion, presumably begins when interrill erosion reaches about 15 tons/ha/year (Toy *et al.*, 2002). Interrill and rill erosions concern about 40% of the sediment moving into the reservoirs (Plata Bedmar *et al.*, 1997). However, gully erosion which is a localized process supply about 60% of total sediment yield to reservoir siltation (Plata Bedmar *et al.*, 1997; Martínez-Casasnovas, 2003; Lesschen *et al.*, 2007).
Extreme and exceptional rainfall events are known being responsible for most of the soil erosion taking place in the Mediterranean areas (Boix-Fayos *et al.*, 2007). They are characterized by short event duration (Cerdan, 2004; Cammeraat, 2002; EEA, 2002; Ramos *et al.*, 1997; Weggel, 1992) and specific return period intervals (Bull *et al.*, 1999; Hooke *et al.*, 2000; Coppus *et al.*, 2002; Garcia-Ruiz *et al.*, 2003). Taking these features into account, erosive rainfall characteristics in semiarid Tunisia were defined by Jebari *et al.,* (2008) relating type of erosion to return period, and intensity of maximum 15-min duration rainfall according to:

1) Interrill erosion:	$1 \leq T < 5$	corresponding to	$38 \leq I_{15} < 65$
2) Rill erosion:	$5 \leq T < 10$	corresponding to	$65 \leq I_{15} < 75$
3) Gully erosion:	$10 \leq T$	corresponding to	$75 \leq I_{15}$

where T is return period in years and I_{15} is maximum 15-min duration rainfall in mm/h.

The above relationships should be regarded as a simplified way to estimate the occurrence of different erosion types depending on the maximum 15-min duration rainfall intensity. The intensity boundaries should not be seen as fixed but rather indicative. Together with additional information on a particular catchment´s situation in the soil degradation cycle the relationships can be used to estimate the risk for different types of erosion in the Dorsal region (see further Jebari *et al.*, 2008).

Methods

Reservoir sediments typically represent an important record of a catchment's erosion history. In fact, they provide information over relatively large time spans and so including main exceptional erosive rainfall events responsible for erosion and siltation (e.g., Price *et al.*, 2000; De Vente, 2005). From this point of view the bathymetric measurements were used to estimate average and maximum siltation rates for each catchment (Tables 2 & 3). Average siltation rate was calculated using the first and the last bathymetric measurements of each reservoir. From these data an annual average siltation was determined (Table 2). These calculations were performed for all reservoirs. For the maximum siltation rate in Table 3 the maximum siltation rate was selected from two successive bathymetric campaigns for a specific reservoir. However, some reservoirs only had one single bathymetric campaign. This was the case for the Mrira, Bou Haya, Baouejer, and Jedeliane reservoirs (Table 3). For these reservoirs maximum siltation could not be determined. The average siltation rate could be

Table 3 Observation periods for reservoirs. For Mrira, Bouhaya, Jedeliane, and Baouejer the period of maximum soil loss could not be determined.

Reservoir	No. bathym. observ. except first one, year of observation	Period for max. soil loss rate	Max. soil loss (tons/ha/year)	Max I_{15} (mm/h)	Return period (years)
1. Arara	(3) 1995-1996-1998	1995-06-08 to 1996-10-10	52.3	60	5
2. Mrira	(1) 1996	-	-	-	-
3. Abdeladim	(3) 1994-1997-1999	1997-08-01 to 1999-07-28	7.4	66	5
4. Bou Haya	(1) 1999				
5. Echar	(2) 1994-1996	1994-12-12 to 1996-06-21	5.6	39	1
6. El Amadi	(2) 2000-2002	2000-07-31 to 2002-08-31	14.7	96	20
7. Baouejer	(2) 1996-1998	-	-	-	-
8. Jédéliane	(1) 1999	-	-	-	-
9. Sadine 1	(3) 1996 (month 06 & 12) - 1998	1994-07-31 to 1996-06-15	47.0	110	50
10. Sadine 2	(4) 1994-1996-1998-2000	1994-06-14 to 1996-05-07	59.1	100	50
11. Es Senega	(3) 1995-1996-1998	1995-05-19 to 1996-06-06	30.8	52	2
12. Hadada	(2) 1994-1996	1994-10-11 to 1996-05-16	24.0	45	2
13. Janet	(3) 1994-1996-1998	1994-10-12 to 1996-05-17	62.8	42	1
14. Brahim Zaher	(4) 1994-1996-1998-1999	1994-12-02 to 1996-09-27	21.9	50	2
15. Abdessadok	(2) 1995-1996	1995-06-07 to 1996-06-05	64.1	64	5
16. Hnach	(2) 1993-1996	1993-10-13 to 1996-05-30	43.2	87	20
17. Fidh b. Naceur	(4) 1993-1996-1998-1999	1998-07-31 to 1999-05-27	28.7	41	1
18. Mrichet El Anze	(4) 1993-1996-1998-1999	1996-05-29 to 1998-03-17	19.5	72	10
19. Fidh Ali	(5) 1993-1996-1997-1998-1999	1996-05-23 to 1997-06-27	49.6	50	2
20. Dekikira	(2) 1995-1996	1995-06-13 to 1996-06-12	72.1	50	2
21. El Gouazine	(4) 1993-1996-1997-1998	1993-07-06 to 1996-06-13	3.2	88	20
22. El Mouidhi	(3) 1994-1996-1998	1994-07-07 to 1996-06-26	38.2	102	50
23. Saadine	(4) 1994-1996-1997-1998	1996-08-29 to 1997-04-03	152.6	122	100
24. El Ogla	(4) 1995-1996-1997-1999	1997-04-03 to 1999-06-06	88.3	74	10
25. Sbaihia	(2) 1994-1996	1994-09-19 to 1996-10-01	23.2	61	5
26. El Melah	(3) 1995-1996-1999	1996-11-15 to 1999-08-12	17.1	110	50
27. Es Seghir	(2) 1995-1996	1995-02-15 to 1996-10-04	5.4	152	100
28. Kamech	(5) 1995-1996-1998-1999 (month 07 & 12)	1995-07-06 to 1996-07-31	50.5	102	50

determined using the storage volume just after construction of the reservoir. Using calculated siltation rates, average and maximum soil loss rates were computed for each catchment.

At the end of the hydrological year 2006-2007, the siltation state of the reservoirs was evaluated through field visits. Accordingly, their average life span was deduced. The latter, was compared to the average depreciation time for reservoirs or water harvesting structures. The average life span for such structures ranges from 20 to 40 years (Anonymous, 2000b; Dendy *et al.*, 1973; Goel *et al.*, 2005; Khybri, 1985; Verma, 1987). Thus, the erosive rainfall events that characterise the different siltation periods are especially important. Consequently, the dates related to the above bathymetric measurement periods (for average and maximum siltation) were used to identify the extreme rainfall events that occurred during these intervals. The maximum 15-min duration events were analysed in order to determine the resulting deposited sediment amount during the corresponding period. They were also used to determine the erosion process contribution to the soil loss rate for all catchments. The spatial distribution of erosive rainfall together with erosion processes were analysed for 22 catchments. Catchments that received specific erosion management and lacking maximum siltation values were discarded from the below spatial analysis.

Since the surface conditions of the 28 catchments were carefully observed and since they present a wide range of degradation stages (Fig. 3) the catchments were divided into degradation groups. Based on the degradation group the life span of the reservoir can be better determined. These groups are also helpful to understand the different siltation responses from one catchment to another independent of climatic, physical, and geographical conditions. The

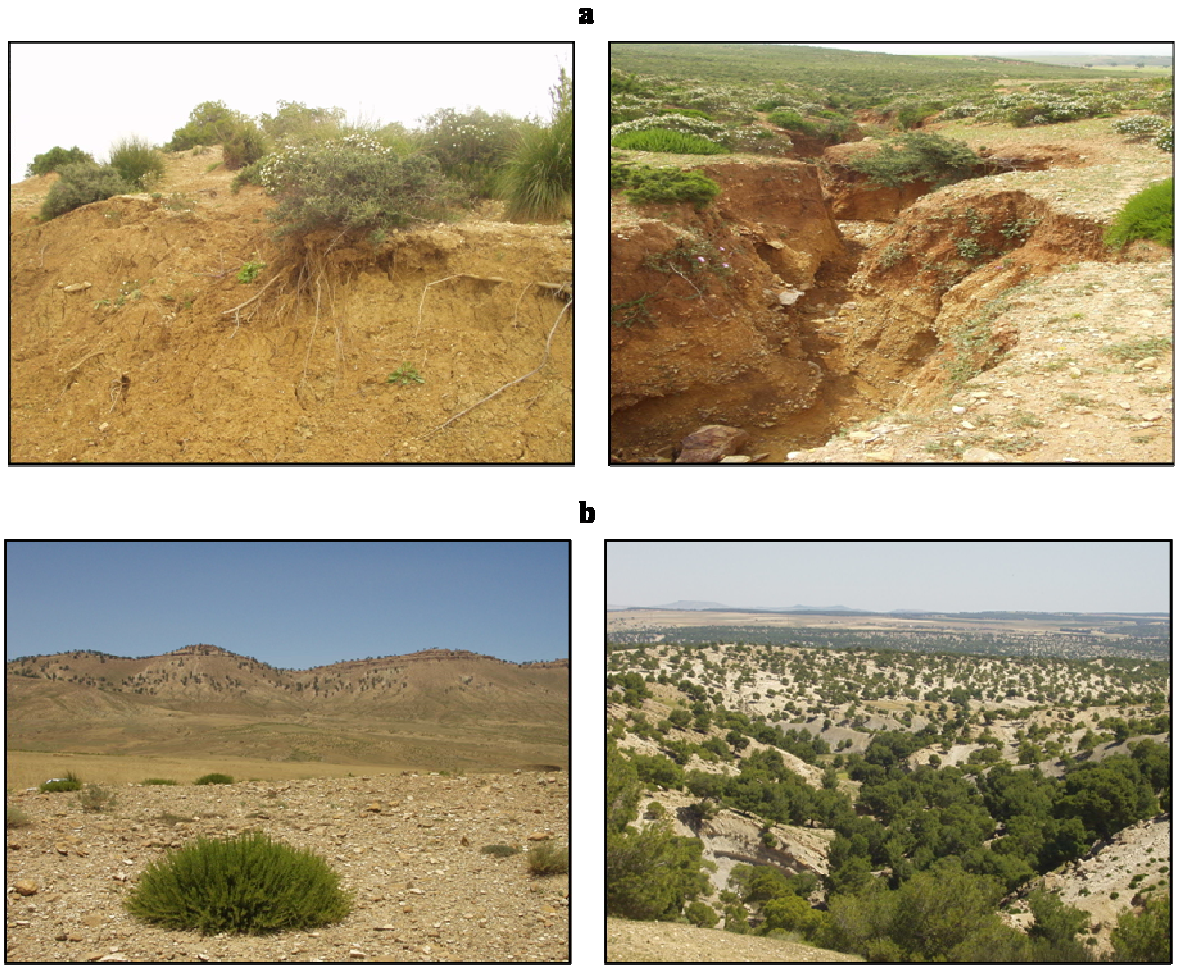

Fig. 3 Soil cover characteristics, original bedrock displayed on the surface at a small (a) and at a large scale (b) in the observation area.

degradation grouping also allows a division into different vulnerability categories depending on where each specific catchment is located in a soil degradation cycle. According to Fig. 3, the dominant landscape over the Dorsal area is characterized by a soil surface horizon that is the original bedrock. This is noticeable at small as well as at large scales.
The above experimental catchments were investigated through field trips and interviews with local farmers, inhabitants, and water engineers. Catchments were characterized through their original bedrock (soft, hard, depth, etc.), their surface horizon aspect (rough, smooth, etc.), and erosion traces (rill and gully). Thus, catchments with similar degradation feature vs. soil erosion rates could be grouped and compared to rainfall intensities. Once organised according to the erosion vulnerability, catchments could be clustered according to a typical "soil degradation cycle" spanning the entire Dorsal area. The procedure used for the catchments was also used at a larger scale for the entire Dorsal area. At this scale, the spatial distribution of rainfall intensities, erosion processes, and the soil loss rates were used to define a "soil degradation front". This front is considered as a degradation centre where erosion is at its maximum. Areas within the soil degradation front may potentially supply large loads of soil particles to downstream areas.

RESULTS

Erosive event characteristics and soil loss rates

The erosive events may be linked to the three different types of erosion namely, interrill, rill, and gully erosion according to Jebari *et al*., (2008). Based on these assumptions, the studied area shows an average of 60 erosive events per year. They are unevenly distributed for different rain gauge stations. The average erosive event was 2.2 per station and year. The average erosive events duration was 105 min with a depth of 24.6 mm, a maximum intensity of 56 mm/h, and an average intensity of 23.5 mm/h. The total number of erosive events representing interrill, rill, and gully erosion was 342, 84, and 65, respectively. The number of rainfall events related to the different erosion types varied depending on rainfall station (Fig. 4(a)). Interrill rainfall events, however, are present for all stations, while rill and gully rainfall events occur occasionally depending on year.
In general, large variation between the erosive rainfall events and the annual average soil loss rate was found (Fig. 4(a) & Table 2). The total number of erosive rainfall events during the 10-year observation period varied from 8 to 29 depending on station. About 8 erosive events at Arara and Barhim Zaher corresponding to an average siltation of 14 and 25 tons/ha/year, while 17 erosive events at Abdeladim, Hadada, and Abdessadok gave a siltation of 3.2, 11.2, and 15.9 tons/ha/year, respectively. About 29 erosive events at Kamech and Ogla corresponding to 24.9 and 36.4 tons/ha/year, respectively. At stations like Jedeliane and Mrichet 20 erosive events gave the same siltation rate of 11.4 tons/ha/year. Similarly for Dekikira and Mouidhi with 22 erosive events resulted in a soil loss equal to 21 tons/ha/year. Noteworthy, Ogla displayed the maximum average soil loss rate among all studied reservoirs (Table 2). This station also had the largest number of erosive rainfall events per year (3.7).
Figure 4(b) illustrates the maximum soil loss depending on catchment. All catchments had 91 recorded erosive rainfall events during the maximum soil loss periods. This corresponded to 68 interrill, 14 rill, and 9 gully erosion events. For these events, all stations except Saadine experienced interill erosion. Nine stations experienced interrill erosion only (Fig. 4(b)). The observed soil loss during these events was 62.8, 49.5, 30.8, and 72.1 tons/ha/year for Janet, Fidh Ali, Es-Senega, and Dekikira, respectively (Table 3). This indicates how important the contribution from interrill erosion is for the reservoir siltation throughout the Tunisian Dorsal

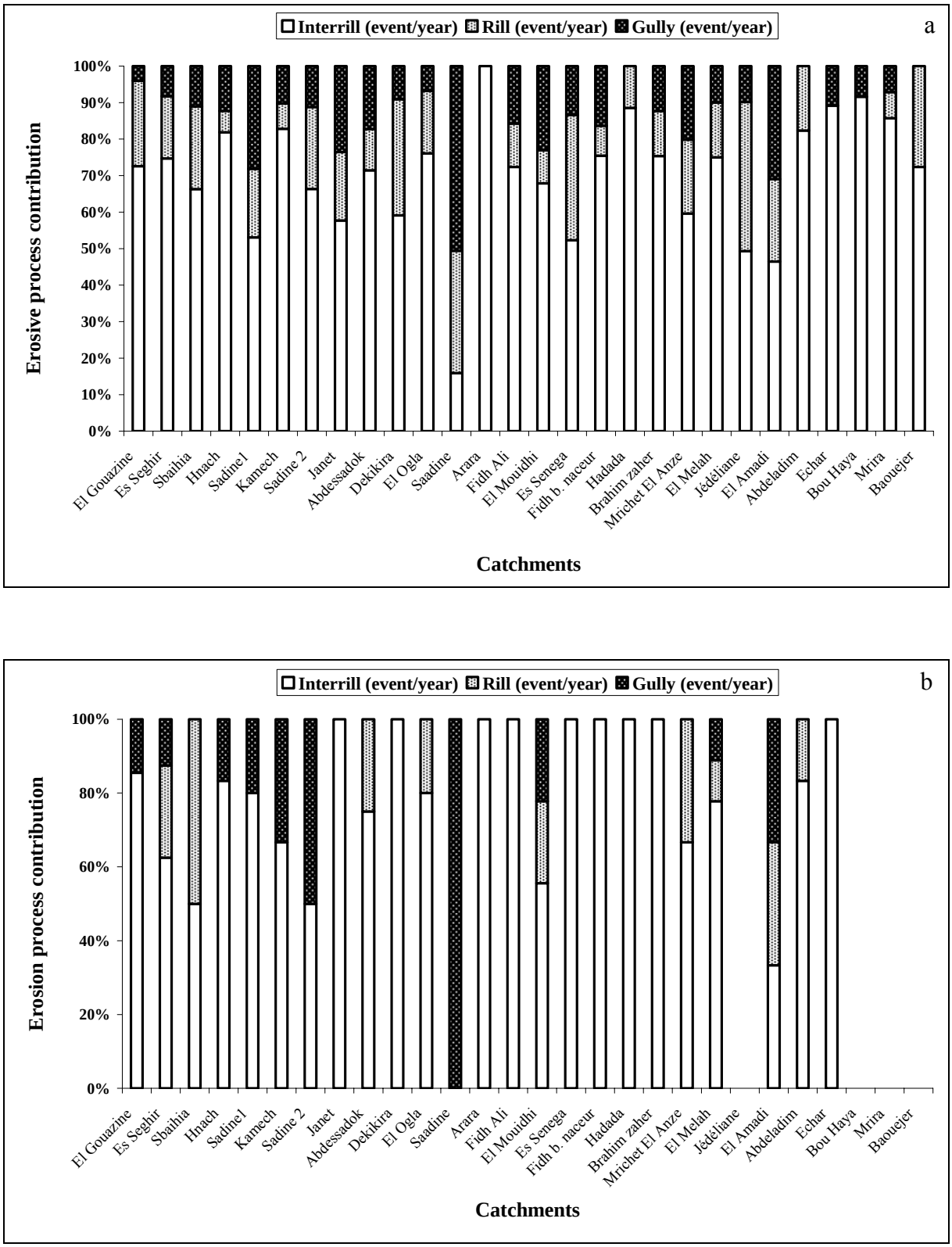

Fig. 4 Relative importance of erosion type depending on catchment. Catchments are listed according to location in the degradation cycle. (a) illustrates the average soil loss and (b) the maximum soil loss.

area in the absence of rill and gully erosion. Interrill together with a single rill event, displayed a maximum soil loss rate of 64.1 tons/ha/year at Abdessadok. For two occurring rill events the maximum soil loss rate reached 88.3 tons/ha/year at Ogla. These two rill events

exceeded what was observed for interrill erosion alone. Joint interrill and rill erosion appears to be able to increase the maximum soil loss by more than 20 tons/ha/year as compared to interrill erosion only (Table 2, 3, & Fig. 4). A catchment that displays gully erosion is Saadine (Fig. 4(b)). This catchment had an average soil loss of 152.2 tons/ha/year (Table 3).
The difference in soil erosion regarding average and maximum values depends on an increase in the annual erosive events by 9%. This is shown by an annual increase of interrill events by about 25% (33 events per year for the average soil loss and 41 events per year for the maximum soil loss period based on 9 stations, among these Dekikira and Ogla). However, different response for individual events may average out for longer periods of time. One such example is the Arara and Kamech catchments. They are situated to the west and east. Although, they are very different in terms of physical properties and rainfall characteristics they present an average similar soil loss of about 25 tons/ha/year and a maximum siltation of about 50 tons/ha/year. The latter value is due to an exceptional 5-year return period event at Arara and a 50-year return period event at El Kamech. In general, the number of erosive events per year shows a wide range of soil erosion rates. A larger number does not necessarily mean a larger soil erosion rate. It has to be remembered that each catchment has its own specific response to number and type of erosive rainfall events.

Soil loss rates and soil degradation cycle

The mean annual soil loss for all catchments was 14.5 tons/ha/yr (Table 2), while the maximum soil loss rate was 44.2 tons/ha/year (Table 3). The mean values varied from 1.7 tons/ha/year for El Gouazine reservoir to 36.4 tons/ha/year for El Ogla (Table 2). Among the 28 catchments studied, 17 display an annual soil loss of more than the permissible limit of 12 tons/ha/yr (Wischmeier and Smith, 1978; Table 1). If we use Masson´s (1972) permissible limit for average soils instead (5 tons/ha/year), we find that 22 catchments are seriously being eroded. at the end of the hydrological year 2006-2007, most reservoirs displayed a rapid siltation. In fact almost half of the reservoirs were already completely filled up with silt. This occurred for an average life span of about 14 years. Referring to the depreciation time mentioned in the literature, the dorsal life time reservoir's is well below average rates.
The observed siltation rates do not show any significant straightforward correlation with the different physical and hydrological features of the studied catchments (Table 1).

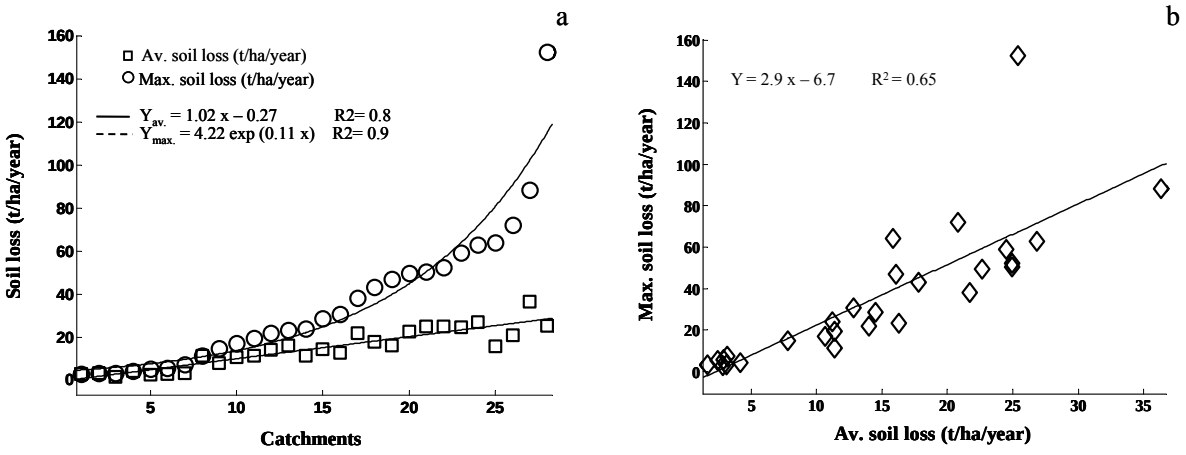

Fig. 5 (a) Distribution of average and maximum soil loss rates, (b) Average vs. maximum soil loss. Catchments are arranged according to increasing values.

This result corroborates findings by Boufaroua et al. (2006). In fact, that study showed limited impact of topography, lithology, and even anthropogenic factors to forecast siltation for the Dorsal reservoirs. However, the distribution of average and maximum soil loss rates for all catchments arranged in an increasing order are shown in Fig. 5(a). The latter displays, respectively, a linear and an exponential distribution. Figure 4(b) shows that there is a strong linear relationship between mean and maximum annual soil loss.

The soil degradation cycle for the different catchments is essential in order to understand the observed siltation rates. Catchments that are at the end of the soil degradation cycle and thus displaying large areas of bare bedrock obviously yield small soil erosion rates. For example, the hard rocky upstream area of Hadada (11.2 tons/ha/year) displays an exhaustion of transported sediments while Janet with deeper soft bedrock layers (26.8 tons/ha/year) shows great availability of transported soil particles. Figure 6 shows examples of soil surface properties from various parts of the Dorsal observation network. These photos of the catchment landscapes tell much about the actual location in the soil degradation cycle and possible erosion rates. Examples of this are Arara, Echar, and Abdeladim with almost no gullies characterising the landscapes (Fig. 6). For the opposite case, Sadine 1, Dekikira, and Saadine show a developed gully network all over their catchment area (Fig. 6).

Predisposition and resistance of small catchments to soil loss depend on the ability of the catchments to deliver soil particles. This ability is conditioned by the soil degradation cycle for each specific catchment. The degradation cycle can be described by three different catchment erosion states according to Fig. 7. The first state (group I in Fig. 7) is related to low soil loss rate and concerns catchments that are protected against rainfall erosivity by several parameters such as erosion and soil restoration management practices. The two catchments El Gouazine and Seghir illustrate this first phase well. Accordingly, they show low siltation rates (Table 2). For example, most of the soil surface in El Gouazine has been modified with soil contour ridges along the topographical isolines in order to prevent runoff and erosion.

The second state corresponds to catchments that are more active in the degradation process since they display deeper soil layers and a soft original bed rock (group II in Fig. 7). The catchments yield soil particles in a generous way and soil loss rate is large. Examples of this are Janet, Sadine2, Kamech, Saadine, and Dekikira where the gully network is well developed. Actually, most of the catchments belong to this second state characterised by badlands.

The third state of the cycle includes catchments that are in their last stage of degradation (group III in Fig. 7). The majority of available soil particles have already been lost to downstream areas. Catchments display modest soil loss rates where the original hard bedrock is uncovered. This last state is displayed by a few catchments to a varying degree. Some examples are Bou Haya, Baouajer, and Abdeladim. The two last catchments are displaying a calcareous crust on the soil surface.

Spatial erosive rainfall and soil erosion

Relying on the same assumptions, regarding links between erosive rainfall intensity and soil erosion type, it is possible to delineate spatial properties of erosive rainfall and soil erosion. Figure 8(a) shows the spatial distribution of erosive rainfall over the Dorsal area estimated from the maximum 15-min duration rainfall (1993-2003). The I_{15} intensities increase anti-clockwise from the crest and downhill surrounding the mountain range above 300 m of altitude. Below this level, I_{15} takes an opposite direction. Therefore, the Dorsal area seems to be shared into an eastern and a western part according to a specific centre. The latter, is localized on the main Dorsal axis at the level of Saadine-Ogla stations. The eastern area

Fig. 6 The Dorsal landscape in general and the experimental catchments in particular display different location in the soil degradation cycle. Numbers correspond to catchment in Table 1.

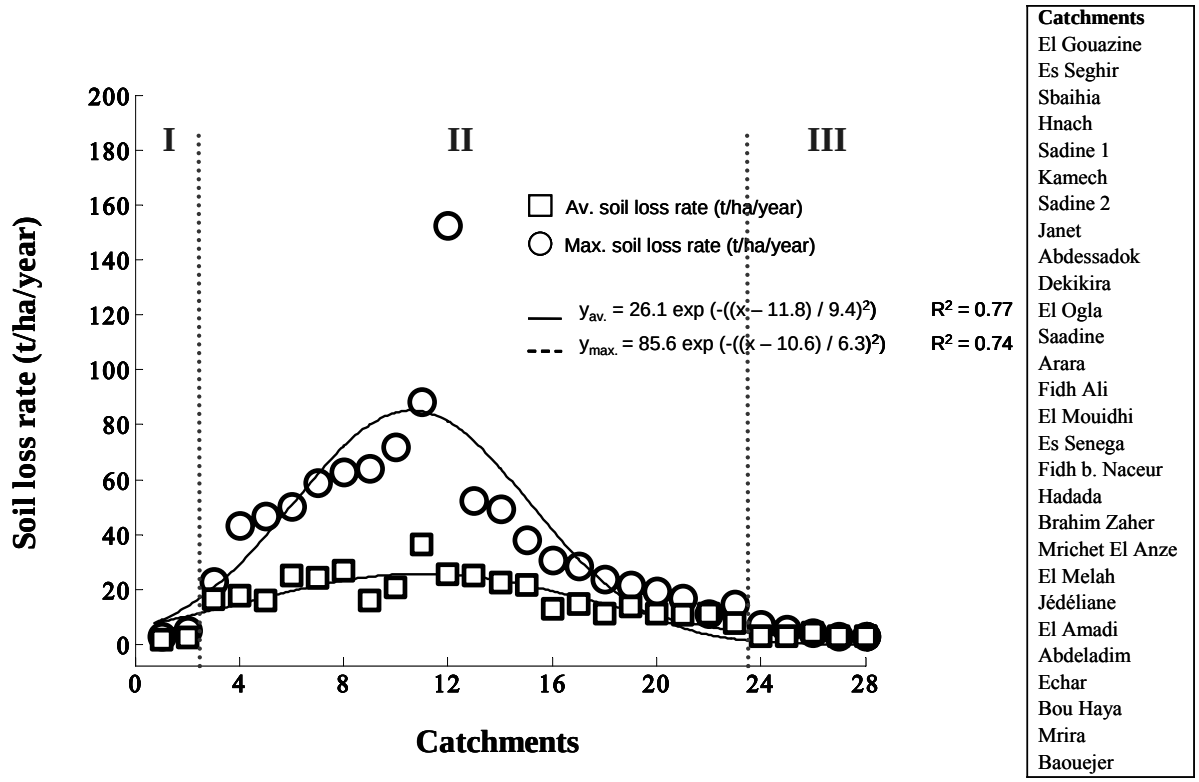

Fig. 7 Soil degradation cycles (I, II, and III) depending on average and maximum soil loss rates. Stations are arranged according to their degradation levels as determined during field visits (according to list to the right).

includes the Cap Bon peninsula and corresponds to the upper end of the Dorsal chain. This part is subject to the north-eastern disturbances that carry large amounts of moisture. They are characterized by large variability and violent storms which can occur during all seasons (Rodier et al., 1981; Fons, 1987). The western parts are watered by north-western disturbances which arrive in Tunisia filled with moisture and give rise to heavy rainfall (INM, 1993). A comparison between the eastern and the western parts in term of rainfall characteristics seems to be relevant for erosion dynamics. In fact, the eastern part displays exceptional events that are 25% more recurrent, 40% more intense, 45% longer in duration, and 28% more important in amount as compared to conditions at the western part (Table 1). One of the reasons for this is that the eastern part presents no continuous important physical barrier for rainfall. Catchment areas here are smaller (30%) presenting shorter concentration times (42%). Consequently, 30% and 40% more average and maximum soil loss have been found (Tables 2, 3). The eastern area also presents an advanced degradation level as compared to the western area.

Figure 8(b,c,d) shows the distribution of soil erosion risk expressed as the average number of erosive events per year based on the spatial pattern for I_{15} (Fig. 8(a)). Figure 8(e,f) shows the spatial distribution of observed soil erosion loss in tons/ha/year calculated from the bathymetric data. The agreement between Fig. 8(b,c,d) and 8(a) is not perfect, at least not at the detailed level. However, the general agreement at a larger scale is quite striking. All estimated erosion types display a maximum near the north-eastern or north-western parts of the Dorsal. This is the same general pattern as for the observed erosion. The interrill risk map displays the largest values for the north-eastern parts of the Dorsal whereas the rill and the gully erosion risks appear to be the greatest in the north-west and the central north-eastern areas.

As seen from Fig. 8(e,f), the observed spatial average and maximum erosion is similar over the Dorsal area. The western part of the Dorsal displays the lowest erosion rates while the mid-eastern parts have the highest rates. Consequently, there is a clear general trend for

observed erosion along the Dorsal axis (broken line in Fig. 8). The trend is increasing towards the mid-eastern Dorsal. The maximum erosion is observed for the Ogla-Saadine stations. These stations respectively present the most important difference in height (735m) and the maximum observed soil loss for the whole network (Table 1, 3).

Some of the discrepancy between estimated and observed erosion rates depends on differences in the erosion cycle for the observed catchments. If all catchments would have had similar soil surface the observed erosion would probably have been more close to the estimated one (from extreme rainfall).

From a large-scale point of view the erosive processes and the availability of potential erosive material can be viewed as a slowly moving "soil degradation front". This soil degradation front coincides with the 300 m altitude at the level of the Ogla-Saadine transverse. It is continuously progressing westward from lower to higher altitude following the main Dorsal axis. Consequently, the situation of catchments in the soil degradation cycle clearly displays the soil particle delivery potential for the Dorsal area. This then determines the progress of the soil degradation front as influenced by extreme rainfall.

The above findings are crucial to determine the most urgent areas where soil erosion control needs to be developed. For this, the main erosion type, exposure to extreme rainfall, degradation front direction, and the most vulnerable catchments within the degradation cycle need to be taken into account. For the Dorsal area it is clear that the 300 m altitude cross-section is an erosion front that needs to be closely monitored and further investigated. Similarly, areas surrounding the Dorsal ridge and areas at mid-slope locations are also necessary to monitor. All these areas need urgent management to halt severe erosion.

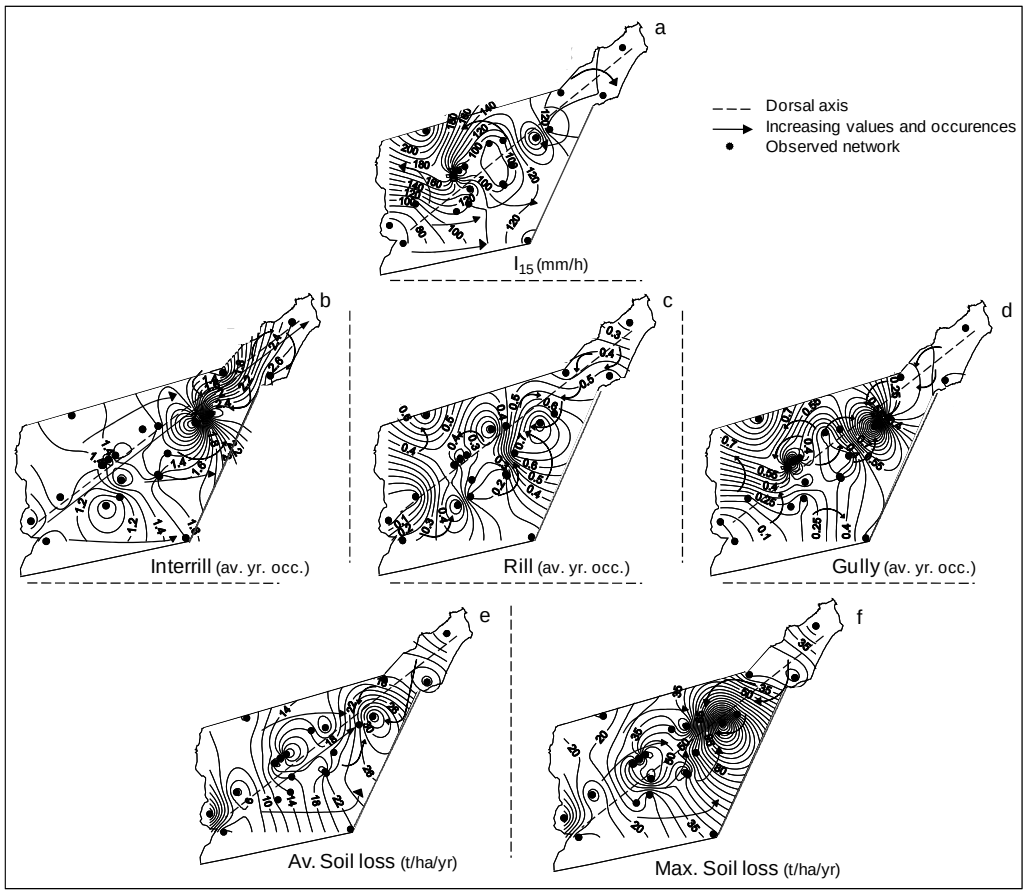

Fig. 8 a) Spatial distribution of maximum 15-min duration rainfall intensity (1993-2003; Jebari *et al*., 2008), b) c) d) estimated number of annual events for different erosion types namely interrill, rill, and gully erosion, and e) f) observed average and the maximum soil loss in tons/ha/year.

CONCLUSIONS

The average soil loss for semiarid Tunisian small catchments is 14.5 tons/ha/year. This induces a rapid siltation of the Dorsal small reservoirs which present a general life-span of about only 14 years. The maximum 15-min duration maximum rainfall was seen to generate meaningful maps of erosion risks at large scales. These maps together with information on situation of a specific catchment in the soil degradation cycle can be used to get a general idea of catchment erosion.

The north-western part of the Dorsal displays the most extreme rainfall erosivity. Consequently, spatial erosion patterns are to some extent similar but are also greatly modified depending on their location in the soil degradation cycle. In general, the north-western parts of the Dorsal display modest soil erosion patterns due to the already severely degraded soil structure. Their soil surface often consists of the hard original bedrock. The greatest soil erosion occurs in the mid-eastern parts of the Dorsal in catchments where deep vulnerable soils have only recently been exposed to severe erosion. In fact, the catchments are a part of the current degradation front of the Dorsal.

The mountain range provides soil particles from two main areas. The first area is the vulnerable catchments located in the second group within the soil degradation cycle. The second area corresponds to the degradation front currently located at about 300 m altitude. This front appears to be moving westward at a distance of more than 80 km perpendicular to the main Dorsal axis range.

The above results can be used for planning purposes to develop mitigation strategies for soil erosion management. At the small scale, such as farming plot, the above approach is less useful due to the effect of local land-use and farming practices. At the larger scale, however, the results can be used to better manage soils and soil covers in the Dorsal area and eventually to decrease the soil erosion and reservoir siltation risks.

Acknowledgements Sihem Jebari and Akissa Bahri thank Mr Habib Farhat, head of the Tunisian Farmland Conservation and Management Department (DG/ACTA) for providing data and all his staff from Kasserine, Siliana, Kairouan, Zaghouan and Nabeul regional departments for valuable time and discussions allocated to this work. They also gratefully acknowledge Mr Ali Debabria for managing the field trips. Ronny Berndtsson was supported by the Swedish International Development Agency.

REFERENCES

Anonymous, (2000b) Project Report of Panjara watershed under NWDPRA of Nurpur block in district Kangra of Himachal Pradesh. *Department of Agriculture, Government of Himachal Pradesh.*

Ben Mamou, A. (1998) Barrages Nebeur, Sidi Salem, Sidi Saad, et Sidi Bou Baker. Quantification, étude sédimentologique et géotechnique des sédiments piégés. Apport des images satellitaires. Thèse de Doctorat Es-Sciences géologiques, présentée à l'Université de Tunis II, Faculté des Sciences de Tunis.

Boix-Fayos, C., Martinez-Mena, M., Calvo-Cases, A., Arnau-Rosalén, E., Albaladejo, J., Castillo, V. (2007) Causes and underlying processes of measurement variability in field erosion plots in Mediterranean conditions. *Earth Surf. Process. Landforms* **32,** 85–101.

Boufaroua, M., Lamachère, J.M., Débabria, A., Ksibi, F. (2006) Prédétermination de l'envasement des lacs collinaires de la Dorsale Tunisienne. *14ème conférence de l'ISCO*. 14-19 Mai, Marrakech, Maroc.

Bull, L.J., Kirkby, M.J., Shannon, J., Hooke, J.M. (1999) The impact of rainstorms on floods in ephemeral channels in southeast Spain. *Catena* **38**, 191–209.

Cammeraat, L.H. (2002) A review of two strongly contrasting geomorphological systems within the context of scale. *Earth Surf. Process. Landforms* **27**, 1201–1222.

Campbell, I.A. (1992) Spatial and temporal variations in erosion and sediment yield. In: Bogen, J., Walling, D.E., and Day, T., Editors, *Erosion and sediment transport monitoring programmes in river basins*. Proc. Internat. Symp., Oslo, 24–28 August, 1992 (1992), pp. 455–465 IAHS Publication No. 210.

Camus, H., Guiguen, N., Ben Younes, M. (1995) *Note sur l'envasement de lacs collinaires en zone semi-aride Tunisienne*. Rapport publié par la Direction de la Conservation des Eaux et du Sol & l'Institut de Recherche pour le Développement en Cooperation (ORSTOM).

Coppus, R., Imeson, AC. (2002) Extreme events controlling erosion and sediment transport in a semi-arid sub-andean valley. *Earth Surf. Process. Landforms* **27**, 1365–1375.

DCES/IRD (1994-2002) *Annuaires hydrologiques des lacs collinaires*. Rapports publiés par la Direction Générale de l'Aménagement et de la Conservation des Terres Agricoles & l'Institut de Recherche pour le Développement. République Tunisienne.

Dendy, F. E., Champion, W. A., Wilson, R. B. (1973) Reservoir sedimentation surveys in the United States. In Ackermann, W. C., White, G. F., Worthington, E. B., editors, *Man-made lakes: their problems and environmental effects*. Geophysical Monograph 17, Washington, DC: American Geophysical Union, 349-357.

De Vente, J., Poesen, J., Verstraeten, G. (2005) The application of semi-quantitative methods and reservoir sedimentation rates for the prediction of basin sediment yield in Spain. *J. Hydrol.* **305,** 63–86.

EEA (1999) Environment in the European Union at the Turn of the Century. European Environmental Agency.

EEA (2000) Down to earth: Soil degradation and suistainable development in Europe. Environmental issue series, European Environmental Agency, No. 16, 32 pp.

EEA (2002) Assessment and reporting on soil erosion. Background and workshop report. European Environmental Agency.

Ennabli, M., Margat, M., Vallee, D. (1998) Pour prévenir les crises de l'eau en Méditerranée, priorité à une meilleure maîtrise des demandes. *Conférence internationale « Eau et Développement durable »,* Paris, 19-21 Mars.

FAO (1994) *Situation mondiale de l'alimentation et de l'agriculture 1993*. FAO Agriculture N°26, 326 p.

Fons, C. (1987) *Météo marine*, 01–68. Les dossiers des éditions du Pen-duick.

García-Ruiz, J.M., Martí-Bono, C., Lorente, A., Begería, S. (2003) Geomorphological consequences of frequent and infrequent rainfall and hydrological events in Pyrenees Mountains of Spain. *Mitigation and adaptation strategies for global change* **7**, 303–320.

Goel, A.K., Kumar, R. (2005) Economic analysis of water harvesting in a mountainous watershed in India. *Agricultural Water Management* **71**, 257–266.

GOPA & GTZ (2005) Elaboration d'une stratégie nationale d'adaptation de l'agriculture tunisienne et des écosystèmes aux changements climatiques. *Pré rapport 1ere phase.*

Herath, M.G., Gopalakrishnan, C. (1999) The Economics of Reservoir Sedimentation: A Case Study of Mahaweli Reservoirs in Sri Lanka. *International Journal of Water Resources Development* **15**, 511–526.

Hooke, J.M., Mant, J.M. (2000) Geomorphological impacts of a flood event on ephemeral channels in SE Spain. *Geomorph.* **34**, 163–180.

ILEC and UNEP (2003) World lake vision- A call to action. International Lake Environement Committee Foundation, and United Nations Environment Programme, Nairobi.

ILEC and Lake Biwa Research Institute (eds.) (1988-1993). *Survey of the State of World Lakes, Vols I-V*. ILEC/UNEP, Kusatsu/Nairobi.

Imeson, A.C. (1990) Climate fluctuations and soil erosion under Mediterranean conditions. *Technical report, International University AMenedez Pelayo*,Valencia, Spain.

IRD (2000) Evaluation du programme lacs et barrages collinaires en Tunisie "Hydromed"; Report published by the Institut de Recherche au Developpement..

Jebari, S., Berndtsson, R., Bahri, A., Boufaroua, M. (2008) Exceptional rainfall characteristics related to erosion risk in semiarid Tunisia. *The Open Hydrol. J*, **2**, 25–33.

Keller, A., Sakthivadivel, R., Seckler, D. (2000) Water scarcity and the role of storage in development. *Research report 39. Colombo Sri Lanka International Water Management Institute (IWMI).*

Khybri, M.L. (1985) Experiences of the transfer of technology in soil and water conservation programme, *Proceedings of the National Seminar on Soil and Water Conservation and Watershed Management New Delhi*, September 17–18 , pp. 299–304.

Kirpich, Z.P. (1940) Time of concentration of small agricultural watersheds. Civil engineering. 10(6), pp 362.

Lal, R. (1976) Soil Erosion Problems on Alfisols in Western Nigeria and Their Control. IITA Monograph 1, IITA, Ibadan, Nigeria, 208 pp.

Lesschen, J.P., Kok, K., Verburg, P.H,. Cammeraat, L.H. (2007) Identification of vulnerable areas for gully erosion under different scenarios of land abandonment in Southeast Spain. *Catena* **71**, 11–0121.

Cerdan, O., Le Bissonnais, Y., Govers, G., Lecomte, V., Van Oost, K., Couturier, A., King, C., Dubreuil, N. (2004). Scale effect on runoff from experimental plots to catchments in agricultural areas in Normandy . *J. Hydrol*. **299**, 4**–**14.

INM (1993) Pluies et nuages convectifs. *Unité de recherche et de developpement. Rapport Interne de l'Institut National de la Météorologie, Tunisie.*

Li, M., Li, Z.B., Ding, W.F., Liu, P.L., Yao, W.Y. (2006) Using rare earth element tracers and neutron activation analysis to study rill erosion process. *Applied radiation and isotopes* **64**, 402–408.

Malam Issa, O., Le Bissonnais, Y., Planchon, O., Favis-Mortlock, D., Silvera, N., and Wainwright, J. (2006) Soil detachment and transport on field- and laboratory-scale interrill areas: erosion processes and the size-selectivity of eroded sediment. *Earth Surf. Process. Landforms* **31**, 929–939.

Martínez-Casasnovas, J.A. (1998) Soil– landscape– erosion. Gully erosion in the Alt Penede`s-Anoia (Catalonia, Spain). A spatial information technology approach: spatial databases, GIS and remote sensing. PhD thesis, University of Lleida, Lleida, Spain.

Martínez-Casasnovas, J.A. (2003) A spatial information technology approach for the mapping and quantification of gully erosion. *Catena* **50**, 293– 308.

Masson, J.M. (1972) L'érosion des sols par l'eau en climat Méditerranéen. Méthodes expérimentales pour l'étude des quantités érodées a l'échelle du champ. La Houille Blanche **8**, 673–679.

Plata Bedmar, A., Cobo Rayan, R., Sanz Montero, E., Go´mez Montan˜a, J.L., Avendan˜o Salas, C. (1997) Influence of the Puentes reservoir operation procedure on the sediment accumulation rate between 1954–1994. *Commission Internationale des Grands Barrages, Proc. 19th Congress Grands Barrages, Florence, Italy, 1997,Q.74, R.52, 835– 847.*

Poesen, J.W.A, Hooke, J.M. (1997). Erosion, flooding and channel management in the Mediterranean environments of southern Europe. *Prog. Phys. Geogr.* **21**, 157–199.

Price, L.E., Fawcett, C.P., Young, P.C. (2000) Modeling reservoir sedimentation and estimating historical deposition rates using a data-based mechanistic (DBM) approach. *Hydrological Sciences Journal* **45**, 237–248.

Ramos, M.C., Nacci, S. (1997) Estabilidad de agregados superficales en suelos del Anoia-penedès (Barcelona) frente al humedecimiento y al impacto de las gotas de lluvia. *Edafologia* **3**, 3–12.

Rodier, J. A., Colombani, J., Claude, J. & Kallel, R. (1981) *Le bassin de la Medjerdha*. Monographie de l'ORSTOM, Paris, France.

Sundborg, A. (1992). Lake and reservoir sedimentation prediction and interpretation. Geografiska Annaler. *Series A, Physical Geography* **74**, 93–100.

Tafangenyasha, C. (1997) Should Benji Dam be dredged? A preliminary impact assessment to dredging a water reservoir in an African national park. *Environmentalist*: **17**, 191–195.

Toy, J.T., Foster, G.R., Renard, K.G. (2002) *Soil erosion: Processes, prediction, measurement and control.* Library of congress cataloging-in-publication data. Edited by John Wiley & Sons, Inc., New York. 338 pp.

UNEP (1994). The pollution of Lakes and Reservoirs (UNEP Environment Library). UNEP/Nairobi.

Verma, H.N. (1987) Studies of an Efficient use of rainwater for rainfed crops. Ph.D Thesis. Division of Agricultural Engineering. IARI, New Delhi.

Weggel, J.R., Rustom, R. (1992) Soil erosion by rainfall and runoff - State of the art. Geotextiles and *Geomembranes* **11**, 551–572.

WCD (2000) *Dams and development. A new framework for Decision-Making*. Earthscan Publications Ltd, London , 356 pp.

Wischmeier, W.H., Smith, D.D. (1958) Rainfall energy and its relationship to soil loss. *Trans. Am. Geophys. Union* **39**, 285–291.

Wischmeier, W.H., Smith, D.D. (1978) *Predicting rainfall erosion losses* – A guide to conservation planning. USDA Agriculture Handbook 537, Washington D.C: GPO.

Woodward, J.C. (1995) Patterns of erosion and suspended sediment yield in Mediterranean river basins, In: Foster IDL, Gurnell AM, Webb BW. (Eds.), Sediment and Water Quality in River Catchments. Wiley, Chichester, 365-389 pp.

Regionalizing fine time-scale rainfall affected by topography in semi-arid Tunisia

SIHEM JEBARI[1], RONNY BERNDTSSON[2], CINTIA UVO[2] & AKISSA BAHRI[1]

1 *National Research Institute for Rural Engineering, Waters, and Forestry (INRGREF), Laboratory on Use of Marginal Quality Water, Hydro-Agricultural Structures and Irrigation System Management, BP 10, Ariana 2080, Tunisia*
sihem.jebari@iresa.agrinet.tn

2 *Department of Water Resources Engineering, Lund University, PO Box 118, SE-22100 Lund, Sweden*

Abstract The characteristics of fine time-scale rainfall are important in many hydrological applications, such as infiltration, erosion and flooding. The spatial properties of such rainfall are, however, seldom known, especially for arid and semi-arid areas. A better knowledge of fine time-scale rainfall and also comparison with daily rainfall may yield possibilities for disaggregation. For this purpose, rainfall data of different time scales, from 1-min to daily, from 25 stations during four years (1995–1998), were spatially analysed by means of spatial correlation, empirical orthogonal function (EOF) and hierarchical clustering. The results show that the spatial correlation is typically non-isotropic and varying, depending on topography and local meteorological settings. Similarly, spatial patterns of EOF are closely related to main atmospheric synoptic situations as influenced by orography and spatial dependence regarding areas with predominant convective and frontal rainfall. The clustering displayed different homogeneous sub-groups over the Tunisian Dorsal Mountains that can be used to better manage the limited water resources that often depend on fine time-scale rainfall variability.

Key words daily rainfall; multivariate analysis; regionalization; semi-arid; Tunisia; fine time-scale rainfall; spatial rainfall patterns; Atlantic mountain range

Régionalisation de la pluie à pas de temps fins affectée par la topographie en Tunisie semi-aride

Résumé Les caractéristiques des pluies à pas de temps fins sont déterminantes pour de nombreux phénomènes hydrologiques comme l'infiltration, l'érosion et les inondations. Leurs propriétés spatiales restent, cependant, peu connues en milieux arides et semi-arides. Une meilleure connaissance de la pluie à pas de temps fin et la comparaison avec la pluie journalière pourrait ouvrir des perspectives de désagrégation. Dans ce but, des données de pluie à différentes échelles de temps, allant de la minute à la journée, de 25 stations et couvrant une période de quatre ans (1995–1998), ont été analysées spatialement à l'aide des méthodes de corrélation spatiale, de fonction orthogonale empirique (FOE) et de classification hiérarchique. Les résultats montrent que la corrélation spatiale est typiquement anisotrope et variable, dépendant de la topographie et des conditions météorologiques locales. De même, les structures spatiales de FOE sont très liées aux principales situations atmosphériques synoptiques, sous influence de l'orographie et de la prédominance des pluies convectives ou frontales. La classification a permis d'identifier différents sous-groupes homogènes couvrant la Dorsale tunisienne, qui peuvent servir à mieux gérer les ressources en eau limitées qui dépendent généralement de la variabilité à pas de temps fin de la pluie.

Mots clefs pluie journalière; analyse multivariable; régionalisation; semi-aride tunisien; pluie à faibles pas de temps; propriétés spatiales; chaîne atlasique

INTRODUCTION

Mediterranean rainfall is characterized by strong irregularity. An amount equal to the annual mean can be recorded in a single rainfall event and large floods are often observed (Doswell, 1982; Conte, 1986; Jansa *et al*., 1996; Buzzi & Foschini, 2000; Homar *et al*., 2002). Due to this, analysing rainfall characteristics in the area is one of the most challenging subjects for hydrologists as well as meteorologists (Andrés *et al*., 2000; Campins *et al*., 2000; Lana *et al*., 2004). Both peculiar topographic conditions and differences in the humidity and temperature distribution may induce substantial modification to the general atmospheric flow in this region (INM, 1988). Orography, for example, may act both as a barrier to atmospheric flow from a dynamic point of

view and as a source of sensible and latent heat. This results in rainfall distribution that is extremely complex in space and time from one mountain range to another (Marquinez *et al*., 2003; Arora *et al*., 2006).

The strong variability of rainfall also influences the rural development progress in terms of water and soil resource availability and use (Cudennec *et al*., 2005). Water storage systems, flood protection, water harvesting structures, and silting trap design are common tasks for rural engineers. Even though there are national programmes for improving water resource availability and protecting downstream areas against floods and erosion, there is often a lack of information, e.g. hydrological data of sufficient detail for engineering applications (e.g. Berndtsson, 1988; MEDEX, 2001).

In view of the above, there is a great need to develop regionalization methodologies for these areas with large variability and to establish links between temporal and spatial rainfall variability. For this purpose, we studied fine time-scale rainfall variability using a unique high-quality database observed at 25 gauges in semi-arid Tunisia over the Dorsal Mountain range. The Dorsal Mountains play a very important role for the water resources in Tunisia, since the rain falling here feeds major rivers and their tributaries over large areas. The Dorsal Mountain range is known as the "water tower of Tunisia". The objective of this study is hence to develop regionalization maps that can be used for developing simulation and engineering tools for fine time-scale rainfall data in the range 1 to 30 min and also to compare with daily rainfall in view of disaggregation possibilities. Statistical properties of the rainfall were investigated using spatial correlation and empirical orthogonal functions. Furthermore, a regionalization was performed using hierarchical clustering. We close with a discussion of practical results and further studies.

MATERIALS AND METHODS

Experimental area

Besides the northern Polar front and northeastern trade winds, the Tunisian climate is affected by a wide range of local factors with distinct characteristics (Bousnina, 1986). These include topographic conditions, marine influences, as well as continental effects. The climate is semi-arid Mediterranean characterized by mild, rainy winters and hot, dry summers. Mediterranean and Polar disturbances are the cause of cyclonic rain during the cold season. The cold and rainy period lasts from November to March with large year-to-year variations. Northwesterly, westerly and southwesterly winds prevail from October to May, whereas from April to September the prevailing winds are from the east, northeast and southeast (Rodier *et al*., 1981). Transition seasons (spring and autumn) are characterized by stormy weather. Rain is irregular and often sudden and strong (e.g. Dhonneur, 1985). The frequency of disturbances affecting Tunisia are as follows (Henia, 1980): 42% of the rain is due to northwestern disturbances, 17% is due to western disturbances, 10% is generated by the northeastern disturbances, 14% comes from the southwest, and, finally, 17% of the rain comes from the Sahara region.

The Dorsal Mountains represent the last part of the Atlas Mountain ranges towards the east (Fig. 1). The Tunisian Dorsal region covers a total area of 12 490 km^2. It includes a chain of high mountain peaks, of which the highest is Chaambi (1544 m).

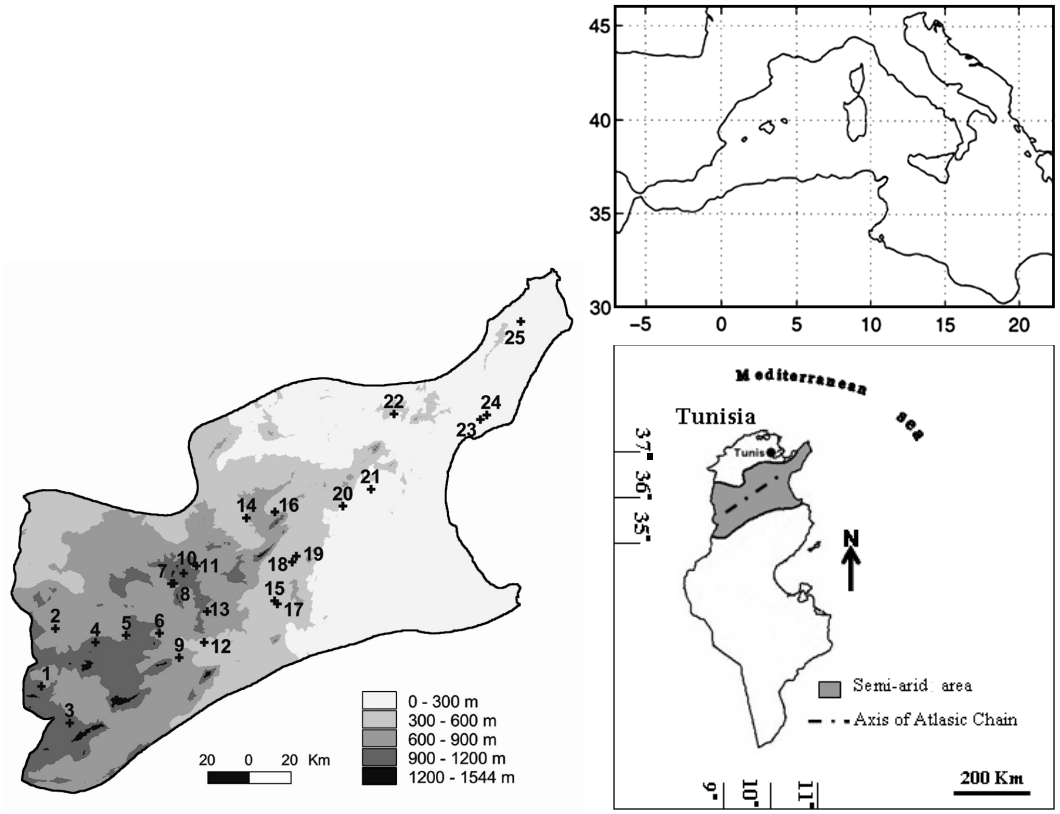

Fig. 1 Topography and raingauge locations.

The Dorsal Mountains stretch through Tunisia from southwest to northeast and end at the Cap Bon Peninsula. The width in the west is about 40 km and it reduces to less than 10 km in the northeast. Altitudes continue to decrease in the same direction. Gammar (1999) defines the Dorsal region as an important orographic region that influences the water resources and natural environment in an important way. A maximum of 110 rainfall days have been observed in the extreme east of the study area and a minimum of 58 rainfall days in the centre. The area also coincides with the 400 mm/year isohyet, which is of a great importance since it is the limit for farming of dry cereals in Tunisia (Houérou, 1969).

A hydrological monitoring network includes about 30 experimental catchments at representative sites along the Tunisian Dorsal range (Fig. 1). Each catchment discharges into a small dam, called a hill reservoir and usually built in an agricultural area. An automatic raingauge is located at each site (D/CES & ORSTOM, 1998) and 25 of these gauges were selected for this study due to a low percentage of missing data (total missing data for the 25 stations during the observation period were less than 1%). The gauging density corresponds to approximately one gauge per 500 km^2. Table 1 gives descriptive statistics for these stations and the recorded rainfall for the analysed 4-year period 1995–1998. However, the statistical properties such as mean value, standard deviation and coefficient of variation given in Table 1 have to be interpreted with great care since the number of data values is just four. Even so, taken together they may indicate the degree of variation. The raingauge network was set up by the EU-funded Programme HYDROMED (Research programme on hill reservoirs in the semi-arid

Table 1 Descriptive characteristics of the Tunisian Dorsal region experimental rainfall network (1995–1998).

Station	Longitude	Latitude	Altitude (m)	Rainy days (year)	Mean (mm/year)	Minimum (mm/year)	Maximum (mm/year)	Std. dev. (mm/year)	Coeff. var. (%)
1 Arara	8°24′25″	35°22′09″	910	71	301.2	239.0	360.8	49.7	17
2. Mrira	8°28′37″	35°36′34″	770	98	378.6	312.5	423.0	54.2	14
3. Abdeladim	8°33′02″	35°13′01″	1030	80	338.3	269.5	429.0	66.9	20
4. Echar	8°40′45″	35°33′11″	970	92	426.6	384.0	513.5	59.0	14
5. Baouejer	8°50′11″	35°34′52″	1010	108	378.5	319.5	440.0	51.3	14
6. Jédéliane	9°00′14″	35°35′27″	1100	73	242.6	140.5	352.5	108.6	45
7. Sadine1	9°03′58″	35°47′49″	842	110	524.1	421.5	598.5	83.3	16
8. Sadine 2	9°04′42″	35°47′53″	950	95	459.2	305.5	559.0	113.7	25
9. Es senega	9°06′18″	35°29′21″	630	64	326.4	229.0	424.0	89.1	27
10. Hadada	9°07′42″	35°50′25″	900	102	397.4	341.0	465.5	52.2	13
11. Janet	9°11′35″	35°52′16″	820	101	447.1	372.5	550.0	85.1	19
12. Brahim zaher	9°14′00″	35°33′12″	570	58	220.6	159.0	278.5	49.5	22
13. Abdessadok	9°14′49″	35°40′52″	845	74	319.0	199.5	367.0	80.2	25
14. Hnach	9°26′55″	36°04′10″	447	76	432.1	378.0	485.5	61.0	14
15. Fidh b. naceur	9°35′20″	35°43′26″	350	65	236.8	170.0	334.0	70.8	30
16. Mrichet	9°35′41″	36°05′37″	590	88	491.6	423.5	612.0	88.1	18
17. Fidh ali	9°36′13″	35°42′40″	280	58	292.4	227.0	344.0	55.5	19
18. Dekikira	9°40′53″	35°53′04″	380	73	376.1	254.5	452.0	85.0	23
19. Gouazine	9°42′13″	35°54′30″	376	71	370.0	270.4	414.5	67.1	18
20. Saadine	9°56′36″	36°06′55″	250	70	389.1	221.0	539.0	130.2	33
21. El ogla	10°05′12″	36°11′02″	160	72	365.4	239.5	451.0	91.9	25
22. Sbaihia	10°12′31″	36°29′43″	320	88	461.4	345.0	629.5	125.7	27
23. El melah	10°39′13″	36°28′01″	90	93	522.8	399.0	664.5	118.4	23
24. Es seghir	10°41′05″	36°29′08″	100	102	572.7	484.5	727.7	107.3	19
25. Kamech	10°52′08″	36°52′18″	95	110	662.6	555.5	929.0	178.1	27

Mediterranean periphery, 1992–2002; IRD, 2000). At present the observation network is managed by the Tunisian Farmland Conservation and Management Department (DG/ACTA). The rainfall measurements were made by tipping bucket raingauges (Type Oedipe V.4, pluvio 91 and pluvio-limni 92; designed and provided by, respectively, the French Elsyde and SERPE-IESM). The raingauges are fully automatic and data are downloaded once a month through data loggers. The collection area of each gauge is 400 cm^2. The capacity of the tipping bucket is 0.5 mm of rainwater and the adding tip diameter of the bucket is 3.5 mm. The raingauges were calibrated for average precipitation intensity. According to SERPE-IESM (1993), the measurement accuracy is ±4% up to 250 mm/h intensity (for 5-min time scale). The rainfall observation system was designed to give reliable rainfall estimates down to at least 1-min values (Colombani, 1988). Time is recorded every second. Therefore, rainfall amounts and intensities can be computed with great accuracy for the range of durations used in the current study.

Data treatment

All statistical analyses were performed on rainfall data normalized by applying logarithmic transformation (zero values were exchanged by 0.001). The logarithmic

transformation satisfies the prerequisites for the normal distribution requirement regarding statistical analyses (e.g. Richman & Lamb, 1985; Jolliffe, 1986; Von Storch *et al.*, 1995; Romero *et al.*, 1999; Korres, 2000; Uvo, 2003). Data were also standardized by subtracting the mean and dividing by the standard deviation (e.g. Von Storch *et al.*, 1995; Livezey, 2005; Ha & Ha, 2006). Normal distribution tests (t-test and Z-test) showed that the normal distribution could not be rejected at a significance level of at least 95% for most of the stations. All numerical computations were made using standard routines of the Matlab software. For pair-wise data analyses, stations were included only if rainfall occurred in at least one of the stations.

In order to evaluate the representativeness of the analysed period as compared to long-term rainfall conditions, several comparisons were made. The longest and most reliable long-term records have been used from eight nearby stations. Figure 2 shows the annual rainfall during the period 1969–2003 including the analysed period 1995–1998. The mean annual rainfall for the longer period was about 406 mm (standard deviation 124 mm). The same value for the period 1995–1998 was 424 mm (standard deviation 104 mm). The 10-year moving average in the figure shows a humid decade, then a dry decade, and finally an average decade in terms of rainfall amount. The latter decade covers our study period and indicates about average rainfall conditions, at least for the annual amounts. Moreover, the four-year observation period average was 1.04 times the decade average. This indicates that the 1995–1998 period was representative as regards the long-term average rainfall amount. If we compare the annual spatial variability for the eight long-term rainfall stations and nearby stations representing the shorter observation period used in this study, we notice that the latter displays minor variation regarding mean annual rainfall (Fig. 3(a) and (b)). In general, however, overall aspects are maintained for long-term rainfall.

It is more difficult to estimate the representativeness as regards fine time-scale rainfall properties since there are very little data to compare with. It might also be questioned if four years of data are enough to represent longer period statistical

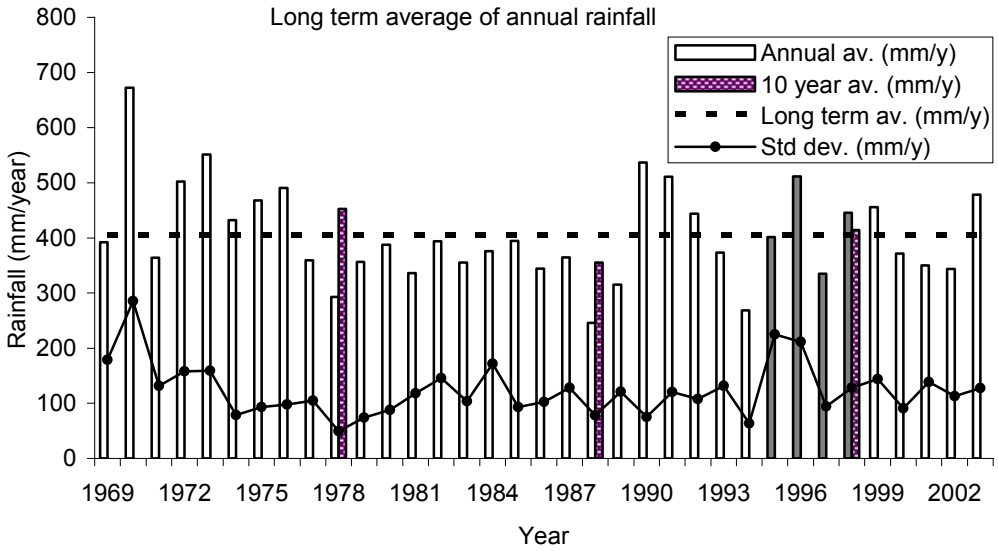

Fig. 2 Annual rainfall over the Tunisian Dorsal region during 1969–2003 (grey bars indicate the periods studied). Source: Tunisian Meteorological Institute.

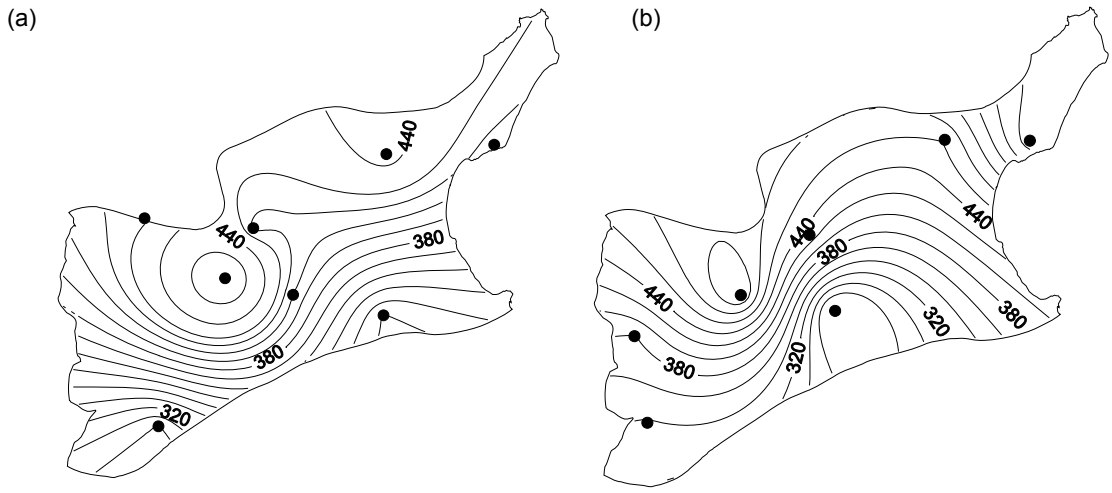

Fig. 3 Spatial variability of annual rainfall (mm/year): (a) 1969–2003; and (b) 1995–1998.

properties. In this case, however, deficiencies in time might be improved by many spatial locations. If the so-called station-year concept (e.g. Baghirathan & Shaw, 1978) is applied to four-year series recorded at 25 independent gauging locations, this would approximate to 100 years of records from one gauge. The station-year concept is based upon independent gauging locations and may be valid for fine time-scale rainfall. As the time period increases this concept is less and less valid. However, based on available data for the region we conclude that the chosen period does not display any tendencies of being unusual in terms of either short-term or long-term spatial rainfall distribution.

Methods

In this study we used multivariate techniques based on covariance or correlation between stations to study rainfall on a regional basis (e.g. Kalkstein *et al*., 1987; Berndtsson, 1988; Kozuchowski *et al*., 1992; Van Regenmortel, 1995; Uvo & Berndtsson, 1996; Andres *et al*., 2000; Chen, 2000; Lana *et al*., 2004; Singh, 2004; Livezey, 2005). Spatial correlation functions were used to investigate the spatial dependence of rainfall for the different time scales: 1, 5, 10, 30 min, and daily rainfall. Empirical orthogonal function (EOF) was used to delineate spatial and dynamic properties of rainfall as used by, e.g. Svensson, (1999), Andres *et al*. (2000), Todd *et al*. (2003), and Tosic (2004). After this, hierarchical clustering was performed for regionalization purposes.

The spatial correlation gives a general quantitative measure of the rainfall variability within an investigated area. It can be expressed in a general way as a function of distance (h) and direction (φ). The lag k (k = time lag) correlation $r_{h,\varphi,k}$ may be plotted with respect to either distance only, or both distance and direction. If the spatial correlation function is isotropic, the correlation–distance diagram contains all necessary information. Otherwise, the correlation function is non-isotropic and the directional information needs to be included (Berndtsson, 1988; Uvo & Berndtsson, 1996). Rainfall gradients in mountainous areas as observed by Gilles *et al*. (2006)

result in large anisotropy in spatial rainfall distribution. Similar properties may be expected for the Dorsal Mountain rainfall.

The EOF technique is similar to principal component analysis (PCA; Hotelling, 1933; Preisendorfer, 1988). The EOF patterns are the eigenvectors (e), of a covariance matrix and, as such, they contain important information of the probability distribution of the variables themselves. These eigenmodes are characterized by several useful properties such as mutual orthogonality and efficient representation of the initial field. The eigenvalues (λ) are defined as the variance of the amplitude, and the rank of each eigenvector is ordered by the magnitude of their eigenvalues, so that the first mode represents the largest part of the total variance, the second mode is the second largest part of the total variance, and so on. The initial data set can be efficiently represented by the first k dominant modes of the analysis. The amplitude of the modes particularly characterizes the time evolution. The space vectors were found using the covariance matrix of the rainfall time series. In general, all modes that were statistically significant or physically justifiable were retained (e.g. Andres *et al*., 2000; Gurgel & Ferreira, 2003; Singh, 2004; Tosic, 2004). To obtain physically meaningful and statistically stable EOF patterns, careful consideration of several factors is needed. These factors include choice of dispersion matrices, sampling errors (e.g. North *et al*., 1982), and rotation of the EOF axes (Richman, 1986). Most commonly, the rotated EOFs are used in the regionalization procedure to resolve the domain dependence problem that is associated with non-rotated EOFs (e.g. Busuioc *et al*., 2001; Livezey, 2005). In our case, results of the EOF analysis were rotated by use of the varimax (orthogonal rotation) procedure (Richman, 1986).

The clustering was achieved by means of routines included in the Matlab software. This analysis was performed with two kinds of input, namely the retained EOF modes on the one hand and the correlation matrix on the other hand. The EOF and correlation data between all raingauges stations were compared with the specific similarity/ dissimilarity, using selected linkage methods grouped into clusters. All analysed time scales were included in this comparison. A classification scheme using Euclidean distance for similarity measurement, together with several linkage techniques, was tested (Kalkstein *et al*., 1987). However, Ward's method (Ward, 1963) appeared to be the most appropriate linkage technique, which gave the most stable and consistent results. This method often produces the most consistent groups in climatic research (e.g. Unal *et al*., 2003). The number of groups was assessed graphically through a dendrogram and then interpreted on a map together with topography and atmospheric circulation.

RESULTS

Spatial correlation

Figure 4, shows the spatial correlation for the investigated rainfall based on different time scales. Results for 5- and 10-min rainfall data are not shown due to general similarities with the 1-min rainfall. As expected, the correlation increases with time scale. The inter-station correlation is generally inhomogeneous and topography appears to greatly influence the dependence. As seen in the figure, shorter convective

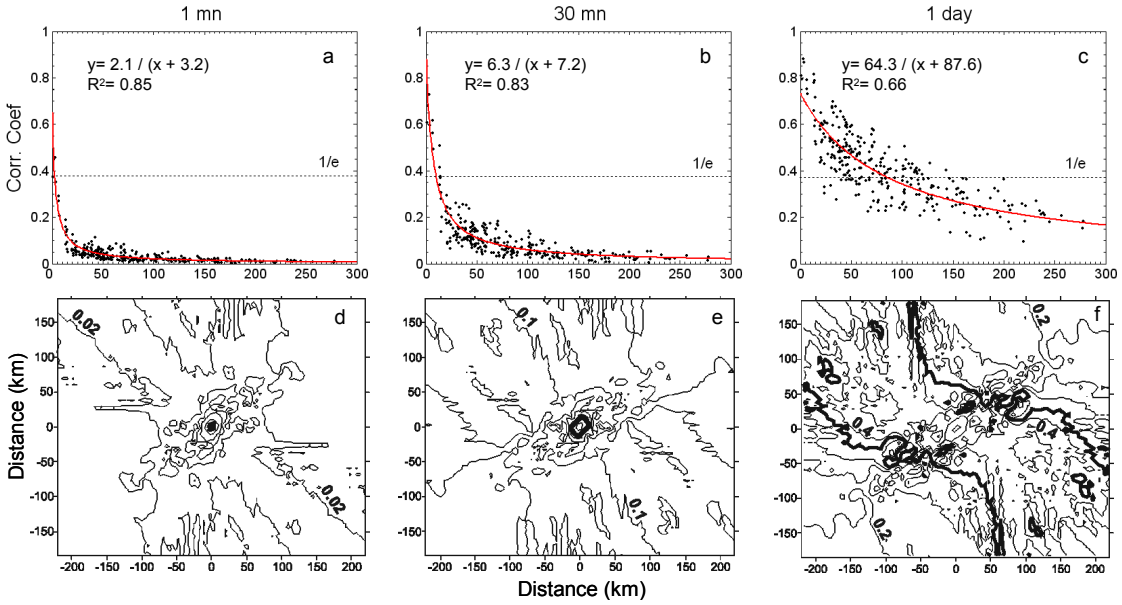

Fig. 4 (a)–(c) Lag zero cross-correlation for 1-, 30-min, and 1-day rainfall *vs* inter-station distance; the solid line has been fitted by regression. (d)–(f) Spatial correlation structures for the same time scales; the bold black line shows the correlation field limit according to the 1/*e* decorrelation isolines.

Table 2 Decorrelation distances and areas (1/*e*) for 1-, 5-, 10-, 30-min, and 1-day time scales.

Time scale	1 min	5 min	10 min	30 min.	1 day
Distance (km)	2.0	6.2	11.8	15.0	70.0
Area (km^2)	12.5	58.7	437.2	706.0	83250.0

rainfall appears to be less affected by topography as compared to daily accumulations. Table 2 presents a summary of decorrelation distances and the correlation field limited by (1/*e*) according to Rodriguez-Iturbe *et al*. (1972). According to the table the decorrelation distance is between 2 and 15 km for 1- to 30-min rainfall. Consequently, the decorrelation distance is clearly less than the average distance between gauges as seen from Fig. 1. Thus, the station-year concept discussed in the Methodology section above appears to be a relevant assumption and hence, the fine time-scale rainfall data represent a much longer period than only 4 years.

Empirical orthogonal function (EOF)

Figure 5 shows the cumulative explained variance for the retained eigenvectors for each of the time scales analysed. For 1-day timescale, the first mode accounts for about 50% of the rainfall variance, yet, for the other analysed time scales, the first mode does not explain more than 20% of the variance. The second mode explains less than 10% for all analysed time scales. It may be assumed that higher modes often represent localized phenomena and not large-scale variability. In general, however, it seems as if the finer the time scale of the rainfall, the more noise and small-scale variation are at hand in the data. Thus, fine time-scale rainfall has a low explained variance. This may indicate the complexity of fine time-scale rainfall and that many different physical

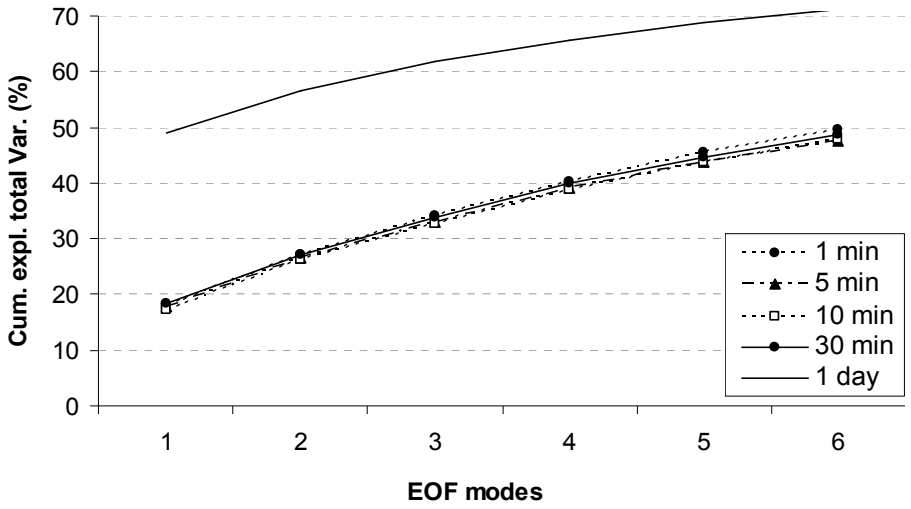

Fig. 5 Cumulative explained variance, for EOF modes 1–6 for 1-, 5-, 10-, 30- min, and 1-day time scales.

variables are responsible for its variation. Therefore, even though explained variation may be low, the different modes may be important in order to explain the dependence of rainfall on local effects such as topography and climatology. Along with this reasoning, modes have been kept due to their statistical significance and, more importantly, their physical explanation (Yarnal, 1984; Kozuchowski *et al.*, 1992; Chen, 2000; Busuioc *et al.*, 2001). Eventually, we ended up with six modes that display quite a good interpretation in terms of the topography and atmospheric circulation patterns known in Tunisia. Consequently, in the following text six modes are kept for further analysis.

The six first spatial modes are shown in Fig. 6 for 1-, 30-min, and 1-day scales. The 5- and 10-min scales were not included in the figure due to general similarities with the 1-min pattern. In general, the modes display large similarities for all time scales. This indicates that fine time-scale rainfall often constitutes the majority of the daily totals. There are, however, some distinct differences between the short-term and the daily data. Plots for the daily rainfall show much more elongated and generally larger rainfall areas as compared to the short-term data, as seen particularly in the second and third modes (Fig. 6(d), (e), (f), (g), (h) and (i)). This reflects the larger variability of fine scale rainfall. Topographic patterns for higher altitudes close to the mountain peaks often display rounded shapes (Fig. 6(f), (l), (o) and (r)). In particular, station 6 situated at 1100 m, station 10 at 900 m, stations 21 and 22 located behind a peak of 1000 m, and finally station 4, are stations that generally display a maximum. The delimitation areas between negative and positive correlations seem to be according to the main direction and the topographic characteristics of the Dorsal region. In fact, for the second mode this delimitation corresponds to about the 600 m altitude isoline (Fig. 6(d), (e) and (f)), whereas, for the third mode, the topographic ridge constitutes a boundary (Fig. 6(g), (h) and (i)). The dynamics of the rainfall phenomenon are very well displayed through the different modes through all time scales. For instance, one can see a northward shift of the rainfall area in modes 3 and 5 from the 1-min to the 1-day rainfall (Fig. 6(h), (i) and (n), (o), respectively).

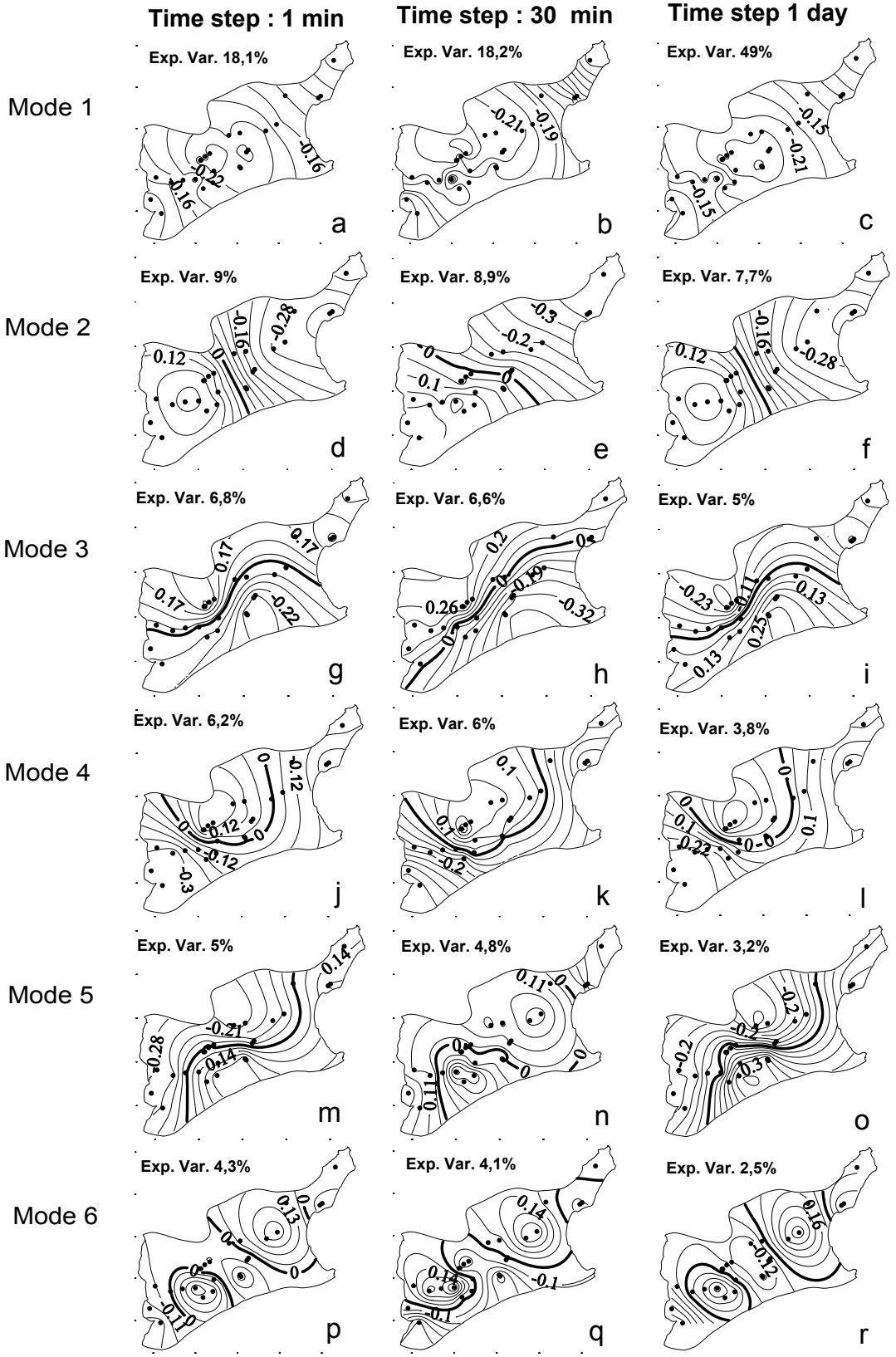

Fig. 6 Six first spatial modes for 1-min, 30-min, and daily rainfall. The bold black line corresponds to the limit between positive and negative values.

In general, the different modes indicate an opposite behaviour between stations situated in the south and those in the north (Mode 3: Fig. 6(g), (h) and (i); Mode 4: Fig. 6(j), (k) and (l); Mode 5: Fig. 6(m), (n) and (o)), and similarly stations located in the eastern part as compared to the western part (Mode 2: Fig. 6(d), (e) and (f)). In fact, atmospheric disturbances feeding the rainfall region are much influenced by the topographic distribution. Even though higher modes continuously explain a lesser degree of variance, up to the sixth mode was kept for interpretation. The reason for this is that all six modes display spatial rainfall patterns typical for most of the atmospheric disturbances known throughout Tunisia in general and in the northern part in particular (see e.g. Henia, 1980; Rodier *et al*., 1981; Dhonneur, 1985; Bousnina, 1986; INM, 1991). Below follows an interpretation of the physics behind each one of the six retained modes.

Mode 1 reflects rainfall due to northwestern disturbances. This type of rainfall is most frequent in winter, with December, January and February being the rainiest months (Henia, 1980; Bousnina, 1986). The disturbance is related to the anticyclone cell of the Azores and originates from the Atlantic Ocean. It then extends towards the Mediterranean Sea and finally arrives in Tunisia from the northwest, filled with moisture that gives rise to heavy rainfall. The effects of these air masses can last for several days. Figure 6(a), (b) and (c) displays the stations as a homogenous group sharing the same behaviour. The correlation structure of the topographical unit is masked by the larger scale (e.g. Sumner, 1983). However, the isolines for the daily time scale are more even and with less topographic detail as compared to the short time scales. This appears reasonable since rainfall during one day generally involves larger areas.

Mode 2 indicates two kinds of disturbances. The first is related to the western rainfall. The origin here is the same as that described above, but the path of the disturbance is more continental as compared to the above northwestern track. As seen in Fig. 6(d), (e) and (f), rain concerns only the western part of the Dorsal region, over a distance of about 100 km. The second type of disturbances are mainly from the north-east. They are blocked by the Dorsal Mountains and westwards by the Azorean and Siberian anticyclone (Rodier *et al*., 1981). These Mediterranean oriental disturbances may carry large amounts of moisture characterized by large variability and violent storms. They can appear in all seasons (Fons, 1987). For fine time-scale rainfall, EOF areas are often delimited by the 600-m contour (Fig. 6(d), (e)). However, daily rainfall involves a larger area and is delimited on an average by the 900-m contour (Fig. 6(f)).

Mode 3 displays a typical northern type rainfall pattern known as the Balearic disturbance. It represents about 15% of the most common Mediterranean low pressure systems (Fons, 1987). Figure 6(g), (h) and (i) displays the opposite behaviour of stations situated on northern and southern slopes, respectively. The delimitation between negative and positive values coincides with the Dorsal peaks. Consequently, the ridges seem to be of a great importance for the rainfall pattern for all time periods. Geographical studies emphasize the fact that the Dorsal Mountain range acts as a barrier to the moist atmospheric flow: for the same altitudes, the difference in precipitation between exposed and sheltered slopes is generally about 50 mm/year (Gammar, 1999).

Mode 4 displays the contribution of cyclonic circulation rainfall. It is well known that winter rainfall in Tunisia is usually associated with the Polar or the Mediterranean

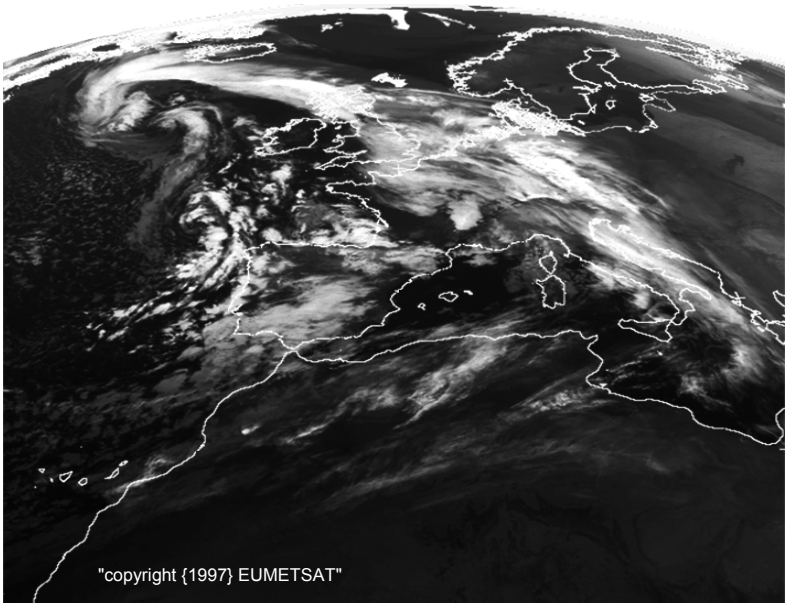

Fig. 7 Example of extension of cyclonic circulation (18/12/1997). Copyright {1997} EUMETSAT.

front. Cyclones are moving low pressure systems which are associated with frontal systems. However, as seen from the example in Fig. 7, the size and dynamics of the cyclonic disturbance usually concern Tunisia only at the dissipating stage. According to this, Fig. 6(j), (k) and (l) shows that only part of the Dorsal area is affected by cyclonic disturbance. The rainfall area for 1- and 30-min time scales is delimited westward by the 850-m contour level and the resulting areas with spatial dependence may be assumed to be due to the effects of single cyclonic remnants. The delimitation for the daily rainfall extends farther to the 1100-m contour. Quite high correlations are shown in the southwestern part. This can be explained by successive remnants of cyclonic disturbances crossing over Tunisia leading to sparse rainfall over the Dorsal region.

Mode 5 can best be described by rainfall associated with the Saharan front, which is the convergence zone between warm tropical air and cold continental or maritime air (Rodier *et al*., 1981). The Saharan depression often originates in the Mediterranean over the Gabes Gulf and then moves north towards the Cap Bon peninsula and the south of Italy. Depending on the origin of the warm current, a stormy evolution due to the Saharan air gaining moisture during its maritime path can be expected (Fons, 1987). For the 1-min rainfall, only the south slope of the Dorsal Mountains and the Cap Bon peninsula appear to be affected (Fig. 6(m) and (n)). However, for daily rainfall (Fig. 6(o)), the rainfall area shrinks and only concerns stations in the western area and the Cap Bon peninsula. This can be explained by the fact that the rainfall type is characterized by heavy storms mainly when influenced by topography as well, or in particular conditions, such as the presence of sub-tropical cast (INM, 1988, 1993).

Mode 6 displays mainly local and small-scale meteorological phenomena as compared to the synoptic large-scale processes described above. This is mainly rainfall from convective clouds. Due to instability, they are characterized by strong up- and downdrafts. For this type of rainfall, the physiographic and thermal features of the

immediate surrounding area are of great importance. However, the highest topographic peaks result in a clear rise in rainfall with small and discontinuous areas within a sub-humid bio-climatic zone that reaches 600 mm/year (Gammar, 1999). In Fig. 6(p), (q) and (r), high values are clearly situated around peaks at about 1000 m altitude from west to east. The three time scales follow the same general pattern. This can be explained by the lifetime of the convective cells, which is typically about one hour (Fons, 1987). In Fig. 6(p), (q) and (r) the delimitation between positive and negative correlation shows a strong curvature that indicates small and discontinuous rainfall areas.

Hierarchical cluster analysis

Cluster analysis was performed using the six EOF modes in order to classify the synoptic situations associated with the mode for major rainfall occurrence (Uvo & Berndtsson, 1996; Busuioc *et al*., 2001; Uvo, 2003). The modes explain simultaneously about 70 and 50% of the total variance for daily and fine time-scale rainfall, respectively. Figure 8 (a), and (b) shows the results of the clustering. The dendrogram for EOF input displays two rather clear sub-groups (Fig. 8(a)). The general pattern related to the minute time scale, is a first subgroup covering the entire Dorsal area surrounding a second subgroup located in the central part. Similarly, the daily scale rainfall displays Subgroup 2 covering the central southern slope of the Dorsal area.

The results from the EOF input were compared to clustering using the correlation matrix as input. Also, the correlation input displays similar clusters as mentioned above. These two clusters can be delimited as seen in Fig. 8(c) and (d). For 1-min data, the results from the EOF and correlation matrix are almost identical. Two large subgroups divide the Dorsal area into an eastern and a western part divided by an altitudinal line of about 600 m. For the daily time-scale rainfall, Subgroup 2 extends eastward reaching lower altitude parts of the Dorsal area (300 m). A second smaller subgroup covers the main part of the Cap Bon Peninsula.

Both the EOF and correlation input display similar results in terms of regionalization and the results therefore appear robust. The two subgroups, identified according to the above description, display rather clear within-group similarities as well as between-group differences regarding rainfall statistics as well as physiographic features. Stations in subgroups 1 and 2 divide the Dorsal area in different ways according to the time scale and the type of input. For 1-min rainfall it appears clear that there is a major difference between the western and the eastern Dorsal ranges. For the daily rainfall this pattern is not noticeable.

The above regional areas could be explained in terms of rainfall mechanisms of the area. The lifetime of frontal rainfall in the area is often only a few hours (Table 3). Rainfall depth and number of events seem to be characterizing properties of the Subgroup 1 above. Instead, mean seasonal rainfall and the daily occurrence of rain producing cells seem to be more important for the second subgroup. The latter group is located at higher altitudes as compared to the first subgroup. Subgroup 2 seems to be related mainly to convective rainfall which may originate from orography in the western part where the average altitude is about 600 m (INM, 1988, 1993).

Autumn and summer rainfall properties are often characterized by the short-term minute time scale. However, the winter and spring rainfall properties are probably

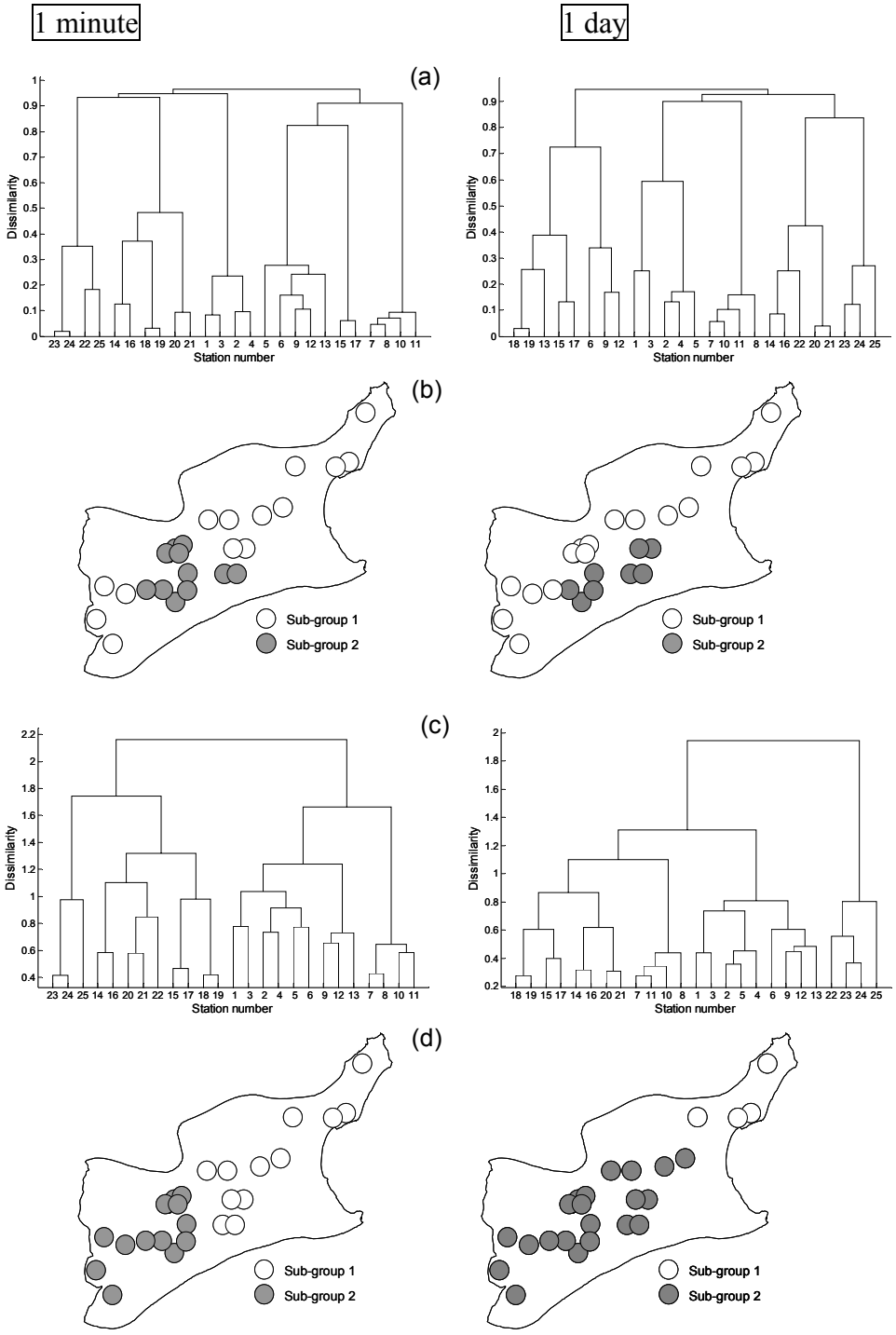

Fig. 8 (a) Cluster dendrogram (6 modes); (b) regionalization (6 modes); (c) cluster dendrogram (correlation matrix); and (d) regionalization (correlation matrix): for 1-min time scales (left) and 1-day time scales (right).

more related to the daily time scale. The EOF results seem more related to summer rainfall depth and maximum rainfall intensity. However, the correlation results appear more related to rainfall depth, number, and duration of events during the autumn, winter and spring seasons. Besides, they also resemble patterns for average rainfall

Table 3 Average duration of the rainfall events.

Rainfall duration (1995–1998), t	Number of rainfall events (%)
24 h ≤ t	0
6 h ≤ t < 24 h	1.4
1 h ≤ t < 6 h	26.9
30 min ≤ t < 1 h	56.7
1 min ≤ t < 30 min	15.0

Rainfall events are separated if raingauge shows less than one tip per hour.
The total rainfall events measured through the Dorsal network is 13 889.

intensity during the spring, autumn and summer periods. Finally, the EOF and correlation inputs respectively describe the localized and the large-scale rainfall variability. This fact makes them rather complementary for rainfall studies.

SUMMARY AND CONCLUSION

The statistical analysis presented herein has revealed some of the similarities and dissimilarities between rainfall for different time scales and related physical mechanisms over the important Dorsal Mountains in central Tunisia. Potentially this analysis may also help to explain the observed variability in water resources in the area. Generally, the inter-station correlation is not homogeneous and topography appears to greatly influence this dependence. The EOF analysis also displayed various spatial rainfall patterns as demonstrated in the resulting regionalization. The classification of stations into homogeneous regions could be done according to two main subgroups based on overall rainfall properties. For fine time-scale (1-min) rainfall there appears to be an important west–east delimitation represented by the 600 m altitude boundary. For daily rainfall this boundary appears less important. Instead, for the 1-day rainfall, the Dorsal Mountain range appears to be more important as a north–south boundary.

Typically, throughout the Dorsal area, frontal rainfall displays a shorter lifetime and occurrence of rain-producing cells seems to be more frequent as compared to surrounding low-lying areas in Tunisia. Consequently, these rainfall properties, typical for both subgroups, are probably an effect of the complex topography in the area.

In general, fine time-scale rainfall displays similarity to daily rainfall. A probable reason for this is that fine scale rainfall often constitutes the major part of daily rainfall in the area. However, as seen above, there are also important similarities between, e.g. spatial 1-min and daily rainfall. Consequently, there are possibilities for successful disaggregation of daily rainfall into shorter period rainfall. However, the noticeable differences in the above regionalization must also be kept in mind when working with the disaggregation tool. This knowledge can be used in models where fine time-scale rainfall properties are the driving mechanism for simulated output, such as erosion estimations in areas where only daily rainfall data are at hand.

Acknowledgements Sihem Jebari and Akissa Bahri thank Mr H. Farhat, head of the Tunisian Farmland Conservation and Management Department (DG/ACTA) and

Mr M. Boufaroua for providing data. They also gratefully acknowledge Mr M. Rajhi, head of the Tunisian Meteorological Institute (INM), and his staff for valuable time and discussions allocated to this work. Ronny Berndtsson and Cintia Uvo were supported by the Swedish Research Council. The study was finalized during a guest research period of Sihem Jebari at the Department of Water Resources Engineering, Lund University, Sweden, sponsored by the Swedish Institute and the Swedish Agency for International Development Cooperation, SIDA.

REFERENCES

Andrés, M., Tomás, C. & De Pablo, F. (2000) Spatial patterns of the daily non-convective rainfall in Castilla y León (Spain). *Int. J. Climatol*. **20**, 1207–1224.

Arora, M., Singh, P., Goel, N. K. & Singh, R. D. (2006) Spatial distribution and seasonal variability of rainfall in a mountainous basin in the Himalayan region. *Water Resour. Manage.* **20**, 489–508.

Baghirathan, V. R. & Shaw, E. M. (1978) Rainfall–depth–frequency studies for Sri Lanka. *J. Hydrol.* **37**, 223–239.

Berndtsson, R. (1988) Spatial hydrological processes in a water resources planning perspective. An investigation of rainfall and infiltration in Tunisia. PhD Thesis, Rep. 1009, Dept of Water Resour. Engng, Lund Univ., 1–315.

Bousnina, A. (1986) *La variabilité des pluies en Tunisie*. Deux. Ser. Geogr., vol. 22, 1–308. Fac. des sci. humaines et sociales de Tunis, Pub. de l'Univ. de Tunis, Tunisia.

Busuioc, A., Chen, D. & Hellström, C. (2001) Temporal and spatial variability of precipitation in Sweden and its link with the large-scale atmospheric circulation. *Tellus* **53A**, 348–367.

Buzzi, A. & Foschini, L. (2000) Mesoscale meteorological features associated with heavy precipitation in the southern Alpine region. *Meteorol. Atmos. Phys*. **72**, 131–146.

Campins, J., Genoves, A., Jansa, A., Guijarro A. A. & Ramis, C. (2000) A catalogue and a classification of surface cyclones for the western Mediterranean. *Int. J. Climatol.* **20**, 969–984.

Chen, D. (2000) A synoptic climatology based on the Lamb classification for Sweden and its application to winter temperature study. *Int. J. Climatol.* **20**, 1067–1076.

Colombani, J. (1988) Autopsie d'un hyétogramme. In: *Troisièmes journées hydrologiques de l'ORSTOM* (Montpellier, 23–24 septembre 1987), 28–37. Publication du laboratoire d'hydrologie de Montpellier, France.

Conte, M. (1986) The meteorological bomb in the Mediterranean: a synoptic climatology. WMO TD no. 128, App. 4, 17–31. World Meteorological Organization, Geneva, Switzerland.

Cudennec, C., Slimani, M. & Le Goulven, P. (2005) Accounting for sparsely observed rainfall space–time variability in a rainfall–runoff model of a semiarid Tunisian basin. *Hydrol. Sci. J.* **50**(4), 617–630.

D/CES & ORSTOM (1998) L'acquisition numérique et autonome de données hydro-pluviométriques. L'expérience d'un réseau pilote Tunisien. *Rapport édité par La Direction de Conservation des Eaux et du Sol ainsi que de l'Institut Français de Recherche Scientifique pour le Développement en Coopération*, 01–33.

Dhonneur, G. (1985) *Traité de Météorologie Tropicale*, 1–151. Publication de la Direction de la Météorologie, France.

Doswell, C. A. (1982) The operational meteorology of convective weather, vol. I, Operational mesoanalysis. *NOAA Tech. Mem. NWS NSSFC-5*.

Fons, C. (1987) *Météo marine*, 01–68. Les dossiers des éditions du Pen-duick.

Gammar, A. M. (1999) La dorsale tunisienne, entre la représentation linéaire et réalité régionale, 39–52. Publication de la faculté des lettres de Manouba, Tunisie.

Gilles, D., Christian, W., Nicole, M., Lucien, H. & Laurent, P. (2006) Topography and recent winter rainfall regime change in temperate western European areas: a case study in the Rhine–Meuse basin. *Int. J. Climatol.* **26**, 785–796.

Gurgel, H. C. & Ferreira N. J. (2003) Annual and interannual variability of NDVI in Brazil and its connections with climate. *Int. J. Remote Sensing* **24**, 3595–3609.

Henia, L. (1980) *Les précipitations pluvieuses dans la Tunisie tellienne*. Publication de l'université de Tunis, Faculté des lettres et sciences humaines de Tunis.

Homar, V., Ramis, C. & Alonso, S. (2002) A deep cyclone of African origin over the western Mediterranean: diagnosis and numerical simulation. *Ann. Geophys.* **20**, 93–106.

Hotelling, H. (1933) Analysis of a complex of statistical variables into principal components. *J. Educ. Psychol.* **24**, 417–441.

Houérou, H. N. (1969) La végétation de la Tunisie steppique et des régions limitrophes. *Ann. Inst. Nat. Rech. Agron. de Tunis* **42**, 622.

INM (1988) Les orages en Tunisie. *Rapport Interne de l'Institut National de la Météorologie, Tunisie.*

INM (1991) Numerical simulation of the Mediterranean cyclones. *Rapport Interne de l'Institut National de la Météorologie, Tunisie.*

INM (1993) Pluie et nuages convectifs*. Unité de recherche et de développement. Rapport Interne de l'Institut National de la Météorologie, Tunisie*.

IRD (2000) Evaluation du programme Lacs et barrages collinaires en Tunisie "Hydromed". *Rapport édité par l'Institut de Recherche Développement.*

Jansa, A., Genoves, A., Riosalido, R. & Carretero, O. (1996) Mesoscale cyclones vs. heavy rain and MCS in the Western Mediterranean. *MAP Newsletter* no. 5, 24–25.

Ha, K. J. & Ha, E. (2006) Climatic change and interannual fluctuations in the long-term record of monthly precipitation for Seoul. *Int. J. Climatol.* **26**, 607–618.

Jollife, I. T. (1986) *Principal Component Analysis*. Springer Series in Statistics, Springer-Verlag, New York, USA.

Kalkstein, L. S., Tan, G. & Skindlov, J. A. (1987) An evaluation of three clustering procedures for use in synoptic climatological classification. *J. Climat. Appl. Met*. **26**, 717–730.

Korres, G. (2000) The ocean response to low-frequency interannual atmospheric variability in the Mediterranean Sea. Part II: Empirical orthogonal functions analysis. *J. Climate* **13,** 732–745.

Kozuchowski, K. M., Wibig, J. & Maheras, P. (1992) Connections between air temperature and precipitation and the geopotential height of the 500 hPa level in a meridional cross-section in Europe. *Int. J. Climatol*. **12**, 343–352.

Lana, X., Martínez, M. D., Serra, C. & Burgueno, A. (2004) Spatial and temporal variability of the daily rainfall regime in Catalonia (northeastern Spain), 1950–2000. *Int. J. Climatol*. **24**, 613–641.

Livezey, B. (2005) Best practices *vs*. misuse of PCA in the analysis of climate variability. The *30th Annual Climate Diagnostics and Prediction Workshop* (24–28 October, The Pennsylvania State University) [proceedings/cdw30_proceedings/Livezey_PCA_PSU.ppt; date of access 2006].

Marquinez, J., Lastra, J., & Garcia, P. (2003) Estimation models for precipitation in mountainous regions: the use of GIS and multivariate analysis. *J. Hydrol.* **270**, 1–11.

MEDEX (Phase 1) (2001) Cyclones that produce high impact weather in the Mediterranean. Research proposal [medex.inm.uib.es/documents/MEDEX2001_research_proposal_v1.pdf; date of access 2003].

North, G .R., Bell, T. L., Cahalan, R. F. & Moeng, F. J. (1982) Sampling errors in the estimation of empirical orthogonal functions. *Mon. Weather Rev*. **110**, 699–706.

Preisendorfer, R. H. (1988) Principal components analysis in meteorology and oceanography. In: *Developments in Atmospheric Sciences, 17*. (Compiled/ed. by Curtis D. Mobley). Elsevier, Amsterdam, The Netherlands.

Richman, M. B. (1986) Rotation of principal components. *J. Climatol*. **6**, 293–335.

Richman, M. B. & Lamb, P. J. (1985) Climatic pattern analysis of 3- and 7-day summer rainfall in the central United States: some methodological considerations and a regionalization. *J. Clim. Appl. Met.* **24**, 1325–1343.

Romero, R., Summer, G., Ramis, C. & Genoves, A. (1999) A classification of the atmospheric circulation patterns producing significant daily rainfall in the Spanish Mediterranean area. *Int . J. Climatol*. **19**, 765–785.

Rodier, J. A., Colombani, J., Claude, J. & Kallel, R. (1981) *Le bassin de la Medjerdha*. Monographie hydrologique de l'Orstom, Paris, France.

Rodriguez-Iturbe, I., Vanmarcke, E. H. & Schaake, J. C. (1972) Problems of analytical methods in hydrologic data collection. In: *Proc. Symp. on Uncertainties in Hydrologic and Water Resources Systems* (Tucson, Arizona, December).

SERPE-IESM (1993) *Pluviomètre* transducteur à impulsions R01-3032. *Notice d'utilisation*, France.

Singh, C. V. (2004) Empirical Orthogonal Function (EOF) analysis of monsoon rainfall and satellite-observed outgoing long-wave radiation for Indian monsoon: a comparative study. *Meteorol. Atmos. Phys.* **85**, 227–234.

Sumner, G. N. (1983) Daily rainfall variability in coastal Tanzania. *Geogr. Ann*. **65A**, 53–66.

Svensson, C. (1999) Empirical orthogonal function analysis of daily rainfall in the upper reaches of the Huai River Basin, China. *Theoret. Appl. Climatol.* **62**, 147–161.

Todd, M. C., Washington, R. & James, T. (2003) Characteristics of summertime daily rainfall variability over South America and the South Atlantic Convergence Zone. *Meteorol. Atmos. Phys*. **83**, 89–108.

Tosic, I. (2004) Spatial and temporal variability of winter and summer precipitation over Serbia and Montenegro. *Theoret. Appl. Climatol*. **77**, 47–56.

Unal, Y., Kindap, T. & Karaca, M. (2003) Redefining the climate zones of Turkey using cluster analysis. *Int. J. Climatol.* **23**, 1045–1055.

Uvo, B. C. (2003) Analysis and regionalization of northern European winter precipitation based on its relationship with the North Atlantic Oscillation. *Int. J. Climatol*. **23**, 1185–1194.

Uvo, C. & Berndtsson, R. (1996) Regionalization and spatial properties of Ceara State rainfall in Northeast Brazil. *J. Geophys. Res. Atmos*. **101**, 4221–4233.

Van Regenmortel, G. (1995) Regionalization of Botswana rainfall during the 1980s using Principal Component Analysis. *Int. J. Meteorol.* **15**, 313–323.

Von Storch, H. Burger, G. Schnur, R. & Von Storch, J. S. (1995) Principal oscillation pattern: a review. *J. Climate* **8**, 377–400.

Ward, J. H. (1963) Hierachical grouping to optimize an objective function. *J. Am. Statist. Assoc.* **58**, 236–244.

Yarnal, B. (1984) The effect of weather map scale on the results of a synoptic climatology. *Int. J. Climatol*. **4**, 481–493.

Received 16 November 2005; accepted 2 July 2007

A scaling approach to enhance rainfall data for erosion estimation in semiarid Tunisia

S. Jebari[1], R. Berndtsson[2], and J. Olsson[3]

[1]National Research Institute for Rural Engineering, Water, and Forestry, Box 10, Ariana 2080, Tunis, Tunisia
[2]Department of Water Resources Engineering, Lund University, Box 118, S-22100 Lund, Sweden
[3]Swedish Meteorological and Hydrological Institute, S-60176 Norrköping, Sweden

Submitted for publication in Hydrology and Earth System Sciences

Abstract. Observations of rainfall data with the necessary fine-scale time resolution are often missing for semiarid areas. In this paper the multifractal properties of a 4-year rainfall time series of 15 min intensity observations from the semiarid Tunisia are investigated. The time series was shown to be the result of a multiplicative cascade process for a sequence range of 100 min within the investigated rainfall events. This sequence is located in the last third of the typical rainfall event. This coincides in general with the most active period of soil erosion during rainfall. The temporal structure of rainfall was reproduced using a disaggregation model. Observed daily rainfall was disaggregated to 15-min time step rainfall. The generated 15-min time series displayed similar fundamental characteristics as the observed series such as event structure, erosive event properties, and scaling behavior. The rainfall duration and depth were, however, slightly under-estimated and this led to an over-estimation of the intensity for the generated series. However, the multifractal methodology appears to be an efficient technique to reproduce the rainfall agressivity for erosive soils where fine-scale rainfall observations are lacking. Thus, the potential of scaling-based approaches in water erosion applications involving this kind of time series seems to have a promising future.

---

1 Introduction

During recent decades different disaggregation approaches have been developed to account for rainfall observation gaps and lack of fine time-scale rainfall data. (e.g., Elshamy, 2007; Guntner et al., 2001; Molnar and Burlando, 2005; Olsson, 1998; Olsson and Berndtsson, 1998; Ormsbee, 1989; Lovejoy and Schertzer, 2005). The temporal rainfall disaggregation is performed based on invariant scaling theory (Schertzer and Lovejoy, 1987; Over and Gupta, 1996; Olsson, 1998; Menabde and Sivapalan, 2000; Sivakumar et al., 2001; Schertzer et al., 2002, Gaume, 2007). The above mentioned scaling behavior is modeled by a cascade process, an approach recommended by Schertzer and Lovejoy (1987), Lovejoy and Shertzer (1990) and Gupta and Waymire (1990; 1993), and originally used in statistical turbulence (e.g., Yaglom, 1966; Mandelbrot, 1974). Cascade models are used to explore the temporal rainfall structure in rare cases (Hubert et al., 1993; Olsson, 1995; Menabde et al., 1997). They distribute rainfall mass on successive regular subdivisions of an interval in a multiplicative manner. Their performance is usually assessed in terms of reproducing some statistical characteristics of the observed time series, such as variance, wet/dry properties, rainfall amount quantiles, autocorrelation, etc. (e.g., Marsan et al., 1996; Svensson et al., 1996; Harris et al., 1998; Menabde et al., 1999; Gunter et al., 2001; Deidda, 2000; Veneziano and Furcolo, 2002; 2003; Olsson and Burlando, 2002; Olsson 2008; Molnar and Burlando, 2005; Hingray et al., 2005).

Enhancement of rainfall data has been one of the main successful and promising applications of the scaling/multiscaling approach (e.g., Kantelhardt, 2008). It has been described as the most powerful concept introduced in rainfall disaggregation modeling over the last two decades. However, applications still remain rare and restricted characterizing the rainfall process (e.g., Thauvin et al., 1998; Venezianoa et al., 2006). Moreover, the physical reasons behind the rainfall scale invariance remain a widely discussed topic. Consequently, researchers have tried to continue to increase the confidence in scaling assumptions, to refine analysis techniques, and to improve modeling ability. Thus, scaling behavior has to be established for rainfall data over different climates and geographical regions (Olsson, 1996; Olsson and Berndtsson, 1998; Kantelhardt, 2008). Besides, it is highly desirable to study causes and consequences of fractal and

multifractal correlations in time series (Kantelhardt, 2008).

Studies on rainfall disaggregation methods in semiarid areas still remain scarce. There is consequently a great need to investigate rainfall properties and test the ability of disaggregating models for the semiarid climate. For this purpose, an observed 15-min rainfall time series from a period of about 4 years from a representative area in the Tunisian Dorsal area was chosen. The site and rainfall resolution were shown as they are related to the water erosion processes in the Tunisian semiarid area (Jebari et al., 2008). The first sections of the paper investigate scaling properties for the observed rainfall time series aiming to define parameters that characterize the multifractal behavior. The following sections aim at testing a disaggregation model proposed by Olsson (1998; 2008). The model is applied to 1-day rainfall accumulations to generate 15-min rainfall time series. A comparison between the observed and the generated data series concerning the temporal rainfall properties in general and erosive rainfall in particular is performed. Finally, some of the practical implications of the results are discussed.

2 Data and methods

2.1 Rainfall data

Rainfall in semiarid areas is characterized by strong irregularities. In the Tunisian Dorsal area, the frontal rainfall displays a short lifetime, while the occurrence of rain-producing cells seems to be more frequent (Jebari et al., 2007). The Jannet catchment is located within the Dorsal area at the heart of semiarid Tunisia (Fig. 1). This region is characterized by especially serious water erosion problems. In fact soil loss rates widely exceed tolerance thresholds given by Wischmeier and Smith (1978) and Masson (1971), who defined these as 12 and 6 tonnes/ha/year, respectively. The Jannet catchment has an erosion of 27 tonnes/ha/year as an average and about 60 tonnes/ha/year for extreme rainfall events (Jebari et al., 2009). Also, the Jannet catchment and the available 15-min rainfall time series appear to be representative of the entire semiarid Tunisia in terms of rainfall agressivity and water erosion processes (Jebari et al., 2008, 2009). The recorded time series concerns the period ranging from 3/2/1995 to 11/9/1998 and displays only about 1% of missing data. The mean annual rainfall for the studied period was 436 mm (standard deviation 140 mm). The same value for the longest (1969-2003) and most reliable long term rainfall record from the semiarid Tunisia was 406 mm (standard deviation 124 mm). The Jannet rain gauge belongs to a monitoring network including 30 experimental catchments all over the Tunisian Dorsal chain (D/CES & Orstom, 1998). Each catchment discharges into a small dam, called a hill reservoir usually located in an agricultural area. The Jannet rain gauge is located on the dike itself, as well as an automatic water level recording gauge.

The Jannet high resolution rainfall was recorded by a fully automatic a rain gauge with an accuracy of ±4% up to 250 mm/h intensity for a 5-min time step. The rain gauge is of tipping bucket type connected to a logger recording data every minute. A rainfall event is defined as separated from another event if a rain gauge showed less than one tip per hour. A total number of 618 station rainfall events were included in the present analysis. This series showed only 2% of events which exceeded 6 hours and a single event reaching 14 hours. The kinetic energy of rainfall could be evaluated as above 3 mm (Kowal et al., 1976). The data used presents 59 specific events according to this condition. Moreover, the erosivity index R proposed by Wischmeier and Smith (1978) considers erosive rainfall as exceeding 12 mm. The Jannet data represent 23 erosive events according to this definition.

2.2 Scaling and multifractal analysis

Scaling and scale invariance of temporal rainfall has received increased attention during the last two decades (e.g., Burlando and Rosso, 1996; Gunter et al., 2001; Hubert et al., 1993; Menabde et al., 1997; Olsson et al., 1992; 1993; Svensson et al., 1996). This implies that statistical properties of the process observed at different scale resolutions are governed by the same relationship. The power spectrum and the probability distribution function properties are two ways to indicate scaling behavior. The spectral analysis (Fourier transform) is considered a powerful tool to assess the scaling invariance in rainfall time series (Malamud and Turcotte, 1999). It requires stationarity of the data and calculates the power spectrum E(f) as a function of the frequency to determine self affine scaling behavior (Hunt, 1951). If the time series spectrum fits a power law form according to (1), thus, the scaling regime characterizes the range of the defined (holds) power law. Spectral analysis is applied to a double logarithmic plot of E(f). Within the above mentioned range, fluctuations at all scales are related to each other by the same scale independent relationship. This indicates that multifractal behavior of the data may be assumed.

$$E(f) \alpha f^{\beta} \quad (1)$$

where f is the frequency and β the spectral exponent deduced from the slope of a linear regression.

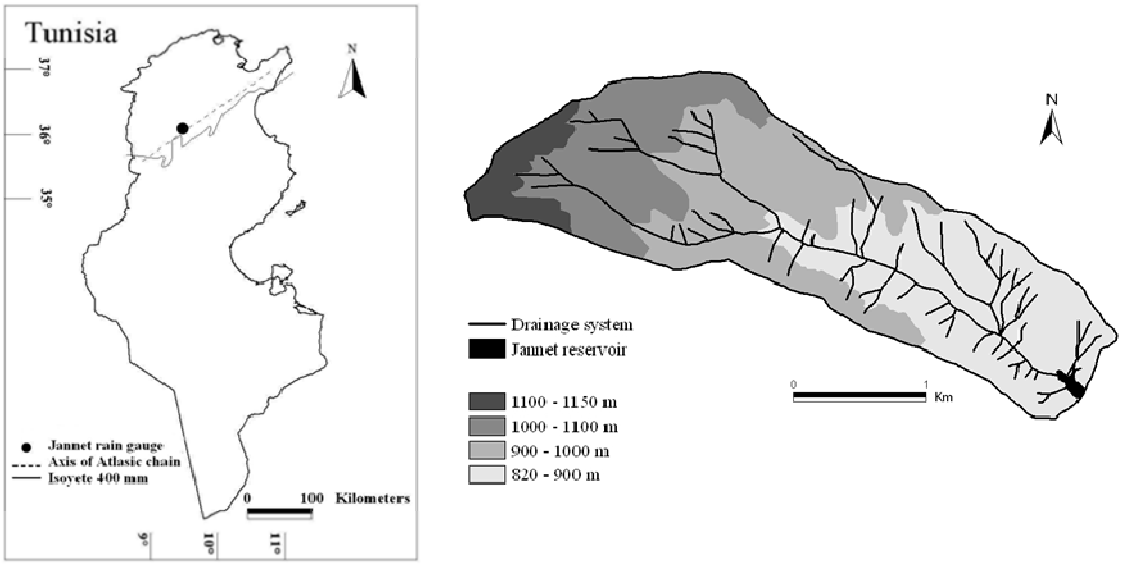

Fig. 1. Jannet rain gauge location and topography

To investigate the multifractal temporal structure of a rainfall time series the scaling of the probability distribution function (pdf) of the data is determined (Schertzer and Lovejoy, 1987). The rainfall intensity is divided by the average intensity of the process on a time scale resolution λ. At each scale step, the average values ε_λ are compared to the threshold specified by λ^q (Frisch and Parisi, 1985; Halsey et al., 1986). The probability $Pr(\varepsilon_\lambda > \lambda^q)$ is estimated as the number of averaged values exceeding λ^q divided by the total number of averaged values at the specific scale step. If the tail of the probability distribution of the rainfall intensity obeys a power law form, so a hyperbolic intermittency characterizes the series (Fraedrich and Larnder, 1993).

To determine the scaling properties of the rainfall time series, the scaling of the statistical moments of the rainfall intensity was examined (Over and Gupta, 1994). The scaling of the moments is described by the exponent function K(q) which satisfies the following expression

$$(\varepsilon_\lambda^q) = \lambda^{K(q)} \qquad (2)$$

where (ε_λ^q) is the average qth moment of the rainfall on a scale specified by λ and K(q) is regarded as a characteristic function of the scaling behavior.

If K(q) plotted as a function of q in a double logarithmic diagram falls on an approximately straight line the data set is monofractal. However, if K(q) is a hyperbolic function, the data is multifractal (Frisch and Parisi, 1985). In theory a hyperbolic behavior implies that sample moments increase with the sample size and may become arbitrarily large and that in practice larger-order moments are dominated by the most extreme values only. The scaling behavior of the series may be investigated by plotting (ε_λ^q) as a function of λ in a log-log diagram. If (2) is valid the curve will exhibit an approximately linear behavior with a slope that is an estimate of K(q). By fitting straight lines to the points corresponding to different values of q, the entire K(q) may be estimated. Owing to uncertainties in the estimation of high order moments (Kumar et al., 1994), the investigations were limited to orders in the range $0 \leq q \leq 4.0$. The divergence of moment results from the multifractal singular behavior at the small scale limit. However, in a large number of realizations, divergence of moments is observed in the form of a linear relation of the empirical function K(q).

2.3 Random cascade model

Cascade processes originate from turbulence theory and describe how some quantity is transferred and concentrated from larger to smaller scales in the processes. Investigations in geophysics often combine multifractal theory and a cascade process model. For instance, several studies displayed that, rainfall time series were multifractal (e.g., Fraedrich and Larnder, 1993; Olsson et al., 1993; Olsson, 1995; Svensson et al., 1996, Olsson and Berndtsson 1998; Schmitt et al., 1998). This indicates that a multiplicative cascade process is responsible for the concentration of water and energy fluxes into successively smaller parts of the atmosphere. Consequently, this may characterize the rainfall process by an infinite hierarchy of intensity-dependent dimensions.

In a multiplicative cascade process the flux is transferred into successively smaller scales by means of multiplicative weights, and the generator specifies the statistical distribution of these weights (Davis et al., 1994). In Schertzer and Lovejoy (1987) K(q) is expressed according to the following:

$$K(q) = \begin{cases} \dfrac{C1\,(q^{\alpha} - q)}{\alpha - 1} & \alpha \neq 1 \\ C1\, q \log(q) & \alpha = 1 \end{cases}$$

where α and C1 are specifying the generator's distribution. A double trace moment is employed to estimate the parameters (Lavallée 1991, Tessier et al., 1993).

In a random cascade, the ensemble moments are shown to be a log-log linear function at the scale of resolution λ_n. The slope of this scaling relationship is a function (Mandelbrot, 1974; Kahane and Peyriere, 1976). The latter function contains important information about the distribution of the cascade generator w, and thus determines the scaling properties of rainfall.
In data analysis, the scaling of the sample moments is used to estimate K(q), and assuming a distribution for the cascade generator w, the parameters of the cascade model can then be estimated. According to this, cascade models have been used to explore the temporal structure for rainfall time series (e.g., Hubert et al., 1993; Olsson, 1995; Menabde et al., 1997). These models allow dropping the critical issue related to the determination of the initial condition of the complex system. The rainfall modeling based on random cascades has been tested under different climate for temporal disaggregation. They perform reasonably well for the reproduction of rainfall statistics and capture the high resolution rainfall variability (Olsson, 1998; Gunter et al, 2001; Molnar and Burlando, 2005; Svensson et al., 1996; Olsson and Berndtsson, 1998; Hingray et al., 2005).

2.4 The disaggregation procedure

The current study focused on the performance of the modified cascade disaggregation model developed by Olsson (1998; 2008). The model was developed for continuous rainfall time series in order to represent the temporal structure of rainfall. Olsson (1998) evaluated the model using 8-min rainfall data from southern Sweden and found it applicable from time scales between approximately 1 hour and 1 week with a uniform distribution of the time series values. After calibration the model was used for disaggregation from approximately 16 hours to 1 hour. It reproduced not only the scaling behavior of the observed data, but also the intermittent nature and the distributional properties of both individual volumes and event-related measures. The disaggregation model is based on the scale invariance concept, so it can in principle be calibrated on the very same data which are to be disaggregated. The disaggregation consists of distribution of the rainfall amount observed at any time step Δt over 2 sub-period time steps Δt/2 (t1 and t2). According to the probabilities P(0/1), P(1/0), and P(x/x). These probabilities are assumed to depend on both the position of the period in the rainfall sequence and the rainfall volume during the period. If P(x/x), the volume in each half is determined based on weights w drawn from a theoretical probability distribution. The disaggregation procedure concerns a volume v corresponding to a period t and the cascade process gives during the first half time t_1 a volume $v_1 = w_1.v$ and a volume $v_2 = w_2.v$ during the second half time t_2. The w_1 and w_2 are multiplicative weights ($0 \leq w \leq 1$). This model has the advantage of extracting the weights by aggregating the time series values two by two (running the cascade backwards).

The described model was developed in order to be applied in semiarid areas for fine-scale time steps (Olsson, 2008). A general Matlab code was developed for disaggregation, parameter estimation, and settings defined to fit the observed data using scale invariant properties of observed rainfall time series. The probability values P(0/1), P(1/0), and P(x/x), were estimated and weights extracted. To do so, the observed 15-min time series values were aggregated into daily values (96 by 96) which then were disaggregated back to 15-min values using the cascade model (8 cascade steps) and calibrated on the very same series. The mean of the empirical probabilities in the range 15-min to 1-day was used as probability values. The disaggregation from 1-day resolution was reproduced 10 times. Consequently, ten 15-min time series were generated.

The evaluation of the applicable scale range of a cascade model designed to represent the temporal structure of rainfall in semiarid Tunisia was performed as a first step. Secondly, the model was used for temporal rainfall disaggregation within this range using 10 realizations. The latter were averaged and compared to the observed time series. Statistical properties related to the rainfall in general and to the erosive events in particular were investigated to evaluate the model output. For this, autocorrelation and empirical probability distribution functions were calculated. The ability of the model to reproduce the scaling behavior of the observed data was studied by calculating statistical moments of various orders.

3 Results and discussion

The agreement between observed and generated time series was quite good. This was especially in terms of zero value percentage, wet period, event depth, and total volume (Table 1). The agressivity potential of generated rainfall was also well represented. In fact the number of 3 mm and 12 mm rainfall events was in the same range for observed and generated series. A slight overestimation of the event depth and an under estimation of the duration induced higher average and maximum intensities for the erosive events (Table 2). The rainfall agressivity related to erosion is reproduced even though the total depth is disaggregated with a reduction of 7%. Finally, the generated time series shows a time shift of about 150 min compared to the observed one.

The maximum intensity observed during the studied period, was about 84 mm/h. referring to the long-term intensity-duration-frequency curves from the Jannet district, the maximum intensity corresponds to a return period of 5 years. Such events are described as being responsible for transporting sediments, mobilizing bed load, channelizing debris flow, and even changing the valley floor (Coppus et al., 2002 ; Garcia-Ruiz et al., 2003; Hooke et al., 2000; Maas et al., 2000). All these characteristics are at hand in the Jannet catchment.

Table 1. The rainfall characteristics related to the observed and the generated series

Time series	Zero values (%)	Event depth (mm)	Wet period (hrs)	Max. 15min depth (mm)	Total depth (mm)
Observed	0.97	0.46 ± 0.94	849.5	21.0	1570.5
Modeled	0.97	0.45 ± 0.88	864.7	19.2	1568.5

Table 2. Comparison between the observed and the generated erosive rainfall events

Erosive event characteristics	No of events (>3mm)	No of events (>13mm)	Mean depth /event (mm)	Mean duration /event (mm)	I_{15}max (mm/h)	Mean int. (mm/h)	Total depth (mm)
Observed	59	23	18.3 ± 7.9	267.4 ± 217.0	52.0 ± 30.4	9.3	420.0
Modeled	58	18	21.7 ± 1.2	218.4 ± 35.5	76.6.0 ± 26.9	11.2	391.0

Figure 2 shows the autocorrelation properties related to the observed and generated time series. For short time lags, the generated autocorrelation is over-estimated compared to the original series. Between 1 and 4 time lags the significant autocorrelation of the observed time series decreases strongly, but the autocorrelation for the generated time series needs about 25 more time steps to reach the same level of autocorrelation. It is observed that a significant correlation exists up to about 40 min for the observed data and about 1000 min for the generated one. These correlations reach zero respectively at 600 and 1500 min. These delays in the function could be due to a temporal persistence that may be related to the fractal properties of the time series (Rodriguez-Iturbe et al., 1989).

The empirical probability distribution function Pr(X>x) for observed and generated time series is displayed in Fig. 3. The hyperbolic tail behavior is evident for both series with the slope qo=1.6 and qg=1.8, respectively. Slopes were estimated from fitted regression lines. These values agree well with the findings of Fraedrich and Larnder (1993), Olsson (1995), and Svensson et al. (1996) for almost similar intensity levels.

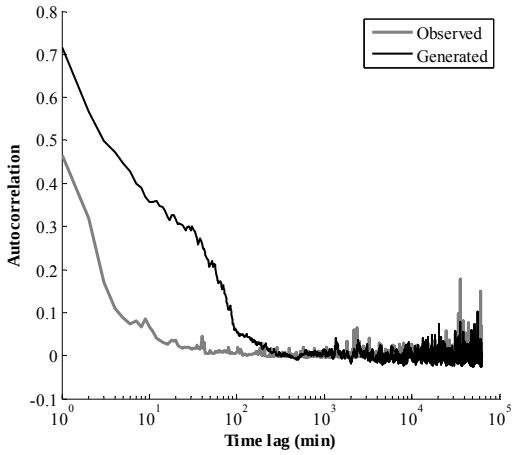

Fig. 2. Autocorrelation function for observed and generated 15-min rainfall time series (15-min time lag). The plot concerns the whole observation period.

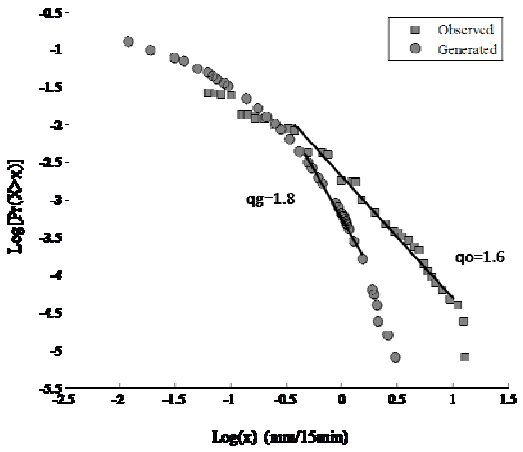

Fig. 3. Empirical probability distribution function Pr(X>x) for observed and generated 15-min rainfall time series. The straight lines have been fitted by regression.

The power law shapes for observed and generated series are shown over a range of frequencies $f^{0.62}$ and $f^{0.91}$. The exponent β was estimated from the solid regression line (Fig. 4(a,b)). This indicates that both series are scaling with a well respected stationarity in this range of scale. Their scaling regime was estimated to be from 15 up to 375 min for the observed data and from 15 up to 225 min for the generated time series. The generated spectrum is observed to be above the observed one (Fig. 4(a,b)).

Consequently, the above rainfall time interval may be expected to exhibit scaling behavior. The upper limits are in contradiction with some previous studies where it was found to be several days (Ladoy, 1993; Olsson, 1995, 1998; Svensson et al., 1996). However, this upper limit may correspond to the higher variability of rainfall events and related to individual meso-scale storms characterizing semiarid areas.

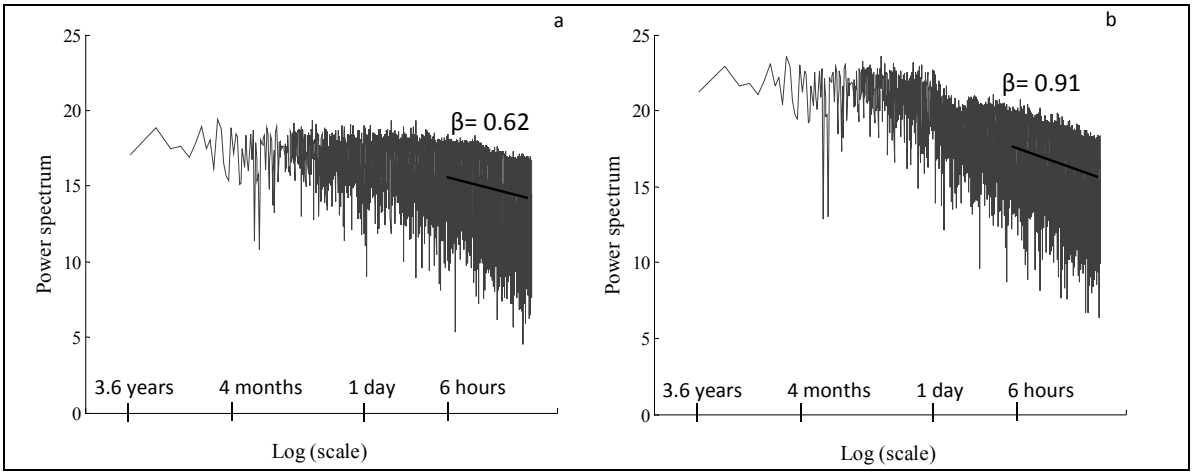

Fig. 4. (a) Spectral density function for observed time series. (b) Spectral density function for generated time series. The straight lines were fitted by regression respecting the significance of the Fourier power spectrum.

Figure 5(a,b) shows statistical moments of various order (q between 0.5 and 4.0) as a function of scale for the observed and the generated data. The log-log linear (power-law) curves of the observed data confirm the scaling behavior. The curves have been fitted by regression lines with an average R^2 of 0.9. The disaggregated data match these very well and it is evident that the model preserves scaling behavior. However, the moment analysis reveals that a multifractal behavior as expressed by (2) is represented from 260 to 360 min for the observed series and from 140 to 260 min for the generated series. Thus, a multifractal behavior is expected to hold for a time range of 100 min for both series. The scaling regime sequence and its length seem to fit the erosive event duration very well (Table 2). This scaling regime appears about four hours after start of rainfall. This coincides with the last third of the event intensity distributions regarding erosive events for the observed data the second half for the generated data. For both series the scaling lasts about 100 min. The latter period also coincides with the most crucial occurrence of the active erosion process that leads to the main part of soil loss. After few hours of rainfall, the soil is water soaked and all cohesion between surface soil particles is lost. Consequently, huge soil loss is induced. This may indicate a physical link between the temporal structure of scaling erosive rainfall events and the soil loss process for semiarid areas.

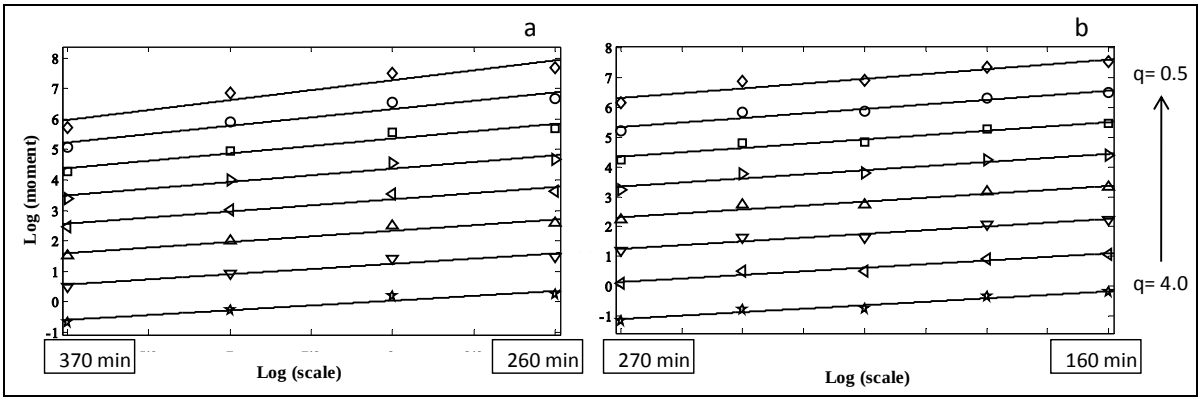

Fig. 5. The average moment as a function of λ in the scaling regime of order q varying from 0.5 to 4.0. (a) Observed series. (b) Generated series. The straight lines have been fitted by regression

4 Conclusion

Rainfall disaggregation techniques are powerful methods for increasing data availability for many areas lacking detailed rainfall observation. Semiarid regions often lack the fine time scale rainfall data necessary for many engineering and environmental applications. In this paper we have investigated a method for enhancing rainfall data to provide input to erosion estimation. The results show that erosive rainfall properties in semiarid Tunisia are characterized by scale invariance. Moreover, they represent a multifractal temporal behavior that appears to coincide with the temporal most active erosion process occurrence.

The cascade model applied to disaggregate the daily time series into 15-min time resolution performed well. It reproduced the main rainfall characteristics in general and respected the erosive properties in particular. The scaling regime and the multifractal behavior were well reproduced. These findings are very promising for a scaling-based approach in soil loss applications over the Tunisian semiarid area where erosion is a serious problem. Continued work with this approach will focus on using the generated rainfall time series by the means of the cascade model as input for a soil loss model. The results from such a model approach can be compared to the downstream erosion rate. The presented approach will also be tested for other rainfall gauges in order to evaluate the general performance.

Acknowledgements. The authors thank Mr. Habib Farhat, head of the Tunisian Farmland Conservation and Management Department (DG/ACTA) for providing data. They are also grateful to the support given to this work by Dr. Nejib Rejeb, head of the National Research Institute for Rural Engineering, Water and Forestry (INRGREF).

References

Burlando, P., and Rosso, R.: Scaling and multiscaling models of depth-duration frequency curves for storm precipitation. *J. Hydrol.,* 187, 45–64, 1996.

Davids, A., Marshak, A., Wiscombe, W., and Cahalan, R.: Multifractal characterizations of nonstationarity and intermittency in geophysical fields: Observed, retrieved or simulated. *J. Geophys. Res.,* 99, 8055–8072, 1994.

Coppus, R., and Imeson, A.C.: Extreme events controlling erosion and sediment transport in a semi-arid sub-andean valley. *Earth Surf. Process. Landforms*, 27, 1365–1375, 2002.

D/CES and ORSTOM : L'acquisition numérique et autonome de données hydro-Pluviométriques, L'expérience d'un réseau pilote Tunisien, *Rapport édité par la Direction de Conservation des Eaux et du Sol ainsi que l'Institut Français de Recherche Scientifique pour le développement en Coopération.,* 01–33, 1998.

Deidda, R.: Rainfall downscaling in a space time multifractal framework. *Water Resour. Res*. 36, 1779–1794, 2000.

Elshamy, M.E., Wheater, H.S., Gedney, N., and Huntingford, C.: Evaluation of the rainfall component of a weather generator for climate impact studies. *J. Hydrol.,* 326, 1–24, 2006.

Fraedrich, K., and Larnder, C.: Scaling regimes of composite rainfall time series. *Tellus* 45., 289–298, 1993.

Frisch, U., and Parisi, G.: *Fully developed turbulence and inter-mittency Proc*. International School of Physics Enrico Fermi, Course LXXXVIII, Italian Physical Society. In: Ghil, M., Benzi, R., Parisi, G. (Eds.), Turbulence and predictability in geophysical fluid dynamics and climate dynamics, North-Holland, Amsterdam, 1985.

Garcia-Ruiz, J.M., Carlos, M.B., Adrián, L., and Santiago, B: Geomorphological consequences of frequent and infrequent rainfall and hydrological events in Pyrenees Mountains of Spain. *Mitig. Adapt. Strat. Glob. Change*., 7, 303–320, 2003.

Gaume, E., Mouhous, N., and Andrieu, H.: Rainfall stochastic disaggregation models: Calibration and validation of a

multiplicative cascade model. *Adv. Water Resour*., 30, 1301–1319, 2007.

Güntner, A., Olsson, J., Calver, A., and Gannon, B.: Cascade-based disaggregation of continuous rainfall time series: the influence of climate. *Hydrol. Earth Syst., Sci.* 5, 145–164, 2001.

Gupta, V.K., and Waymire, E.: Multiscaling properties of spatial rainfall and river flow distributions. *J. Geophys. Res.,* 95, 1999–2009, 1990.

Gupta,V. K., and Waymire, E.C.: A statistical analysis of mesoscale rainfall as a random cascade. *J. Appl. Meteorol.,* 32, 251–267, 1993.

Halsey, T. C., Jensen, M. H., Kadanoff, L. P., Procaccia, I., and Shraiman, B.: Fractal measures and their singularities: the characterization of strange sets. *Phys. Rev. Letters* 33.,1141–1151, 1986.

Harris, D., Menabde, M., Seed, A., and Austin, G.: Breakdown Coefficients and scaling properties of rain fields. *Nonlinear Proc. Geophys.,* 5, 93–104, 1998.

Hingray, B., and Ben Haha, M.: Statistical performances of deterministic and models for rainfall series disaggregation. *Atmos. Res.,* 77,152–175, 2005.

Hooke, J.M., and Mant, J.M.:Geomorphological impacts of a flood event on ephemeral channels in SE Spain. *Geomorphology*.,34, 163–180, 2000.

Hubert, P., and Carbonnel, J.P. : *Analyse multifractale et precipitations extremes*. Proc. Sixth Scientific Assembly of the Inter-national Association of Meteorology and Atmospheric Physics and Fourth Scientific Assembly of the International Association of Hydrological Sciences, Yokohama, Japan, 11–23July, 1993.

Hubert, P., Tessier, Y., Lovejoy, S., Schertzer, D., Schmitt, F., Ladoy, P., Carbonnel, J. P., Violette, S. and Desurosne, I.: Multifractals and extreme rainfall events. *Geophys. Res. Lett.,* 20, 931–941, 1993.

Hunt, G.A. (1951) Random Fourier transforms. *Trans. Amer. Math. Soc.* 71, 1–38.

Jebari, S., Berndtsson, R., Bahri, A., and Boufaroua, M.:Spatial soil loss risk and reservoir siltation in semi arid Tunisian. Accepted for publication *in Hydrol. Sc. J*., 2009.

Jebari, S., Berndtsson, R., Bahri, A., and Boufaroua, M.: Exceptionel Rainfall Characteristics Related to Erosion Risk in Semiarid Tunisia. *The Open Hydrol. J.,* 2., 25–33, 2008.

Jebari, S., Berndtsson, R., Uvo, C. and Bahri, A.: Regionalizing fine time-scale rainfall affected by topography in semi-arid Tunisia. *Hydrol. Sci. J.,* 52, 1199–1215, 2007.

Kahane, J.P. and Peyriere, J.: Sur certaines martingales de Benoit Mandelbort. *Adv. Math*., 22, 131-145, 1976.

Kantelhardt, J.W.: Factal and Multifractal Time Series. *Phy. Data* Xiv:0804.0747v1. Free PDF:s from Universitetsbibliotekets printed journals, 2008.

Kowal, J.M., and Kassam, A.H.: Energy load and instantaneous intensity of rainstorms at Samaru, northern Nigeria. *Samaru Res. Bull*., 267,185–197, 1976.

Kumar, P., Guttarp, P., and Foufoula-Georgiou, E.: A probability weighted moment test to assess simple scaling. *Stoch. Hydrol. Hydraul*., 8,173–183, 1994.

Ladoy, P., Schmitt, F., Schertzer, D., and Lovejoy, S. : Variabilité temporelle multifractale des observations pluviométriques a Nîmes. *C. R. Acad. Sci.,* 317, 775–782, 1993.

Lavallee, D.: Multifractal techniques: analysis and simulation of turbulent fields. PhD thesis, McGill University, Montreal, Canada, 1991.

Lovejoy, S. and Schertzer, D.: Multifractals, universality classes and satellite and radar measurements of cloud and rain fields. *J. Geophy. Res.*, 95, 2021–2034, 1990.

Lovejoy, S., and Schertzer, D.: Multifractals, cloud radiances and rain, *J. Hydrol*., 322, 59–88, 2005.

Maas, G.S., Macklin, G.E., Warburton. J., Woodward, J.C., and Meldrum, E.: A 300-year history of flooding in an Andean mountain river system: the Rio Alizos, southern Bolivia. *Technical Report, Balkema, Rotterdam*,2000.

Malamud, B., and Turcotte, D.: Self affine time series: measure of weak and strong persistence. *J. Stat. Plan. Inference.,* 80,173–196, 1999.

Mandelbrot, B.: Intermittent turbulence in self similar cascades: divergence of high moments and dimension of the carrier. *J. Fluid Mech*., 62, 331–350, 1974.

Marsan, D., Schertzer, D., and Lovejoy, S.: Causal space time multifractal processes: predictability and forecasting of rain fields. *J. Geophys. Res*., 101, 26333–26346,1996.

Masson, J.M. : L'érosion des sols par l'eau en climat Méditerranéen, Méthodes expérimentales pour l'étude des quantités érodées à l'échelle du champ, Thèse de Docteur-Ingenieur USTL Montpellier, 1971.

Menabde, M., and Sivapalan, M.,: Modeling of rainfall time series and extremes using the bounded random cascades and Levy-stable distributions. *Water Resour. Res.,* 36, 3293– 3300, 2000.

Menabde, M., Harris, D., Seed, A., Austin, G., and Stow, D.: Multiscaling properties of rainfall and bounded random cascades. *Water Resour. Res.,* 33, 2823– 2830, 1997.

Menabde, M., Seed, A., and Pegram, G.: A simple scaling model for extreme rainfall. *Water Resour. Res*., 35, 335–339, 1999.

Molnar, P., and Burlando, P.: Preservation of rainfall properties in stochastic disaggregation by a simple random cascade model. *Atmos. Res.,* 77, 137–151, 2005.

Olsson, J., Niemczynowicz, J. Berndtsson, R. and Larson, M.: An Analysis of the rainfall Time Structure by Box Counting – Some Practical Implications. *J. Hydrol*., 137, 261–277, 1992.

Olsson, J., Niemczynowicz, J., and Berndtsson, R.: Fractal analysis if high resolution rainfall time series. *J. Geophys. Res.,* 98, 65–74, 1993.

Olsson, J.: Limits and characteristics of the multifractal behavior of a high-resolution rainfall time series. *Nonlinear Proces. Geophys*., 2, 23–29,1995.

Olsson, J.: Scaling and fractal properties of rainfall, Analysis and modeling of rain gauge data. PhD Thesis, Rep. 1014, Dept of Water Resourc. Engng, Lund Univ, 1996.

Olsson, J.: Evaluation of a cascade model for temporal rainfall disaggregation. *Hydrol. Earth Syst. Sci.,* 2, 19–30, 1998.

Olsson, J., and Berndtsson , R.: Temporal rainfall disaggregation based on scaling properties. *Water Sci. Technol,*. 37, 73–79, 1998.

Olsson, J., and Burlando, P.: Reproduction of temporal scaling by a rectangular pulse rainfall model. *Hydrol. Proc.,* 16, 611–630, 2002.

Olsson, J.: Development and Matlab implementation of the cascade-based disaggregation model. Report, 2008.

Ormsbee, L.E.: Rainfall disaggregation model for continuous hydrologic modeling. *J. Hydraul. Eng.,* 115, 507–525, 1989.

Over, T. M., and Gupta,V. K.: Statistical analysis of mesoscale rainfall: dependence of a random cascade generator on large-scale forcing. *J. Appl. Meteorol*., 33, 1526–1542, 1994.

Over, T. M., and Gupta, V. K.: A space–time theory of mesoscale rainfall using random cascades. *J. Geophys. Res.,* 101, 26319– 26331, 1996.

Rodriguez-Iturbe I., DePower, F., Sharifi, M., and Georgakakos, K.: Chaos in rainfall. *Water Resour. Res.,* 25, 67–75, 1989.

Schertzer, D., and Lovejoy, S.: Physical modeling and analysis of rain and clouds by anisotropic scaling of multiplicative processes. *J. Geophys. Res*., 92, 9693–9714, 1987.

Schertzer, D., Tchiguirinskaia, I., Lovejoy, S., Hubert, P., and Bendjoudi, H.: Which chaos in the rainfall-runoff process? A discussion on ''Evidence of chaos in the rainfall-runoff process''. *Hydrol. Sci. J.,* 47, 139–147, 2002.

Schmitt, F., Vannitesm, S., and Barbosa, A.: Modeling of rainfall time series using two-state renewal processes and multifractals. *J. Geophy. Res*., 103, 23181–23193, 1998.

Sivakumar, B., Sorooshian, S., Gupta, H. V., and Gao, X.: A chaotic approach to rainfall disaggregation. *Water Resour. Res*., 37, 61–72, 2001.

Svensson, C., Olsson, J., and Berndtsson, R.: Multifractal properties of daily rainfall in two different climates. *Water Resour. Res*., 32, 2463–2472, 1996.

Tessier, Y., Lovejoy, S., and Schertzer, D.: Universal multifractals: theory and observations for rain and clouds. *J. Appl. Meteorol*., 32,223–250, 1993.

Thauvin, V., Gaume, E., and Roux, C.: A short time-step point rainfall stoshastic model. *Water Sci. Technol*., 11, 37–45, 1998.

Veneziano, D., and Furcolo, P.: Multifractality of rainfall and scaling of the IDF curves. *Water Resour. Res.,* 38, 12–42, 2002.

Veneziano, D., and Furcolo, P.: Marginal distribution of stationary multifractal measures and their haar wavelet coefficients. *Fractals .,* 11, 253–270, 2003.

Veneziano, D., Furcolo, P., and Iacobellis, V.: Imperfect scaling of time and space –time rainfall. *J. Hydrol*., 322, 105–109, 2006.

Wischmeier, W.H., and Smith, D.D.: *Predicting rainfall erosion losses* – A guide to conservation planning. USDA Agriculture Handbook 537, Washington D.C: GPO, 1978.

Yaglom, Y.: The influences of fluctuations in energy dissipation on the shape turbulence characteristics in the inertial interval, *Sow. Phys. Dekl*., 11, 26–29, 1966.

Soil erosion estimation based on rainfall disaggregation

S. Jebari[1] and J. Olsson[2]

[1]National Research Institute for Rural Engineering, Waters, and Forestry, Box 10, Ariana 2080, Tunis, Tunisia
[2]Swedish Hydrological and Meteorological Institute, S-60176 Norrköping, Sweden

Submitted for publication to Hydrology and Earth System Sciences

Abstract. Soil loss estimation remains one of the most difficult research tasks all over the world. Current simulation tools are still not detailed enough to allow for realistic scenarios to handle soil erosion problems. A common problem is often the lack of rainfall data at a sufficient level of detail. The present study uses a cascade disaggregation model to generate short time scale rainfall data, needed to calculate the erosivity index in erosion modeling. The model is used to determine the spatial soil loss rate by the Universal Soil Loss Equation and a GIS approach. Comparison between observed and generated data in terms of erosive rainfall characteristics shows that the erosivity factor is overestimated by some 30%. This was caused by an over-estimation of short rainfall events. Consequently, different duration limits beyond which erosive events could be considered within the generated series were used to estimate the model performance curve. This provided a suitable duration limit needed to reproduce the observed erosivity. The procedure showed that generated series that only considered rainfall events longer than 45 min is almost perfect. It provides a soil loss rate with only 5% over-estimation. Moreover, using Masson and Wischmeier-Smith's limit intervals it gives a realistic spatial erosion distribution. The results are promising and can be used to better manage erosion-prone soils.

---

1 Introduction

Water erosion problems are seriously affecting agricultural areas and extending worldwide degrading lands (e.g., Eswaran et al., 2001). The potential consequences raise important issues like the global food security and the loss of reservoir capacity for irrigation and energy production (Pimentel et al., 1995; Crosson, 1997; Lal, 1998; WCD, 2000; Lomborg, 2001). Consequently, improved methods are urgently needed to better estimate where in a catchment the soil loss risks are the greatest. Also, methods that can yield erosion assessment at the regional scale, determine sediment yield, and predict of soil loss distribution are required. However, these tasks still remain among the main challenges in soil erosion research since sufficiently detailed observations of hydrological variables in small watersheds are often lacking (e.g., Van Rompaey and Govers, 2002; De Vente 2005; Haregeweyn et al., 2006). Especially, the non-availability of recorded short-term rainfall data is considered the principal limitation to statistical modeling of risk, in general, and the rainfall erosivity factor in particular (White, 1997; Sonneveld and Nearing, 2003; Yang et al., 2003a). The erosivity factor (R), describes the ability of rainfall to erode soil (Wischmeier and Smith, 1978). It is known as a region specific parameter (Yu, 1998). A second problem is that this factor may increase in the future due to the global warming process (Yang et al., 2003; Nearing et al., 2004). Research for the northern Mediterranean basin has emphasized the importance of soil erosion (Poesen and Hooke, 1997; EEA, 1999; Boix-Fayos, 2007). However, the situation can be even more serious for the southern parts of the basin. Especially for the North African countries it is expected that water and soil resources will continue to deteriorate (GOPA&GTZ, 2005; Gobin et al., 2004, Ennabli, 2007). Consequently, to better control water erosion it is crucial to overcome data limits. A possible way is to use the fractal approach and disaggregation of rainfall (Veneziano et al., 2006; Kantelhardt, 2008). The disaggregation approach could address the rainfall fine time scale scarcity in several climate types (e.g., Olsson 1995; Svensson et al., 1996; Olsson and Berndtsson, 1998; Gunter et al., 2001; Molnar and Burlando, 2005). This seems to be also true in semiarid Tunisia, where the disaggregation of daily rainfall into shorter period rainfall has been shown to be possible (Jebari et al., 2007; Jebari et al., 2009, manuscript). Hence, the objective of the current study was to evaluate the performance of the Olsson cascade disaggregation model (1998; 2008) in estimating the soil loss rate for the Dorsal semiarid area in Tunisia. The model was applied to disaggregate daily rainfall into 15-min rainfall time series for the small agricultural Jannet catchment. The generated time series was used to determine the rainfall erosivity as input to the Universal Soil Loss Equation (USLE) and GIS modeling approach to estimate sediment yield and to display the spatial distribution of the erosion rates. Finally, the observed water erosion rates were compared to the modeled ones. The results show that the disaggregation method can be used to better estimate soil erosion and this lead to better planning of water and soil conservation measures.

2 Methods

2.1 Rainfall records and siltation measurements

In Mediterranean conditions, the water erosion process and reservoir siltation are event-based (e.g., Bois-Fayos et al., 2007; Walling, 1988; Uson et al., 2001; Romkens et al., 2002; Vrieling, 2006). This is probably caused by the great portion of convective rainfall. Rainfall in semiarid Tunisia is convective in 72% of the cases with a duration less than 1 hour (Jebari et al., 2007). Moreover, 12% of the rainfall events are exceptional with regard to 15-min rainfall intensity which is characterized by large values right from the start of rainfall (Jebari et al., 2008). This can cause great raindrop impact initiating detachment of soil particles particularly in the beginning of the rainy period (August-October) when the soil lies bare after a long dry period. Consequently, the maximum 15-min duration rainfall intensity was studied for the 1995-1998 period in order to characterize observed erosive rainfall events. The latter are specified in Table 1 according to number of events, depth, duration, maximum intensity (I_{max15}), average intensity, kinetic energy, and finally the corresponding erosivity factor (R). The observations used are based on the rainfall analysis of a monitored rain gauge network including 30 experimental catchments over the Tunisian Dorsal (HYDROMED, 1992-2002; SERST-IRD, 2000; Albergel and Rejeb, 1997). Each catchment discharges into a small reservoir. The rain gauge is fully automatic and of tipping bucket type connected to a logger recording data every minute (Colombani, 1988). The descriptive statistics for recorded rainfall event during the analyzed period (1994-1998) displays missing data less than 1%. A rainfall event is defined as separated from another event if a rain gauge shows less than one tip per hour. Besides the rainfall records, bathymetric measurements were periodically undertaken. These measurements were made by echo-sounding the water depths along pre-defined transects (Camus et al., 1995). At least 400 measuring points defined by three Cartesian coordinates (x, y, and z) were used. The change in reservoir volume was deduced from the difference from one observation time to another. In order to compare siltation rates between the different bathymetric campaigns, the deposited sediment volume on the bottom of the reservoirs was converted into transported mass of soil using an average of 1.5 t/m^3 as apparent density (Ben Mammou, 1998). Siltation data for the reservoir are available from annually published hydrological reports (DCES/IRD, 1994-2002). These are used to estimate average and maximum siltation rates delivered at the outlet of a catchment usually needed to design reservoirs and to preserve the storage water capacity (Jebari et al., 2009).

2.2 Studied catchment

From the above described hydrological and sedimentological observation network, the Jannet catchment was chosen for erosion modeling based on the fractal rainfall model (Fig. 1). The catchment is representative for the Dorsal area in terms of rainfall properties and soil loss rate (Jebari et al., 2007; 2009; 2009, manuscript). Jannet displays a mean annual rainfall of 447 mm, is situated at 800 m altitude, covers an area of 5.41 km^2, displays a mean slope of 16%, and a drainage density of about 7 km/km^2. Its reservoir was created in 1992 with an initial volume of about $95.5 \cdot 10^3$ m^3. The reservoir was subject of three bathymetric measurement campaigns (1994-1996-1998). The 10-year reservoir siltation corresponds to an average annual soil loss of 32.5 t/ha/yr since it was completely silted up by the end of the hydrological year of 2002-2003. An excessive soil loss rate of about 60 t/ha/yr was observed between the bathymetric campaigns of 12/10/1994 and 17/5/1996. However, the period corresponding to the disaggregation analysis involves two bathymetric measurements (12/10/1994-12/5/1998) and shows a soil loss rate of 27 t/ha/yr. The depreciation time of the reservoir is estimated below the average (Goel et al., 2005, Verma 1987; Anonymous, 2000b).

The Jannet catchment is seriously eroded and shows an annual soil loss of more than permissible levels mentioned in the literature. In fact, Wischmeier and Smith (1978) give the soil loss tolerance to 12 t/ha/yr defined as “the maximum level of soil erosion that will permit a level of crop productivity to be sustained economically and indefinitely”. Experiments throughout the Tunisian semiarid area have determined the average tolerable soil loss to about 2.5, 5, and 10 t/ha/yr for a thin, average, and thicker soil, respectively (Masson, 1971). The Jannet soil degradation level can be explained by the deep soft bedrock layer that characterizes the area and an active soil degradation process mainly generated by dominating interrill erosion (Jebari et al., 2009).

2.3 Soil Erosion Model

Physically-based models require large data and still have limitation in predicting basin sediment yields (e.g., Renschler and Harbor, 2002). However, simplified empirical models such as the Universal Soil Loss Equation (USLE; Wischmeier and Smith, 1965), presents a simple structure with easy application to available data (Bartsch et al., 2002). It reasonably estimates the soil erosion and sediment yield caused by interrill and rill erosion.

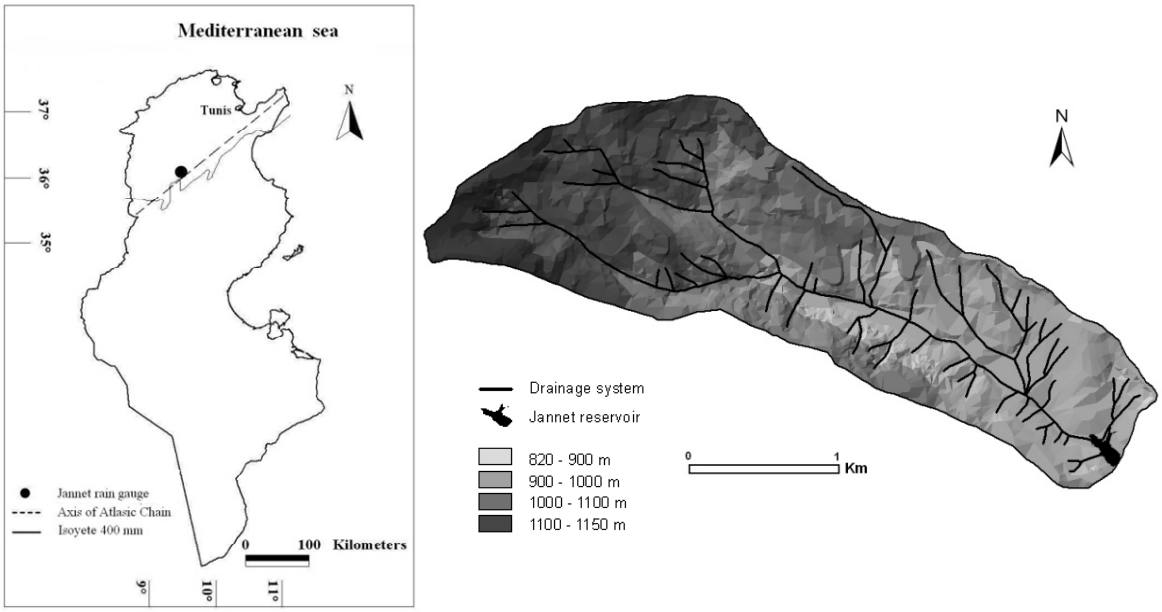

Fig. 1. Jannet rain gauge location and catchment topography

The interrill erosion process affects the largest areas and has an essential role in the erosion (Toy et al., 2002; Malam Issa et al., 2006; EEA, 2002). Moreover, in the Dorsal semiarid area it is the dominant erosion mechanism and crucial for reservoir siltation (Jebari et al., 2009). Since several decades ago, USLE is the most frequently applied model for estimating the annual soil loss from rainfall erosivity, topography, and land-use. Besides, it has been widely applied and tested at the watershed scale (Williams and Berndt, 1972; Griffin et al., 1988; Dickinson and Collins, 1998; Jain et al., 2001; Lee, 2004), the country scale (Gay et al., 2002), and the continent scale (Van der Knijff et al., 2000). The USLE equation is used to determine mean annual soil loss A (t/ha/yr) as a function of six erosion factors:

$$A = R * K * L * S * C * P \qquad (1)$$

where R is rainfall erosivity factor (m·t/ha·h), K (t·ha/m·t) is soil erodibility factor, L is length factor (m), S is slope factor (%), C is crop management factor (unit-less) and P a conservation practice factor (unit-less).

2.3.1 Rainfall erosivity factor (R)

The rainfall erosivity is considered by researchers as a more important factor in estimating erosion response than other environmental variables (e.g., Nearing et al., 1990). It is based on the kinetic energy (KE) and the maximum intensity (I) in a 30-min period (Wischmeier and Smith, 1958; Lal, 1976). In fact, the kinetic energy of rainfall is the potential ability of rain to detach soil and to splash. It can be evaluated above 3 mm (Kowal et al., 1976) and remains constant for rainfall intensities exceeding 76 mm/h (Hudson, 1965). The erosivity factor is calculated for precipitation exceeding 12.7 mm, a rate proposed by Wischmeier and Smith (1978) as erosive rainfall. Areas with high potential rainfall erosivity factor present high risk of severe soil erosion for which soil conservation structures may be necessary. Krishnaswamy et al. (2001) showed that R is the origin of the spatial variability of sediment yield and it increases from high mountains to valleys. The rainfall erosivity factor of Jannet station was computed by analyzing rainfall for 15-min periods. The latter period, was found representative regarding occurring erosion processes in the Tunisian semiarid dorsal catchments (Jebari et al., 2008). Each erosive event in the Jannet area is characterized by its depth, duration, average, and maximum intensity. Moreover, the observed and the generated erosivity factor (R) are respectively calculated from the different erosive rainfall events. The R values can be used as input to erosion modeling in order to estimate erosion rates and to better manage erosion risks in catchments with serious degradation. For the entire Jannet catchment, the observed and the generated R factors were assumed constant.

2.3.2 Soil erodibility factor (K)

The soil erodibility factor (K) represents the susceptibility of soil to erosion under standard plot conditions. The value can be locally measured since it depends on soil properties. Soils differ in their resistance to erosion according to the texture, structure, soil moisture, roughness, and organic matter content. The K factor was defined by using the Tunisian soil map (DRES 1979, scale: 1/200000), Tunisian experiments conducted in the semiarid area, and tables given in the literature (Wischmeier and Smith, 1978; Dangler et al, 1976; Cormary, 1963). The erodibility values and their spatial distribution are displayed in Figure 2.

2.3.3 Topographic factor (LS)

The percent slope layer was determined from a digital elevation model (DEM) developed for the Jannet area using a topographical map with a vertical resolution of 10 m (Tunisian National Topographical Service, Makthar map 1922, sheet 53, 1:50000). The contour lines were digitized, rastered, and linearly interpolated. The slope length was assumed fixed to 15 m according to Ogawa et al. (1997). The topographical factor LS was determined using the equation recommended by Morgan and Davidson (1991). Its spatial distribution is shown in Figure. 2.

2.3.4 Crop management (C) and conservation practice (P) factors

The crop management factor C, is defined as the ratio of soil loss from land cropped under specified conditions to the corresponding clean-tilled continuous fallow on identical soil and slope under the same rainfall conditions (Wischmeier and Smith, 1978). Their values account for different types of soil cover in a catchment and lower value was given to the forest cover which indicates a better cover as compared to the other land cover types. The Conservation practice factor (P) is the ratio of soil loss with a specific support practice to the corresponding loss with up and down slope cultivation. These factors depend on land/cover information of the catchment area. For the Jannet catchment they were derived from aerial photo interpretation (Agricultural and Water Resources Ministry, mission 1998; scale: 1/20000; photo: TU_17_28/ TU_18_28 TU_18_29/). The digitalization of these photos was used as tool to allocate the C and P factors for different land use classes. Their corresponding values are defined as recommended in the literarture (Wischmeier, 1975; Hudson, 1985; Masson, 1971; Heusch, 1970, CTFT, 1979). The values and the spatial distribution of both factors are displayed in Figure 2.

2.4 Disaggregation rainfall procedure

The spatial erosivity of the area was determined using a cascade disaggregation model (Olsson, 1988). This model was modified in order to be applied on semiarid fine-scale rainfall time steps (Olsson 2008). A Matlab code was used for disaggregation, parameter estimation, and settings defined to fit the observed data. The code distributes the observed rainfall amount during time step Δt over 2 sub-time steps $\Delta t/2$ (t_1 and t_2). The Jannet 15-min rainfall time series were aggregated into daily values (96 by 96) which were then disaggregated back to 15-min values using the cascade model (8 cascade steps) calibrated on the same series. The mean of the empirical probabilities in the range 15 min to 1 day was used as probability values. The disaggregation from 1 day resolution was reproduced 10 times. The average of the generated series was used in the current study to calculate the erosivity factor needed to estimate soil loss in the USLE model. Details of the disaggregation procedure can be found in Jebari et al. (2009, manuscript) and the resulting erosivity factors are shown in Table 1.

The results from the disaggregation procedure were divided in to five rainfall duration limits. These durations were 30, 45, 60, 75, and 90 minutes. Consequently, erosive events with duration longer than these limits were used to calculate erosivity factors. The different series of erosivity factors were used to construct a model performance curve (Fig. 3). This curve was used to compare short erosive rainfall event characteristics and to select a suitable duration limit for the Jannet catchment conditions and average rainfall erosivity value (Table 2).

The comparison between observed and generated erosivity values was based on three erosion classes. The first case is related to Masson's erosion classes, the second case considers the Wischmeier-Smith's erosion limits, and the third case presents the recent commonly used erosion classes (Irvem et al., 2007; Onyando et al., 2005; Pandey et al., 2007).

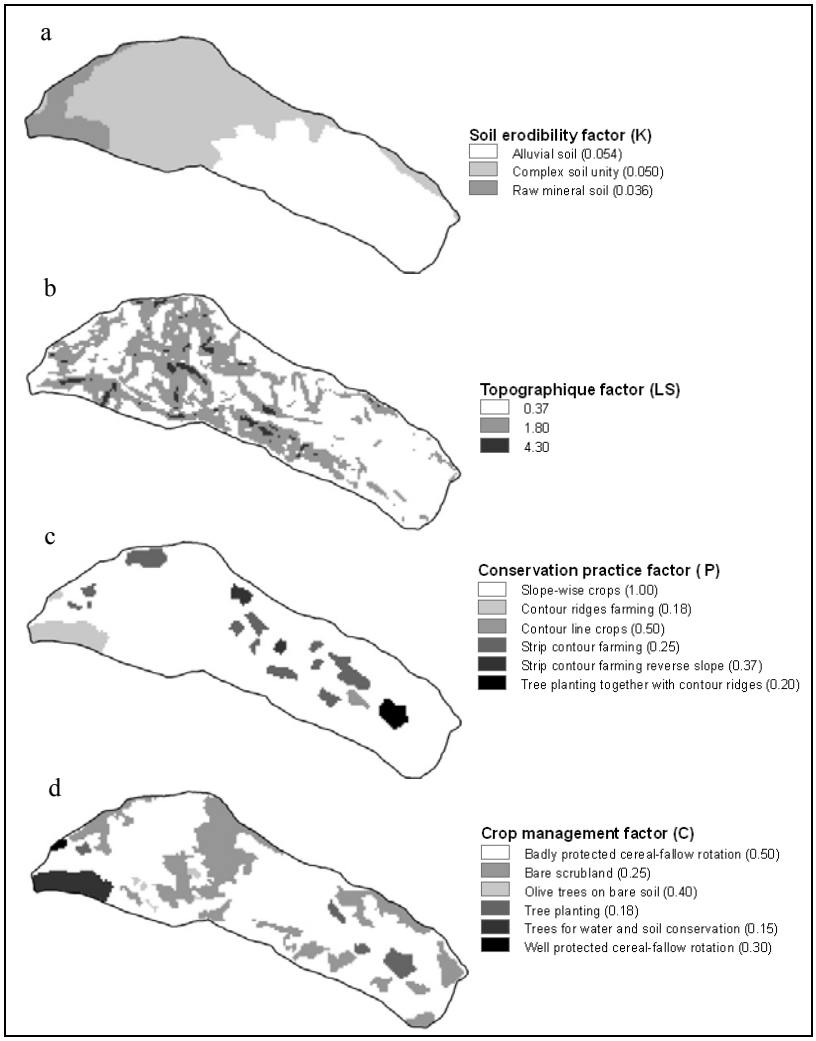

Fig. 2. Thematic map layers used to estimate the spatial distribution of soil loss using USLE equation. (a) Soil erodibility factor layer. (b) Topographic factor layer. (c) Conservation practice factor layer. (d) Crop management factor layer.

2.5 Generation of the thematic layers and estimation of soil loss

The GIS and aerial photo interpretation provided spatial input data for the USLE model. Together, they allowed an accurate, quick, and inexpensive tool to analyze soil erosion and estimate of erosion within a watershed (Millward & Mersey, 1999; Wang et al., 2003; Onyando et al. (2005) Pandey et al., 2007). The GIS technique involves discretizing the studied area into small regular grid cells which are considered a basic operational unit for erosion analysis and assumed a closed plot (Kinnell, 2001; Renschler et al., 1997; Fistikoglu and Harmancioglu, 2002). Subsequently, annual average soil loss for the catchment was computed from the sum of all grid cells. For the Jannet catchment the preparation of the thematic maps as spatial data base was performed to run the USLE model. Consequently, the watershed boundary, land cover aerial photos, and soil maps were digitized and/or transferred as GIS layers in ARC view 3.3 (Geographic Information System). The 10 m resolution DEM (digital elevation model) of the watershed was performed by interpolating the digitized contour intervals. All data were spatially organized using the GIS with the same resolution and co-ordinate system. The Jannet watershed was divided into regular 25*25 m grids and the erosivity factor was used as a uniform constant layer. This procedure was followed by the overlay of the five parameter layers (R, K, LS, C, and P). The USLE/GIS approach was calibrated for the Jannet catchment by comparing calculated soil loss rate with observed deposited sediment in a downstream reservoir.

3 Results and discussion

3.1 Estimation of rainfall erosivity values

The observed 23 erosive rainfall events during the studied period had a total depth of 420 mm. This represented about 25% of the total catchment rainfall. The average erosive event depth was 18.3±7.9 mm with a maximum intensity of 52 mm/h and an average duration of 267.4±217.0 min. However, the annual average erosivity value found was 79.9 m.t/ha.h (Fig. 2). Characteristics of observations are compared to the generated data ($Gen._{Tot.}$) and displayed in Table 2. The disaggregation model reproduced erosive events with an over-estimation regarding depth and maximum intensity. Moreover, it underestimated the number of events and its duration.

Table 2 Performance of the disaggregation model in reproducing erosive rainfall characteristics with duration less than 45 minutes.

Erosive event characteristics	Obs. data	Gen. data	Perfor. (%)
Nb. Events	4	2.6	-35.0
Tot. Depth (mm)	63.0	54.4	-13.5
Av. Depth /Ev. (mm)	15.7	23.8	+33.8
Av. Duration/Ev. (min)	37.7	38.0	+1.4
Av. I_{max15} /Ev. (mm/h)	43.0	55.6	+22.6
Av. Int./Ev. (mm/h)	26.6	41.1	+35.2
Av. KE/Ev. (MJ/ha.mm)	397.3	591.5	+32.8
Av. R/Ev. (m.t/ha.h)	24.6	70.5	+65.1
Max. I_{max15} (mm/h)	52.0	68.4	+23.9
Max. KE (MJ/ha.mm)	461.5	795.5	+41.9
Max. R (m.t/ha.h)	27.8	99.7	+72.1

Consequently, this led to underestimation of the annual kinetic energy and overestimation of the annual erosivity (Table 1). The average annual generated erosivity was 110.7 m.t/ha.h. This was an overestimation of about 30% compared to the observed value.

The observed and the generated erosivity values were incorporated in the USLE/GIS methodology to calculate the erosion of the Jannet catchment. The observed and the generated average soil loss rates were 27.0 and 37.4 t/ha/yr, respectively. Consequently, this was an overestimation of about 30%.

3.2 The disaggregation model performances

To investigate the performance of the disaggregation model erosivity factors were calculated for five different event durations. These were 30, 45, 60, 75, and 90 minutes, respectively. The corresponding generated erosivity factors were 104.5, 83.5, 71.5, 67.3, 57.6 (m·t/ha·h), respectively. These values show an overestimation of 23.5% and 4.5 % for the two first duration limits and an underestimation of 10.3, 15.5, and 27.7% for the three last duration limits, respectively. These values were used to plot a disaggregation model performance curve shown in Figure 3.

Table 1 Comparison between observed and generated rainfall time series ($Gen._{Tot.}$ & $Gen._{Part.}$). The partially generated series take into account events >45 minutes only.

Erosive event characteristics	Obs. data	Tot. Gen. data	Part. Gen. data	Perfor. (%) (Obs-Tot. Gen)	Perfor. (%) (Obs-Part. Gen)
Nb. Events	23	18	17.5	-21.7	-23.9
Tot. Depth (mm)	420.1	391.0	355.2	-6.9	-15.4
Av. Depth /Ev. (mm)	18.3±7.9	21.7±9.7	21.5±9.5	+18.5	+17.4
Av. Duration/Ev. (min)	267.4±217.0	218.3±151.1	235.2±148.7	-18.3	-12.0
Av. I_{max15} /Ev. (mm/h)	18.8±14.5	25.2±18.3	22.5±16.4	+34	+19.6
Av. Int./Ev. (mm/h)	9.3±11.5	11.1±12.3	8.5±7.3	+19.3	-8.6
Av. KE/Ev. (MJ/ha.mm)	359.3±199.0	447.1±248.9	432.0±235.7	+19.6	+16.8
Av. R/Ev. (m.t/ha.h)	11.4±14.4	21.9±30.8	18.0 ±24.6	+47.9	+36.6
Max. I_{max15} (mm/h)	52.0	77.1	67.2	+32.5	+22.6
Max. KE (MJ/ha.mm)	1198.0	1108.6	1087.0	-8.1	-10.2
Max. R (m.t/ha.h)	66.4	116.1	96.0	+42.8	+30.8
Annual KE (MJ/ha.mm)	2361.1	2278.7	2012.6	-3.6	-17.3
Annual R (m.t/ha.h)	79.9	110.7	83.5	+27.3	+4.3

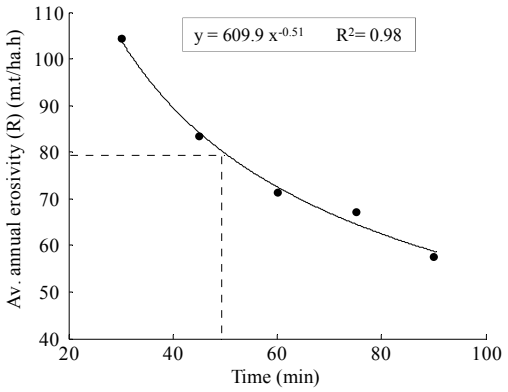

Fig. 3. The generated erosivity factors for the different rainfall duration limits. The dotted line displays the suitable duration limit needed to reproduce the observed erosivity.

The performance curve shows that the generated erosivities are increasing when the duration limit is decreasing. The general behavior can be compared to the observed and generated short duration erosive events in Table 2. The difference characterizing these is important. Table 2 displays that generated depth and intensity result in an erosivity factor exceeding the observed one by 65%. Moreover, the average erosivity factor for an observed erosive event is about 25 m·t/ha·h, meanwhile, the generated value is about 65.4 m·t/ha·h. Even though these events are rare, they are highly overestimated by the disaggregation model. However, the model performance curve was used to select a suitable duration limit approximately equal to 50 min from Fig. 3. However, the disaggregation model did not generate 50 min duration only 45 min duration limit. Consequently, this duration limit was selected as the best alternative for generating erosivity factor and average soil loss rate. These were 83.5 m·t/ha·h and 28.5 t/ha/yr, respectively. Compared to the observed erosion this was a slight overestimation of less than 5%.

3.3 The spatial erosion distribution

The USLE/GIS methodology presented above was applied to give a quantitative erosion estimate in the Jannet catchment. Observed and generated erosion maps include the annual erosive rainfall. The erosivity for totally observed ($Gen._{Tot.}$) and partially generated ($Gen._{Part.}$) series were 79.9, 110.7, and 83.5 m·t/ha·h, respectively. The corresponding soil loss rates were 27.0, 37.4, and 28.2 t/ha/yr, respectively, which corresponded to an overestimation of about 30 and 5%. Figure 4 shows the corresponding spatial soil erosion over the catchment. It is seen that the low soil loss rates involve a limited area of the catchment. However, the high rates are related to larger areas. In fact, rates less than 5 and 15 t/ha/yr are found for 15 and 27%, respectively, of the entire catchment area. These rates involve localized plots which are quite limited and subject to water and soil conservation practices. Meanwhile, if we consider high erosion levels ranging from 30 to 100 t/ha/yr, we notice that 50% of the catchment area is affected (Fig. 4). Such areas are distributed all over the catchment at both upstream and downstream areas. Moreover, the extreme soil loss rate is about 250 t/ha/year and covers an area of 70 hectares which corresponds to 13% of the whole catchment. This category of soil loss is observed at upstream areas above 1000 m altitude and representing a slope of about 15% (Fig. 5).

Both Fig. 4 and 5 show a similar spatial distribution of extreme soil loss as compared to the observations. However, the corresponding values for the total and partially generated data are 345 and 260 t/ha/yr, respectively.

The spatial erosion distribution which were prepared according to Masson's, Wischmeier-Smith's, and recent erosion classes display promising results for the partially generated case. In fact, the latter displays a very good agreement with the observed situation for the two first erosion classes (Fig. 4). As far as the third erosion classes are concerned, the spatial difference is seen for the intervals related to 30-60, 60-100, and >100 t/ha/year. The corresponding areas 71.0 and 41.7 hectares are under-estimated and the final 119.6 hectare area is overestimated.

The comparison between observed and total generation seems to be more complex. The spatial distribution of erosion according to Masson's erosion classes displays an underestimation and an overestimation of about 3.5 hectares for the two first soil loss intervals, respectively. However, an underestimation of 25 hectares characterizes the third soil loss interval (5-10 t/ha/yr). The same area in the next interval (>10 t/ha/year) is overestimated. For the Wischmeier-Smith soil loss interval and the totally generated case, the area is about 30 hectares underestimated as compared to observations for the first soil loss interval. For the second interval the same area is overestimated. For the "recent erosion classes", the two first soil loss intervals are similar as for the observations. However, for the three last erosion intervals (30-60, 60-100, and >100), the differences concern 71.0 and 83.7 hectares as over-estimation and 161.7 hectares as underestimation, respectively.

Usually the overestimated and underestimated areas are compensated for in the different soil loss intervals. However, overestimated areas are characterized the highest soil loss rates (>100 t/ha/yr) and underestimated are mainly characterized by the low soil loss intervals.

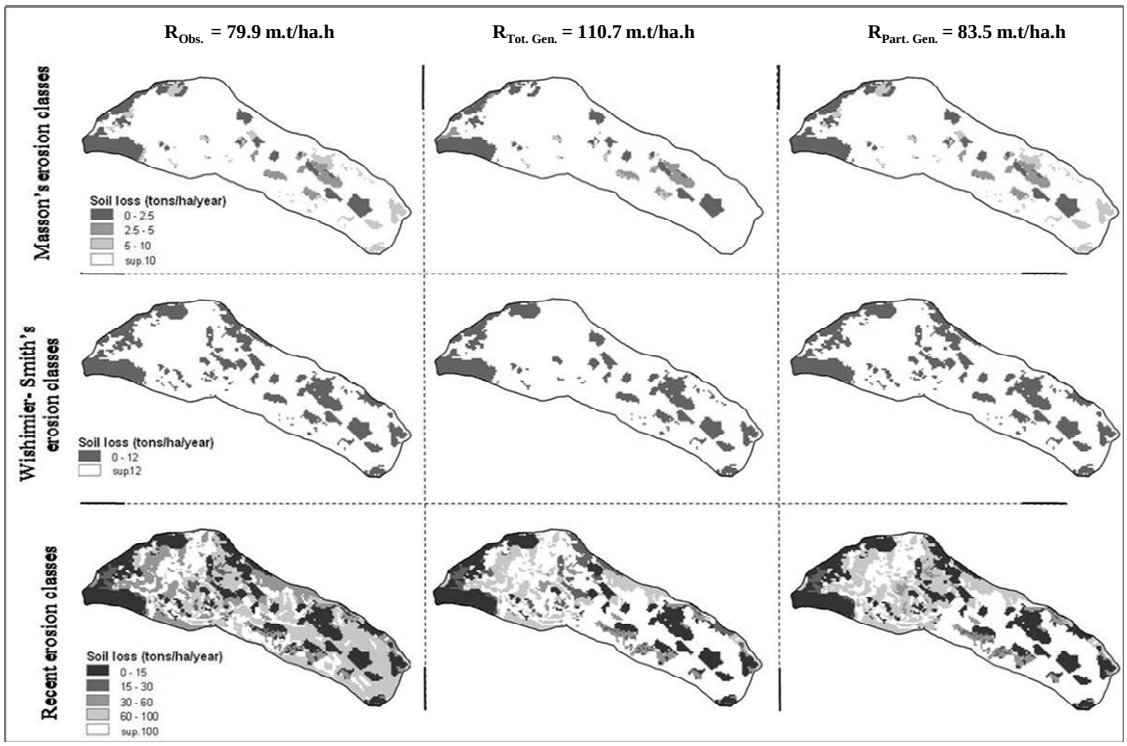

Fig. 4. Comparison between the spatial erosion distribution of the observed and the generated soil loss in the Jannet watershed. This is performed according to three erosion clusters namely: a) Masson's erosion classes, b) Wishmier-Smith's erosion classes, and c) recent erosion classes.

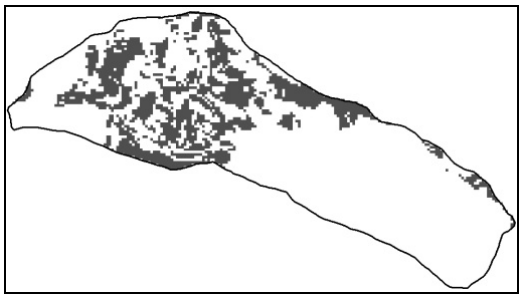

Fig. 5. Spatial distribution of extreme soil loss rates over the Jannet catchment.

The spatial distribution of the extreme soil loss values are exactly the same for the three used erosivity factors (Fig.5). For observed soil loss rates >100 t/ha/yr the spatial erosion displays a uniform distribution that is spread over the entire catchment (Fig. 6). Conversly, and for the same category of soil loss rate, the generated maps show overestimated downstream areas for altitude less than 1000 m. This large area is spotted by areas of lower soil loss rates that mainly involve water and soil conservation techniques (Fig. 6). Moreover, the observed map corresponding to the soil loss rate ranging from 60 to 100 t/ha/yr concerns areas situated in downstream but limited upstream areas above 1100 m altitude. Meanwhile, as opposed to observations both generated maps reproduce slightly larger upstream areas and almost no downstream degraded areas (Fig. 6).

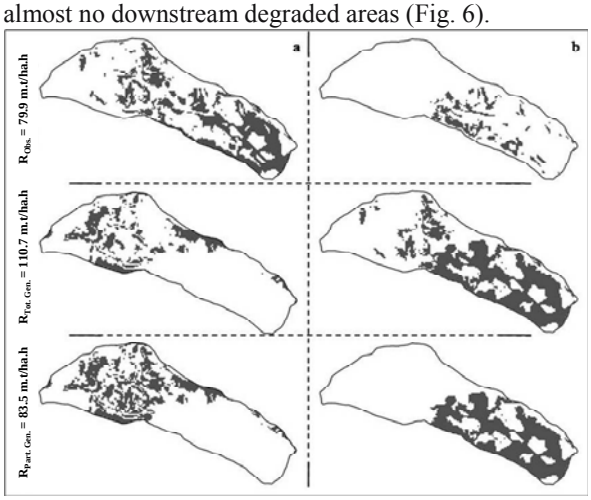

Fig. 6. Comparison between the observed and generated spatial soil loss distribution according to the "recent erosion classes". This is performed for soil loss category: a) from 60 to 100 tonnes/ha/yr and b) >100 t/ha/yr.

4 Conclusion

This analysis focused on evaluating the performance of a cascade rainfall disaggregation model in providing accurate and reliable soil loss estimation at the scale of small semiarid Mediterranean catchments. To do this, the Olsson's disaggregation model was applied to the Jannet catchment rainfall data. Preliminary results showed that the generated erosivity factor overestimated the spatial distribution of soil loss by 30%. However, the use of generated series with rainfall duration limit provided better agreement. The use of several duration limits for estimating erosivity showed that erosive events >45 minutes and gave an average erosivity factor of 83.5 m·t/ha·h which was only 5% higher than the observed one. Consequently, the presented methodology could be used to estimate spatial soil erosion levels even where no fine time-scale rainfall observations exist. The method needs to be tested on more catchments with actual data to evaluate its robustness.

Acknowledgements. The authors thank Mr. Habib Farhat, head at the Tunisian Farmland Conservation and Management Department (DG/ACTA) for providing data. They are also grateful to Prof. Ronny Berndtsson and Dr. Hedia Chakroun for valuable suggestions and comments related to this work. The support of Dr. Nejib Rejeb, head of the National Research Institute for Rural Engineering, Water and Forestry (INRGREF) is gratefully acknowledged.

References

Albergel, J., and Rejeb, N.: Les lacs collinaires en Tunisie: Enjeux, contraintes et perspectives. Comptes rendus de *l'Académie d'Agriculture de France*., 83, 77–104, 1997.

Anonymous.: Project Report of Panjara watershed under NWDPRA of Nurpur block in district Kangra of Himachal Pradesh. Departement of Agriculture, Government of Himachal Pradesh, 2000b.

Bartsch, K.P., Mietgroet, H.V., Boettinger, J., and Dobrowolski, J.P.: Using empirical erosion models and GIS to determine erosion at Camp William, Utah. *J. Soil Water Conserv.*, 57(1), 29–37, 2002.

Ben Mammou, A.: Barrages Nebeur, Sidi Salem, Sidi Saad, et Sidi Bou Baker. Quantificaton, étude sédimentologique et géotechnique des sédiments piégés. Apport des images satellitaires. Thèse de Doctorats Es-Sciences Géologiques, présentée à l'Université de Tunis II, Faculté des Sciences de Tunis, 1998.

Boix–Fayos, C., Martinez-Mena, M., Calvo-Cases, A., Arnau-Rosalén, E., Albaladejo, J., and Castilo, V.: Causes and underlying processes of measurement variability in field erosion plots in Mediterranean conditions. *Earth Surf. Process. Landforms*., 32, 85–101, 2007.

Camus, H., Guiguen, N., and Ben Younes, M.: Note sur l'envasement des lacs collinaires en zone semi-aride Tunisienne. Rapport publié par la Direction de la Conservation des Eaux et du Sol et l'Institut de Recherche pour le Développement en Cooperation (ORSTOM), 1995.

Colombani, J.: Autopsie d'un hyétogramme. In: Troisièmes journées hydrologiques de l'ORSTOM (Montpellier, 23-24 septembre 1987), 28-37. Publication du Laboratoire d'hydrologie de Montpellier, Fance, 1988.

Cormary., Y.: Projet type CES. Utilisation des photographies aériennes. Intégration des paramètres climatiques, pédologiques et agricoles dans l'élaboration d'un projet de CES sur le bassin versant de l'Oued Hallouf. Dossier CGR. N°.30 Note CES-C5, 1963.

Crosson, P.: Will erosion threaten agricultural productivity? *Environment*., 39 (8), 4–12, 1997.

Dangler, E, W., El-Swaify, S, A., Ahuja, L.R., and Barnett, A.P.: Erodibility of selected Hawaii soils by rainfall simulation, Agricultural research service, US Department of Agriculture, western region, 113p, 1976.

DCES/IRD: Annuaires hydrologiques des lacs collinaires. Rapports publiés par la Direction Générale de l'Aménagement et de la Conservation des Terres Agricoles et l'Institut de Recherche pour le Développement. République Tunisienne, 1994-2002.

De Vente, J., Poesen, J., and Verstraeten, G.: The application of semi-quantitative methods and reservoir sedimentation rates for the prediction of basin sediment yield in Spain. *J. Hydrol.*, 305, 63–86, 2005.

Dickinson, A., and Collins, R.: Predicting erosion and sediment yield at the catchment scale, Soil erosion at multiple scales. CAB Int., 317–342, 1998;

EEA: Environement in the European Union at the turn of the century. (Environmental assessment report 2). Copenhagen, Denmark: European Environment Agency, 1999.

EEA: Assessment and reporting on soil erosion. Background and workshop report. European Environmental Agency, 2002.

Ennabli, M.: la gestion durable des ressources en eau. Communication presentée lors des journées scientifiques de l'INRGREF, 2007.

Eswaran, H., Lal, R., and Reich, P.F.: Land degradation: an overview. In: Bridges, E.M., Hannam, I.D., Oldeman, L.R., Penning de Vries, F.W.T., Scherr, S.J., Sombatpanit, S. (Eds.), Response to Land Degradation. Science Publishers Inc, Enfield, NH, USA, pp., 20–35, 2001.

Fistikoglu, O., and Harmancioglu, N.B.: Integration of GIS with USLE in assessment of soil erosion. *Water Resour. Manag.*, 16, 447–467, 2002.

Gay, M., Cheret, V., and Denux, J.P.: Apport de la télédétection dans l'identification du risque d'érosion. *La Houille Blanche*., 1, 81– 86, 2002.

Gobin, A., Jones, R., Kirkby, M., Campling, P., Govers, G., Kosmas, C., and Gentile, A.R.: Indicators for pan-European assessment and monitoring of soil erosion by water. *Environ. Sci. Policy.*, 7, 25–38, 2004.

Goel A.K., and Kumar R.: Economic analysis of water harvesting in a mountainous xatershed in India. *Agricul. Water Manag.,* 71, 257–266, 2005.

GOPA and GTZ: Elaboration d'une stratégie nationale d'adaptation de l'agriculture tunisienne et des

écosystèmes aux changements climatiques. Pré rapport 1ere phase, 2005.

Griffin, M.L., Beasley, D.B., Fletcher, J.J., and Foster, G.R.: Estimating soil loss on topographically non-uniform field and farm units. *J. Soil Water Conserv*., 43, 326–331, 1988.

Gunter, A., Olsson, J., Calver, A., and Gannon, B.: Cascade-based disaggregation of continuous rainfall time series: the influence of climate. *Hydrol. Earth Syst. Sci*., 5, 145–164, 2001.

Heusch, B.: L'Erosion du Pré-Rif. Une étude quantitative de l'érosion hydrique dans les collines marneuses du Pré-Rif occidental. Rapport de la station de recherches forestières de Rabat., T.12, 176 p., 1970.

Hudson, N.W.: the Influence of Rainfall on the Mechnics of Soil Erosion with particular reference to Northen Rhodesia. MSc. Thesis, Univ. of Cape Rown, 1965.

Hudson, N.: Soil Conservation, Batsford Academic and Educational, London, 1985.

Irvem, A., Topaloglu, F., and Uygur, V.: Estimating spatial distribution of soil loss over seyhan iver Bassin in Turkey. *J. Hydrol*., 336, 30-37, 2007.

Jain, SK, Kumar, S., and Varghese, J.: Estimation of soil erosion for a Himalayan watershed using a GIS technique. *Water Resour. Manag*., 15, 41–54, 2001.

Jebari, S., Berndtsson, R., Uvo, C., and Bahri, A.: Regionalzing fine time-scale rainfall affected by topography in semi-aride Tunisia. *Hydrol. Sc. J*., 52, 1199–1215, 2007.

Jebari, S., Berndtsson, R., Bahri, A., and Boufaroua, M.: Exceptionel Rainfall Characteristics Related to Erosion Risk in Semiarid Tunisia. *The Open Hydrol. J*., 9, 25–33, 2008.

Jebari, S., Berndtsson, R., Bahri, A., and Boufaroua, M.: Spatial soil loss risk and reservoir siltation in semi arid Tunisian. Accepted for publication in *Hydrol. Sc. J*., 2009.

Jebari, S., Berndtsson, R., Olsson, J.: Scaling approach to enhance rainfall data for erosion estimation in semiarid Tunisia. Submitted to: *Hydrol. Earth Syst. Sc*., 2009.

Kantelhardt, J.W.: factal and Multifractal Time Series. arXiv:0804.0747v1 [physics.data-an] 4 Apr 2008.

Kowal, J.M., and Kassam, A.H.: Energy load and instantaneous intensity of rainstorms at Samaru Nigeria. *Tropical Agric*., 53 185–197, 1976.

Kinnell, P. I. A.: Slope length factor for applying the USLE-M to erosion in grid cells. *Soil & Tillage Research*., 58, 11–17, 2001.

Krishnaswamy, J., Richter, D.D., Halpin, P.N., and Hofmockel, M.S.: Spatial Patterns of suspended sediment yield in a humid tropical watershed in Costa Rica. *Hydrol. Process*., 15, 2237–2257, 2001.

Lal, R.: Soil erosion problems on alfisols in western Nigeria and their control. IITA Monograph 1, IITA, Ibadan, Nigeria 208 pp., 1976.

Lal, R.: Soil erosion impact on agronomic productivity and environment quality. *Critical Reviews in Plant Sciences*. 17, 319– 464, 1998.

Lomborg, B.: The Skeptical Environmentalist: Measuring the Real State of the World. Cambridge University Press, Cambridge, UK, 2001.

Lee, S.: Soil erosion assessment and its verification using the universal soil loss equation and geographic information system: A case study at Boun, Korea. *Environmental Geology*., 45, 457–465, 2004.

Malam Issa, O., Le Bissonnais, Y., Planchon, O., Favis-Mortlock, D., Silvera, N., and Wainwright, J.: Soil detachment and transport on field-and laboratory-scale interrill areas: erosion processes and the size-selectivity of eroded sediment. *Earth Surf. Proc. Landf*., 31, 929–939, 2006.

Masson, J.M.: L'érosion des sols par l'eau en climat Méditerranéen. Méthodes expérimentales pour l'étude des quantités érodées à l'échelle du champ Thèse de Docteur-Ingénieur, USTL Montpellier, 1971.

Millward, A. A., and Mersey, J. E.: Adapting the RUSLE to model soil erosion potential in a mountainous tropical watershed. *Catena*., 38, 109–129, 1999.

Molnar, P., and Burlando, P.: Preservation of rainfall properties in stochastic disaggregation by a simple random cascade model. *Atmos. Res*., 77, 137–151, 2005.

Morgan, R.P.C., and Davidson, D. A.: Soil Erosion and Consevation, Longman Goup, U.K, 1991.

Nearing, M.A., Ascough, L.D., and Laften, J.M.: Sensitivity analysis of the WEPP hillslope pofile erosion model. *Trans. ASAE*., 33, 839–849, 1990.

Nearing, M.A., Pruski, F.F., and O'Neal, M.R.: Expected climate change impacts on soil erosion rates: a review. *J. Soil and Water Cons.,* 59, 43–50, 2004.

Ogawa, S., Saito, G., Mino, N., Uchida S., Khan, N. M., and Shafiq, M.: Estimation of soil erosion using USLE and Landsat TM in Pakistan (ACRS 1–5). Retrieved from GIS development.net, 1997.

Olsson, J.: Limits and characteristics of the multifractal behavior of a high-resolution rainfall time series. *Nonlinear Processes in Geophysics*., 2, 23–29, 1995.

Olsson, J.: Evaluation of a cascade model for temporal rainfall disaggregation. *Hydrol. Earth Syst. Sci*., 2, 19–30, 1998.

Olsson, J., and Berndtsson, R.: Temporal rainfall disaggregation based on scaling properties. *Water Sci. Technol.*, 37, 73–79, 1998.

Olsson, J.: Development and Matlab implementation of the cascade-based disaggregation model. Working report, 2008.

Onyando, J.O., Kisoyan, P., and Chemelil M.C.: Estimation of potential soil erosion for River Perkerra catchment in Kenya. *Water Resour. Manag*., 19,133–143, 2005.

Pandey, A., Chowdary, V.M., and Mal, B.C.: Identification of critical erosion prone areas in the small agricultural watershed using USLE, GIS and remote sensing. *Water Resour. Manag*., 21,729–746, 2007.

Pimentel, D., Harvey, C., Resosudarmo, P., Sinclair, K., Kurz, D., McNair, M., Crist, S., Shpritz, L., Fitton, L., Saffouri, R., and Blair, R.: Environmental and Economic Costs of Soil Erosion and Conservation Benefits. *Science*., 267, 1117–1123, 1995.

Poesen, J.W.A., and Hooke, J.M.: Erosion, flooting and channel management in the Mediterranean environments of southern Europe. *Prog. Phys. Geogr*., 21, 157–199, 1997.

Renschler, C., Diekkruger, B., and Mannaerts, C.: Regionalization in surface runoff and soil erosion risk evaluation, in Regionalization of Hydrology. IAHS Publishers, UK., 254, 233–241, 1997.

Renschler, C.S., and Harbor, J.: Soil erosion assessment tools from point to regional scales-the role of geomorphologists in land management research and implementation. *Geomorphology*., 47, 189–209, 2002.

Romkens, M.J.M., Helming, K., and Prasad, S.N.: Soil erosion under different rainfall intensities, surface roughness, and soil water regimes. *Catena*., 46: 103–123, 2002.

SERST-IRD.: Evaluation conjointe du programme de recherche : Lacs et barrages collinaires en Tunisie. 2000.

Svensson, C., Olsson, J., and Berndtsson, R.: Multifractal properties of daily rainfall in two different climates. *Water Resources Research*., 32, 2463–2472, 1996.

Sonneveld, B., and Nearing, M.A.: A nonparametric/ parametric analysis of the Universal Soil Loss Equation. *Catena* 52, 9–21, 2003.

Toy, J.T., Foster, G.R., and Renard, K.G.: Soil erosion: Processes, prediction, measurement and control. Library of congress cataloging-in-publication data . Edited by Jhon Wiley et & Sons, Inc., NewYork., 338 pp, 2002.

Uson, A., and Ramos, MC.: An improved rainfall erosivity index obtained from experimental interrill soil losses in soils with a Mediterranean climate. *Catena*., 43: 293–305, 2001.

Van der Knijff, J.M., Jones, R.J.A., and Montanarella, L.: Soil erosion risk assessment in Europe. EUR 19044 EN, European Soil Bureau, Space Application Institute, JRC, Ispra, Italy, p. 34, 2000.

Van Rompaey, A.J.J., and Govers, G.: Data quality and model complexity for regional scale soil erosion prediction. *Geomorphology*., 16, 663–680, 2002.

Veneziano, D., Furcolo, P., and Iacobellis, V.: Imperfect scaling of time and space–time rainfall. *J. Hydrol*., 322, 105–109, 2006.

Verma, H.N.: Studies of an efficient use of rainwater for rainfed crops. Ph.D Thesis. Division of Agriculture Engineering. IARI, New Delhi, 1987.

Vrieling, A.: Satellite remote sensing for water erosion assessment: A review. *Catena*., 65, 2–18, 2006.

Walling, D.E.: Erosion and sediment yield research – some recent perspectives. *J. Hydrol*. 100, 113–141, 1988.

Wang, G., Gertner, G., Fang, S., and Anderson, A. B.: Mapping multiple variables for predicting soil loss by geostatistical methods with TM images and a slope map. *Photog. Eng. Remote Sensing*., 69, 889–898, 2003.

WCD.: Dams and development. A new framework for Decision-Making. Earthscan Publications Ltd, London., 356 pp, 2000.

White, S., Garcia-Ruiz, J.M., Marti, C., Valero, B., Errea, M.P., and Gomez-Villar, A.: The Biescas campsite disaster in the Central Spanish Pyrenees, and its temporal and spatial context. *Hydrol. Process*., 11, 1797–1818, 1996.

Williams, R., and Berndt, H.D.: Sediment yield computed with universal equation. *J. Hydrau. Div*., *ASCE* 98 (HY12). 2087–2098, 1972.

Wischmeier, W.H., and Smith, D.D.: Rainfall energy and its relationship to soil loss. *Trans., Am. Geophys. Union*., 39, 285–291, 1958.

Wischmeier, W.H., and Smith, D.D.: Predicting rainfall-erosion losses from cropland east of Rocky Mountains: guide for selection of practices for soil and water conservation. US Department of Agriculture, Agricultural handbook 282, 1965.

Wischmeier, W.H.: New developments in estimating water erosion. The 29th Annual meeting of the SSS of America, august 1974, Syracuse, NewYork., pp179-195, 1975.

Wischmier, W.H., and Smith, D.D.: Predicting rainfall erosion losses – A guide to conservation planning. USDA Agriculture Handbook 537, Washington D.C: GPO, 1978.

Yang, H., Shen, J., and Hu, S.: Evaluating waste treatment, recycle and reuse in industrial system, an application of the emergy approach. *Ecol. Model*., 160, 13–21, 2003.

Yu, B.: Rainfall erosivity and its estimation for Australia's tropics. *Australian Journal of Soil Research* ., 36, 143–165, 1998.